ISSN 1007-9327 (print)
ISSN 2219-2840 (online)

World Journal of *Gastroenterology*

World J Gastroenterol 2018 December 7; 24(45): 5057-5188

Published by Baishideng Publishing Group Inc

World Journal of Gastroenterology

Contents

Weekly Volume 24 Number 45 December 7, 2018

World Journal of Gastroenterology

Contents

Weekly Volume 24 Number 45 December 7, 2018

AIMS AND SCOPE

World Journal of Gastroenterology (*World J Gastroenterol*, *WJG*, print ISSN 1007-9327, online ISSN 2219-2840, DOI: 10.3748) is a peer-reviewed open access journal. *WJG* was established on October 1, 1995. It is published weekly on the 7th, 14th, 21st, and 28th each month. The *WJG* Editorial Board consists of 642 experts in gastroenterology and hepatology from 59 countries.

The primary task of *WJG* is to rapidly publish high-quality original articles, reviews, and commentaries in the fields of gastroenterology, hepatology, gastrointestinal endoscopy, gastrointestinal surgery, hepatobiliary surgery, gastrointestinal oncology, gastrointestinal radiation oncology, gastrointestinal imaging, gastrointestinal interventional therapy, gastrointestinal infectious diseases, gastrointestinal pharmacology, gastrointestinal pathophysiology, gastrointestinal pathology, evidence-based medicine in gastroenterology, pancreatology, gastrointestinal laboratory medicine, gastrointestinal molecular biology, gastrointestinal immunology, gastrointestinal microbiology, gastrointestinal genetics, gastrointestinal translational medicine, gastrointestinal diagnostics, and gastrointestinal therapeutics. *WJG* is dedicated to become an influential and prestigious journal in gastroenterology and hepatology, to promote the development of above disciplines, and to improve the diagnostic and therapeutic skill and expertise of clinicians.

INDEXING/ABSTRACTING

World Journal of Gastroenterology (*WJG*) is now indexed in Current Contents®/Clinical Medicine, Science Citation Index Expanded (also known as SciSearch®), Journal Citation Reports®, Index Medicus, MEDLINE, PubMed, PubMed Central and Directory of Open Access Journals. The 2018 edition of Journal Citation Reports® cites the 2017 impact factor for *WJG* as 3.300 (5-year impact factor: 3.387), ranking *WJG* as 35th among 80 journals in gastroenterology and hepatology (quartile in category Q2).

NAME OF JOURNAL
World Journal of Gastroenterology

ISSN
ISSN 1007-9327 (print)
ISSN 2219-2840 (online)

LAUNCH DATE
October 1, 1995

FREQUENCY
Weekly

EDITORIAL OFFICE
Ze-Mao Gong, Director
World Journal of Gastroenterology
Baishideng Publishing Group Inc
7901 Stoneridge Drive, Suite 501,
Pleasanton, CA 94588, USA
Telephone: +1-925-2238242
Fax: +1-925-2238243
E-mail: editorialoffice@wjgnet.com
Help Desk: http://www.f6publishing.com/helpdesk
http://www.wjgnet.com

PUBLISHER
Baishideng Publishing Group Inc
7901 Stoneridge Drive, Suite 501,
Pleasanton, CA 94588, USA
Telephone: +1-925-2238242
Fax: +1-925-2238243
E-mail: bpgoffice@wjgnet.com
Help Desk: http://www.f6publishing.com/helpdesk
http://www.wjgnet.com

PUBLICATION DATE
December 7, 2018

World Journal of Gastroenterology

Submit a Manuscript: http://www.f6publishing.com

World J Gastroenterol 2018 December 7; 24(45): 5057-5062

DOI: 10.3748/wjg.v24.i45.5057

ISSN 1007-9327 (print) ISSN 2219-2840 (online)

EDITORIAL

Methodology to develop machine learning algorithms to improve performance in gastrointestinal endoscopy

Thomas de Lange, Pål Halvorsen, Michael Riegler

Thomas de Lange, Department of Transplantation, Oslo University Hospital, Oslo 0424, Norway

Thomas de Lange, Institute of Clinical Medicine, University of Oslo, Oslo 0316, Norway

Pål Halvorsen, Michael Riegler, Center for Digital Engineering Simula Metropolitan, Fornebu 1364, Norway

Pål Halvorsen, Michael Riegler, Department for Informatics, University of Oslo, Oslo 0316, Norway

ORCID number: Thomas de Lange (0000-0003-3989-7487); Pål Halvorsen (0000-0003-2073-7029); Michael Riegler (0000-0002-3153-2064).

Author contributions: de Lange T, Halvorsen P and Riegler M contributed to the concept and design of the editorial, drafting of the manuscript and final approval of the manuscript.

Supported by the grants from Norwegian Research Council, No. 282315.

Conflict-of-interest statement: de Lange T declares no conflict of interests; Halvorsen P reports grants from Norwegian Research Council during the conduct of the study; and grants from Norwegian Research Council outside the submitted work; Riegler M declares no conflict of interests.

Manuscript source: Invited manuscript

Correspondence author to: Thomas de Lange, MD, PhD, Associate Professor, Department of transplantation, Oslo University Hospital and Institute of Clinical Medicine, University of Oslo, Postboks 4956 Nydalen, Oslo 0424, Norway. t.d.lange@medisin.uio.no

Telephone: +47-22118080

Received: September 7, 2018
Peer-review started: September 7, 2018
First decision: October 4, 2018
Revised: October 25, 2018
Accepted: November 2, 2018
Article in press: November 2, 2018
Published online: December 7, 2018

Abstract

Assisted diagnosis using artificial intelligence has been a holy grail in medical research for many years, and recent developments in computer hardware have enabled the narrower area of machine learning to equip clinicians with potentially useful tools for computer assisted diagnosis (CAD) systems. However, training and assessing a computer's ability to diagnose like a human are complex tasks, and successful outcomes depend on various factors. We have focused our work on gastrointestinal (GI) endoscopy because it is a cornerstone for diagnosis and treatment of diseases of the GI tract. About 2.8 million luminal GI (esophageal, stomach, colorectal) cancers are detected globally every year, and although substantial technical improvements in endoscopes have been made over the last 10-15 years, a major limitation of endoscopic examinations remains operator variation. This translates into a substantial inter-observer variation in the detection and assessment of mucosal lesions, causing among other things an average polyp miss-rate of 20% in the colon and thus the subsequent development of a number of post-colonoscopy colorectal cancers. CAD systems might eliminate this variation and lead to more accurate diagnoses. In this editorial, we point out some of the current challenges in the development of efficient computer-based digital assistants. We give examples of proposed tools using various techniques, identify current challenges, and give suggestions for the development and assessment of future CAD systems.

Key words: Endoscopy; Artificial intelligence; Deep

learning; Computer assisted diagnosis; Gastrointestinal

Core tip: Assisted diagnosis using artificial intelligence and recent developments in computer hardware have enabled the narrower area of machine learning to equip the endoscopists with potentially powerful tools for computer assisted diagnosis systems. The success depends on various factors; optimizing algorithms, image database quality and size and comparison with existing systems.

de Lange T, Halvorsen P, Riegler M. Methodology to develop machine learning algorithms to improve performance in gastrointestinal endoscopy. *World J Gastroenterol* 2018; 24(45): 5057-5062 Available from: URL: http://www.wjgnet.com/1007-9327/full/v24/i45/5057.htm DOI: http://dx.doi.org/10.3748/wjg.v24.i45.5057

INTRODUCTION

Gastrointestinal (GI) endoscopy is a cornerstone for diagnosis and treatment of diseases in the GI tract. About 2.8 million luminal GI cancers (esophageal, stomach, colorectal) are detected globally every year, and many of these might be prevented through improved endoscopic performance and systematic high-quality screening in high incidence areas[1]. These cancers represent a substantial health challenge for society with a mortality rate of about 65%[2], and colorectal cancer is the third most common cause of cancer mortality among both women and men[3]. Despite substantial technical improvements in endoscopes over the last 10-15 years, a major limitation of endoscopic examinations is operator variation. This variation depends on operator skill, perceptual factors, personality characteristics, knowledge, and attitude[4]. This translates into a substantial inter-observer variation in the detection and assessment of mucosal lesions[5,6], leading to an average polyp miss-rate of 20% in the colon[7]. All of these factors can to some extent be alleviated by substantial educational efforts, but they cannot be eliminated entirely[8]. Thus, developing an automated computer-based support system for the detection and characterization of mucosal lesions would be an important contribution to eliminating the current variation in endoscopists' performance.

Artificial intelligence (AI) is the area of computer science that aims to create intelligent machines that mimic human behavior, and assisted diagnosis using AI has been a holy grail in the field of medicine for many years. Such machines have long been the realm of fiction, but recent developments in computer hardware have enabled the narrower field of machine learning to develop potentially highly accurate computer assisted diagnosis (CAD) systems. At its most basic, machine learning is the practice of using algorithms to parse data, learn from the data, and then make a prediction, and in the medical domain such systems are used to detect or classify a disease. Research and development of such systems is currently under way in many medical domains like retina scans, various cancer screening systems, and skin cancer detection[9-11]. However, there exist methodological issues that need to be addressed both for creating and improving automated diagnosis algorithms.

MACHINE LEARNING IN ENDOSCOPY

Automated detection of anomalies in the GI tract have been proposed for diseases such as Barrett's esophagus, gastric cancer, angiectasia, celiac disease, and polyp detection and characterization, and a number of methods and algorithms have been tested in recent years[12-18]. The methods and algorithms range from simpler traditional machine learning methods to more recently developed deep learning approaches[19,20].

An example of a simple system is a search-based system using various global features in the images[21]. It extracts (complex) image features like color histograms and textures and feeds these features into a classifier for determining whether an object is present or not. For example, such a system might determine the presence of an object by calculating the distance of the feature vector from the vectors in the model. An important advantage of systems based on simple methods is that they can be easier to understand and their results can be easier to explain to medical personnel[22-24].

The current state-of-the-art and the most commonly used methods are based on deep neural networks. These networks work as an interconnected group of nodes, akin to the vast network of neurons in the human brain[25]. Such networks typically consist of an input and an output layer, as well as multiple hidden convolutional, pooling, fully connected, and normalization layers. Typically, each input image will pass through the layers in order to classify an object with probabilistic values between 0 and 1. There exist several variations of deep neural networks. For image and video analysis, convolutional neural networks (CNNs) are the most common. CNNs can be used to perform either segmentation (the exact marking of a finding in the image[26]) or classification (a more global point of view on the image, such as a general statement like "this image contains a polyp"[22,27,28]). Another promising method for image analysis is generative adversarial networks (GANs). GANs consist of two neural networks competing with each other in a zero-sum game framework during the training phase. The generator network generates new data instances using an inverse convolutional network by upsampling random noise to an image. The other network, the discriminator, takes the generated image and the training set and checks for authenticity. This means that the discriminator decides whether the data belong to or are

classified in the actual training dataset or not. GANs can also be defined as conditional GANs that have an image as input instead of random noise and that transform this image into another image. This can be used to create, for example, segmentation masks. An example of a GAN-based method is described by Pogorelov *et al*[22,29]. The approach presented in their papers uses conditional GANs with a normal image from the colon as input, and the algorithm segments the finding in the image. This noise segmentation is then cleaned in a post-processing step that leads to a clear segmentation. Many of these approaches have yielded promising results regarding detection accuracy, with some achieving numbers above 90%, but many run too slowly to be used in a clinically useful system providing real-time feedback. Some comparisons of different approaches are given by Pogorelov *et al*[22,26] and Riegler *et al*[30].

IMAGE DATABASE QUALITY

A sufficient amount of data is vital in machine learning, and the creation of algorithms usually relies on large databases. This is especially true for deep learning, which is currently the standard for image analysis[31]. However, the quality of the database is also essential, and it is crucial that all the images and videos are annotated correctly. The computer learns from analyzing the given data, and thus erroneous learning will lead to incorrect diagnoses. Therefore, when collecting data and making a dataset the recommendations below should be followed

There are variations between observers, and to reduce this bias the ground truth assessment should involve at least three observers[32]. However, the required agreement between the observers and the degree of confidence is not known and requires further studies. The goal regarding the diagnostic thresholds for such a technique is to reach more than 90% positive predictive value for correct classification of the lesions[33].

A potential problem in machine learning is over-fitting. Many of the datasets show obvious examples of medical findings, and the similarity of the different images often results in overfitting. Thus, overfitting occurs when the learning algorithm learns the data too well and therefore also captures the noise of the data, *e.g.*, when the model or the algorithm fits the data too well, or if the model or algorithm shows low bias but high variance. Therefore, too many similar samples should be avoided in order to avoid such "overtraining". A diverse dataset is therefore recommended to better enable correct disease detection in new data.

Many datasets are limited in size, and many assess their systems using too few samples. Many argue that the dataset should be as large as possible[34], but others show that machine learning can also work on smaller datasets using transfer learning[30,35], which has recently found frequent use in the context of medical image problems[36,37]. Note that there is no "one size fits all" answer. The amount of required training data is dependent on many different aspects of the experiment, but a general rule of thumb is to have around 1000 images per class for deep learning applications. In the Kvasir dataset[38], at least 1000 images per class are provided for different findings.

One general problem is that several of the existing datasets are cumbersome to use in terms of permission, for example, several of the listed sets in Table 1[38-44] are restricted. To enable subsequent comparisons, it is best is to use an open dataset.

The most important take-away message is that clean and complete data are one of the most important parts of a good detection system. This means that spending the time to create a high-quality database is very important and is directly connected to the quality of the following steps.

SYSTEM ASSESSMENT

Comparing published research is challenging, and an increasing number of research communities are targeting this problem by creating public available datasets and encouraging reproducible experiments. In order to enable full comparisons, not only the same datasets should be used, but the datasets should also be split between training and test sets in an equal way. Furthermore, the more information the better, and one should use as many of the common metrics as possible as described by Pogorelov *et al*[38]. For detection accuracy, the raw numbers for true positives, true negatives, false positives, and false negatives are important, and metrics based on these like sensitivity (recall), precision, specificity, accuracy, Matthews correlation coefficient, and F1 score should be calculated. Finally, a metric for processing speed in terms of time per image or frame should be included, and although this depends on the hardware that is used, it gives an indication as to whether the system can run in real time.

We must also emphasize that there is a difference in how anomaly detection is defined. In the area of computer science, detection per frame or image is the standard, but in the medical domain, reporting a detection per instance (at least once in a sequence of frames of the same finding) is common. If possible, one should include both definitions.

CONCLUSION

Researchers have sought for many years to develop efficient AI tools to assist in medical diagnosis. Enabled by recent hardware developments, several research groups are now working on machine learning-based medical systems and have obtained promising results. Thus, we have observed a rapid increase in publications related to AI in GI endoscopy over the last two years. However, as described above, there are still large variations in the

Table 1 Some existing image datasets for gastrointestinal endoscopy

Dataset	Findings	Frames	Usage
CVC-356[39]	Polyps	1706	©, by request
CVC-612[40]	Polyps	1962	©, by request
CVC-12k[41]	Polyps	11954	©, by request
Kvasir[38]	Polyps, esophagitis, ulcerative colitis, Z-line, pylorus, cecum, dyed polyp, dyed resection margins, stool	8000	Open academic
Nerthus[41]	Stool - categorization of bowel cleanliness	1350	Open academic
GIANA'17[42]	Angiectasia	600	©, by request
ASU-Mayo polyp database[43]	Polyps	18781	©, by request
CVC-ClinicDB	Polyps	612	©, by request
ETIS-Larib Polyp DB	Polyps	1500	©, by request
KID[44]	Angiectasia, bleeding, inflammations, polyps	2500 + 47 videos	Open academic

tested datasets, and insufficient metrics are being used. In order to enable full comparisons between methods, the same datasets should be utilized, and as many of the common metrics as possible should be used[38]. Another limitation is that the lesion characterization systems rely on advanced endoscopic functionality like narrow-band imaging, endocytoscopy, or volumetric laser endomicroscopy, to which most endoscopy units do not have access, especially in low-income countries[45]. Still, it is not proven that these techniques improve endoscopy performance, and validation in live endoscopies is still required. Therefore, there is still a long road ahead before such systems can be put into practice, and much research, development, and clinical testing still needs to be performed. To produce the best possible and the most comparable results, the recommendations given here should be followed.

REFERENCES

1 **Brenner H**, Kloor M, Pox CP. Colorectal cancer. *Lancet* 2014; **383**: 1490-1502 [PMID: 24225001 DOI: 10.1016/S0140-6736(13)61649-9]
2 World Health Organization - International Agency for Research on Cancer. Estimated cancer incidence, mortality and prevalence world-wide in 2012. Available from: URL: http://globocan.iarc.fr/Default.aspx. 2012
3 **Torre LA**, Bray F, Siegel RL, Ferlay J, Lortet-Tieulent J, Jemal A. Global cancer statistics, 2012. *CA Cancer J Clin* 2015; **65**: 87-108 [PMID: 25651787 DOI: 10.3322/caac.21262]
4 **Hewett DG**, Kahi CJ, Rex DK. Efficacy and effectiveness of colonoscopy: how do we bridge the gap? *Gastrointest Endosc Clin N Am* 2010; **20**: 673-684 [PMID: 20889071 DOI: 10.1016/j.giec.2010.07.011]
5 **Lee SH**, Jang BI, Kim KO, Jeon SW, Kwon JG, Kim EY, Jung JT, Park KS, Cho KB, Kim ES, Park CG, Yang CH; DeaguGyeongbook Gastrointestinal Study Group. Endoscopic experience improves interobserver agreement in the grading of esophagitis by Los Angeles classification: conventional endoscopy and optimal band image system. *Gut Liver* 2014; **8**: 154-159 [PMID: 24672656 DOI: 10.5009/gnl.2014.8.2.154]
6 **van Doorn SC**, Hazewinkel Y, East JE, van Leerdam ME, Rastogi A, Pellisé M, Sanduleanu-Dascalescu S, Bastiaansen BA, Fockens P, Dekker E. Polyp morphology: an interobserver evaluation for the Paris classification among international experts. *Am J Gastroenterol* 2015; **110**: 180-187 [PMID: 25331346 DOI: 10.1038/ajg.2014.326]
7 **Lanspa SJ**, Lynch HT. Quality indicators for colonoscopy and the risk of interval cancer. *N Engl J Med* 2010; **363**: 1371; author reply 1373 [PMID: 20879889 DOI: 10.1056/NEJMc1006842]
8 **Rondonotti E**, Soncini M, Girelli CM, Russo A, Ballardini G, Bianchi G, Cantù P, Centenara L, Cesari P, Cortelezzi CC, Gozzini C, Lupinacci G, Maino M, Mandelli G, Mantovani N, Moneghini D, Morandi E, Putignano R, Schalling R, Tatarella M, Vitagliano P, Villa F, Zatelli S, Conte D, Masci E, de Franchis R; AIGO, SIED and SIGE Lombardia. Can we improve the detection rate and interobserver agreement in capsule endoscopy? *Dig Liver Dis* 2012; **44**: 1006-1011 [PMID: 22858420 DOI: 10.1016/j.dld.2012.06.014]
9 **Gulshan V**, Peng L, Coram M, Stumpe MC, Wu D, Narayanaswamy A, Venugopalan S, Widner K, Madams T, Cuadros J, Kim R, Raman R, Nelson PC, Mega JL, Webster DR. Development and Validation of a Deep Learning Algorithm for Detection of Diabetic Retinopathy in Retinal Fundus Photographs. *JAMA* 2016; **316**: 2402-2410 [PMID: 27898976 DOI: 10.1001/jama.2016.17216]
10 **Ciompi F**, Chung K, van Riel SJ, Setio AAA, Gerke PK, Jacobs C, Scholten ET, Schaefer-Prokop C, Wille MMW, Marchianò A, Pastorino U, Prokop M, van Ginneken B. Towards automatic pulmonary nodule management in lung cancer screening with deep learning. *Sci Rep* 2017; **7**: 46479 [PMID: 28422152 DOI: 10.1038/srep46479]
11 **Esteva A**, Kuprel B, Novoa RA, Ko J, Swetter SM, Blau HM, Thrun S. Dermatologist-level classification of skin cancer with deep neural networks. *Nature* 2017; **542**: 115-118 [PMID: 28117445 DOI: 10.1038/nature21056]
12 **Swager AF**, van der Sommen F, Klomp SR, Zinger S, Meijer SL, Schoon EJ, Bergman JJGHM, de With PH, Curvers WL. Computer-aided detection of early Barrett's neoplasia using volumetric laser endomicroscopy. *Gastrointest Endosc* 2017; **86**: 839-846 [PMID: 28322771 DOI: 10.1016/j.gie.2017.03.011]
13 **Hirasawa T**, Aoyama K, Tanimoto T, Ishihara S, Shichijo S, Ozawa T, Ohnishi T, Fujishiro M, Matsuo K, Fujisaki J, Tada T. Application of artificial intelligence using a convolutional neural network for detecting gastric cancer in endoscopic images. *Gastric Cancer* 2018; **21**: 653-660 [PMID: 29335825 DOI: 10.1007/s10120-018-0793-2]
14 **Leenhardt R**, Vasseur P, Li C, Saurin JC, Rahmi G, Cholet F, Becq A, Marteau P, Histace A, Dray X; CAD-CAP Database Working Group. A neural network algorithm for detection of GI angiectasia during small-bowel capsule endoscopy. *Gastrointest Endosc* 2018 [PMID: 30017868 DOI: 10.1016/j.gie.2018.06.036]
15 **Mori Y**, Kudo SE, Chiu PW, Singh R, Misawa M, Wakamura K, Kudo T, Hayashi T, Katagiri A, Miyachi H, Ishida F, Maeda

Y, Inoue H, Nimura Y, Oda M, Mori K. Impact of an automated system for endocytoscopic diagnosis of small colorectal lesions: an international web-based study. *Endoscopy* 2016; **48**: 1110-1118 [PMID: 27494455 DOI: 10.1055/s-0042-113609]

16 **Mori Y**, Kudo SE, Misawa M, Saito Y, Ikematsu H, Hotta K, Ohtsuka K, Urushibara F, Kataoka S, Ogawa Y, Maeda Y, Takeda K, Nakamura H, Ichimasa K, Kudo T, Hayashi T, Wakamura K, Ishida F, Inoue H, Itoh H, Oda M, Mori K. Real-Time Use of Artificial Intelligence in Identification of Diminutive Polyps During Colonoscopy: A Prospective Study. *Ann Intern Med* 2018; **169**: 357-366 [PMID: 30105375 DOI: 10.7326/M18-0249]

17 **Yuan Y**, Meng MQ. Deep learning for polyp recognition in wireless capsule endoscopy images. *Med Phys* 2017; **44**: 1379-1389 [PMID: 28160514 DOI: 10.1002/mp.12147]

18 **Wang P,** Xiao X, Glissen Brown JR, Berzin TM, Tu M, Xiong F, Hu X, Liu P, Song Y, Zhang D, Yang X, Li L, He J, Yi X, Liu J, Liu X. Development and validation of a deep-learning algorithm for the detection of polyps during colonoscopy. *Nat Biomed Eng* 2018; **2**: 741-748 [DOI:10.1038/s41551-018-0301-3]

19 **Zhou T**, Han G, Li BN, Lin Z, Ciaccio EJ, Green PH, Qin J. Quantitative analysis of patients with celiac disease by video capsule endoscopy: A deep learning method. *Comput Biol Med* 2017; **85**: 1-6 [PMID: 28412572 DOI: 10.1016/j.compbiomed.2017.03.031]

20 **Lequan Yu**, Hao Chen, Qi Dou, Jing Qin, Pheng Ann Heng. Integrating Online and Offline Three-Dimensional Deep Learning for Automated Polyp Detection in Colonoscopy Videos. *IEEE J Biomed Health Inform* 2017; **21**: 65-75 [PMID: 28114049 DOI: 10.1109/JBHI.2016.2637004]

21 **Riegler M,** Pogorelov K, Halvorsen P, de Lange T, Griwodz C, Johansen D, Schmidt PT, Eskeland SL. Eir - efficient computer aided diagnosis framework for gastrointestinal endoscopies. *CBMI* 2016; 1-6 [DOI: 10.1109/CBMI.2016.7500257]

22 **Pogorelov K,** Ostroukhova O, Jeppsson M, Espeland H, Griwodz C, de Lange T, Johansen D, Riegler M, Halvorsen P. Deep learning and hand-crafted feature based approaches for polyp detection in medical videos. *IEEE CBMS* 2018 [DOI: 10.1109/CBMS.2018.00073]

23 **Hong D**, Tavanapong W, Wong J, Oh J, de Groen PC. 3D Reconstruction of virtual colon structures from colonoscopy images. *Comput Med Imaging Graph* 2014; **38**: 22-33 [PMID: 24225230 DOI: 10.1016/j.compmedimag.2013.10.005]

24 **Riegler M,** Larson M, Lux M, and Kofler C. How 'how' reflects what's what: Content-based exploitation of how users frame social images. *ACM MED MER* 2014; 397-406 [DOI: 10.1145/2647868.2654894]

25 **LeCun Y**, Bengio Y, Hinton G. Deep learning. *Nature* 2015; **521**: 436-444 [PMID: 26017442 DOI: 10.1038/nature14539]

26 **Pogorelov K,** Riegler M, Eskeland SL, de Lange T, Johansen D, Griwodz C, Schmidt PT, Halvorsen P. Efficient disease detection in gastrointestinal videos - global features versus neural networks. *Multimed Tools Appl* 2017; 76: 22493-22525 [DOI: 10.1007/s11042-017-4989-y]

27 **Shin Y**, Balasingham I. Automatic polyp frame screening using patch based combined feature and dictionary learning. *Comput Med Imaging Graph* 2018; **69**: 33-42 [PMID: 30172091 DOI: 10.1016/j.compmedimag.2018.08.001]

28 **Alammari A,** Islam AR, Oh J, Tavanapong W, Wong J, De Groen PC. Classification of ulcerative colitis severity in colonoscopy videos using CNN. *ACM ICIME* 2017; 139-144 [DOI: 10.1145/3149572.3149613]

29 **Pogorelov K,** Ostroukhova O, Petlund A, Halvorsen P, de Lange T, Espeland H, Kupka T, Griwodz C, Riegler M. Deep learning and handcrafted feature based approaches for automatic detection of angiectasia. *IEEE BHI* 2018 [DOI: 10.1109/BHI.2018.8333444]

30 **Riegler M,** Pogorelov K, Eskeland SL, SchmidtPT, Albisser Z, Johansen D, Griwodz C, Halvorsen P, de Lange T. From annotation to computer-aided diagnosis: Detailed evaluation of a medical multimedia system. *ACM Trans Multimedia Comput Commun* 2017; **13**: 26:1-26:26 [DOI: 10.1145/3079765]

31 **Litjens G**, Kooi T, Bejnordi BE, Setio AAA, Ciompi F, Ghafoorian M, van der Laak JAWM, van Ginneken B, Sánchez CI. A survey on deep learning in medical image analysis. *Med Image Anal* 2017; **42**: 60-88 [PMID: 28778026 DOI: 10.1016/j.media.2017.07.005]

32 **Gottlieb K**, Hussain F. Voting for image scoring and assessment (VISA)--theory and application of a 2 + 1 reader algorithm to improve accuracy of imaging endpoints in clinical trials. *BMC Med Imaging* 2015; **15**: 6 [PMID: 25880066 DOI: 10.1186/s12880-015-0049-0]

33 **Rex DK**, Kahi C, O'Brien M, Levin TR, Pohl H, Rastogi A, Burgart L, Imperiale T, Ladabaum U, Cohen J, Lieberman DA. The American Society for Gastrointestinal Endoscopy PIVI (Preservation and Incorporation of Valuable Endoscopic Innovations) on real-time endoscopic assessment of the histology of diminutive colorectal polyps. *Gastrointest Endosc* 2011; **73**: 419-422 [PMID: 21353837 DOI: 10.1016/j.gie.2011.01.023]

34 **Chen XW,** Lin X. Big data deep learning: challenges and perspectives. *IEEE Access* 2014; 2: 514-525 [DOI: 10.1109/ACCESS.2014.2325029]

35 **Riegler M,** Lux M, Griwodz C, Spampinato C, de Lange T, Eskeland SL, Pogorelov K, Tavanapong W, Schmidt PT, Gurin C, Johansen D, Johansen H, Halvorsen P. Multimedia and medicine: Teammates for better disease detection and survival. *ACM on Multimedia Conference* 2016; 968-977 [DOI: 10.1145/2964284.2976760]

36 **Younghak Shin**, Balasingham I. Comparison of hand-craft feature based SVM and CNN based deep learning framework for automatic polyp classification. *Conf Proc IEEE Eng Med Biol Soc* 2017; **2017**: 3277-3280 [PMID: 29060597 DOI: 10.1109/EMBC.2017.8037556]

37 **Shin HC**, Roth HR, Gao M, Lu L, Xu Z, Nogues I, Yao J, Mollura D, Summers RM. Deep Convolutional Neural Networks for Computer-Aided Detection: CNN Architectures, Dataset Characteristics and Transfer Learning. *IEEE Trans Med Imaging* 2016; **35**: 1285-1298 [PMID: 26886976 DOI: 10.1109/TMI.2016.2528162]

38 **Pogorelov K,** Randel KR, Griwodz C,Eskeland SL, de Lange T, Johansen D, Spampinato C, Dang-Nguyen DT, Lux M, Schmidt PT, Riegler M, and Halvorsen P. Kvasir: A multi- class image dataset for computer aided gastrointestinal disease detection. *ACM on Multimedia Systems Conference* 2017; 164-169 [DOI: 10.1145/3083187.3083212]

39 **Bernal J,** Aymeric H. Miccai endoscopic vision challenge polyp detection and segmentation. Accessed December, 2017 Available from: URL: https://endovissub2017-giana.grand-challenge. org/home/

40 **Bernal J**, Sánchez FJ, Fernández-Esparrach G, Gil D, Rodríguez C, Vilariño F. WM-DOVA maps for accurate polyp highlighting in colonoscopy: Validation vs. saliency maps from physicians. *Comput Med Imaging Graph* 2015; **43**: 99-111 [PMID: 25863519 DOI: 10.1016/j.compmedimag.2015.02.007]

41 **Pogorelov K,** Randel KR, de Lange T, Eskeland SL, Griwodz C, Johansen D, Spampinato C, Taschwer M, Lux M, Schmidt PT, Riegler M, Halvorsen P. Nerthus: A bowel preparation quality video dataset. *ACM on Multimedia Systems Conference* 2017; 170-174 [DOI: 10.1145/3083187.3083216]

42 **Bernal J,** Aymeric H. Gastrointestinal image analysis (GIANA) angiodysplasia D&L challenge. Accessed November, 2017 Available from: URL: https://endovissub2017-giana.grand-challenge. org/home/

43 **Tajbakhsh N**, Gurudu SR, Liang J. Automated Polyp Detection in Colonoscopy Videos Using Shape and Context Information. *IEEE Trans Med Imaging* 2016; **35**: 630-644 [PMID: 26462083 DOI: 10.1109/TMI.2015.2487997]

44 **Koulaouzidis A**, Iakovidis DK, Yung DE, Rondonotti E, Kopylov U, Plevris JN, Toth E, Eliakim A, Wurm Johansson G, Marlicz W, Mavrogenis G, Nemeth A, Thorlacius H, Tontini GE. KID Project: an internet-based digital video atlas of capsule endoscopy for

research purposes. *Endosc Int Open* 2017; **5**: E477-E483 [PMID: 28580415 DOI: 10.1055/s-0043-105488]
45 **Wang Z**, Meng Q, Wang S, Li Z, Bai Y, Wang D. Deep learning-based endoscopic image recognition for detection of early gastric cancer: a Chinese perspective. *Gastrointest Endosc* 2018; **88**: 198-199 [PMID: 29935613 DOI: 10.1016/j.gie.2018.01.029]

P- Reviewer: Hashimoto R, Shichijo S **S- Editor**: Ma RY
L- Editor: A **E- Editor**: Huang Y

World Journal of Gastroenterology

Submit a Manuscript: http://www.f6publishing.com

World J Gastroenterol 2018 December 7; 24(45): 5063-5075

DOI: 10.3748/wjg.v24.i45.5063

ISSN 1007-9327 (print) ISSN 2219-2840 (online)

REVIEW

Alcoholic liver disease: Utility of animal models

Arantza Lamas-Paz, Fengjie Hao, Leonard J Nelson, Maria Teresa Vázquez, Santiago Canals, Manuel Gómez del Moral, Eduardo Martínez-Naves, Yulia A Nevzorova, Francisco Javier Cubero

Arantza Lamas-Paz, Fengjie Hao, Eduardo Martínez-Naves, Francisco Javier Cubero, Department of Immunology, Ophthalmology and ORL, Complutense University School of Medicine, Madrid 28040, Spain

Arantza Lamas-Paz, Fengjie Hao, Eduardo Martínez-Naves, Yulia A Nevzovova, Francisco Javier Cubero, 12 de Octubre Health Research Institute (imas12), Madrid 28041, Spain

Leonard J Nelson, Institute for Bioengineering (IBioE), School of Engineering, Faraday Building, The University of Edinburgh, Edinburgh EH9 3 JL, Scotland, United Kingdom

Maria Teresa Vázquez, Department of Human Anatomy and Embryology, Complutense University School of Medicine, Madrid 28040, Spain

Santiago Canals, Instituto de Neurociencias, Consejo Superior de Investigaciones Científicas, Universidad Miguel Hernández, San Juan de Alicante 03550, Spain

Manuel Gómez del Moral, Department of Cell Biology, Complutense University School of Medicine, Madrid 28040, Spain

Yulia A Nevzorova, Department of Genetics, Physiology and Microbiology, Faculty of Biology, Universidad Complutense, Madrid 28040, Spain

Yulia A Nevzorova, Department of Internal Medicine III, University Hospital RWTH Aachen, Aachen 52062, Germany

ORCID number: Arantza Lamas-Paz (0000-0001-5857-4320); Fengjie Hao (0000-0002-6734-265X); Leonard J Nelson (0000-0002-4197-4843); Maria Teresa Vázquez (0000-0003-3537-0901); Santiago Canals (0000-0003-2175-8139); Manuel Gómez del Moral (0000-0002-0642-8142); Eduardo Martínez-Naves (0000-0001-8136-9042); Yulia A Nevzorova (0000-0003-1390-8002); Francisco Javier Cubero (0000-0003-1499-650X).

Author contributions: Lamas-Paz A and Hao F equally contributed to the manuscript writing and figure design; Nelson LJ, Vázquez MT, Canals S, Gómez del Moral M and Martínez-Naves E critiqued the manuscript, checked English language and provided fundamental guidance. Nevzorova YA and Cubero FJ outlined and corrected the review and provided guidance.

Supported by the MINECO Retos, No. SAF2016-78711 and SAF2017-87919R; EXOHEP-CM, No. S2017/BMD-3727; the AMMF Cholangiocarcinoma Charity, No. 2018/117; the COST Action, No. CA17112; Ramón y Cajal, No. RYC-2014-15242 and No. RYC-2015-17438; grant of ERAB, No. EA 14/18; Gilead Liver Research Scholar 2018, No. 44/2018; Ministerio de Sanidad, Servicios Sociales e Igualdad, No. 2017I065; and the UCM group "Lymphocyte Immunobiology", No. 920631 (imas12-associated, Ref. IBL-6). German Research Foundation (SFB/TRR57/P04 and DFG NE 2128/2-1); Interdisciplinary Center for Clinical Research from the Faculty of Medicine at RWTH Aachen University (IZKF/E8-2).

Conflict-of-interest statement: The authors declare that they have no conflict of interest.

Manuscript source: Invited manuscript

Correspondence author to: Francisco Javier Cubero, BSc, MSc, PhD, Assistant Professor, Department of Immunology, Ophthalmology and ORL, Complutense University School of Medicine, c/Doctor Severo Ochoa 9, Madrid 28040, Spain. fcubero@ucm.es
Telephone: +34-91-3941385
Fax: +34-91-394164

Received: October 19, 2018
Peer-review started: October 19, 2018
First decision: November 1, 2018
Revised: November 8, 2018
Accepted: November 9, 2018
Article in press: November 9, 2018
Published online: December 7, 2018

Abstract

Alcoholic liver disease (ALD) is a major cause of acute

and chronic liver injury. Extensive evidence has been accumulated on the pathological process of ALD during the past decades. However, effective treatment options for ALD are very limited due to the lack of suitable *in vivo* models that recapitulate the full spectrum of ALD. Experimental animal models of ALD, particularly rodents, have been used extensively to mimic human ALD. An ideal animal model should recapitulate all aspects of the ALD process, including significant steatosis, hepatic neutrophil infiltration, and liver injury. A better strategy against ALD depends on clear diagnostic biomarkers, accurate predictor(s) of its progression and new therapeutic approaches to modulate stop or even reverse the disease. Numerous models employing rodent animals have been established in the last decades to investigate the effects of acute and chronic alcohol exposure on the initiation and progression of ALD. Although significant progress has been made in gaining better knowledge on the mechanisms and pathology of ALD, many features of ALD are unknown, and require further investigation, ideally with improved animal models that more effectively mimic human ALD. Although differences in the degree and stages of alcoholic liver injury inevitably exist between animal models and human ALD, the acquisition and translational relevance will be greatly enhanced with the development of new and improved animal models of ALD.

Key words: Steatohepatitis; Cirrhosis; Hepatocellular carcinoma; Alcoholic liver disease; Reactive oxygen species

Core tip: Alcoholism is now considered a global health issue. Although significant progress has been made in our understanding of the mechanisms and pathology of alcoholic liver disease (ALD), many features of ALD remain unidentified - requiring further investigation with improved animal models that more effectively emulate human ALD. In this Review, we provide an update on the prevalence, current and emerging experimental models, as well as the pathophysiology of ALD.

Lamas-Paz A, Hao F, Nelson LJ, Vázquez MT, Canals S, Gómez del Moral M, Martínez-Naves E, Nevzorova YA, Cubero FJ. Alcoholic liver disease: Utility of animal models. *World J Gastroenterol* 2018; 24(45): 5063-5075 Available from: URL: http://www.wjgnet.com/1007-9327/full/v24/i45/5063.htm DOI: http://dx.doi.org/10.3748/wjg.v24.i45.5063

INTRODUCTION

Alcohol has been part of human culture for thousands of years. Excessive alcohol consumption is the oldest form of liver injury known to civilization. Currently, alcohol abuse is an important global health problem with a significant socioeconomic burden in most societies. The term alcoholic liver disease (ALD) comprises a range of disorders including simple steatosis, steatohepatitis, cirrhosis, and end-stage hepatocellular carcinoma (HCC).

Animal models are frequently used to emulate and understand the underlying mechanisms of human disease. However, over the last decades, a great variety of animal models for ALD have been developed with different outcomes. To find the "ideal" experimental model for ALD would greatly help the study of the pathogenesis and thus development of new therapeutic strategies for the treatment of ALD. However, most models do not recapitulate the full spectrum of human ALD. A clinically-relevant model should induce certain characteristics, including: severe steatosis, hepatocellular damage and hepatic infiltration.

This review provides an overview of the pros and cons of the most frequently used experimental models of ALD, and the advances and implementation of new animal models that show great potential. We also discuss the recapitulation of pathological events in such models that commonly occur in human ALD.

PATHOPHYSIOLOGY OF ALD

Alcohol abuse has a long history although it was not until the 20th century when it was studied with a scientific perspective. In 1965, pioneering work by Lieber and colleagues[1] identified the hepatotoxic function of alcohol, instead of the malnutrition effect, previously assumed. ALD is now recognized as a complex disease induced by alcohol abuse with a broad spectrum of liver diseases. These range from simple steatosis to more severe forms of injury, including steatohepatitis, cirrhosis and HCC[2,3].

Following absorption in the gastrointestinal tract (GI), only 2% to 10% of total ingested ethanol is directly eliminated through the lung, the kidney and sweat in an unchanged form[4]. Most ethanol will undergo metabolic processing in the liver (Figure 1). First, ethanol (C_2H_6O) is oxidized and transformed into acetaldehyde (C_2H_4O) in hepatocytes. This step is mainly achieved by the enzyme alcohol dehydrogenase (ADH); although alternative minor pathways are involved including the catalase enzyme pathway (which has low expression in the liver), and the microsomal ethanol oxidation system (MEOS) - which depends on cytochrome P450 (CYP450) enzymes, particularly cytochromes P450 2E1 (CYP2E1)[4]. Successive oxidation reactions take place: Acetaldehyde loses hydrogen, and is metabolized to acetate (C_2H_3O), under the catalysis of acetaldehyde dehydrogenase (ALDH). Major reactions in this process require the coenzyme nicotinamide adenine dinucleotide (NAD^+) for transferring hydrogen, and the amount of reducing equivalents (NADH) is increased as a result. It has been reported that the change in NAD^+/NADH ratio favours hepatic triglyceride accumulation and fatty acid synthesis[4].

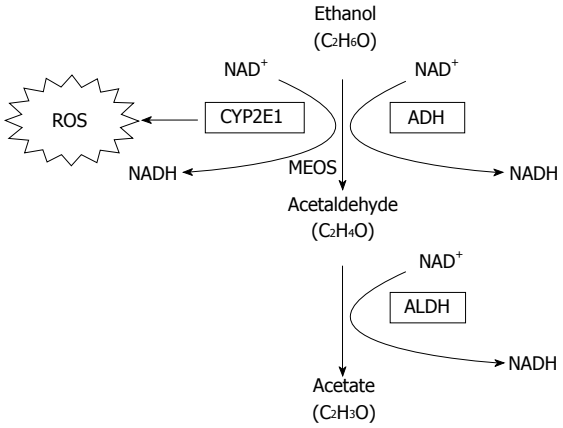

Figure 1 Alcohol metabolism in hepatocytes. Ethanol is oxidized to acetaldehyde through action of the enzyme alcohol dehydrogenase and cytochrome P450 isoenzyme 2E1 a major component of the microsomal enzyme oxidation system. Acetaldehyde is subsequently metabolized to acetate by acetaldehyde dehydrogenase. In this process coenzyme nicotinamide adenine dinucleotide is reduced to coenzyme nicotinamide adenine dinucleotide reduced. The metabolism of ethanol increases generation of reactive oxygen species, including hydroxyethyl, superoxide anion and hydroxyl radicals, which contribute to oxidative stress and also can react with other cellular molecules, forming adducts (proteins, lipids or DNA). ADH: Alcohol dehydrogenase; CYP2E1: Cytochrome P450 isoenzyme 2E1; MEOS: Microsomal enzyme oxidation system; ALDH: Acetaldehyde dehydrogenase; NAD^+: Nicotinamide adenine dinucleotide; NADH: Nicotinamide adenine dinucleotide reduced; ROS: Reactive oxygen species.

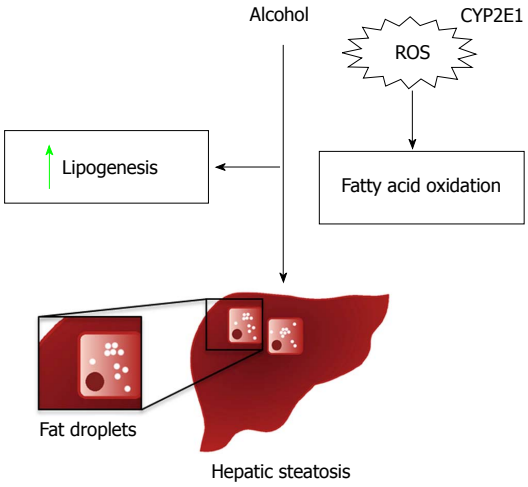

Figure 2 Alcohol induces fatty liver disease. Alcohol causes the accumulation of fat droplets in hepatocytes increasing the lipogenesis and decreasing the fatty acid oxidation. CYP2E1: Cytochrome P450 isoenzyme 2E1; ROS: Reactive oxygen species.

Another feature of alcohol metabolism is the generation of reactive oxygen species (ROS), which are largely regulated (and which can be exacerbated) by the CYP2E1 family[5]. These active radicals are usually produced by the mitochondria, endoplasmic reticulum (ER) or Kupffer cells (KCs). They rapidly form a variety of active metabolites which can further contribute to oxidative stress in hepatocytes[6]. Last but not least, acetaldehyde, the major metabolite of ethanol, is a powerful hepatotoxin. Multiple studies indicate acetaldehyde-induced liver injury *via* mechanisms that promote glutathione depletion, ROS toxicity and lipid peroxidation[7-9] (Figure 1).

Thus, ethanol metabolism can lead to direct biochemical changes in hepatocytes, including cytotoxic metabolites, accumulation of ROS and lipid peroxidation. Importantly, all of these effects can further trigger complex pathological responses that eventually cause damage in the liver. Patterns involved in alcohol-induced liver injury include inflammation, different types of cell death (mainly apoptosis and necrosis), steatosis, fibrogenesis, and even liver regeneration (Figure 2).

Statistically, only about the 35% of ALD patients go on to develop ALD with liver fibrosis. Alcohol-induced damage in liver significantly increases the production of cytokines, chemokines, other soluble mediators and components of the innate immune system[10,11]. This pro-inflammatory environment causes the activation of hepatic stellate cells (HSCs) and myofibroblasts, increasing the production of extracellular matrix (ECM) proteins, which can subsequently induce fibrogenesis in the liver[12]. HSC is the main source of ECM proteins but also a critical target in alcoholic liver fibrosis. Acetaldehyde and adducts such as malondialdehyde (MDA) or 4-hydroxynonenal (4-HNE) directly affect HSC activation and collagen-I genes *via* different signalling cascades[13]. Another crucial mechanism of alcohol-promoting liver fibrosis is associated with endotoxin and immune responses. Studies have shown correlation between alcohol administration, endotoxin in blood and KCs[14]. In the intestine, alcohol impairs tight junctions (TJs) - increasing gut permeability between epithelial cells, thus allowing the gut-derived bacterial endotoxin, lipopolysaccharide (LPS), to enter the liver *via* the portal vein[15]. It is common to see increased levels of serum LPS in ALD patients. KCs, the principal immune cells in the liver, are involved in this process. Several studies have shown that increased LPS levels induced by alcohol stimulate KCs to generate ROS and cytokines. These inflammatory mediators subsequently activate HSCs *via* a Toll-like receptor 4 (TLR4) signalling pathway, which eventually results in enhanced, chronic production of ECM proteins - and promotion of fibrogenesis[16,17]. Additionally, HSCs are also enriched with TLR4 that directly bind, and thus activate through LPS signalling[18]. To summarize, alcohol-stimulated liver fibrosis is a result of a robust immune response involving many types of liver cells and different signal transduction pathways. Fibrosis can develop into alcoholic cirrhosis, which is an advanced stage of liver fibrosis (occurring in 8%-20% of heavy drinkers) - this event is a significant risk factor for HCC. Such pathophysiological transitions will certainly reveal unique mechanisms, requiring more detailed studies and more realistic models[19,20].

HISTORY OF EXPERIMENTAL MODELS

The use of animals as models for scientific study is

a very old practice of human civilization. Acquiring knowledge and experience from his predecessors, Galen of Pergamum (2nd century BC), a Roman physician, greatly improved techniques for dissection and vivisection of animals, and further used them to study cardiovascular and neural anatomy extensively[21].

However, landmark findings in anatomy and physiology in ancient times were largely based on observation, inference and extrapolation of animal physiology to humans.

A Flemish anatomist, Vesalius (1514-1564), a physician and surgeon, was also a pioneer in animal modelling. He compared the similarity and differences between human body and other animal species, overturning the work of Galen - dogma which held for nearly 2000 years. He also recognized the value of animal experiment in teaching and performed vivisection of animals for medical students at his courses. Among the list of new, animal experimentalists, were scholars such as William Harvey (1578-1657). Using results from elegant and sophisticated experiments on live animals, Harvey published his revolutionary work *De Motu Cordis* in 1628, in which he described the anatomic and functional properties of the heart and vascular system from many species with remarkable accuracy[22,23].

The 20th century has witnessed unprecedented advances in biological and medical science. Innovations such as the invention of antibiotics, new diagnostic methods and surgical techniques, chemo- and radiotherapy for cancer, and improved vaccination. Saving millions of lives and significantly increased the average life expectancy. In the past few decades, the use of animal modelling increased dramatically - further supporting the development of medical science. Currently, animal species (model organisms) frequently used in laboratories include: rodents (mouse and rat), zebrafish, swine, rhesus, guinea pig, rabbit, cat, and dog. However it is mammalian rodent models that are the most frequently used - several important advantages: (1) Rodents are highly-resistant to successive in-breeding, with less genetic variability between individual animals (and generations); (2) Their short lifespan and a fast rate of reproduction allows more rapid accumulation of data; (3) Rodents are small in size and easy to handle for most experimental procedures; and (4) Costs are low per animal in terms of initial purchase cost, housing and maintenance. Altogether, rodents provide a model system for study of alcohol effects on mammalian physiology, are amenable to a tremendous array of experimental questions, and are highly-efficient in both time and budget.

Transgenics has become an important tool for generating animal models of human disease. Transgenics involves the addition of foreign genetic information (nucleic acids) to animals, often for specific inhibition of endogenous gene expression. However, despite the generation of several transgenic and knockout models, the development of relevant models has theoretical and technical challenges. Indeed, many ALD-associated genes of interest have not been fully identified and gene addition or inactivation can yield inconclusive results. Some models relevant to ALD are transgenic mice for human CYP2E1 and $p47^{phox}$ NADPH oxidase-deficient mice[24].

CURRENT EXPERIMENTAL MODELS OF ALD

Early attempts of studying ALD with animal models began in the 1950s - using primarily rodents (mice, rats, hamsters, guinea pigs), and primates. An early study using six animal species in parallel was designed to detect their voluntary consumption of alcohol[25]. The data interestingly suggested that golden hamster had a clear preference for alcohol solution (about 88% of their total liquid intake amount), while all other species significantly prefer water over alcohol (with rabbits as the only exception that consumed both drinks at comparable levels). In another study, baboons receiving alcohol-containing diet for 3-4 years, all developed severe hepatic injury (liver fibrosis or cirrhosis), which closely resembled all the pathological stages of human ALD. Thus primates are considered an ideal animal model of studying ALD[26]. However, ethical issues, and the now very tight regulatory controls on the use of primates, as well as high cost and time, prevent the use of primates for the study of ALD in most laboratories. Thus, although rodents (mainly mice and rats), are still the preferred animal species to mimic ALD in human, such models fail to display the complete disease spectrum of human ALD[27,28].

Various hypotheses have been proposed to explain the disparity in liver injury between human and rodents after ethanol exposure. Notably, most rodents have a natural aversion to alcohol and tend to consume ethanol only for calories rather than for craving. In addition, the catabolic rate in rodents is 5 times faster than in humans[29]. These characteristics lead to less damage in rodents, after alcohol exposure, than humans. In addition to effects of alcohol metabolism, difference in the innate immune systems must be carefully considered as immune responses and the pattern of inflammation all play a critical role in the pathology of ALD. For example, the balance between neutrophils and lymphocytes in the blood differs greatly in mice and humans: neutrophils account for 50%-70% of total leukocytes in human blood (10%-25% in mice); whereas lymphocytes comprise 75%-90% of leukocytes in mouse blood, compared with 30%-50% in humans[30]. The physio-/pathophysiological consequences of these differences remain largely unknown. Studies have however demonstrated that mice exhibit greater resistance against endotoxin-induced inflammation, thus experiments usually require a higher ethanol challenge to create the extent of damage comparable with humans[31].

The response to alcohol and the development of

ALD in humans varies considerably between individuals, and ethnic groups. Besides familiar risk factors such as age, diet, and smoking - genetic differences among individuals or ethnic groups are also of great significance. A genotyping study in Asian populations, showed that approximately 50% of Chinese and Taiwanese have low ALDH activity compared with Western nations, due to different genetic polymorphisms in the ALDH2*2 allele[32]. Similarly, diverse outcomes after receiving alcohol application are also seen in different rodent strains. In one case study, mice from 14 commercially acquired inbred strains received ethanol diet (up to 27 mg/kg body weight per day) with an intragastric enteral feeding model for 28 d; all strains exhibited comparable caloric intake and blood alcohol concentration (BAC) levels after the feeding[33]. Interestingly, mice from strains NZW/LacJ, C57BL/10J, FVB/NJ, BALB/cByJ showed severe liver injury compared with mice from WSB/EiJ, PWD/PHJ, C3H/HeJ, AKR/J strains. These results indicated that the marked difference in sensitivity to alcoholic liver injury, was strongly dependent on the mouse strain. Thus, careful consideration of the strain/ desired traits and experimental outcomes should be undertaken when considering an experimental model of ALD. In another study, rats from three different strains (Long Evans, Sprague Dawley, Fisher 344) were fed with an isocaloric liquid diet containing ethanol (equivalent to 37% of the total caloric intake) for 8 wk[34]. All three strains exhibited equally increased BAC, but significantly varied in body weight, alanine aminotransferase (ALT), triglycerides and cholesterol levels. Notable differences were also found in proinflammatory parameters including TNF-α, IL-6 and interleukin-1beta (IL-1β), indicating different degrees of hepatic inflammation after alcohol administration among the three strains. Moreover, dramatic variations were detected between the three strains in some critical enzymes of ethanol metabolism including ADH1, ADH2, AHD3, Catalase, and CYP2E1, suggesting the inequality of alcoholic liver damage may be partly due to different rates of ethanol metabolism between all strains.

Numerous models employing rodent animals have been established to investigate the effects of acute and chronic alcohol exposure on the initiation and progression of ALD (Table 1). To achieve the desired animal model of alcohol disorder, consideration should be given to such factors as amount, route and duration of ethanol given to the animal, and, as mentioned above, the particular animal strain. The amount and duration of ethanol applied to the animal should be sufficient to maintain both a consistently high level of BAC, and long enough to create an acute or chronic injury. In addition, the route of alcohol delivery also plays a critical role in determining the effect of a model. Studies of alcohol administration using vapour inhalation, intravenous, or intraperitoneal injection have been widely reported. These approaches can overcome the unwillingness to imbibe alcoholic beverage in most rodents, and accurately control the amount of ethanol absorbed. However, despite the high level of BAC in rats and mice, these models fail to mimic the natural alcohol "drinking" *i.e., via* the oral route, ingestion and subsequent metabolic processes in humans. As a result, such models are more frequently employed in the field of addiction and behavioural studies, rather than in studies related to alcoholic-induced liver damage[35-37].

Focusing on the effects of alcohol on the GI and liver, rodent models of oral alcohol ingestion have been developed and extensively utilized. By engaging the rodents in "voluntary drinking", these approaches largely replicate the overall process of human drinking habits as well as the general effects of alcohol on liver and intestine. Patterns of alcohol exposure in humans include both short-/ and long-term drinking. Whilst acute liver injury occurs even after 4-5 acute or binge episodes, within a period of several hours, chronic damage accumulates over many years of continuous ethanol consumption. In rodents, gastric intubation is commonly used to administer ethanol dosages of 4-6 g/kg body weight to induce acute hepatic injury. One study using this approach, followed by LPS injection, demonstrated that acute ethanol administration exacerbated hepatic damage caused by endotoxin[38]. Compared with acute animal models using only one or a few gavages, chronic models of alcohol feeding typically last 4-12 wk, usually with a specially designed diet. As acute and chronic alcoholic injury in the liver share remarkable overlap in their pathology, an increasing number of studies combine both models (chronic plus binge model), to better emulate current drinking patterns in humans.

Lieber-DeCarli liquid diet

One of the earliest and most successful diets designed specifically for studying the effect of alcohol consumption *in vivo* is the Lieber-DeCarli liquid diet. It was first introduced by Lieber *et al*[39] in 1963 in response to the need for a more accurate *in vivo* research model for ALD. In a previous study, rats received a 15% (v/v) solution of ethanol instead of drinking water for 177 d. Afterwards, no obvious liver injury (including steatosis and fibrosis) were found in the ethanol-only feeding groups but mainly in groups fed also with a diet of nutritional deficiency[40]. The investigators suggested that the damage to liver after alcohol consumption was a consequence of malnutrition. Thus, it was widely accepted that alcohol alone has no hepatotoxic risk.

In 1960s, in a series of studies, Lieber *et al*[1,41-43] designed a diet containing ethanol and other nutritional components. They demonstrated that when rats received adequate diet, the absorption of alcohol was insufficient to cause significant liver damage, due to their natural aversion to ethanol. This aversion can be overcome when rats had access only to an ethanol-containing liquid diet formula but with no other food or drink. In this case, the daily intake of ethanol in rats can reach 12-18 g/kg, which was two to three times more than that achieved from drinking the ethanol-only

Table 1 Comparison of experimental models of alcoholic liver disease

Models	Animal model	Characteristics	Advantages and disadvantages
Lieber-DeCarli liquid diet[27,28]	Rat/mice	Chronic ethanol feeding (4-12 wk)	Easy to perform Marked elevation of ALT Short term feeding with no mortality rate No liver fibrosis
	Rat/mice	Chronic ethanol feeding + single/multiple binges (4-6 wk)	Easy to perform Marked elevation of ALT and marked steatosis Long term feeding + multiple binges with a high mortality rate No liver fibrosis
	Rat/mice	+ Second hit: DEN, LPS, CCl_4, APAP (4-12 wk)	Easy to perform Marked elevation of ALT and marked steatosis Long term feeding + multiple binges + injection with a high mortality rate Liver fibrosis
Ethanol *ad libitum* feeding[27,28]	Mice	Oral alcohol in drinking water (10 d/1-2 wk)	Easy to perform Minimal elevation of ALT and mild steatosis Short-or long-term feeding with no mortality rate No liver fibrosis
The Tsukamoto-French model[27,28]	Rat/mice	Intragastric infusion (2-3 mo)	Difficult to perform Requirement for intensive medical care Marked elevation of ALT and steatosis Long-term feeding with a high mortality rate Mild liver fibrosis
The NIAA model[47]	Mice	LDE + single ethanol binge	Cost and time efficient High blood alcohol levels Liver injury Inflammation Fatty liver
	Rat /mice	LDE + 3 ethanol binges	Cost and time efficient Increased blood alcohol levels Augmented liver injury Increases in ERK1/2
Ethanol + CCl_4 treatment[106]	Mice	4% ethanol liquid diet + 2 times IP CCl_4 injection per week (8 wk)	Easy to perform Toxic components Elevated acetaldehyde levels Liver fibrosis

Lieber-DeCarli liquid diet with different variants, ethanol *ad libitum* feeding and the Tsukamoto-French and the NIAA model. ALT: Alcoholic liver disease; DEN: Diethylnitrosamine; LPS: Lipopolysaccharide; CCl_4: Carbon tetrachloride; APAP: Acetaminophen; LDE: Lieber-De Carli ethanol diet; IP: Intraperitoneal.

solution. Notably, higher BACs were also observed (100 to 150 mg/dL)[39,44,45]. Using this approach, in seminal work, Lieber *et al*[46] observed significant steatosis in the liver and concluded that alcohol alone is a pathological factor that can induce liver disease. In the next decade, they further detected that this process was influenced by other factors such as gender, dietary fat, the essential nutrients methionine and choline, and vitamin A. These findings opened a new era for ALD research. The liquid diet formula in these studies later became known as the Lieber-DeCarli ethanol (LDE) and Lieber-DeCarli control (LDC) diets, and are now a standard experimental model for the study of ALD[47].

The Lieber-DeCarli diet is an isocalorically-controlled liquid diet in that the total caloric content (0.6-1.0 cal/mL) in the diet remains unchanged, while specific components vary to serve different groups and experimental objectives. The LDC diet, often used for pair-fed control groups, is formulated from several key parts of nutrition: Casein (consisting of methionine and cystine), contributes 18% of total calories; fat, derived from olive and corn oils, makes up 35% of total calories; fat-soluble vitamins (A, D, E, K) and water-soluble vitamin B_{12}, minerals and fiber; the remaining formula (dextrin and maltose mixture) provided the majority of energy (47% of the total calories)[42,44,45]. In the ethanol-containing formula (LDE diet), an amount equal to 36% of total calories of the dextrin and maltose mixture is removed and replaced by isocalorically measured alcohol[42,44,45]. Of note, when applying the LDE diet, the amount of ethanol in the diet should be increased gradually during a primer period of approximate five days, in which the concentration of ethanol increases from zero to the final concentration (in most studies 50 g/L). This short priming period allows the animal to adapt to the ethanol-contained diet gradually, thus ensuring the effect of

subsequent formal feeding.

The feeding period using the LDE model usually varies from 4 wk to 12 wk in mouse and 1-9 mo in rat[48-58]. In most studies, there was a marked elevation of serum ALT and aspartate aminotransferase (AST), with a 6-fold average increase in hepatic triglycerides[46]. Moreover, varying degrees of hepatic steatosis was widely observed in the experimental group. However, no other major hepatic pathological changes, particularly severe forms such as fibrosis, have been reported with the LDE diet feeding model, including long feeding periods of up to nine months in rat[58]. A possible explanation for this limitation is that the LDE diet can only maintain a relatively low BAC in animals, compared with other feeding models such as patients with advanced stage ALD[27].

Many attempts have since been made to elevate the effect of LDE diet - to induce more sever forms of liver injury, in order to overcome its limitations. The general aim would be better mimicking the pathogenesis of ALD in human, in particular its advanced forms. It is not rare for physicians to observe that advanced alcoholic hepatitis (AH) occurs in patients who have a long history of chronic drinking, but also have one or several more recent heavy binge drinking experiences[59,60]. In this context, the chronic-binge ethanol feeding rodents model, which combines a chronic feeding period using LDC diet and one or multiple binges has been introduced and widely accepted[28]. To perform this model, the LDE diet (5% v/v) is given for four weeks to create chronic liver injury as described above. In addition, single or multiple binges are applied by intragastric gavage twice a week during the chronic feeding phase. For gavage, absolute ethanol is diluted to 32% (v/v) in tap water and the recommended dosage of alcohol is calculated at 5 g/kg body weight[61]. It has been reported that in this model, the BAC in rodents can reach 200 to 500 mg/dL, with remarkable elevation of transaminases in serum and significant steatosis in liver[60,62].

Besides binge drinking, other hepatotoxins can subsequently be added during the chronic feeding phase of the LDE diet to provide a "second hit" and increase liver damage, such as: diethylnitrosamine (DEN), LPS, carbon tetrachloride (CCl_4), or acetaminophen (APAP)[63-66]. These studies have expanded the use of the LDC diet and provided useful insight into the effects of ethanol on the initiation and progression of severe liver injuries such as cirrhosis or HCC.

Ethanol ad libitum feeding

The *ad libitum* alcohol feeding model was one of the earliest animal models used for ALD study in rodents[40]. Alcohol is administrated in tap water serving as the only source of drinking water for animals, whilst animals have free access to a standard rodent chow diet. The *ad libitum* feeding model is simple to perform, and easy to manipulate the precise concentration of ethanol in the water. The "voluntary" consumption of alcohol with the normal diet mimics the typical drinking pattern in humans; *i.e.,* intermittent alcohol use with ordinary food intake. Partly due to its great flexibility, protocols used in different studies have varied considerably. The concentration of ethanol solution varied from 10%-40% (v/v), and the period of alcohol administration used in different groups can range from 8 wk, and up to 70 wk, without significant mortality[67-70]. In most studies, the *ad libitum* feeding model is sufficient to induce liver damage with clear steatosis and elevation of ALT and AST, but without more advanced lesions of fibrosis or cirrhosis[68,70,71].

Despite its convenience, *ad libitum* feeding method has limitations compared to other ALD animal models. Noticeably, rodents show strong natural aversion to alcohol, as they tend to drink less ethanol than expected[25]; whilst the rate of alcohol metabolism in rodents is much faster than in humans. These factors prevent the rats or mice from achieving high BAC consistently after chronic ethanol *ad libitum* feeding. The relatively low levels of BAC may be one of the main reasons for some misconceptions of early ALD studies[40]. Mice receiving ethanol *ad libitum* of 20% (v/v) alcohol solution for eight weeks reached BACs between 50-70 mg/dL[67]. Whereas only moderate increase in serum ethanol (to 90 mg/dL) was reported in an early study, where rats were given 40% ethanol solution daily, up to 29 wk[68]. High BAC (up to 150 mg/dL) was also reported indicating wide variations of BAC after ethanol *ad libitum* application[72]. Unlike the LDC diet, which is a nutrition-balanced diet ensuring equal calories in the presence or absence of alcohol content, it is very challenging to evaluate the nutritional status when applying *ad libitum* feeding.

Although the ethanol *ad libitum* feeding model is useful as a "standalone" model of mild alcoholic liver injury, an increasing number of studies combined it with other stressors to stimulate inflammation, fibrosis or HCC in liver. Noticeably, consistent long-term feeding can be substituted by *ad libitum* feeding for long-term periods of time due to its low mortality rate. In one study, 15 different mouse strains were tested with ethanol *ad libitum* from 8 wk to 78 wk[69]. More recently, secondary factors have been introduced including other dietary models such as the high-fat diet and high-fructose diet, to evaluate whether such dietary factors potentiate chronic alcohol-induced liver injury[70,73]. Other studies combining ethanol *ad libitum* feeding model with well-known hepatic stressors like DEN, diallyl disulphide (DADS), phenobarbital, and CCl_4 - typically induced advanced liver injury, including inflammation, fibrosis and HCC[67,72,74,75]. In summary, ethanol *ad libitum* feeding is a simple and reproducible approach to introduce alcohol in rodents, is amenable to the introduction of secondary hits - and is thus widely used by many laboratories for ALD study.

The Tsukamoto-French intragastric infusion model

Although oral alcohol administration including *ad libitum* feeding and ethanol-containing LDC diet has proved a

convenient and effective way to apply alcohol in rodents, it has several limitations. Generally, the average BAC of rodents received oral alcohol administration is usually observed below 150 mg/dL, compared with human levels. Moreover, liver steatosis is the major pathological change in studies conducting oral ethanol application (without a second stressor), where no fibrosis or cirrhosis is found. To overcome these limitations, a new feeding model of direct infusion through a surgically implanted intragastric cannula was developed in 1984, also known as Tsukamoto-French (TF) model[76,77].

Compared with other feeding models of oral administration, the TF infusion model has several distinct advantages. By circumventing the natural aversion to alcohol that generally exists in rodent animals, the TF model removes the barrier on the amount of alcohol that is consumed by the animals. An early study employed liquid diet with alcohol (reaching as high as 49% of total calories) with 30-d infusion. Rats developed severe hepatic steatosis and focal necrosis with a high average BAC (216 mg/dL), and highly elevated ALT and AST levels[78]. More importantly, the TF model also allows easy manipulation of the food content in order to create the desired model of liver damage. When progressively increased ethanol intake (32%-47% of total calories), combined with high fat diet (25% of total calories as fat), fibrosis started to develop in rats within 30 d of feeding, and was observed in all animals after 120 d of feeding[79]. Furthermore, this group also showed that by adding carbonyl iron (0.25% w/v) into the high fat/ethanol-containing diet - by the end of 16 wk most mice developed fibrosis, to different extents, whilst 2 out of the 20 mice developed liver cirrhosis[80].

Even after only 4 wk of intragastric infusion, the average BAC in mouse experiment can reach as high as 300-350 mg/dL, and peak BACs above 400 mg/dL can occur. This reflects a substantially greater level of alcoholic intoxication, achieved by the TF infusion model, over other alcohol feeding regimes[81]. Altogether, in rodents the TF model produces a sequence of liver damage that closely resembles human ALD, *i.e.,* progressive steatosis, fibrosis, cirrhosis with focal necrosis and immune cell infiltration[82].

There are however several potential drawbacks of the TF model. First, the implantation of intragastric tube requires high technical and surgical competences in small animal handling and surgery. Extensive and stringent post-operative care is also essential as early contamination can increase mortality. In addition, the post-operative maintenance work can be a challenge, as the infusion cannula is usually kept *in situ* often for 2-3 mo. The open access nature of the cannula increases the possibility of infection and irritation that may affect the results or result in death. Therefore, animal health and welfare, physiological signs and any pathological changes demand close monitoring. These stringencies make the TF an expensive model that cannot be performed by all laboratories. However, rats with implanted cannula (TF model) and daily food infusion have been kept and maintained for as long as 6 months, indicating once achieved successfully, the intragastric infusion can be a reliable model for investigating experimental dietary conditions in ALD[83].

As a feeding model initially designed for studying ethanol intake in rodents, the TF model has actually produced results with more severe alcoholic liver injury than in other alcohol administration methods. Additionally, the TF model has also been employed in studies focusing on obesity-associated disorders such as non-alcoholic fatty liver disease (NAFLD)[84]. To sum up, the TF rodent model is an effective and reliable approach for ALD study as well as studies related to other metabolic complications associated with diet.

The National Institute on Alcohol Abuse and Alcoholism NIAA model

The group of Gao *et al*[28] developed a chronic-plus-binge alcohol feeding mouse model in 2013 (Table 1). This model mimics acute-on-chronic alcoholic liver injury in patients. The model consists of 5 d of adaptation to the liquid diet. Subsequently, mice are fed a LDE containing 5% (v/v) ethanol for 10 d. A single dose of ethanol (5 g/kg body weight) is given at day 11 and 9 h later animals are euthanased. This model specifically triggers high levels of alcohol in blood, liver injury, fatty liver and inflammation.

The NIAA model has since then been modified: A single binge (5 g/kg) or repeated intragastric infusions of alcohol (5 g/kg, 32% v/v, 3 doses, 12-h intervals) were added following chronic feeding with the LDE diet (5% v/v, 4-7 wk). The advantage of this modification is that the binge increases the neutrophil infiltration in mice[47].

COMPARISON OF HUMAN AND MURINE ALD

Although there are several mouse models of ALD, differences exist between human and mouse in mild and early forms of ALD.

In human ALD, serum liver function tests and liver histology analyses reveal high concentrations of the enzymes ALT and AST, steatosis, ballooning of hepatocytes, neutrophil infiltration and Mallory-Denk hyaline inclusions in the liver[28]. Nevertheless, mouse models of mild and early ALD do not reflect the observed human pathology at each stage.

The model of *ad libitum* feeding with the LDC ethanol diet in mice for 4 wk, results in only mild steatosis and minor elevation of serum ALT, with low-level inflammation[85-89]. Twelve weeks of stepwise feeding with the LDC diet containing ethanol shows fatty liver, but mild elevation of ALT in serum.

The TK model induces severe steatosis, mild liver inflammation and mild fibrosis through continuous intragastric feeding. This model is very useful for the study of ALD pathogenesis (Figure 2), but, as

mentioned, it is expensive, has technical limitations and requires intensive medical care[77,78,90,91].

Acute gavage of a single dose or multiple doses' of ethanol induces only hepatic steatosis with a slight elevation in serum ALT and AST enzymes[89,92-94]. Administration of various concentrations of ethanol in drinking water given as the only water source for longer-term periods has been shown to cause immune abnormalities and mild steatosis, but has little effect on serum ALT/ AST levels and liver inflammation[69,71].

STRATEGIES FOR THE FUTURE: HUMANIZED RODENT MODELS

The development of animal models of ALD has led to remarkable progress in the study of ALD over the last 6 decades. However, many of the models described have intrinsic weaknesses and do not fully recapitulate each stage and facet of human ALD. Following ingestion, ethanol is processed through the classical drug disposition routes: Absorption, Distribution, Metabolism and Excretion (ADME). Multiple factors and systems participate in this complex process and can affect, directly and indirectly, the pathogenesis and final outcome of ALD. Due to obvious species differences in physiology and pathology between rodents and humans, translation of results from rats or mice to humans is problematic. However, next generation experimental animals having certain features of human physiology are being developed that can better resemble the effects of disease in the human body.

The concept of "humanized rodent models" refers to mice or rats engrafted with functional human cells and tissues. Human cell and tissue types used in the development of humanized rodents include: Immune cells, hepatocytes, skin tissue, pancreatic islets, uterine endometrium, and neural cells[95]. Humanized liver in experimental animals has become an attractive target due to the high regenerative potential of the liver. Early attempts using isolated hepatocytes in rodent models in the 1970s. shifted gradually from ectopic transplantation to in-liver engraftment[96-100]. However, one major difficulty preventing these models from becoming effective therapies, is that numbers of functional repopulated hepatocytes after transplantation are still insufficient[101]. In the 1990s, breakthroughs came with the introduction of several transgenic mouse lines. The first model was developed by Sandgren *et al*[102] with exclusive expression of a protease, urokinase plasminogen activator (uPA) in hepatocytes. Overturf *et al*[103] developed a mouse model which targeted disruption of fumarylacetoacetate hydrolase (Fah) - regulated by 2-cyclohexane-1,3-dione (NTBC). With their extraordinary capacity for repopulation of hepatocytes, the engraftment efficiency of transplanted hepatocytes in transgenic models was substantially enhanced compared with normal mice[104].

Humanized animal models offer a novel approach, with tremendous opportunity to explore ALD, and to produce more reliable and robust data, that will ultimately be easier to translate from bench to bedside. For example, Cederbaum *et al*[105] employed humanized CYP2E1 knock-in mice and discovered significantly elevated liver damage in this group after 3 wk of ethanol feeding, suggesting a major role of CYP2E1 in alcoholic steatosis and oxidant stress. However, there is still a long way before humanized rodent models can become a single, standard model for ALD study. Major challenges include the residual host innate immune system, as well as impaired differentiation and maturation of the human immune cell population due to, for example, differences between human and mouse cytokines. However, these drawbacks will not prevent humanized animal model from being viewed as a promising strategy for the future.

CONCLUSION

Alcoholism is now recognized as a major global health issue. Health and socio-economic consequences of alcohol consumption represent a heavy burden world-wide. Although significant progress has been made in gaining better knowledge on the mechanisms and pathology of ALD, many features of ALD are unknown, and require further investigation, ideally with animal models that more effectively mimic human ALD.

Nonetheless, the development of ALD models in rodent has also undergone a significant evolution in terms of representing different stages of human ALD. The early *ad libitum* model revealed liver damage after alcohol administration but have the major limitation of natural aversion in rodent. By adding isocaloric ethanol into the diet to keep nutritional balance, the development of the LDC diet successfully overcame the aversion issue and brought the study of ALD into a new era. The TF model then allowed more control of ethanol intake - effectively increasing liver damage following large amount of alcohol infusion. However, current ALD animal models fail to replicate the all-round spectrum of ALD in patients, particularly ALD in advanced stages. As mentioned, 20%-40% of heavy drinkers tend to develop ALD with severe alcoholic hepatitis, liver fibrosis and cirrhosis or even HCC - after 10 years of excessive alcohol consumption. In contrast, the major change in rodent after ethanol-only application with all models is restricted to hepatic steatosis, even with long-term feeding. Importantly, fibrosis or cirrhosis only appears when secondary insults to the liver have been employed.

In the future, an ideal model of ALD in rodent would effectively mimic, step-wise, each stage of how alcohol adversely affects the liver in humans. Key facets of such a model would address processes such as: Ethanol metabolism/ ADME, oxidative stress, ROS production and immune system activation. These are crucial events particularly in advanced fibrotic liver disease. Presently, rodent models remain useful tools for us to improve our knowledge of ALD. Although differences

in the degree and stages of alcoholic liver injury exist among rats, mice and humans' - data acquisition and translational relevance will be greatly enhanced with the development of new and improved animal models of ALD.

REFERENCES

1 **Lieber CS**, Jones DP, Decarli LM. Effects of prolonged ethanol intake: production of fatty liver despite adequate diets. *J Clin Invest* 1965; **44**: 1009-1021 [PMID: 14322019 DOI: 10.1172/JCI105200]
2 **Gao B**, Bataller R. Alcoholic liver disease: pathogenesis and new therapeutic targets. *Gastroenterology* 2011; **141**: 1572-1585 [PMID: 21920463 DOI: 10.1053/j.gastro.2011.09.002]
3 **Louvet A**, Mathurin P. Alcoholic liver disease: mechanisms of injury and targeted treatment. *Nat Rev Gastroenterol Hepatol* 2015; **12**: 231-242 [PMID: 25782093 DOI: 10.1038/nrgastro.2015.35]
4 **Lieber CS**. Metabolism of alcohol. *Clin Liver Dis* 2005; **9**: 1-35 [PMID: 15763227 DOI: 10.1016/j.cld.2004.10.005]
5 **Cederbaum AI**. Cytochrome P450 2E1-dependent oxidant stress and upregulation of anti-oxidant defense in liver cells. *J Gastroenterol Hepatol* 2006; **21** Suppl 3: S22-S25 [PMID: 16958665 DOI: 10.1111/j.1440-1746.2006.04595.x]
6 **Cederbaum AI**. Alcohol metabolism. *Clin Liver Dis* 2012; **16**: 667-685 [PMID: 23101976 DOI: 10.1016/j.cld.2012.08.002]
7 **Espina N**, Lima V, Lieber CS, Garro AJ. In vitro and in vivo inhibitory effect of ethanol and acetaldehyde on O6-methylguanine transferase. *Carcinogenesis* 1988; **9**: 761-766 [PMID: 3365837]
8 **Müller A**, Sies H. Role of alcohol dehydrogenase activity and the acetaldehyde in ethanol- induced ethane and pentane production by isolated perfused rat liver. *Biochem J* 1982; **206**: 153-156 [PMID: 6751324]
9 **Lieber CS**, Baraona E, Hernández-Muñoz R, Kubota S, Sato N, Kawano S, Matsumura T, Inatomi N. Impaired oxygen utilization. A new mechanism for the hepatotoxicity of ethanol in sub-human primates. *J Clin Invest* 1989; **83**: 1682-1690 [PMID: 2708529 DOI: 10.1172/JCI114068]
10 **Friedman SL**. Mechanisms of hepatic fibrogenesis. *Gastroenterology* 2008; **134**: 1655-1669 [PMID: 18471545 DOI: 10.1053/j.gastro.2008.03.003]
11 **Bataller R**, Brenner DA. Liver fibrosis. *J Clin Invest* 2005; **115**: 209-218 [PMID: 15690074 DOI: 10.1172/JCI24282]
12 **Cubero FJ**, Urtasun R, Nieto N. Alcohol and liver fibrosis. *Semin Liver Dis* 2009; **29**: 211-221 [PMID: 19387920 DOI: 10.1055/s-0029-1214376]
13 **Mello T**, Ceni E, Surrenti C, Galli A. Alcohol induced hepatic fibrosis: role of acetaldehyde. *Mol Aspects Med* 2008; **29**: 17-21 [PMID: 18164754 DOI: 10.1016/j.mam.2007.10.001]
14 **Thurman RG**, Bradford BU, Iimuro Y, Knecht KT, Connor HD, Adachi Y, Wall C, Arteel GE, Raleigh JA, Forman DT, Mason RP. Role of Kupffer cells, endotoxin and free radicals in hepatotoxicity due to prolonged alcohol consumption: studies in female and male rats. *J Nutr* 1997; **127**: 903S-906S [PMID: 9164260 DOI: 10.1093/jn/127.5.903S]
15 **Szabo G**, Bala S. Alcoholic liver disease and the gut-liver axis. *World J Gastroenterol* 2010; **16**: 1321-1329 [PMID: 20238398 DOI: 10.3748/wjg.v16.i11.1321]
16 **Seki E**, De Minicis S, Osterreicher CH, Kluwe J, Osawa Y, Brenner DA, Schwabe RF. TLR4 enhances TGF-beta signaling and hepatic fibrosis. *Nat Med* 2007; **13**: 1324-1332 [PMID: 17952090 DOI: 10.1038/nm1663]
17 **Jagavelu K**, Routray C, Shergill U, O'Hara SP, Faubion W, Shah VH. Endothelial cell toll-like receptor 4 regulates fibrosis-associated angiogenesis in the liver. *Hepatology* 2010; **52**: 590-601 [PMID: 20564354 DOI: 10.1002/hep.23739]
18 **Inokuchi S**, Tsukamoto H, Park E, Liu ZX, Brenner DA, Seki E. Toll-like receptor 4 mediates alcohol-induced steatohepatitis through bone marrow-derived and endogenous liver cells in mice. *Alcohol Clin Exp Res* 2011; **35**: 1509-1518 [PMID: 21463341 DOI: 10.1111/j.1530-0277.2011.01487.x]
19 **Morgan TR**, Mandayam S, Jamal MM. Alcohol and hepatocellular carcinoma. *Gastroenterology* 2004; **127**: S87-S96 [PMID: 15508108]
20 **McKillop IH**, Schrum LW. Role of alcohol in liver carcinogenesis. *Semin Liver Dis* 2009; **29**: 222-232 [PMID: 19387921 DOI: 10.1055/s-0029-1214377]
21 **Guerrini A**. Experimenting with Humans and Animals: From Galen to Animal Rights. Baltimore: Johns Hopkins University Press, 2003
22 **Gregory A**. Harvey's Heart: The Discovery of Blood Circulation. New York: Totem Books, 2001
23 **Shackelford J**. William Harvey and the Mechanics of the Heart. New York: Oxford University Press, 2003
24 **Butura A**, Nilsson K, Morgan K, Morgan TR, French SW, Johansson I, Schuppe-Koistinen I, Ingelman-Sundberg M. The impact of CYP2E1 on the development of alcoholic liver disease as studied in a transgenic mouse model. *J Hepatol* 2009; **50**: 572-583 [PMID: 19157621 DOI: 10.1016/j.jhep.2008.10.020]
25 **Arvola A**, Forsander O. Comparison between water and alcohol consumption in six animal species infree choice experiments. *Nature* 1961; **191**: 819-820 [PMID: 13684626]
26 **Lieber CS**, Leo MA, Mak KM, DeCarli LM, Sato S. Choline fails to prevent liver fibrosis in ethanol-fed baboons but causes toxicity. *Hepatology* 1985; **5**: 561-572 [PMID: 4018729]
27 **Brandon-Warner E**, Schrum LW, Schmidt CM, McKillop IH. Rodent models of alcoholic liver disease: of mice and men. *Alcohol* 2012; **46**: 715-725 [PMID: 22960051 DOI: 10.1016/j.alcohol.2012.08.004]
28 **Bertola A**, Mathews S, Ki SH, Wang H, Gao B. Mouse model of chronic and binge ethanol feeding (the NIAAA model). *Nat Protoc* 2013; **8**: 627-637 [PMID: 23449255 DOI: 10.1038/nprot.2013.032]
29 **Holmes RS**, Duley JA, Algar EM, Mather PB, Rout UK. Biochemical and genetic studies on enzymes of alcohol metabolism: the mouse as a model organism for human studies. *Alcohol Alcohol* 1986; **21**: 41-56 [PMID: 2937415]
30 **Mestas J**, Hughes CC. Of mice and not men: differences between mouse and human immunology. *J Immunol* 2004; **172**: 2731-2738 [PMID: 14978070]
31 **Copeland S**, Warren HS, Lowry SF, Calvano SE, Remick D; Inflammation and the Host Response to Injury Investigators. Acute inflammatory response to endotoxin in mice and humans. *Clin Diagn Lab Immunol* 2005; **12**: 60-67 [PMID: 15642986 DOI: 10.1128/CDLI.12.1.60-67.2005]
32 **Eng MY**, Luczak SE, Wall TL. ALDH2, ADH1B, and ADH1C genotypes in Asians: a literature review. *Alcohol Res Health* 2007; **30**: 22-27 [PMID: 17718397]
33 **Tsuchiya M**, Ji C, Kosyk O, Shymonyak S, Melnyk S, Kono H, Tryndyak V, Muskhelishvili L, Pogribny IP, Kaplowitz N, Rusyn I. Interstrain differences in liver injury and one-carbon metabolism in alcohol-fed mice. *Hepatology* 2012; **56**: 130-139 [PMID: 22307928 DOI: 10.1002/hep.25641]
34 **Denucci SM**, Tong M, Longato L, Lawton M, Setshedi M, Carlson RI, Wands JR, de la Monte SM. Rat strain differences in susceptibility to alcohol-induced chronic liver injury and hepatic insulin resistance. *Gastroenterol Res Pract* 2010; **2010**: pii:312790 [PMID: 20814553 DOI: 10.1155/2010/312790]
35 **DeNoble VJ**, Mele PC, Porter JH. Intravenous self-administration of pentobarbital and ethanol in rats. *Pharmacol Biochem Behav* 1985; **23**: 759-763 [PMID: 4080762]
36 **Zhang P**, Bagby GJ, Xie M, Stoltz DA, Summer WR, Nelson S. Acute ethanol intoxication inhibits neutrophil beta2-integrin expression in rats during endotoxemia. *Alcohol Clin Exp Res* 1998; **22**: 135-141 [PMID: 9514298]
37 **Slawecki CJ**, Somes C, Ehlers CL. Effects of prolonged ethanol exposure on neurophysiological measures during an associative learning paradigm. *Drug Alcohol Depend* 2000; **58**: 125-132 [PMID: 10669063]
38 **Enomoto N**, Ikejima K, Bradford B, Rivera C, Kono H, Brenner DA, Thurman RG. Alcohol causes both tolerance and sensitization of rat Kupffer cells via mechanisms dependent on endotoxin.

Gastroenterology 1998; **115**: 443-451 [PMID: 9679050]
39 **Lieber CS**, Jones DP, Medelson J, DeCarli LM. Fatty liver, hyperlipemia and hyperuricemia produced by prolonged alcohol consumption, despite adequate dietary intake. *Trans Assoc Am Physicians* 1963; **76**: 289-300
40 **Best CH**, Hartroft WS. Liver damage produced by feeding alcohol or sugar and its prevention by choline. *Br Med J* 1949; **2**: 1002-1006, pl [PMID: 15393035]
41 **Lieber CS**, DeCarli LM. Study of agents for the prevention of the fatty liver produced by prolonged alcohol intake. *Gastroenterology* 1966; **50**: 316-322 [PMID: 5948329]
42 **DeCarli LM**, Lieber CS. Fatty liver in the rat after prolonged intake of ethanol with a nutritionally adequate new liquid diet. *J Nutr* 1967; **91**: 331-336 [PMID: 6021815 DOI: 10.1093/jn/91.3_Suppl.331]
43 **Lieber CS**, DeCarli LM. Ethanol oxidation by hepatic microsomes: adaptive increase after ethanol feeding. *Science* 1968; **162**: 917-918 [PMID: 4386718]
44 **Lieber CS**, DeCarli LM. The feeding of alcohol in liquid diets: two decades of applications and 1982 update. *Alcohol Clin Exp Res* 1982; **6**: 523-531 [PMID: 6758624]
45 **Lieber CS**, DeCarli LM. Liquid diet technique of ethanol administration: 1989 update. *Alcohol Alcohol* 1989; **24**: 197-211 [PMID: 2667528]
46 **de la M Hall P**, Lieber CS, DeCarli LM, French SW, Lindros KO, Järveläinen H, Bode C, Parlesak A, Bode JC. Models of alcoholic liver disease in rodents: a critical evaluation. *Alcohol Clin Exp Res* 2001; **25**: 254S-261S [PMID: 11391080]
47 **Guo F**, Zheng K, Benedé-Ubieto R, Cubero FJ, Nevzorova YA. The Lieber-DeCarli Diet-A Flagship Model for Experimental Alcoholic Liver Disease. *Alcohol Clin Exp Res* 2018; **42**: 1828-1840 [PMID: 30025151 DOI: 10.1111/acer.13840]
48 **Nevzorova YA**, Cubero FJ, Hu W, Hao F, Haas U, Ramadori P, Gassler N, Hoss M, Strnad P, Zimmermann HW, Tacke F, Trautwein C, Liedtke C. Enhanced expression of c-myc in hepatocytes promotes initiation and progression of alcoholic liver disease. *J Hepatol* 2016; **64**: 628-640 [PMID: 26576483 DOI: 10.1016/j.jhep.2015.11.005]
49 **Tammen SA**, Dolnikowski GG, Ausman LM, Liu Z, Sauer J, Friso S, Choi SW. Aging and alcohol interact to alter hepatic DNA hydroxymethylation. *Alcohol Clin Exp Res* 2014; **38**: 2178-2185 [PMID: 25070523 DOI: 10.1111/acer.12477]
50 **Park JK**, Shao M, Kim MY, Baik SK, Cho MY, Utsumi T, Satoh A, Ouyang X, Chung C, Iwakiri Y. An endoplasmic reticulum protein, Nogo-B, facilitates alcoholic liver disease through regulation of kupffer cell polarization. *Hepatology* 2017; **65**: 1720-1734 [PMID: 28090670 DOI: 10.1002/hep.29051]
51 **Ambade A**, Satishchandran A, Gyongyosi B, Lowe P, Szabo G. Adult mouse model of early hepatocellular carcinoma promoted by alcoholic liver disease. *World J Gastroenterol* 2016; **22**: 4091-4108 [PMID: 27122661 DOI: 10.3748/wjg.v22.i16.4091]
52 **Alund AW**, Mercer KE, Pulliam CF, Suva LJ, Chen JR, Badger TM, Ronis MJ. Partial Protection by Dietary Antioxidants Against Ethanol-Induced Osteopenia and Changes in Bone Morphology in Female Mice. *Alcohol Clin Exp Res* 2017; **41**: 46-56 [PMID: 27987315 DOI: 10.1111/acer.13284]
53 **Bang CS**, Hong SH, Suk KT, Kim JB, Han SH, Sung H, Kim EJ, Kim MJ, Kim MY, Baik SK, Kim DJ. Effects of Korean Red Ginseng (Panax ginseng), urushiol (Rhus vernicifera Stokes), and probiotics (Lactobacillus rhamnosus R0011 and Lactobacillus acidophilus R0052) on the gut-liver axis of alcoholic liver disease. *J Ginseng Res*2014; **38**: 167-172 [PMID: 25378990 DOI: 10.1016/j.jgr.2014.04.002]
54 **Varghese J**, James JV, Sagi S, Chakraborty S, Sukumaran A, Ramakrishna B, Jacob M. Decreased hepatic iron in response to alcohol may contribute to alcohol-induced suppression of hepcidin. *Br J Nutr* 2016; **115**: 1978-1986 [PMID: 27080262 DOI: 10.1017/S0007114516001197]
55 **Sun Q**, Zhong W, Zhang W, Zhou Z. Defect of mitochondrial respiratory chain is a mechanism of ROS overproduction in a rat model of alcoholic liver disease: role of zinc deficiency. *Am J Physiol Gastrointest Liver Physiol* 2016; **310**: G205-G214 [PMID: 26585415 DOI: 10.1152/ajpgi.00270.2015]
56 **Okazaki S**, Nagoya S, Tateda K, Katada R, Mizuo K, Watanabe S, Yamashita T, Matsumoto H. Experimental rat model for alcohol-induced osteonecrosis of the femoral head. *Int J Exp Pathol* 2013; **94**: 312-319 [PMID: 24020403 DOI: 10.1111/iep.12035]
57 **Cubero FJ**, Nieto N. Ethanol and arachidonic acid synergize to activate Kupffer cells and modulate the fibrogenic response via tumor necrosis factor alpha, reduced glutathione, and transforming growth factor beta-dependent mechanisms. *Hepatology* 2008; **48**: 2027-2039 [PMID: 19003881 DOI: 10.1002/hep.22592]
58 **Leo MA**, Lieber CS. Hepatic fibrosis after long-term administration of ethanol and moderate vitamin A supplementation in the rat. *Hepatology* 1983; **3**: 1-11 [PMID: 6681608]
59 **Zakhari S**, Li TK. Determinants of alcohol use and abuse: Impact of quantity and frequency patterns on liver disease. *Hepatology* 2007; **46**: 2032-2039 [PMID: 18046720 DOI: 10.1002/hep.22010]
60 **Aroor AR**, Jackson DE, Shukla SD. Elevated activation of ERK1 and ERK2 accompany enhanced liver injury following alcohol binge in chronically ethanol-fed rats. *Alcohol Clin Exp Res* 2011; **35**: 2128-2138 [PMID: 21790671 DOI: 10.1111/j.1530-0277.2011.01577.x]
61 **Marhenke S**, Buitrago-Molina LE, Endig J, Orlik J, Schweitzer N, Klett S, Longerich T, Geffers R, Sánchez Muñoz A, Dorrell C, Katz SF, Lechel A, Weng H, Krech T, Lehmann U, Dooley S, Rudolph KL, Manns MP, Vogel A. p21 promotes sustained liver regeneration and hepatocarcinogenesis in chronic cholestatic liver injury. *Gut*2014; **63**: 1501-1512 [PMID: 24092862 DOI: 10.1136/gutjnl-2013-304829]
62 **Shukla SD**, Pruett SB, Szabo G, Arteel GE. Binge ethanol and liver: new molecular developments. *Alcohol Clin Exp Res* 2013; **37**: 550-557 [PMID: 23347137 DOI: 10.1111/acer.12011]
63 **Rafacho BP**, Stice CP, Liu C, Greenberg AS, Ausman LM, Wang XD. Inhibition of diethylnitrosamine-initiated alcohol-promoted hepatic inflammation and precancerous lesions by flavonoid luteolin is associated with increased sirtuin 1 activity in mice. *Hepatobiliary Surg Nutr* 2015; **4**: 124-134 [PMID: 26005679 DOI: 10.3978/j.issn.2304-3881.2014.08.06]
64 **Muñoz NM**, Katz LH, Shina JH, Gi YJ, Menon VK, Gagea M, Rashid A, Chen J, Mishra L. Generation of a mouse model of T-cell lymphoma based on chronic LPS challenge and TGF-β signaling disruption. *Genes Cancer* 2014; **5**: 348-352 [PMID: 25352951 DOI: 10.18632/genesandcancer.32]
65 **Karaca G**, Xie G, Moylan C, Swiderska-Syn M, Guy CD, Krüger L, Machado MV, Choi SS, Michelotti GA, Burkly LC, Diehl AM. Role of Fn14 in acute alcoholic steatohepatitis in mice. *Am J Physiol Gastrointest Liver Physiol* 2015; **308**: G325-G334 [PMID: 25524063 DOI: 10.1152/ajpgi.00429.2013]
66 **McCuskey RS**, Bethea NW, Wong J, McCuskey MK, Abril ER, Wang X, Ito Y, DeLeve LD. Ethanol binging exacerbates sinusoidal endothelial and parenchymal injury elicited by acetaminophen. *J Hepatol* 2005; **42**: 371-377 [PMID: 15710220 DOI: 10.1016/j.jhep.2004.11.033]
67 **Brandon-Warner E**, Walling TL, Schrum LW, McKillop IH. Chronic ethanol feeding accelerates hepatocellular carcinoma progression in a sex-dependent manner in a mouse model of hepatocarcinogenesis. *Alcohol Clin Exp Res* 2012; **36**: 641-653 [PMID: 22017344 DOI: 10.1111/j.1530-0277.2011.01660.x]
68 **Keegan A**, Martini R, Batey R. Ethanol-related liver injury in the rat: a model of steatosis, inflammation and pericentral fibrosis. *J Hepatol* 1995; **23**: 591-600 [PMID: 8583149]
69 **Cook RT**, Schlueter AJ, Coleman RA, Tygrett L, Ballas ZK, Jerrells TR, Nashelsky MB, Ray NB, Haugen TH, Waldschmidt TJ. Thymocytes, pre-B cells, and organ changes in a mouse model of chronic ethanol ingestion--absence of subset-specific glucocorticoid-induced immune cell loss. *Alcohol Clin Exp Res* 2007; **31**: 1746-1758 [PMID: 17681030 DOI: 10.1111/j.1530-0277.2007.00478.x]
70 **Song M**, Chen T, Prough RA, Cave MC, McClain CJ. Chronic Alcohol Consumption Causes Liver Injury in High-Fructose-Fed

Male Mice Through Enhanced Hepatic Inflammatory Response. *Alcohol Clin Exp Res* 2016; **40**: 518-528 [PMID: 26858005 DOI: 10.1111/acer.12994]
71 **Meadows GG**, Blank SE, Duncan DD. Influence of ethanol consumption on natural killer cell activity in mice. *Alcohol Clin Exp Res* 1989; **13**: 476-479 [PMID: 2679200]
72 **McCaskill ML**, Hottor HT, Sapkota M, Wyatt TA. Dietary diallyl disulfide supplementation attenuates ethanol-mediated pulmonary vitamin D speciate depletion in C57Bl/6 mice. *BMC Nutr* 2015; **1**: [PMID: 27536382 DOI: 10.1186/s40795-015-0012-z]
73 **Tan TC**, Crawford DH, Jaskowski LA, Subramaniam VN, Clouston AD, Crane DI, Bridle KR, Anderson GJ, Fletcher LM. Excess iron modulates endoplasmic reticulum stress-associated pathways in a mouse model of alcohol and high-fat diet-induced liver injury. *Lab Invest* 2013; **93**: 1295-1312 [PMID: 24126888 DOI: 10.1038/labinvest.2013.121]
74 **Abraham P**, Wilfred G, Ramakrishna B. Oxidative damage to the hepatocellular proteins after chronic ethanol intake in the rat. *Clin Chim Acta* 2002; **325**: 117-125 [PMID: 12367775]
75 **Chae HB**, Jang LC, Park SM, Son BR, Sung R, Choi JW. An experimental model of hepatic fibrosis induced by alcohol and CCl4: can the lipopolysaccharide prevent liver injury induced by alcohol and CCl4? *Taehan Kan Hakhoe Chi* 2002; **8**: 173-178 [PMID: 12499803]
76 **Tsukamoto H**, Reidelberger RD, French SW, Largman C. Long-term cannulation model for blood sampling and intragastric infusion in the rat. *Am J Physiol* 1984; **247**: R595-R599 [PMID: 6433728]
77 **Ueno A**, Lazaro R, Wang PY, Higashiyama R, Machida K, Tsukamoto H. Mouse intragastric infusion (iG) model. *Nat Protoc* 2012; **7**: 771-781 [PMID: 22461066 DOI: 10.1038/nprot.2012.014]
78 **Tsukamoto H**, French SW, Benson N, Delgado G, Rao GA, Larkin EC, Largman C. Severe and progressive steatosis and focal necrosis in rat liver induced by continuous intragastric infusion of ethanol and low fat diet. *Hepatology* 1985; **5**: 224-232 [PMID: 3979954]
79 **Tsukamoto H**, Towner SJ, Ciofalo LM, French SW. Ethanol-induced liver fibrosis in rats fed high fat diet. *Hepatology* 1986; **6**: 814-822 [PMID: 3758935]
80 **Tsukamoto H**, Horne W, Kamimura S, Niemelä O, Parkkila S, Ylä-Herttuala S, Brittenham GM. Experimental liver cirrhosis induced by alcohol and iron. *J Clin Invest* 1995; **96**: 620-630 [PMID: 7615836 DOI: 10.1172/JCI118077]
81 **Nanji AA**, French SW. Animal models of alcoholic liver disease--focus on the intragastric feeding model. *Alcohol Res Health* 2003; **27**: 325-330 [PMID: 15540804]
82 **French SW**. Intragastric ethanol infusion model for cellular and molecular studies of alcoholic liver disease. *J Biomed Sci* 2001; **8**: 20-27 [PMID: 11173972 DOI: 10.1159/000054009]
83 **Nanji AA**, Mendenhall CL, French SW. Beef fat prevents alcoholic liver disease in the rat. *Alcohol Clin Exp Res* 1989; **13**: 15-19 [PMID: 2646971]
84 **Deng QG**, She H, Cheng JH, French SW, Koop DR, Xiong S, Tsukamoto H. Steatohepatitis induced by intragastric overfeeding in mice. *Hepatology* 2005; **42**: 905-914 [PMID: 16175602 DOI: 10.1002/hep.20877]
85 **Cohen JI**, Roychowdhury S, McMullen MR, Stavitsky AB, Nagy LE. Complement and alcoholic liver disease: role of C1q in the pathogenesis of ethanol-induced liver injury in mice. *Gastroenterology* 2010; **139**: 664-674, 674.e1 [PMID: 20416309 DOI: 10.1053/j.gastro.2010.04.041]
86 **Mandrekar P**, Ambade A, Lim A, Szabo G, Catalano D. An essential role for monocyte chemoattractant protein-1 in alcoholic liver injury: regulation of proinflammatory cytokines and hepatic steatosis in mice. *Hepatology* 2011; **54**: 2185-2197 [PMID: 21826694 DOI: 10.1002/hep.24599]
87 **Hu M**, Wang F, Li X, Rogers CQ, Liang X, Finck BN, Mitra MS, Zhang R, Mitchell DA, You M. Regulation of hepatic lipin-1 by ethanol: role of AMP-activated protein kinase/sterol regulatory element-binding protein 1 signaling in mice. *Hepatology* 2012; **55**: 437-446 [PMID: 21953514 DOI: 10.1002/hep.24708]
88 **Liangpunsakul S**, Rahmini Y, Ross RA, Zhao Z, Xu Y, Crabb DW. Imipramine blocks ethanol-induced ASMase activation, ceramide generation, and PP2A activation, and ameliorates hepatic steatosis in ethanol-fed mice. *Am J Physiol Gastrointest Liver Physiol* 2012; **302**: G515-G523 [PMID: 22194417 DOI: 10.1152/ajpgi.00455.2011]
89 **Leung TM**, Lu Y, Yan W, Morón-Concepción JA, Ward SC, Ge X, Conde de la Rosa L, Nieto N. Argininosuccinate synthase conditions the response to acute and chronic ethanol-induced liver injury in mice. *Hepatology* 2012; **55**: 1596-1609 [PMID: 22213272 DOI: 10.1002/hep.25543]
90 **Xu J**, Lai KKY, Verlinsky A, Lugea A, French SW, Cooper MP, Ji C, Tsukamoto H. Synergistic steatohepatitis by moderate obesity and alcohol in mice despite increased adiponectin and p-AMPK. *J Hepatol* 2011; **55**: 673-682 [PMID: 21256905 DOI: 10.1016/j.jhep.2010.12.034]
91 **Kisseleva T**, Cong M, Paik Y, Scholten D, Jiang C, Benner C, Iwaisako K, Moore-Morris T, Scott B, Tsukamoto H, Evans SM, Dillmann W, Glass CK, Brenner DA. Myofibroblasts revert to an inactive phenotype during regression of liver fibrosis. *Proc Natl Acad Sci USA* 2012; **109**: 9448-9453 [PMID: 22566629 DOI: 10.1073/pnas.1201840109]
92 **Zhou Z**, Wang L, Song Z, Lambert JC, McClain CJ, Kang YJ. A critical involvement of oxidative stress in acute alcohol-induced hepatic TNF-alpha production. *Am J Pathol* 2003; **163**: 1137-1146 [PMID: 12937155]
93 **Beier JI**, Kaiser JP, Guo L, Martínez-Maldonado M, Arteel GE. Plasminogen activator inhibitor-1 deficient mice are protected from angiotensin II-induced fibrosis. *Arch Biochem Biophys* 2011; **510**: 19-26 [PMID: 21501583 DOI: 10.1016/j.abb.2011.04.001]
94 **Kao E**, Shinohara M, Feng M, Lau MY, Ji C. Human immunodeficiency virus protease inhibitors modulate Ca2+ homeostasis and potentiate alcoholic stress and injury in mice and primary mouse and human hepatocytes. *Hepatology* 2012; **56**: 594-604 [PMID: 22407670 DOI: 10.1002/hep.25702]
95 **Fujiwara S**. Humanized mice: A brief overview on their diverse applications in biomedical research. *J Cell Physiol* 2018; **233**: 2889-2901 [PMID: 28543438 DOI: 10.1002/jcp.26022]
96 **Matas AJ**, Sutherland DE, Steffes MW, Mauer SM, Sowe A, Simmons RL, Najarian JS. Hepatocellular transplantation for metabolic deficiencies: decrease of plasms bilirubin in Gunn rats. *Science* 1976; **192**: 892-894 [PMID: 818706]
97 **Jirtle RL**, Biles C, Michalopoulos G. Morphologic and histochemical analysis of hepatocytes transplanted into syngeneic hosts. *Am J Pathol* 1980; **101**: 115-126 [PMID: 6108719]
98 **Kusano M**, Mito M. Observations on the fine structure of long-survived isolated hepatocytes inoculated into rat spleen. *Gastroenterology* 1982; **82**: 616-628 [PMID: 7060884]
99 **Gupta S**, Chowdhury NR, Jagtiani R, Gustin K, Aragona E, Shafritz DA, Chowdhury JR, Burk RD. A novel system for transplantation of isolated hepatocytes utilizing HBsAg-producing transgenic donor cells. *Transplantation* 1990; **50**: 472-475 [PMID: 2402796]
100 **Ponder KP**, Gupta S, Leland F, Darlington G, Finegold M, DeMayo J, Ledley FD, Chowdhury JR, Woo SL. Mouse hepatocytes migrate to liver parenchyma and function indefinitely after intrasplenic transplantation. *Proc Natl Acad Sci USA* 1991; **88**: 1217-1221 [PMID: 1899924]
101 **Shafritz DA**, Oertel M. Model systems and experimental conditions that lead to effective repopulation of the liver by transplanted cells. *Int J Biochem Cell Biol*2011; **43**: 198-213 [PMID: 20080205 DOI: 10.1016/j.biocel.2010.01.013]
102 **Sandgren EP**, Palmiter RD, Heckel JL, Daugherty CC, Brinster RL, Degen JL. Complete hepatic regeneration after somatic deletion of an albumin-plasminogen activator transgene. *Cell* 1991; **66**: 245-256 [PMID: 1713128]
103 **Overturf K**, Al-Dhalimy M, Tanguay R, Brantly M, Ou CN, Finegold M, Grompe M. Hepatocytes corrected by gene therapy are selected in vivo in a murine model of hereditary tyrosinaemia type I. *Nat Genet* 1996; **12**: 266-273 [PMID: 8589717 DOI: 10.1038/ng0396-266]
104 **Rhim JA**, Sandgren EP, Degen JL, Palmiter RD, Brinster RL. Replacement of diseased mouse liver by hepatic cell transplantation.

Science 1994; **263**: 1149-1152 [PMID: 8108734]

105 **Lu Y**, Wu D, Wang X, Ward SC, Cederbaum AI. Chronic alcohol-induced liver injury and oxidant stress are decreased in cytochrome P4502E1 knockout mice and restored in humanized cytochrome P4502E1 knock-in mice. *Free Radic Biol Med* 2010; **49**: 1406-1416 [PMID: 20692331 DOI: 10.1016/j.freeradbiomed.2010.07.026]

106 **Kwon HJ**, Won YS, Park O, Chang B, Duryee MJ, Thiele GE, Matsumoto A, Singh S, Abdelmegeed MA, Song BJ, Kawamoto T, Vasiliou V, Thiele GM, Gao B. Aldehyde dehydrogenase 2 deficiency ameliorates alcoholic fatty liver but worsens liver inflammation and fibrosis in mice. *Hepatology* 2014; **60**: 146-157 [PMID: 24492981 DOI: 10.1002/hep.27036]

P- Reviewer: Ji G, Kim DJ **S- Editor**: Ma RY **L- Editor**: A
E- Editor: Huang Y

World Journal of Gastroenterology

Submit a Manuscript: http://www.f6publishing.com

World J Gastroenterol 2018 December 7; 24(45): 5076-5080

DOI: 10.3748/wjg.v24.i45.5076

ISSN 1007-9327 (print) ISSN 2219-2840 (online)

MINIREVIEWS

Montezuma's revenge - the sequel: The one-hundred year anniversary of the first description of "post-infectious" irritable bowel syndrome

Mark S Riddle, Patrick Connor, Chad K Porter

Mark S Riddle, Department of Preventive Medicine and Biostatistics, Uniformed Services University, Bethesda, MD 20814, United States

Patrick Connor, Military Enteric Disease Group, Department of Military Medicine, Royal Centre for Defence Medicine, Birmingham Research Park, Birmingham B15 2SQ, United Kingdom

Chad K Porter, Department of Enteric Diseases, Naval Medical Research Center, Silver Spring, MD 20910, United States

ORCID number: Mark S Riddle (0000-0002-0607-7880); Patrick Connor (0000-0001-7258-1690); Chad K Porter (0000-0001-5411-4159).

Author contributions: Riddle MS performed the majority of the writing; Porter CK provided input in writing the paper; Connor P provided input in writing the paper.

Conflict-of-interest statement: There is no conflict of interest associated with any of the author contributions in this manuscript.

Manuscript source: Unsolicited manuscript

Correspondence author to: Mark S Riddle, MD, Full Professor, Department of Preventive Medicine and Biostatistics, Uniformed Services University, 4301 Jones Bridge Rd, Bethesda, MD 20814, United States. Mark.riddle@usuhs.edu
Telephone: +1-301-2950777
Fax: +1-301-2959769

Received: July 12, 2018
Peer-review started: July 12, 2018
First decision: August 27, 2018
Revised: August 28, 2018
Accepted: October 5, 2018
Article in press: October 5, 2018
Published online: December 7, 2018

Abstract

One-hundred years have passed since the original description of the commonly described phenomenon of persistent abdominal symptoms being triggered by an acute enteric infection. This first account was generated out of astute observations by Sir Arthur Hurst in World War I. Additional descriptions followed from military and non-military practitioners adding the evidence which has transitioned this recognized condition from association to causation. While mechanistic understanding is an area of active pursuit, this historical accounting of a centuries progress highlights important advances and contributions of military medicine and scientists to advances benefiting global populations.

Key words: Post-infectious irritable bowel syndrome; Medical history; Military medicine; Gastroenteritis; Travelers' diarrhea; Functional gastrointestinal disorder; Bacterial diarrhea

Core tip: There are several reviews in the literature describing the clinical phenomenon of post-infectious irritable bowel syndrome including its history. However, this is the first review to consider the earliest description dating back nearly 100 years ago and describe the role of the individuals and context of discoveries that were

made, and the important contributions that military medicine has lended towards further understanding.

Riddle MS, Connor P, Porter CK. Montezuma's revenge - the sequel: The one-hundred year anniversary of the first description of "post-infectious" irritable bowel syndrome. *World J Gastroenterol* 2018; 24(45): 5076-5080 Available from: URL: http://www.wjgnet.com/1007-9327/full/v24/i45/5076.htm DOI: http://dx.doi.org/10.3748/wjg.v24.i45.5076

INTRODUCTION

"It takes good guts to be a good soldier"
-Anonymous Civil War Observer

This reflection, though lost in attribution, transcends centuries where it was likely first remarked to describe the necessary qualities of nerve and grit required for military service in the 19th century[1]. However, it is possible the original intent was due to the fact that in the Civil War (and conflicts immemorial) the success in battle may well have depended on one's gastrointestinal constitution as much as bravery. Wars were once lost by the frequent alimentary casualties which rendered mass numbers of troops ineffectual and, before the advent of antibiotics and intravenous and oral rehydration, would kill by the thousands[2,3].

But an even more transcendent meaning emerged decades later in 1918 where Sir Arthur Hurst first described the condition of frequently unexplainable chronic bowel problems well after a soldier's acute bout of dysentery had resolved[4]. Hurst, a British Physician and co-founder of the British Gastrointestinal Society, is recognized as a transformative and leading physician of the 20th century with an early career specializing in neurology where he made substantial contributions in understanding the etiology of War Neuroses during his appointment to the Royal Army Medical Corps in support of the Crimean War[5]. During duty assignments in Lemnos and Salonika, Hurst diagnosed and treated the broad range of ailments of ill and injured service members returning from the Gallipoli and Macedonia World War I battle fronts and methodically catalogued these observations in first and second editions of Medical Diseases of War[4]. In a section on Colitis and Irritability of the Colon following Dysentery of Chapter XII in the second edition, he recounts (p. 167):

"Patients who have recovered from an acute attack of dysentery frequently remain unfit for a considerable period, which may even extend to years. The symptoms are due to the chronic colitis, which may follow either amoebic or bacillary dysentery after the specific infection has died out…In most cases the patient suffers from alternating attacks of constipation and diarrhoea, the latter often being brought on by aperients taken for the relief of the former, or it may follow an indiscretion in diet or exposure to cold…The diarrhoea may only last for a few hours, or it may continue for two or three days, the attacks being separated by intervals of several weeks or months…Sometimes the attacks of diarrhoea cease to occur, but intractable constipation remains and the general symptoms persist, though in a lessened degree."

One can imagine that he thought these observations of persistent abdominal symptoms after an acute bout of dysentery were unusual and shared such accounts with his colleagues who were treating similar patients. Dr. Hurst goes on further to relay accounts from his colleague, Thomas G Morehead of the Royal College of Physicians of Ireland who was treating patients in Egypt from the Gallipoli front and made similar observations as follows:

"…severe abdominal distension developed from four to eight months after the patient had apparently recovered from an attack of dysentery. They complained of a feeling of fullness in the abdomen, with dyspnea and general dyspeptic symptoms. The bowels were regular, and nothing abnormal was found except enourmous tympanitic distension of the abdomen…"

These descriptions of non-ulcerative persistent abdominal symptoms spanning complaints of diarrhea, constipation, dyspepsia and bloating following an acute gastrointestinal infection are most likely the earliest written description of what we now regard to be post-infectious functional gastrointestinal disorders (FGD). This now expansively described phenomenon of incident FGDs after acute enteric infection has been detailed in a number of systematic reviews[6-8]. While there may have been alternative differential diagnoses including essential nutrient deficiencies, unmasking of organic bowel disease or chronic intestinal infections, the historical accounts from World War I indicate that patients with these symptoms were relatively common, had adequate intake of fresh fruits and vegetables (at least after returning home), lacked features of inflammatory bowel disease, and had cleared chronic infections (at least of amoeba). While the lack of detailed microbiological and endoscopic description leaves open the question of patho-etiology and association in Sir Arthur Hurst's account, the distinct characteristics of the "Post-dysenteric Irritable Colon Syndrome" describes features strikingly similar to the symptoms of PI FGD described today.

Following this earliest description of chronic gastrointestinal consequences of the Great War, a young Surgeon-Lieutenant physician epidemiologist in the Royal Navy, Gordon T. Stewart, detailed nearly 500 cases of hospital admitted acute and chronic amoebic and bacillary dysentery in service members serving in World War II[9]. In Stewart's 1950 paper in the British Medical Journal acute and chronic diarrheal and dysentery cases were

characterized with specific etiologies identified, treatment recorded, and follow-up at three months and beyond with repeated assessments for infectious etiologies associated with recurrent symptoms. An important contribution of this report was the thorough culture and microscopic work-ups for infections in addition to sigmoidoscopy for those with persistent infections. Twenty-nine of the 228 (12.7%) admitted to the Combined Services Hospital and 49 of the 246 (19.9%) patients treated at the Liverpool Tropical Diseases Centre were identified as having persistent colitis symptoms despite appropriate treatment and no evidence of persistent infection. Among the 49 persistent diarrheal cases followed in Liverpool, sigmoidoscopy was conducted with 27 showing no signs of overt inflammation and these were classified as "Functional Post-Dysenteric Colitis". The remaining 22 had evidence of inflammation (some with ulceration and bleeding) and evidence of persistent infection mucosal scrapings and were labeled "Ulcerative Post-Dysenteric Colitis". Treatments, including large doses of soluble and insoluble sulphonamides, penicillin, and chiniofon retention enemas yielded eventual improvement in all but 4 patients, who persisted with "idiopathic ulcerative colitis". Among the functional cases, the authors noted that the patients had a tendency towards concomitant neurotic and anxiety features and generally resolved over time but continued to persist indefinitely in a few.

In the intervening years, while the "functional irritable colon" patient was recognized as not-infrequent diagnosis, little original research was conducted until 1962, when Chaudhary and Truelove reported on a large case series of 130 patients with the "Irritable Colon Syndrome" being cared for at the Radcliff Infirmary at Oxford[10]. They observed that the condition was more predominant in women and first diagnosis occurred between 20 and 59 years of age, and over 60% reported symptoms being present for over a year (and more than 10 years in 24%). From their detailed description of quality, quantity and location of pain and associated bowel movement patterns they further classified these patients into two distinct groups: (1) A spastic colon group characterized by colonic pain and variable bowel habits with periodic constipation or diarrhea or both alternating, and (2) a painless diarrhea group defined by patients without pain but who had chronic diarrhea. While lacking adequate study design, the authors did comment upon possible predisposing causes based on extensive patient histories. Most notable was the observation that in 26% of patients' symptoms clearly started after a proven or presumptive episode of dysentery. Among those with "post-infective" irritable colon syndrome, a majority (63%) had resolved compared to only 29% of those cases which were not ascribed to follow a bout of infectious dysentery, suggesting a more favorable prognosis. Psychological co-morbidities were important factors in both post-dysentery and "idiopathic" cases.

Interestingly, it would be another three decades before the first study on post-infectious irritable bowel syndrome (PI-IBS) was published where an adequate control group was utilized to explore disease incidence and risk. In 1999, Rodríguez and Ruigómez utilized medical encounter data from the United Kingdom General Practice Research Database to conduct a retrospective cohort study among a population with a bacteriologically-confirmed gastroenteritis episode and a comparator population subsequently followed for incident irritable bowel syndrome[11]. Medical encounter data were augmented with practitioner case-diagnosis validation surveys. IBS was identified in 4% of subjects with bacterial gastroenteritis, 12-fold higher than the rate in the comparative population with no history of gastroenteritis in the preceding year.

In just the past 20 years, the scientific literature has greatly expanded with more than 30 independent studies in which exposed subjects with infectious gastroenteritis consistently demonstrate a 4-fold increase in the risk of IBS compared to unexposed subjects with the highest rates observed after protozoal infection (41.9%) compared to bacterial (13.9%) or viral etiologies (6.4%)[6]. Similar risk estimates have been reported after travelers' diarrhea[7], and the first modern epidemiological study defining PI-IBS among military travelers was reported in 2011 following acute infectious diarrhea episodes among United States troops deployed to Egypt and Turkey[12]. Features which appear to increase the risk include more severe disease, longer disease, female gender and psychological comorbidities, though not entirely consistently across the multiple studies[6]. Additionally, the syndrome tends to be more commonly associated with the diarrhea-predominant IBS phenotype.

Though the historical readings behind the centenary description of the origins of PI-IBS and studies of recent times may be of interest, we focus on the nature and challenges remaining in developing our understanding of etiology in the "functional" diseases as well as the sometimes limiting paradigm of Koch's postulates in ascertaining disease causality. Traditionally, Koch's postulates proved effective at establishing disease-pathogen relationships for acute illness but often falls short with more complex associations beyond one-pathogen, one-disease models[13,14]. An alternative paradigm is considered in Hill's criteria which includes strength of association, consistency of effect, specificity of effect, temporality, biological gradient or dose response, and biological plausibility to form the basis of an argument for causation[15]. For PI-IBS, strength, consistency, specificity, temporality and biological gradient are clearly evident. Where the field is focused and uncertainty remains, is in the area of biological plausibility. While intensive studies have explored the patho-etiological underpinning post-infectious IBS, unfortunately a unifying mechanism has not emerged. Rather there appears to be multiple mechanisms to disease progression including low-grade inflammation[16,17], microbiome dysbiosis[18], epithelial barrier dysfunction[19], and auto-immunity[20], bringing added complexity to potential treatment and preventive

solutions. Thus, while much as been learned over the 100 years since Hurst made his first observations, we are presently improved only in our ability to provide symptomatic therapies and an ability to put a name to the symptoms of an often frustrated patient. We remain without a diagnostic test, preventative or cure.

Finally, the appending of another contribution to the list of important discoveries and medical advancements by military medicine and science is noteworthy. Whether it be through the contributions of British Navy Captain James Lind in treating and preventing scurvy[21], advancements of anesthesia during the Civil War[22], development and use of mobile X-ray diagnostics in World War I by Marie Curie[23], use of intramedullary nails to help heal fractures by the German military medical services during World War II[24], pioneering contributions by Robert Phillips in the advancement of oral rehydration therapy after World War II[25], advances in use of frozen blood products[26] during the Viet Nam war which are currently used today in saving countless lives around the world, or the early aggressive use of trauma management techniques in Iraq and Afghanistan[27], many lives have been and continue to be saved throughout the world from these military lead medical advances. While the incalculable wastage of life and well-being that is attributed to armed conflict cannot be compared to the value of innovation that is often born out of necessity to retain dominance, the efforts to save and preserve life and limb by the many dedicated clinicians and researchers to their uniformed patients are laudable. Sir Arthur Hurst's astute inquiry and tireless dedication to his patients is also recognized and clearly led to further interest, investigation and advancement of understanding by those he mentored and taught.

CONCLUSION

As legend would tell, Montezuma II, was the 9th Aztec Emperor between 1502 to 1520 when the Spanish, led by Hernan Cortés, began the conquest of modern day Mexico in the early 16th century[28]. Montezuma, who had perhaps observed the powerful Spanish forces with guns and cannons and crossbows and knew that his forces would be a poor match, attempted strategic diplomacy and appeasement to the invading Conquistadors and invited them into the city-capitol, Tenochtitlan, to negotiate. However, relations would quickly sour with skirmishes between arriving Spanish reinforcements and accusations of betrayal eventually led to Cortés taking Montezuma prisoner. Plunder and chaos in Tenochtitlan ensued and in an effort by to quell the masses, Cortés had Montezuma address the crowds from the palace roof to which he was met with hurled stones and spears from his own people and died three days later of his wounds (though some claim that Cortés had him strangled). Reinforcements would arrive, and smallpox disease spread throughout the susceptible native population assuring the fall of the Aztec Empire in a few short months.

According to the tenets of Aztec religion, the soul went to one of three places after death: the sun, the underworld, or the lower sky[29]. Interestingly, souls of fallen warriors and women that died in childbirth would transform into hummingbirds that followed the sun on its journey through the sky. Aztec religion ascribed the emperors (called tlatoani, translated "Great Speaker") unique supernatural powers such as shape shifting, foreseeing the future, and even immortality where they were thought to take up life in the afterworld with abilities to have impact of the world they left. While there is no written documentation of any edict of revenge, a belief is held by some that Montezuma lives on and awaits the opportunity to come back to life to banish the invaders and rescue his loyal people[30]. Others attribute the persistent scourge of acute travelers' diarrhea among those visiting the lands of the Aztec as an enduring message sent by Montezuma to those visiting from other countries to think twice about ideas of colonization of foreign lands. While previously ascribed to the acute watery diarrhea so frequently encountered, perhaps Montezuma's full plan for revenge was designed to have some such visitors develop an enduring reminder that might live in their bowels for years after. Then again, this could all be a myth.

REFERENCES

1 **Bollet AJ.** Civil war medicine: Challenges and triumphs. Tuczon, Ariz: Galen Press; 2002
2 **Gear HS**. Hygiene Aspects of the El Alamein Victory. *Br Med J* 1944; **1**: 383-387 [PMID: 20785331]
3 **Connor P**, Farthing MJ. Travellers' diarrhoea: a military problem? *J R Army Med Corps* 1999; **145**: 95-101 [PMID: 10420348]
4 **Hurst AF**. Medical diseases of the war. London: E Arnold; 1918
5 **Jones E**. War neuroses and Arthur Hurst: a pioneering medical film about the treatment of psychiatric battle casualties. *J Hist Med Allied Sci* 2012; **67**: 345-373 [PMID: 21596724 DOI: 10.1093/jhmas/jrr015]
6 **Klem F**, Wadhwa A, Prokop LJ, Sundt WJ, Farrugia G, Camilleri M, Singh S, Grover M. Prevalence, Risk Factors, and Outcomes of Irritable Bowel Syndrome After Infectious Enteritis: A Systematic Review and Meta-analysis. *Gastroenterology* 2017; **152**: 1042-1054.e1 [PMID: 28069350 DOI: 10.1053/j.gastro.2016.12.039]
7 **Schwille-Kiuntke J**, Mazurak N, Enck P. Systematic review with meta-analysis: post-infectious irritable bowel syndrome after travellers' diarrhoea. *Aliment Pharmacol Ther* 2015; **41**: 1029-1037 [PMID: 25871571 DOI: 10.1111/apt.13199]
8 **Halvorson HA**, Schlett CD, Riddle MS. Postinfectious irritable bowel syndrome--a meta-analysis. *Am J Gastroenterol* 2006; **101**: 1894-1899; quiz 1942 [PMID: 16928253 DOI: 10.1111/j.1572-0241.2006.00654.x]
9 **Stewart GT**. Post-dysenteric colitis. *Br Med J* 1950; **1**: 405-409 [PMID: 15410136]
10 **Chaudhary NA**, Truelove SC. The irritable colon syndrome. A study of the clinical features, predisposing causes, and prognosis in 130 cases. *Q J Med* 1962; **31**: 307-322 [PMID: 13878459]
11 **Rodríguez LA**, Ruigómez A. Increased risk of irritable bowel syndrome after bacterial gastroenteritis: cohort study. *BMJ* 1999; **318**: 565-566 [PMID: 10037630]
12 **Trivedi KH**, Schlett CD, Tribble DR, Monteville MR, Sanders JW, Riddle MS. The impact of post-infectious functional gastrointestinal disorders and symptoms on the health-related quality of life of US military personnel returning from deployment to the Middle East.

Dig Dis Sci 2011; **56**: 3602-3609 [PMID: 21647652 DOI: 10.1007/s10620-011-1766-z]
13 **Evans AS**. Causation and disease: the Henle-Koch postulates revisited. *Yale J Biol Med* 1976; **49**: 175-195 [PMID: 782050]
14 **Marshall BJ**, Armstrong JA, McGechie DB, Glancy RJ. Attempt to fulfil Koch's postulates for pyloric Campylobacter. *Med J Aust* 1985; **142**: 436-439 [PMID: 3982345]
15 **Szklo M**. Epidemiology: beyond the basics. 2nd ed. Sudbury: Jones and Bartlett Publishers; 2007
16 **Gwee KA**, Collins SM, Read NW, Rajnakova A, Deng Y, Graham JC, McKendrick MW, Moochhala SM. Increased rectal mucosal expression of interleukin 1beta in recently acquired post-infectious irritable bowel syndrome. *Gut* 2003; **52**: 523-526 [PMID: 12631663]
17 **Spiller R**, Garsed K. Infection, inflammation, and the irritable bowel syndrome. *Dig Liver Dis* 2009; **41**: 844-849 [PMID: 19716778 DOI: 10.1016/j.dld.2009.07.007]
18 **Sundin J**, Rangel I, Fuentes S, Heikamp-de Jong I, Hultgren-Hörnquist E, de Vos WM, Brummer RJ. Altered faecal and mucosal microbial composition in post-infectious irritable bowel syndrome patients correlates with mucosal lymphocyte phenotypes and psychological distress. *Aliment Pharmacol Ther* 2015; **41**: 342-351 [PMID: 25521822 DOI: 10.1111/apt.13055]
19 **Jalanka-Tuovinen J**, Salojärvi J, Salonen A, Immonen O, Garsed K, Kelly FM, Zaitoun A, Palva A, Spiller RC, de Vos WM. Faecal microbiota composition and host-microbe cross-talk following gastroenteritis and in postinfectious irritable bowel syndrome. *Gut* 2014; **63**: 1737-1745 [PMID: 24310267 DOI: 10.1136/gutjnl-2013-305994]
20 **Pimentel M**, Morales W, Pokkunuri V, Brikos C, Kim SM, Kim SE, Triantafyllou K, Weitsman S, Marsh Z, Marsh E, Chua KS, Srinivasan S, Barlow GM, Chang C. Autoimmunity Links Vinculin to the Pathophysiology of Chronic Functional Bowel Changes Following Campylobacter jejuni Infection in a Rat Model. *Dig Dis Sci* 2015; **60**: 1195-1205 [PMID: 25424202 DOI: 10.1007/s10620-014-3435-5]
21 **Lind J**. A Treatise of the Scurvy. In three parts. Containing an inquiry into the nature, causes, and cure, of that disease. Edinburgh1753
22 **Weiss ED**. The second sacrifice: costly advances in medicine and surgery during the Civil War. *Yale J Biol Med* 2001; **74**: 169-177 [PMID: 11501713]
23 **Coppes-Zantinga AR**, Coppes MJ. Silhouette. Marie Curie's contributions to radiology during World War I. *Med Pediatr Oncol* 1998; **31**: 541-543 [PMID: 9835914]
24 **Pierach CA**. Give me a break: Gerhard Küntscher and his nail. *Perspect Biol Med* 2014; **57**: 361-373 [PMID: 25959350 DOI: 10.1353/pbm.2014.0021]
25 **Savarino SJ**. A legacy in 20th-century medicine: Robert Allan Phillips and the taming of cholera. *Clin Infect Dis* 2002; **35**: 713-720 [PMID: 12203169 DOI: 10.1086/342195]
26 **Henkelman S**, Noorman F, Badloe JF, Lagerberg JW. Utilization and quality of cryopreserved red blood cells in transfusion medicine. *Vox Sang* 2015; **108**: 103-112 [PMID: 25471135 DOI: 10.1111/vox.12218]
27 **Chatfield-Ball C**, Boyle P, Autier P, van Wees SH, Sullivan R. Lessons learned from the casualties of war: battlefield medicine and its implication for global trauma care. *J R Soc Med* 2015; **108**: 93-100 [PMID: 25792616 DOI: 10.1177/0141076815570923]
28 **Schulz E**. Montezuma II2018.
29 **Dwyer H**, Stout M, Stout M. Aztec history and culture. New York, NY: Gareth Stevens Pub, 2013
30 **Mikulska K**. Did the Aztec Tlatoani possess supernatural or divine powers? Available from: URL: http://www.mexicolore.co.uk/aztecs/home/did-aztec-rulers-possess-divine-powers2011

P- Reviewer: Dumitrascu DL, Thompson RR **S- Editor**: Wang XJ
L- Editor: A **E- Editor**: Huang Y

World Journal of Gastroenterology

Submit a Manuscript: http://www.f6publishing.com

World J Gastroenterol 2018 December 7; 24(45): 5081-5094

DOI: 10.3748/wjg.v24.i45.5081

ISSN 1007-9327 (print) ISSN 2219-2840 (online)

MINIREVIEWS

Multidisciplinary approach for post-liver transplant recurrence of hepatocellular carcinoma: A proposed management algorithm

Kin Pan Au, Kenneth Siu Ho Chok

Kin Pan Au, Department of Surgery, Queen Mary Hospital, Hong Kong, China

Kenneth Siu Ho Chok, Department of Surgery and State Key Laboratory for Liver Research, The University of Hong Kong, Hong Kong, China

ORCID number: Kin Pan Au (0000-0002-7138-9805); Kenneth Siu Ho Chok (0000-0001-7921-3807).

Author contributions: Chok KSH proposed the study; Au KP and Chok KSH conducted the literature review and wrote up the manuscript.

Conflict-of-interest statement: None of the authors has any conflict of interest.

Manuscript source: Invited manuscript

Correspondence author to: Kenneth Siu Ho Chok, FRCS (Ed), Associate Professor, Department of Surgery, The University of Hong Kong, 102 Pok Fu Lam Road, Hong Kong, China. chok6275@hku.hk
Telephone: +86-852-22553025
Fax: +86-852-28165284

Received: September 1, 2018
Peer-review started: September 1, 2018
First decision: October 14, 2018
Revised: October 21, 2018
Accepted: November 7, 2018
Article in press: November 7, 2018

Published online: December 7, 2018

Abstract

A large number of liver transplants have been performed for hepatocellular carcinoma (HCC), and recurrence is increasingly encountered. The recurrence of HCC after liver transplantation is notoriously difficult to manage. We hereby propose multi-disciplinary management with a systematic approach. The patient is jointly managed by the transplant surgeon, physician, oncologist and radiologist. Immunosuppressants should be tapered to the lowest effective dose to protect against rejection. The combination of a mammalian target of rapamycin inhibitor with a reduced calcineurin inhibitor could be considered with close monitoring of graft function and toxicity. Comprehensive staging can be performed by dual-tracer positron emission tomography-computed tomography or the combination of contrast computed tomography and a bone scan. In patients with disseminated recurrence, sorafenib confers survival benefits but is associated with significant drug toxicity. Oligo-recurrence encompasses recurrent disease that is limited in number and location so that loco-regional treatments convey disease control and survival benefits. Intra-hepatic recurrence can be managed with graft resection, but significant operative morbidity is expected. Radiofrequency ablation and stereotactic body radiation therapy (SBRT) are effective alternative strategies. In patients with more advanced hepatic disease, regional treatment with trans-arterial chemoembolization or intra-arterial Yttrium-90 can be considered. For patients with extra-hepatic oligo-recurrence, loco-regional treatment can be considered if practical. Patients with more than one site of recurrence are not always contraindicated for curative treatments. Surgical resection is effective for patients with pulmonary oligo-recurrence, but adequate lung function is a pre-

requisite. SBRT is a non-invasive and effective modality that conveys local control to pulmonary and skeletal oligo-recurrences.

Key words: Hepatocellular carcinoma; Recurrence; Liver transplantation

Core tip: We propose a multi-disciplinary management algorithm for recurrent hepatocellular carcinoma after liver transplantation. The combination of a mammalian target of rapamycin inhibitor with a reduced calcineurin inhibitor can be considered. Staging is performed to differentiate between disseminated recurrence and oligo-recurrence. In patients with disseminated recurrence, sorafenib may confer survival benefits but is associated with significant toxicity. Oligo-recurrence encompasses recurrent disease that is limited in number and location so that loco-regional treatments convey disease control and survival benefits. Intra-hepatic and extra-hepatic oligo-recurrences can be managed with surgical resection, ablative therapy or regional treatments depending on the disease status.

Au KP, Chok KSH. Multidisciplinary approach for post-liver transplant recurrence of hepatocellular carcinoma: A proposed management algorithm. *World J Gastroenterol* 2018; 24(45): 5081-5094 Available from: URL: http://www.wjgnet.com/1007-9327/full/v24/i45/5081.htm DOI: http://dx.doi.org/10.3748/wjg.v24.i45.5081

INTRODUCTION

Despite stringent selection criteria, recurrence occurs in 6%-18% of patients transplanted for hepatocellular carcinoma (HCC)[1-4]. Since the implementation of the Model for End-Stage Liver Disease (MELD) system, patients waitlisted for HCC have been given increased priority for cadaveric grafts[5]. More liver transplants have been performed for HCC, and recurrence is more frequently encountered[6]. The recurrence of HCC after liver transplantation is notoriously difficult to manage. Experience is limited in the literature, and there is considerable debate concerning various systemic and local treatments. The objective of the present narrative review is to summarize the current available literature and propose a management algorithm for recurrence after liver transplantation.

A literature search was performed on PubMed (United States National Library of Medicine, National Institutes of Health, United States) for relevant English articles with a combination of keywords: "liver transplantation" with "hepatocellular carcinoma recurrence" or "HCC recurrence" and/or "immunosuppression" and/or "targeted therapy" and/or "immunotherapy" and/or "resection" and/or "ablation" and/or "stereotactic body radiotherapy" or "SBRT". The references of the selected papers were reviewed for additional relevant articles.

UNIQUE PERSPECTIVES OF POST-TRANSPLANT RECURRENCE

Systemic disease

After liver transplantation, any recurrence is, by definition, metastasis from the native liver. The culprit is either the presence of undiagnosed distant metastasis before transplantation or spillage of tumour cells during transplantation. Even an isolated recurrence implicates solitary metastasis and represents a local phenomenon of the systemic event, which highlights the importance of systemic therapy and the input of oncology as a critical component of the therapeutic strategy.

Immuno-compromised state

Immunity is the primary defence against cancer[7]. The adaptive immune system recognizes and eliminates tumour cells based on their expression of tumour-specific antigens[8]. Termed concomitant immunity, the immune response induced by the primary tumour inhibits the growth of secondaries[9]. However, after liver transplantation, concomitant immunity is suppressed pharmacologically. Any microscopic tumour *in vitro* can progress without immune surveillance. It was observed that post-transplant HCC recurrence progresses significantly faster than in patients treated with hepatic resection[10].

Calcineurin inhibitors, *e.g.,* tacrolimus and cyclosporine, form the cornerstones of maintenance immunosuppression in liver transplantation. In addition to host immune suppression, they promote tumour progression *via* non-immune-mediated pathways related to augmented transforming growth factor expression[11,12]. From a retrospective series of 70 HCC patients treated with liver transplantation, quantified cyclosporine exposure was identified as an independent risk factor for HCC recurrence[13]. Subsequently, Vivarelli *et al*[14] confirmed that high tacrolimus exposure independently predicted HCC recurrence. Immunosuppressive therapy affects the course of tumours in transplant patients and must be fully addressed in the comprehensive management of a recurrence.

Immuno-maintenance phase of the transplant

Throughout the course of treatment, the liver graft must be maintained. Reduction of immunosuppression increases the risk of graft rejection. Medical therapies potentially affect liver function. The use of immunotherapy is particularly concerned with immune-mediated graft injury. While formulating the treatment strategy, the benefits of the treatment must be balanced

with the potential toxicities towards the liver graft.

PROPOSED TREATMENT ALGORITHM

The patient is jointly managed by the transplant surgeon, physician, oncologist and radiologist under a multidisciplinary approach.

IMMUNOSUPPRESSION

Whenever a recurrence is diagnosed, the immunosuppressant should be reviewed. Considering that immune failure contributes to cancer progression, immunosuppression should be tapered to the lowest effective dose protecting against rejection. Moreover, the regimen of immunosuppression warrants reconsideration.

Mammalian target of rapamycin inhibitor

Mammalian target of rapamycin (mTOR) is a protein involved in a signalling pathway that controls cellular growth and proliferation[15]. Rapamycin, more commonly known as sirolimus, inhibits the mTOR pathway to restrain regulatory T-cell proliferation[16]. Apart from immune modulation, mTOR is also involved in HCC pathogenesis and is associated with poor tumour biology[17-19]. Sirolimus has been investigated in a phase II trial showing promising efficacy against advanced HCC[20]. With the theoretical advantage over tumour control, sirolimus has been extensively investigated as immunosuppression therapy for patients engrafted for HCC[21-27] (Table 1).

The highest level of evidence came from a prospective trial conducted by Geissler *et al*[21], where 525 patients were randomized to receive either a sirolimus-based or an mTOR inhibitor-free regimen. In the study group, sirolimus was incorporated 4-6 wk after transplantation, with or without a concomitant calcineurin inhibitor. The overall and recurrence free survival rates were improved up to 5 years (overall survival: 79.4% *vs* 70.3%; P = 0.048) and 3 years (disease-free survival: 80.6% *vs* 72.3%; P = 0.0499). The proportion of patients with acute rejection appeared to be higher in the sirolimus group (23.4% *vs* 17.0%, respectively; P = 0.07), but the difference did not reach statistical significance. The results were in concordance with an updated meta-analysis that demonstrated a survival benefit in patients receiving sirolimus-based immunosuppression therapy (OR = 1.68; CI = 1.21-2.33)[23]. From the pooled results of 11 studies, the risk of graft rejection or hepatic artery thrombosis was not increased. Sirolimus was generally well tolerated. In a small proportion of patients (0-8.3%), sirolimus was discontinued for drug toxicity, mostly due to oral ulcers[28].

Everolimus is a derivative of sirolimus with a shorter elimination half-life (30 h *vs* 60 h) and a quicker time to steady state (4 d *vs* 6 d)[29,30]. The clinical advantage is easier dose adjustment. Everolimus received evaluation in a phase III trial for its role in advanced primary HCC that progressed despite sorafenib therapy[31]. However, no further survival benefit was observed upon switching to everolimus (overall survival: 7.6 mo *vs* 7.3 mo). Everolimus has been evaluated in prospective trials for its efficacy in liver transplantation, although they were not focused on oncological outcomes. In a prospective multicentre study, everolimus with a reduced dose of tacrolimus was associated with better preserved renal function (estimated glomerular filtration rate decline over 36 mo: 7.0 mL/min/1.73 m^2 *vs* 15.5 mL/min/1.73 m^2; P = 0.005) compared with the standard dose of tacrolimus[32]. A similar regimen was studied in another prospective trial with a composite primary endpoint comprising rejection and graft loss[33]. Notably, in patients transplanted for HCC, recurrence was only observed in the control arm with a standard dose of tacrolimus (5/62 *vs* 0/62) after 12 mo of follow up. A direct comparison between everolimus and sirolimus was made in a meta-analysis[34]. Patients on everolimus had significantly fewer recurrences than those on sirolimus or calcineurin inhibitors (4.1% *vs* 10.5% *vs* 13.8%, respectively; P < 0.05). However, everolimus-treated recipients had a shorter follow-up time (13 mo *vs* 30 mo *vs* 43.2 mo, respectively) and fewer advanced tumours (HCC within Milan criteria: 84% *vs* 60.5% *vs* 74%, respectively; P < 0.05). The study did not compare survival, and no definite conclusions were drawn.

The data on mTOR inhibitor therapy for established recurrence after liver transplantation remain scarce. However, a combination of either sirolimus or everolimus with reduced-dose tacrolimus has been proven to be safe and effective in reducing recurrence[24,28,33]. There is inadequate evidence to recommend the optimal serum level of tacrolimus in this combination. In our experience, a sub-therapeutic level of tacrolimus might suffix. From Geissler's prospective trial it appears that Siroliums monotherapy might be adequate for some patients[21]. From a registry database comprising 2491 patients transplanted for HCC, sirolimus was the only maintenance immunosuppressant affecting survival (5-year survival: 83.1% *vs* 68.7%, P < 0.05)[27]. Based on these findings, it appears sensible to incorporate an mTOR inhibitor with a reduced calcineurin inhibitor upon the diagnosis of recurrence. Overall, immunosuppression should be individualized and tapered to spare the remaining anti-tumour immunity. Patients should be closely monitored for liver function throughout the course of cancer treatment.

STAGING

Because post-transplant recurrence is essentially metastatic disease, complete staging is essential to guide subsequent management. Dual tracer positron emission tomography-computed tomography (PET-CT) has been validated for pre-transplant staging for HCC patients[35]. During the examination, a whole-body survey, both functional and structural, is performed for

Table 1 Mammalian target of rapamycin inhibitors for patients engrafted for hepatocellular carcinoma

	No. (SRL/non-SRL)	5-year OS (%)	5-year DFS (%)	HAT (%)	ACR (%)	Discontinuation for toxicity (%)
Prospective controlled trial						
Geissler *et al*[21], 2016	261/264	79.4/70.3[3]	72.6/68.4	-	23.4/17.0	-
Meta-analysis						
Liang *et al*[22], 2012	332/2615	OR: 2.47[3]	1 yr: OR 2.41[3]	OR: 1.32	-	-
Zhang *et al*[23], 2018	7695	OR: 1.68[3]	1 yr: OR 2.13[3]	-	-	-
Case-control						
Vivarelli *et al*[24],2010	31/31	-	3 yr 86/56[3]	0/0	3.2/3.2	-
Retrospective cohort						
Zimmerman *et al*[25],2007	45/52	80/62	78.8/54	2.4/1.9	20/19.6	-
Zhou *et al*[28], 2008[1]	27/46	19.8 ± 1.2/16.0 ± 1.4[2,3]	17.3 ± 1.4/15.9 ± 1.6[2]	0/0	30.4/19.6	8.3
Chinnakotla *et al*[26], 2009	121/106	80/50[3]	-	1.9/2	62.8/54.7	0
Toso *et al*[27], 2010	109/2382	83.1/68.7[3]	-	-	-	-

[1]All tumours were beyond Milan criteria; [2]Median survival in months; [3]Statistically significant. SRL: Sirolimus; OS: Overall survival; DFS: Disease-free survival; HAT: Hepatic artery thrombosis; ACR: Acute cellular rejection.

comprehensive staging. The two radioisotopes, namely C11-acetate and fludeoxyglucose (FDG), complement each other. C11-acetate is sensitive for well-differentiated HCC, but tumours with more unfavourable biology may have a predilection towards FDG[36]. Combining two tracers enhances sensitivity to detect occult metastasis. Dual tracer PET-CT is especially advantageous over computed tomography (CT) to diagnose bone metastasis (sensitivity 97% *vs* 72%, respectively; $P < 0.05$) and is not uncommon in patients with recurrence after liver transplantation[37].

Albeit effective, dual-tracer PET-CT may not be widely available. When contrast CT is performed as an alternative, it is better coupled with a skeletal survey using bone scan. Bone is the third most common site of recurrence after the lung and liver, affecting 20% of patients with recurrence[38]. The objective of radiological staging is to determine whether the recurrence is disseminated or limited, *i.e.*, oligo-recurrence. While disseminated recurrence is managed primarily with systemic therapy, limited recurrence may be better controlled with additional loco-regional treatment. It has been observed that R0 resection conferred a survival benefit in selected candidates with isolated and resectable metastasis[39].

DISSEMINATED RECURRENCE

Disseminated recurrence is primarily managed with systemic treatment with the intention to prolong survival rather than to pursue cure.

Targeted therapy

Sorafenib is a multi-tyrosine kinase inhibitor with activity against vascular endothelial growth factor-2 and -3, platelet-derived growth factor receptor and Ras ligand[40]. It inhibits tumour signalling and angiogenesis pathways involved in HCC pathogenesis. In a randomised controlled trial, sorafenib was shown to prolong the median survival of patients with advanced HCC for 3 mo (10.7 mo *vs* 7.9 mo, $P < 0.001$)[41]. The major drawback was a poorly tolerated side effects profile. Hand-foot skin reaction and gastrointestinal disturbances were reported in 21% and 39% of the patients, respectively. Although mostly graded as 1 and 2 in severity, drug-related adverse events have led to discontinuation of sorafenib in 29% of the patients.

The efficacy of sorafenib in post-transplant HCC recurrence has been studied in numerous retrospective series, mostly in combination with an mTOR inhibitor (Table 2)[42-52]. Sorafenib and mTOR inhibition had synergistic effects on tumour growth in xenograft mice[53]. Ras blockade silenced the feedback signalling of mTOR inhibition, leading to upregulation of its anti-tumour activity[54]. A retrospective cohort reported by De'Angelis *et al*[45] provided insights into the use of sorafenib in patients with advanced recurrence. The outcomes of 15 patients treated with sorafenib were compared with those of 24 patients receiving best supportive care. Sorafenib was stared at 400 mg twice daily. More patients in the sorafenib group received an mTOR inhibitor due to the time effect, but the difference did not reach statistical significance (46.7% *vs* 16.7%, $P = 0.13$). Sorafenib conferred disease control (partial response or stable disease) in 11 of the 15 patients (73.4%), translating into a survival benefit (median OS: 41.4 mo *vs* 19.1 mo; $P = 0.013$). Notably, there was a high proportion of patients requiring dose reduction (53.3%) or discontinuation of treatment (13.3%) due to drug toxicity.

Gomez-Martin *et al*[50] addressed the safety of combining sorafenib with an mTOR inhibitor in a post-transplant setting. In the multicentre cohort consisting of 31 patients with recurrent HCC, the immunosuppression was shifted to mTOR inhibitor therapy with initiation of sorafenib as systemic treatment. Most toxicities were grade 1 or 2. However, 2 episodes of gastric bleeding and 1 episode of cerebral haemorrhage were reported. The gastric bleedings were diffuse mucosal oozing unrelated to portal hypertension or ulcer disease. Thus, sorafenib appears to be effective to prolong

Table 2 Sorafenib for recurrent hepatocellular carcinoma after liver transplantation

	No. (SFN/BSC)	Duration after LT (mo)	mTOR inhibitor (yes/no)	Response rate (% complete/partial/stable)	Median OS (mo)	Time to progression (mo)	Drug toxicity leading to	
							Dose reduction (% patient)	Discontinuation (% patient)
Meta-analysis								
Mancuso *et al*[42],2015	113	13.6	-	0/4.8/44.4	10.5	5.6	42.8	31.9
Retrospective cohort								
Sposito *et al*[43], 2013	15/24	38.1/15.7[2]	7/8	-	21.3/11.8[2]	8.8/10.2	53.3	4.1
De'Angelis *et al*[45], 2016	15/18	18	7/8	0/26.6/46.8	41.4/19.1[2]	-	53.3	13.3
Pinero *et al*[46], 2016	10/10	-	7/3	-	20/12.5	5/3[2]	90	20
Case series								
Yoon *et al*[47], 2010	13	12.3	1/12	0/0/46	5.4	2.9	30.7	0
Kim *et al*[48],2010	9	12.4	7/2	11/0/44	-[1]	-	-	0
Vitale *et al*[49], 2012	10	7	10/0	0/20/60	18	8	40	30
Gomez-Martin *et al*[50], 2012	31	22.6	31/0	0/3.8/50	19.3	6.77	25.8	-
Weinmann *et al*[51], 2012	11	37.5	9/2	0/0/36	20.1	4.1	73	18
Sotiropoulos *et al*[52], 2012	14	8	14/0	-	25	-	33	17
Zavaglia *et al*[44], 2013	11	12	7/4	0/18/9	5	17	90	-

[1]Median survival not reached; [2]Statistically significant. SFN: Sorafenib; BSC: Best supportive care; LT: Liver transplant; mTOR: Mammalian target of rapamycin; OS: Overall survival.

survival after recurrence but at the cost of significant toxicity. Combination treatment with an mTOR inhibitor should be avoided in patients with potential bleeding complications.

Immunotherapy

Immunotherapy directs the host immunity towards the tumour[55]. The physiological immune response is regulated by immune checkpoints[56]. Immunotherapy consists of antibodies directed against these immune checkpoints on the T-cell surface to prompt reactions against tumour antigens. Examples include ipilimumab that targets cytotoxic T-lymphocyte-associated antigen 4 (CTLA-4) and nivolumab and pembrolizumab that target programmed cell death protein 1 (PD-1). Nivolumab has been validated in a large phase II trial for its safety and efficacy against primary HCC[57]. Nivolumab 3 mg/kg was given every 2 wk to 214 patients with advanced HCC. Disease control was achieved in 64% of all patients, including 61% of patients who had previously failed sorafenib treatment. The overall survival was 83% at 6 mo. There was a favourable side effect profile compared with that of sorafenib. Only 2%-4% of patients discontinued nivolumab due to drug toxicity.

However, immune checkpoint modulation of cell-mediated immunity is implicated in transplant organ tolerance[58,59]. Downregulation of these pathways may inadvertently lead to transplant rejection[60]. In fact, clinical trials for immune checkpoint inhibitors often exclude solid organ transplant recipients due to the fear of graft injury[61,62]. Current experience in immunotherapy after liver transplantation is confined to case reports and small series[63-66] (Table 3). Limited survival (0.3 mo to 3 mo) was observed among the 10 patients treated with anti-PD-1. The salvage nature of immunotherapy must be considered while interpreting the results. Most patients had developed disease progression with sorafenib. Moreover, the clinical decision to employ immunotherapy for transplant patients is usually much delayed until treatment failure is evident. Although the therapeutic effect is considered rapid for immunotherapy, a 3-m interval is usually necessary before the treatment response can be evaluated[57]. In the reports, the rather limited survival interval after immunotherapy might not allow the efficacy of immunotherapy to be assessed.

Acute rejection occurred in 3 of the 10 reported cases receiving anti-PD-1 treatment. Although a limited number of events precludes risk factor analysis, a hypothesis could be proposed. Two patients with rejection were relatively young, aged 14 and 20 years, respectively. A young age is a recognized risk factor for acute rejection after liver transplantation, and more aggressive immunosuppression is usually employed[67]. A long duration after transplantation is usually protective of acute rejection. However, the trend is not obvious from this series of observations. Practically, most recurrence occurs early after transplantation as well.

The differential effect of PD-1 and CTLA-4 blockade on rejection may also have implications[68]. Among the 5 reported liver transplant patients treated with immunotherapy for melanoma, rejection was observed only in patients receiving a PD-1 inhibitor[66,69-71] (Table 3). These clinical observations concurred with the findings from *in vitro* studies. Using a murine model it was demonstrated that the PD-1 pathway may play a stronger role in allograft tolerance than CTLA-4 and that PD-1 blockade could be associated with a higher risk of transplant rejection[72]. However, the effect of CTLA-4 blockade on HCC control has not been systematically investigated. The role of immunotherapy in treating HCC recurrence after liver transplantation remains largely unknown. The potential efficacy should not be overlooked but has to be balanced with its safety[73]. Further study in a large patient cohort is warranted to elucidate optimal patient selection.

Table 3 Immunotherapy for recurrent hepatocellular carcinoma after liver transplantation

Patient	Age	Ref.	Tumour	Agent	Years after LT	Immunosuppression	Prior sorafenib	Response	OS (mo)	Rejection
1	41	De Toni *et al*[63], 2017	HCC	Nivolumab	1	Low dose tacrolimus	Yes	No	-	No
2[1]	20	Friend *et al*[64], 2017	HCC	Nivolumab	4	Sirolimus	-	-	1	Yes
3[1]	14	Friend *et al*[64], 2017	HCC	Nivolumab	3	Tacrolimus	-	-	1	Yes
4	70	Varkaris *et al*[65], 2017	HCC	Pembrolizumab	8	Low dose tacrolimus	Yes	No	3	No
5	57	DeLeon *et al*[66], 2018	HCC	Nivolumab	2.7	Tacrolimus	Yes	No	1.2	No
6	56	DeLeon *et al*[66], 2018	HCC	Nivolumab	7.8	MMF/sirolimus	Yes	No	1.1	No
7	35	DeLeon *et al*[66], 2018	HCC	Nivolumab	3.7	Tacrolimus	Yes	No	1.3	No
8	64	DeLeon *et al*[66], 2018	HCC	Nivolumab	1.2	Tacrolimus	Yes	-[2]	0.3	No
9	68	DeLeon *et al*[66], 2018	HCC	Nivolumab	1.1	Sirolimus	Yes	-	0.7	Yes
10	70	Varkaris *et al*[65], 2017	HCC	Pembrolizumab	6	Low dose tacrolimus	Yes	No	3	No
11	59	Ranganath *et al*[69], 2015	Melanoma	Ipilimumab	8	Tacrolimus	-	-	-	No
12	67	Morales *et al*[70], 2015	Melanoma	Ipilimumab	8	Sirolimus	-	-	-	No
13	55	DeLeon *et al*[66], 2018	Melanoma	Pembrolizumab	5.5	MMF/everolimus	-	-	-	No
14	63	DeLeon *et al*[66], 2018	Melanoma	Pembrolizumab	3.1	MMF/prednisolone	-	-	-	Yes
15	62	Kuo *et al*[71], 2018	Melanoma	Ipilimumab and pembrolizumab	6	Sirolimus	-	-	-	Yes

[1]Fibrolamella hepatocellular carcinoma; [2]Multiorgan failure, unrelated to immunotherapy. HCC: Hepatocellular carcinoma; LT: Liver transplant; OS: Overall survival.

MANAGEMENT OF OLIGO-RECURRENCE

Historically, distant recurrence is considered to be terminal. Post-transplant recurrence is, by definition, distant metastasis from the native liver and has been managed with palliative intent. However, the new notions of oligo-recurrence have led to a paradigm shift in the management of cancer recurrence or metastasis. First introduced by Hellman and Weichselbaum in 1995, the term described recurrent disease that was limited in number and location so that loco-regional treatments improved survival[74]. Oligo-recurrence represents a therapeutic opportunity that allows the patient to be treated with a curative strategy. Due to the improvement in systemic therapy, a durable cure is no longer a remote possibility in patients with limited disease. The concept has gained substantial popularity, and oligo-recurrences have been managed with a combination of systemic and loco-regional treatments with promising results[75]. A stringent definition for oligo-recurrence in terms of the number, size, or distribution of tumour is impractical. A pragmatic view to the concept is a rational use of loco-regional therapy in patients for whom disease burden is limited.

Role of surgery

The results for surgical resection have been retrospectively reported for patients with intra-hepatic or extrahepatic oligo-recurrence (Table 4)[4,39,76-79]. Patients eligible for surgical treatment ranged from 25% to 50%. The lung and liver were common sites for resection (Table 4). Survival benefits have been consistently demonstrated in patients treated with surgery, with a median survival of 28 mo to 65 mo observed for patients receiving surgery, compared with 5 mo to 15 mo in those receiving systemic treatment only[4,39,76-79].

Selection bias was inevitable because surgical candidates were invariably patients with localized disease and a better prognosis. In the most recent series, patient selection was further refined with an additional criterion being the absence of progression while on systemic treatment[79]. The genuine benefit conveyed by surgery could be questioned because the selected patients had a limited disease burden and more favourable tumour biology. However, a prospective randomized trial is unlikely under the current setting to be given ethical concern. A matched retrospective comparison is also difficult due to the intrinsic differences between the patients with oligo- and disseminated recurrence.

Reviewing the current literature, long-term survival after post-transplant recurrence has been achieved with surgical resection. Across numerous reported series, surgical treatment remained an independent predictor of superior survival after recurrence[4,76,77,79]. Surgery is supported as the treatment of choice in patients with resectable recurrence, especially when the tumour

Table 4 Surgery for recurrent hepatocellular carcinoma after liver transplantation

	No. resection/total (%)	Site of resection	Median OS in months		Selection criteria	Resection: Independent predictor of survival
			Overall	Resection/no resection		
Comparative study						
Roayaie *et al*[4], 2004	18/57 (31.6)	Liver (n = 8), lung (n = 7), adrenal (n = 2), chest wall (n = 1)[1]	8.7	-	Technical feasibility	Yes
Kornberg *et al*[76], 2010	7/16 (43.8)	Liver (n = 2), lung (n = 2), others (n = 3)	10.5	65/5[5]	-	Yes
Valdivieso *et al*[39], 2010	11/23 (47.8)	Liver (n = 2), lung (n = 2), adrenal (n = 2), abdominal lymph node (n = 2)	-	32.3 ± 21.5/11.9 ± 6.9[2,5]	Technical feasibility	-
Sapisochin *et al*[77], 2015	38/121 (31.4)	-	-	31/12/5[3,5]	Technical feasibility	Yes
Bodzin *et al*[78], 2017	25/106 (23.6)	lung (n = 8), bone (n = 6), intra-abdominal (n = 4), liver (n = 3), brain (n = 2)	10.6	27.8/10.6/3.7[3,5]	-	-
Fernandez-Sevilla *et al*[79], 2017	22/70 (31.4)[4]	-	19	35/15[5]	Technical feasibility. No progression with systemic treatment	Yes

[1]Include radiofrequency ablation of liver lesion (n = 2); [2]R0 resection *vs* no R0 resection; [3]Resection *vs* non-surgical treatment *vs* best supportive care; [4]R0/1 resection *vs* no R0/1 resection; [5]Statistically significant. OS: Overall survival.

biology is favourable.

HEPATIC OLIGO-RECURRENCE

At this point, a differentiation must be made between intra-hepatic recurrence of the primary tumour and development of *de novo* hepatocellular carcinoma. The former occurs early after transplantation, usually within the first 2 years and represents metastatic deposits of the primary HCC into the liver graft. The latter develops late, years after transplantation, when the liver graft becomes cirrhotic secondary to chronic injury. Common culprits are the recurrence of primary liver diseases, diffuse ischaemic biliary injury (DIBI) or chronic rejection. *De novo* HCC resembles the usual situation in a non-transplant recipient where the disease could be presumed to be localized in the liver. Local treatments offer the opportunity of disease control before systemic dissemination. However, the graft function status must be considered when selecting the optimal therapeutic strategy.

Graft resection

This review focuses on genuine intra-hepatic recurrence. In the setting of primary HCC, surgical resection with partial hepatectomy confers favourable oncological outcomes[80]. Surgical resection is therefore given full consideration here when macroscopic disease is confined within the liver. Because recurrence usually occurs early, graft function is preserved and rarely precludes hepatectomy. Resectability is more determined by disease burden. A tumour-free future remnant with adequate volume is the prerequisite for graft hepatectomy. The main concern for graft resection is morbidity. Graft resection is technically challenging due to extensive hilar adhesions. Immunosuppressed patients are susceptible to infective complications. Graft resection for recurrence has been reported in several retrospective series in small numbers (Table 5)[81-83]. High morbidity (60%-80%), but no mortality, was reported. In the first series, infective complications occurred in 63% patients, including 5 Gram-negative bacteraemia requiring intravenous antibiotics[83]. Two series reported oncological outcomes[82,84], with 3-year overall survival rates ranging from 50% to 70%. Graft resection appears to be a feasible treatment for recurrent HCC, offering the chance of long-term survival. However, high morbidity, especially infection complications, is expected.

Radiofrequency ablation

Due to the significant morbidity associated with graft resection, the role of ablative treatments has been investigated. Radiofrequency ablation (RFA) is a thermal ablative technique delivered *via* a needle electrode. For primary HCC, RFA offers equivalent local control as resection for small tumours less than 3 cm in size[85]. The advantage is that it can be performed percutaneously under radiological guidance. A favourable location would be away from the major vasculature and adjacent organs. RFA becomes more appealing when a small tumour is situated in the deep parenchyma, where major hepatectomy is necessitated for resection. In the setting of post-transplant recurrence, the additional benefit is the avoidance of morbidities associated with re-laparotomy in an immunocompromised patient.

One retrospective cohort compared RFA with resection for post-transplant HCC recurrence[84]. In the

Table 5 Graft resection for recurrent hepatocellular carcinoma after liver transplantation

	No.	Morbidity (%)	Mortality (%)	3-yr OS (%)
Case series				
Marangoni *et al*[83], 2008	11[1]	81[2]	0	-
Sommacale *et al*[81], 2013	8[3]	62[4]	0	-
Chok[82], 2015	3	-	0	66.7

[1]Hepatocellular carcinoma (HCC) (n = 4), ischaemic cholangiopathy (n = 2), segmental hepatic artery thrombosis (HAT) (n = 2), others (n = 5); [2]Small bowel perforation (n = 1), bile leak (n = 1), intra-abdominal collection (n = 1), wound infection (n = 1), sepsis (n = 5); [3]HCC (n = 3), bile leak (n = 1), recurrent segmental cholangitis (n = 1), hydatid cyst (n = 1), segmental HAT (n = 1), biliary cyst (n = 1); [4]Statistically significant. OS: Overall survival.

reported series, 15 patients were treated with surgery while 11 received RFA. The author reported similar 3-year (51% *vs* 51%, P = 0.88) and 5-year (35% *vs* 28%, P = 0.88) overall survivals in two groups. However, both hepatic and extra-hepatic recurrences were included, and the results represented the outcomes of heterogeneous procedures. Morbidity and mortality after graft resection were not reported.

Stereotactic body radiation therapy

Stereotactic body radiation therapy (SBRT) is a precise method of delivering ablative radiation by tomographic modulation. Intense and focused doses of radiation are given in a few or single fractions. SBRT for post-transplant HCC recurrence has several theoretical advantages. The radiation beam is focused on the tumour, sparing the adjacent normal liver parenchyma. A higher dose of radiation is delivered while the risk of collateral damage is minimized[86]. Moreover, SBRT is delivered over fewer treatment days than the 10-20 d for conventional radiotherapy, during which systemic therapy is usually deferred. SBRT is usually completed in 1-5 fractions, allowing systemic treatment to be commenced early.

Moreover, it is now established in pre-clinical models that stereotactic radiation upregulates anti-tumour immunity[87-89]. High-dose radiation stimulate antigen-presenting cells, leading to the activation and proliferation of tumour-specific cytotoxic T cells[89]. The abscopal response (from "ab scopus", meaning away from target) denotes this systemic effect leading to the regression of metastatic lesions outside the irradiation field[90]. Interestingly, abscopal effect is synergistically enhanced when combined with immunotherapy-mediated PD-1 blockade[87], which potentially confers a further clinical advantage to SBRT for recurrent HCC because the role of systemic therapy is crucial.

SBRT has been investigated in several prospective studies for primary HCC[91-94]. In these series, the tumour size ranged from 2 cm to 7 cm. At 2 years after ablation, local control was achieved in 80% to 95% of patients. The figure compares favourably with that reported for RFA of small tumours[95,96]. In contrast to RFA, vascular invasion is not a contraindication[97,98]. In direct retrospective comparison, local control was found to be superior in the SBRT group for tumours more than 2 cm in size (HR: 3.35; P = 0.025). Grade III or above morbidity was similar (SBRT *vs* RFA: 5% *vs* 11%; P = 0.31). While RFA loses efficacy with increasing tumour size[99,100], SBRT seems to be as effective when treating larger tumours. To date, the role of SBRT for post-transplant HCC recurrence has yet to be systematically evaluated. While systemic control is of utmost importance, the potential of the SBRT and immunotherapy combination should be conscientiously explored.

Trans-arterial chemoembolization

In patients with multifocal intra-hepatic recurrence, trans-arterial chemoembolization (TACE) offers the opportunity of regional control. Ko *et al*[101] first reported the results of TACE for recurrent HCC after liver transplantation with 1- and 3-year survival rates of 47.9% and 6.0%, respectively. However, in their series, 64.3% of patients developed concomitant extra-hepatic metastasis, which could have affected the oncological outcome as well. Zhou *et al*[102] prospectively compared TACE versus systemic therapy in patients with unresectable intra-hepatic recurrence. Survival benefits were achieved in the TACE arm (P = 0.013), indicating that regional control could have contributed to the improvement in overall survival. Notably, both studies reported no major morbidity after graft liver TACE. In Zhou *et al*[102]'s series of 14 patients, no biliary complications were observed over a median follow up of 14.5 mo.

Trans-arterial radioembolization

Intra-arterial irradiation with Yttrium-90 (Y-90) micro-spheres has gained popularity in recent years to treat unresectable HCC. Injected through the feeding vessels, these microspheres emit high-dose radiation after entrapment at the pre-capillary level. In a large-scale longitudinal cohort comprising 291 patients, Y-90 achieved a 40%-60% response rate[103]. The median survival was 17.2 mo in patients with Child's A cirrhosis. In contrast to TACE, portal vein thrombosis is not a contraindication. Considering the potential synergistic effect of irradiation and immunotherapy, clinical studies are ongoing to investigate the benefit of combining Y-90 and anti-PD1 therapy for primary HCC. Their results will shed light on further applications concerning post-transplant HCC recurrence.

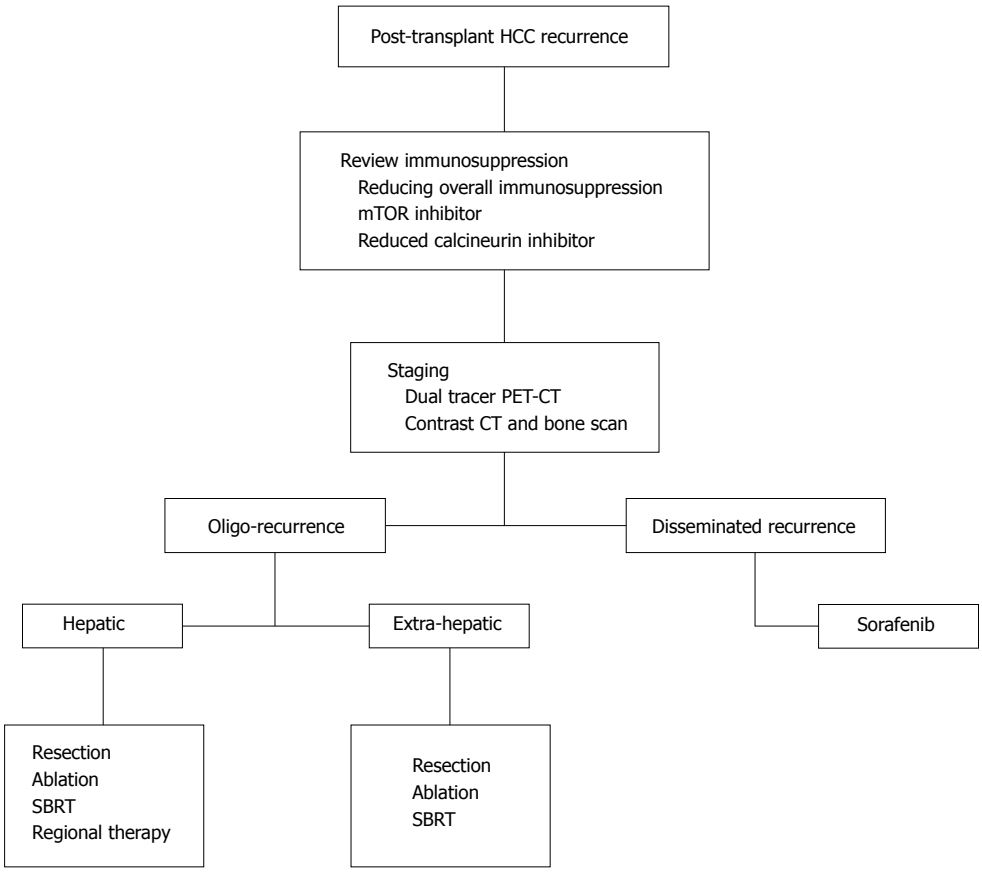

Figure 1 Multidisciplinary approach to manage post-transplant hepatocellular carcinoma recurrence. HCC: Hepatocellular carcinoma; PET-CT: Positron emission tomography-computed tomography; SBRT: Stereotactic body radiation therapy.

EXTRA-HEPATIC OLIGO-RECURRENCE

The lung is the most common site for extra-hepatic recurrence, followed by the bone[4,38,103]. In the literature, the largest series of pulmonary metastatectomy after liver transplantation was reported by Hwang *et al*[104]. Among 43 patients with lung recurrence, 23 were selected for surgery based on the feasibility of complete resection with sufficient pulmonary function after surgery. Patients were resected for up to 3 tumours, regardless of laterality. Over a mean follow up of 33 mo, 4 patients (17.4%) remained disease-free. The resection group had a significantly greater 5-year survival rate (44.7% *vs* 12.8%; $P = 0.017$). There was no operative mortality or morbidity. The results from this retrospective study indicate that pulmonary resection for oligo-recurrence is safe and offers the chance for long-term survival.

Five patients in the resection group had prior extra-pulmonary recurrence successfully treated with loco-regional treatments (3 intrahepatic recurrences ablated with RFA, 1 adrenal and 1 diaphragmatic recurrence excised). Among the 19 patients who developed recurrences after pulmonary resection, 13 received further loco-regional therapy (pulmonary and extra-pulmonary) to enhance disease control. From this series, the notion of oligo-recurrence management was well demonstrated.

When pulmonary metastatectomy is precluded by inadequate lung function, SBRT is considered an alternative[105]. In a German multicentre cohort, 700 patients were treated with SBRT for inoperable pulmonary oligometastasis. The two-year local control and overall survival rates were reported as 82.1% and 54.4%, respectively. Grade 2 or higher pneumonitis occurred in 4.5%-6.5% of patients. SBRT has also been used to treat skeletal oligometastasis from visceral malignancies[106-109]. The 1-year local control rates were 83% and 91% in patients with and without prior radiotherapy, respectively[109]. Stereotactic irradiation was well tolerated with the most common toxicity reported as a transient pain flare[108]. SBRT has been evaluated to treat skeletal metastasis from HCC with a local control rate up to 79% to 88%[110,111]. With these promising results, the role of SBRT for skeletal oligo-recurrence after transplantation should be further explored.

CONCLUSION

To date, experience in managing post-transplant recurrence remains limited. Paucity of high level evidence renders a systematic review or meta-analysis difficult. We hereby propose a multi-disciplinary management algorithm with a systematic approach based on centre experience and best available evidence (Figure 1). The

patient is jointly managed by the transplant surgeon, physician, oncologist and radiologist. Following a diagnosis of recurrence, immunosuppression is reviewed. Immunosuppressants should be tapered to the lowest effective dose protecting against rejection. mTOR inhibitors are associated with anti-tumour effects and are potentially beneficial to tumour control. The combination of an mTOR inhibitor with a reduced calcineurin inhibitor can be considered with close monitoring of graft function and toxicity.

Comprehensive staging is mandatory due to the systemic disease nature. Dual-tracer PET-CT is an effective modality for staging. When contrast CT is used, it is better coupled with a bone scan. The essence of staging is to delineate the extent of disease. In patients presenting with disseminated recurrence, sorafenib may confer survival benefits but is associated with significant drug toxicity and is generally poorly tolerated. Dose reduction is frequently required. Patients at risk of bleeding complications should be avoided for the mTOR and sorafenib combination. In patients with poor tolerance to sorafenib, enrolment into a clinical trial may be beneficial. Disease progression is monitored biochemically with the serum level of AFP and radiologically with reassessment scans. Whenever disease regression is evident, the patients should be reviewed for the feasibility of loco-regional treatment. Additional local control may be beneficial to overall disease progression.

Oligo-recurrence encompasses recurrent disease limited in number and location so that loco-regional treatments convey disease control and survival benefits. Intra-hepatic recurrence can be managed with graft resection, but significant operative morbidity is expected. RFA and SBRT are effective alternative strategies. In patients with more advanced hepatic disease, regional treatment with TACE or intra-arterial Yttrium-90 can be considered. For patients with extra-hepatic oligo-recurrence, loco-regional treatment can be considered if practical. Patients with more than one site of recurrence are not always contraindicated for curative treatments. Surgical resection is effective for patients with pulmonary oligo-recurrence, but adequate lung function is a pre-requisite. SBRT is a non-invasive and effective modality that conveys local control to pulmonary and skeletal oligo-recurrences.

Recurrence of HCC after liver transplantation remains a deadly disease with rapid progression. However, with improved treatment modalities, long-term surviving patients are more frequently observed. More aggressive therapeutic strategies in selected patients with a limited disease burden appear to provide more favourable results than palliative measures. A multidisciplinary team is a comprehensive and coordinated approach to manage patients with post-transplant HCC recurrence.

REFERENCES

1 **Yoo HY**, Patt CH, Geschwind JF, Thuluvath PJ. The outcome of liver transplantation in patients with hepatocellular carcinoma in the United States between 1988 and 2001: 5-year survival has improved significantly with time. *J Clin Oncol* 2003; **21**: 4329-4335 [PMID: 14581446 DOI: 10.1200/JCO.2003.11.137]

2 **Zavaglia C**, De Carlis L, Alberti AB, Minola E, Belli LS, Slim AO, Airoldi A, Giacomoni A, Rondinara G, Tinelli C, Forti D, Pinzello G. Predictors of long-term survival after liver transplantation for hepatocellular carcinoma. *Am J Gastroenterol* 2005; **100**: 2708-2716 [PMID: 16393224 DOI: 10.1111/j.1572-0241.2005.00289.x]

3 **Regalia E**, Fassati LR, Valente U, Pulvirenti A, Damilano I, Dardano G, Montalto F, Coppa J, Mazzaferro V. Pattern and management of recurrent hepatocellular carcinoma after liver transplantation. *J Hepatobiliary Pancreat Surg* 1998; **5**: 29-34 [PMID: 9683751]

4 **Roayaie S**, Schwartz JD, Sung MW, Emre SH, Miller CM, Gondolesi GE, Krieger NR, Schwartz ME. Recurrence of hepatocellular carcinoma after liver transplant: patterns and prognosis. *Liver Transpl* 2004; **10**: 534-540 [PMID: 15048797 DOI: 10.1002/lt.20128]

5 **Wiesner RH**, Freeman RB, Mulligan DC. Liver transplantation for hepatocellular cancer: the impact of the MELD allocation policy. *Gastroenterology* 2004; **127**: S261-S267 [PMID: 15508092]

6 **Yao FY**, Bass NM, Ascher NL, Roberts JP. Liver transplantation for hepatocellular carcinoma: lessons from the first year under the Model of End-Stage Liver Disease (MELD) organ allocation policy. *Liver Transpl* 2004; **10**: 621-630 [PMID: 15108253 DOI: 10.1002/lt.20159]

7 **Swann JB**, Smyth MJ. Immune surveillance of tumors. *J Clin Invest* 2007; **117**: 1137-1146 [PMID: 17476343 DOI: 10.1172/JCI31405]

8 **Altman JD**, Moss PA, Goulder PJ, Barouch DH, McHeyzer-Williams MG, Bell JI, McMichael AJ, Davis MM. Phenotypic analysis of antigen-specific T lymphocytes. *Science* 1996; **274**: 94-96 [PMID: 8810254]

9 **Ruggiero RA**, Bustuoabad OD, Bonfil RD, Meiss RP, Pasqualini CD. "Concomitant immunity" in murine tumours of non-detectable immunogenicity. *Br J Cancer* 1985; **51**: 37-48 [PMID: 2981538]

10 **Yokoyama I**, Carr B, Saitsu H, Iwatsuki S, Starzl TE. Accelerated growth rates of recurrent hepatocellular carcinoma after liver transplantation. *Cancer* 1991; **68**: 2095-2100 [PMID: 1655200]

11 **Hojo M**, Morimoto T, Maluccio M, Asano T, Morimoto K, Lagman M, Shimbo T, Suthanthiran M. Cyclosporine induces cancer progression by a cell-autonomous mechanism. *Nature* 1999; **397**: 530-534 [PMID: 10028970 DOI: 10.1038/17401]

12 **Maluccio M**, Sharma V, Lagman M, Vyas S, Yang H, Li B, Suthanthiran M. Tacrolimus enhances transforming growth factor-beta1 expression and promotes tumor progression. *Transplantation* 2003; **76**: 597-602 [PMID: 12923450 DOI: 10.1097/01.TP.0000081399.75231.3B]

13 **Vivarelli M**, Cucchetti A, Piscaglia F, La Barba G, Bolondi L, Cavallari A, Pinna AD. Analysis of risk factors for tumor recurrence after liver transplantation for hepatocellular carcinoma: key role of immunosuppression. *Liver Transpl* 2005; **11**: 497-503 [PMID: 15838913 DOI: 10.1002/lt.20391]

14 **Vivarelli M**, Cucchetti A, La Barba G, Ravaioli M, Del Gaudio M, Lauro A, Grazi GL, Pinna AD. Liver transplantation for hepatocellular carcinoma under calcineurin inhibitors: reassessment of risk factors for tumor recurrence. *Ann Surg* 2008; **248**: 857-862 [PMID: 18948815 DOI: 10.1097/SLA.0b013e3181896278]

15 **Faivre S**, Kroemer G, Raymond E. Current development of mTOR inhibitors as anticancer agents. *Nat Rev Drug Discov* 2006; **5**: 671-688 [PMID: 16883305 DOI: 10.1038/nrd2062]

16 **Thomson AW**, Turnquist HR, Raimondi G. Immunoregulatory functions of mTOR inhibition. *Nat Rev Immunol* 2009; **9**: 324-337 [PMID: 19390566 DOI: 10.1038/nri2546]

17 **Bjornsti MA**, Houghton PJ. The TOR pathway: a target for cancer therapy. *Nat Rev Cancer* 2004; **4**: 335-348 [PMID: 15122205 DOI: 10.1038/nrc1362]

18 **Zhou Q**, Lui VW, Yeo W. Targeting the PI3K/Akt/mTOR pathway in hepatocellular carcinoma. *Future Oncol* 2011; **7**: 1149-1167 [PMID: 21992728 DOI: 10.2217/fon.11.95]

19 **Zhou L**, Huang Y, Li J, Wang Z. The mTOR pathway is associated with the poor prognosis of human hepatocellular carcinoma. *Med Oncol* 2010; **27**: 255-261 [PMID: 19301157 DOI: 10.1007/s12032-009-9201-4]

20 **Decaens T**, Luciani A, Itti E, Hulin A, Roudot-Thoraval F, Laurent A, Zafrani ES, Mallat A, Duvoux C. Phase II study of sirolimus in treatment-naive patients with advanced hepatocellular carcinoma. *Dig Liver Dis* 2012; **44**: 610-616 [PMID: 22459565 DOI: 10.1016/j.dld.2012.02.005]

21 **Geissler EK**, Schnitzbauer AA, Zülke C, Lamby PE, Proneth A, Duvoux C, Burra P, Jauch KW, Rentsch M, Ganten TM, Schmidt J, Settmacher U, Heise M, Rossi G, Cillo U, Kneteman N, Adam R, van Hoek B, Bachellier P, Wolf P, Rostaing L, Bechstein WO, Rizell M, Powell J, Hidalgo E, Gugenheim J, Wolters H, Brockmann J, Roy A, Mutzbauer I, Schlitt A, Beckebaum S, Graeb C, Nadalin S, Valente U, Turrión VS, Jamieson N, Scholz T, Colledan M, Fändrich F, Becker T, Söderdahl G, Chazouillères O, Mäkisalo H, Pageaux GP, Steininger R, Soliman T, de Jong KP, Pirenne J, Margreiter R, Pratschke J, Pinna AD, Hauss J, Schreiber S, Strasser S, Klempnauer J, Troisi RI, Bhoori S, Lerut J, Bilbao I, Klein CG, Königsrainer A, Mirza DF, Otto G, Mazzaferro V, Neuhaus P, Schlitt HJ. Sirolimus Use in Liver Transplant Recipients With Hepatocellular Carcinoma: A Randomized, Multicenter, Open-Label Phase 3 Trial. *Transplantation* 2016; **100**: 116-125 [PMID: 26555945 DOI: 10.1097/TP.0000000000000965]

22 **Liang W**, Wang D, Ling X, Kao AA, Kong Y, Shang Y, Guo Z, He X. Sirolimus-based immunosuppression in liver transplantation for hepatocellular carcinoma: a meta-analysis. *Liver Transpl* 2012; **18**: 62-69 [PMID: 21964956 DOI: 10.1002/lt.22441]

23 **Zhang ZH**, Li LX, Li P, Lv SC, Pan B, He Q. Sirolimus in Liver Transplant Recipients with Hepatocellular Carcinoma: An Updated Meta-Analysis. *J Invest Surg* 2018; 1-10 [PMID: 29557691 DOI: 10.1080/08941939.2018.1447053]

24 **Vivarelli M**, Dazzi A, Zanello M, Cucchetti A, Cescon M, Ravaioli M, Del Gaudio M, Lauro A, Grazi GL, Pinna AD. Effect of different immunosuppressive schedules on recurrence-free survival after liver transplantation for hepatocellular carcinoma. *Transplantation* 2010; **89**: 227-231 [PMID: 20098287 DOI: 10.1097/TP.0b013e3181c3c540]

25 **Zimmerman MA**, Trotter JF, Wachs M, Bak T, Campsen J, Skibba A, Kam I. Sirolimus-based immunosuppression following liver transplantation for hepatocellular carcinoma. *Liver Transpl* 2008; **14**: 633-638 [PMID: 18324656 DOI: 10.1002/lt.21420]

26 **Chinnakotla S**, Davis GL, Vasani S, Kim P, Tomiyama K, Sanchez E, Onaca N, Goldstein R, Levy M, Klintmalm GB. Impact of sirolimus on the recurrence of hepatocellular carcinoma after liver transplantation. *Liver Transpl* 2009; **15**: 1834-1842 [PMID: 19938137 DOI: 10.1002/lt.21953]

27 **Toso C**, Merani S, Bigam DL, Shapiro AM, Kneteman NM. Sirolimus-based immunosuppression is associated with increased survival after liver transplantation for hepatocellular carcinoma. *Hepatology* 2010; **51**: 1237-1243 [PMID: 20187107 DOI: 10.1002/hep.23437]

28 **Zhou J**, Wang Z, Wu ZQ, Qiu SJ, Yu Y, Huang XW, Tang ZY, Fan J. Sirolimus-based immunosuppression therapy in liver transplantation for patients with hepatocellular carcinoma exceeding the Milan criteria. *Transplant Proc* 2008; **40**: 3548-3553 [PMID: 19100435 DOI: 10.1016/j.transproceed.2008.03.165]

29 **Kirchner GI**, Meier-Wiedenbach I, Manns MP. Clinical pharmacokinetics of everolimus. *Clin Pharmacokinet* 2004; **43**: 83-95 [PMID: 14748618 DOI: 10.2165/00003088-200443020-00002]

30 **Shipkova M**, Hesselink DA, Holt DW, Billaud EM, van Gelder T, Kunicki PK, Brunet M, Budde K, Barten MJ, De Simone P, Wieland E, López OM, Masuda S, Seger C, Picard N, Oellerich M, Langman LJ, Wallemacq P, Morris RG, Thompson C, Marquet P. Therapeutic Drug Monitoring of Everolimus: A Consensus Report. *Ther Drug Monit* 2016; **38**: 143-169 [PMID: 26982492 DOI: 10.1097/FTD.0000000000000260]

31 **Zhu AX**, Kudo M, Assenat E, Cattan S, Kang YK, Lim HY, Poon RT, Blanc JF, Vogel A, Chen CL, Dorval E, Peck-Radosavljevic M, Santoro A, Daniele B, Furuse J, Jappe A, Perraud K, Anak O, Sellami DB, Chen LT. Effect of everolimus on survival in advanced hepatocellular carcinoma after failure of sorafenib: the EVOLVE-1 randomized clinical trial. *JAMA* 2014; **312**: 57-67 [PMID: 25058218 DOI: 10.1001/jama.2014.7189]

32 **Fischer L**, Saliba F, Kaiser GM, De Carlis L, Metselaar HJ, De Simone P, Duvoux C, Nevens F, Fung JJ, Dong G, Rauer B, Junge G; H2304 Study Group. Three-year Outcomes in De Novo Liver Transplant Patients Receiving Everolimus With Reduced Tacrolimus: Follow-Up Results From a Randomized, Multicenter Study. *Transplantation* 2015; **99**: 1455-1462 [PMID: 26151607 DOI: 10.1097/TP.0000000000000555]

33 **Jeng LB**, Lee SG, Soin AS, Lee WC, Suh KS, Joo DJ, Uemoto S, Joh J, Yoshizumi T, Yang HR, Song GW, Lopez P, Kochuparampil J, Sips C, Kaneko S, Levy G. Efficacy and safety of everolimus with reduced tacrolimus in living-donor liver transplant recipients: 12-month results of a randomized multicenter study. *Am J Transplant* 2018; **18**: 1435-1446 [PMID: 29237235 DOI: 10.1111/ajt.14623]

34 **Cholongitas E**, Mamou C, Rodríguez-Castro KI, Burra P. Mammalian target of rapamycin inhibitors are associated with lower rates of hepatocellular carcinoma recurrence after liver transplantation: a systematic review. *Transpl Int* 2014; **27**: 1039-1049 [PMID: 24943720 DOI: 10.1111/tri.12372]

35 **Cheung TT**, Ho CL, Lo CM, Chen S, Chan SC, Chok KS, Fung JY, Yan Chan AC, Sharr W, Yau T, Poon RT, Fan ST. 11C-acetate and 18F-FDG PET/CT for clinical staging and selection of patients with hepatocellular carcinoma for liver transplantation on the basis of Milan criteria: surgeon's perspective. *J Nucl Med* 2013; **54**: 192-200 [PMID: 23321459 DOI: 10.2967/jnumed.112.107516]

36 **Cheung TT**, Chan SC, Ho CL, Chok KS, Chan AC, Sharr WW, Ng KK, Poon RT, Lo CM, Fan ST. Can positron emission tomography with the dual tracers [11 C]acetate and [18 F]fludeoxyglucose predict microvascular invasion in hepatocellular carcinoma? *Liver Transpl* 2011; **17**: 1218-1225 [PMID: 21688383 DOI: 10.1002/lt.22362]

37 **Ho CL**, Chen S, Cheng TK, Leung YL. PET/CT characteristics of isolated bone metastases in hepatocellular carcinoma. *Radiology* 2011; **258**: 515-523 [PMID: 21062922 DOI: 10.1148/radiol.10100672]

38 **Pecchi A**, Besutti G, De Santis M, Del Giovane C, Nosseir S, Tarantino G, Di Benedetto F, Torricelli P. Post-transplantation hepatocellular carcinoma recurrence: Patterns and relation between vascularity and differentiation degree. *World J Hepatol* 2015; **7**: 276-284 [PMID: 25729483 DOI: 10.4254/wjh.v7.i2.276]

39 **Valdivieso A**, Bustamante J, Gastaca M, Uriarte JG, Ventoso A, Ruiz P, Fernandez JR, Pijoan I, Testillano M, Suarez MJ, Montejo M, Ortiz de Urbina J. Management of hepatocellular carcinoma recurrence after liver transplantation. *Transplant Proc* 2010; **42**: 660-662 [PMID: 20304217 DOI: 10.1016/j.transproceed.2010.02.014]

40 **Wilhelm S**, Carter C, Lynch M, Lowinger T, Dumas J, Smith RA, Schwartz B, Simantov R, Kelley S. Discovery and development of sorafenib: a multikinase inhibitor for treating cancer. *Nat Rev Drug Discov* 2006; **5**: 835-844 [PMID: 17016424 DOI: 10.1038/nrd2130]

41 **Llovet JM**, Ricci S, Mazzaferro V, Hilgard P, Gane E, Blanc JF, de Oliveira AC, Santoro A, Raoul JL, Forner A, Schwartz M, Porta C, Zeuzem S, Bolondi L, Greten TF, Galle PR, Seitz JF, Borbath I, Häussinger D, Giannaris T, Shan M, Moscovici M, Voliotis D, Bruix J; SHARP Investigators Study Group. Sorafenib in advanced hepatocellular carcinoma. *N Engl J Med* 2008; **359**: 378-390 [PMID: 18650514 DOI: 10.1056/NEJMoa0708857]

42 **Mancuso A**, Mazzola A, Cabibbo G, Perricone G, Enea M, Galvano A, Zavaglia C, Belli L, Cammà C. Survival of patients treated with sorafenib for hepatocellular carcinoma recurrence after liver transplantation: a systematic review and meta-analysis. *Dig Liver Dis* 2015; **47**: 324-330 [PMID: 25641331 DOI: 10.1016/j.dld.2015.01.001]

43 **Sposito C**, Mariani L, Germini A, Flores Reyes M, Bongini M, Grossi G, Bhoori S, Mazzaferro V. Comparative efficacy of sorafenib versus best supportive care in recurrent hepatocellular carcinoma after liver transplantation: a case-control study. *J Hepatol* 2013; **59**: 59-66 [PMID: 23500153 DOI: 10.1016/j.jhep.2013.02.026]

44 **Zavaglia C**, Airoldi A, Mancuso A, Vangeli M, Viganò R, Cordone G, Gentiluomo M, Belli LS. Adverse events affect sorafenib efficacy in patients with recurrent hepatocellular carcinoma after liver transplantation: experience at a single center and review of the literature. *Eur J Gastroenterol Hepatol* 2013; **25**: 180-186 [PMID: 23044808 DOI: 10.1097/MEG.0b013e328359e550]

45 **de'Angelis N**, Landi F, Nencioni M, Palen A, Lahat E, Salloum C, Compagnon P, Lim C, Costentin C, Calderaro J, Luciani A, Feray C, Azoulay D. Role of Sorafenib in Patients With Recurrent Hepatocellular Carcinoma After Liver Transplantation. *Prog Transplant* 2016; **26**: 348-355 [PMID: 27555074 DOI: 10.1177/1526924816664083]

46 **PiñeroF**, MarcianoS, AndersM. Sorafenib for Recurrent Hepatocellular Carcinoma after Liver Transplantation: A South American Experience

47 **Yoon DH**, Ryoo BY, Ryu MH, Lee SG, Hwang S, Suh DJ, Lee HC, Kim TW, Ahn CS, Kim KH, Moon DB, Kang YK. Sorafenib for recurrent hepatocellular carcinoma after liver transplantation. *Jpn J Clin Oncol* 2010; **40**: 768-773 [PMID: 20494947 DOI: 10.1093/jjco/hyq055]

48 **Kim R**, El-Gazzaz G, Tan A, Elson P, Byrne M, Chang YD, Aucejo F. Safety and feasibility of using sorafenib in recurrent hepatocellular carcinoma after orthotopic liver transplantation. *Oncology* 2010; **79**: 62-66 [PMID: 21071991 DOI: 10.1159/000319548]

49 **Vitale A**, Boccagni P, Kertusha X, Zanus G, D'Amico F, Lodo E, Pastorelli D, Ramirez Morales R, Lombardi G, Senzolo M, Burra P, Cillo U. Sorafenib for the treatment of recurrent hepatocellular carcinoma after liver transplantation? *Transplant Proc* 2012; **44**: 1989-1991 [PMID: 22974889 DOI: 10.1016/j.transproceed.2012.06.046]

50 **Gomez-Martin C**, Bustamante J, Castroagudin JF, Salcedo M, Garralda E, Testillano M, Herrero I, Matilla A, Sangro B. Efficacy and safety of sorafenib in combination with mammalian target of rapamycin inhibitors for recurrent hepatocellular carcinoma after liver transplantation. *Liver Transpl* 2012; **18**: 45-52 [PMID: 21932373 DOI: 10.1002/lt.22434]

51 **Weinmann A**, Niederle IM, Koch S, Hoppe-Lotichius M, Heise M, Düber C, Schuchmann M, Otto G, Galle PR, Wörns MA. Sorafenib for recurrence of hepatocellular carcinoma after liver transplantation. *Dig Liver Dis* 2012; **44**: 432-437 [PMID: 22265328 DOI: 10.1016/j.dld.2011.12.009]

52 **Sotiropoulos GC**, Nowak KW, Fouzas I, Vernadakis S, Kykalos S, Klein CG, Paul A. Sorafenib treatment for recurrent hepatocellular carcinoma after liver transplantation. *Transplant Proc* 2012; **44**: 2754-2756 [PMID: 23146514 DOI: 10.1016/j.transproceed.2012.09.022]

53 **Newell P**, Toffanin S, Villanueva A, Chiang DY, Minguez B, Cabellos L, Savic R, Hoshida Y, Lim KH, Melgar-Lesmes P, Yea S, Peix J, Deniz K, Fiel MI, Thung S, Alsinet C, Tovar V, Mazzaferro V, Bruix J, Roayaie S, Schwartz M, Friedman SL, Llovet JM. Ras pathway activation in hepatocellular carcinoma and anti-tumoral effect of combined sorafenib and rapamycin in vivo. *J Hepatol* 2009; **51**: 725-733 [PMID: 19665249 DOI: 10.1016/j.jhep.2009.03.028]

54 **Carracedo A**, Baselga J, Pandolfi PP. Deconstructing feedback-signaling networks to improve anticancer therapy with mTORC1 inhibitors. *Cell Cycle* 2008; **7**: 3805-3809 [PMID: 19098454 DOI: 10.4161/cc.7.24.7244]

55 **Couzin-Frankel J**. Immune therapy steps up the attack. *Science* 2010; **330**: 440-443 [PMID: 20966228 DOI: 10.1126/science.330.6003.440]

56 **Pardoll DM**. The blockade of immune checkpoints in cancer immunotherapy. *Nat Rev Cancer* 2012; **12**: 252-264 [PMID: 22437870 DOI: 10.1038/nrc3239]

57 **El-Khoueiry AB**, Sangro B, Yau T, Crocenzi TS, Kudo M, Hsu C, Kim TY, Choo SP, Trojan J, Welling TH Rd, Meyer T, Kang YK, Yeo W, Chopra A, Anderson J, Dela Cruz C, Lang L, Neely J, Tang H, Dastani HB, Melero I. Nivolumab in patients with advanced hepatocellular carcinoma (CheckMate 040): an open-label, non-comparative, phase 1/2 dose escalation and expansion trial. *Lancet* 2017; **389**: 2492-2502 [PMID: 28434648 DOI: 10.1016/S0140-6736(17)31046-2]

58 **Riella LV**, Paterson AM, Sharpe AH, Chandraker A. Role of the PD-1 pathway in the immune response. *Am J Transplant* 2012; **12**: 2575-2587 [PMID: 22900886 DOI: 10.1111/j.1600-6143.2012.04224.x]

59 **Tanaka K**, Albin MJ, Yuan X, Yamaura K, Habicht A, Murayama T, Grimm M, Waaga AM, Ueno T, Padera RF, Yagita H, Azuma M, Shin T, Blazar BR, Rothstein DM, Sayegh MH, Najafian N. PDL1 is required for peripheral transplantation tolerance and protection from chronic allograft rejection. *J Immunol* 2007; **179**: 5204-5210 [PMID: 17911605]

60 **Zhang T**, Fresnay S, Welty E, Sangrampurkar N, Rybak E, Zhou H, Cheng XF, Feng Q, Avon C, Laaris A, Whitters M, Nagelin AM, O'Hara RM Jr, Azimzadeh AM. Selective CD28 blockade attenuates acute and chronic rejection of murine cardiac allografts in a CTLA-4-dependent manner. *Am J Transplant* 2011; **11**: 1599-1609 [PMID: 21749640 DOI: 10.1111/j.1600-6143.2011.03624.x]

61 **Hodi FS**, O'Day SJ, McDermott DF, Weber RW, Sosman JA, Haanen JB, Gonzalez R, Robert C, Schadendorf D, Hassel JC, Akerley W, van den Eertwegh AJ, Lutzky J, Lorigan P, Vaubel JM, Linette GP, Hogg D, Ottensmeier CH, Lebbé C, Peschel C, Quirt I, Clark JI, Wolchok JD, Weber JS, Tian J, Yellin MJ, Nichol GM, Hoos A, Urba WJ. Improved survival with ipilimumab in patients with metastatic melanoma. *N Engl J Med* 2010; **363**: 711-723 [PMID: 20525992 DOI: 10.1056/NEJMoa1003466]

62 **Robert C**, Thomas L, Bondarenko I, O'Day S, Weber J, Garbe C, Lebbe C, Baurain JF, Testori A, Grob JJ, Davidson N, Richards J, Maio M, Hauschild A, Miller WH Jr, Gascon P, Lotem M, Harmankaya K, Ibrahim R, Francis S, Chen TT, Humphrey R, Hoos A, Wolchok JD. Ipilimumab plus dacarbazine for previously untreated metastatic melanoma. *N Engl J Med* 2011; **364**: 2517-2526 [PMID: 21639810 DOI: 10.1056/NEJMoa1104621]

63 **De Toni EN**, Gerbes AL. Tapering of Immunosuppression and Sustained Treatment With Nivolumab in a Liver Transplant Recipient. *Gastroenterology* 2017; **152**: 1631-1633 [PMID: 28384452 DOI: 10.1053/j.gastro.2017.01.063]

64 **Friend BD**, Venick RS, McDiarmid SV, Zhou X, Naini B, Wang H, Farmer DG, Busuttil RW, Federman N. Fatal orthotopic liver transplant organ rejection induced by a checkpoint inhibitor in two patients with refractory, metastatic hepatocellular carcinoma. *Pediatr Blood Cancer* 2017; **64** (12) [PMID: 28643391 DOI: 10.1002/pbc.26682]

65 **Varkaris A**, Lewis DW, Nugent FW. Preserved Liver Transplant After PD-1 Pathway Inhibitor for Hepatocellular Carcinoma. *Am J Gastroenterol* 2017; **112**: 1895-1896 [PMID: 29215617 DOI: 10.1038/ajg.2017.387]

66 **DeleonTT**, SalomaoMA, AqelBA. Pilot evaluation of PD-1 inhibition in metastatic cancer patients with a history of liver transplantation: the Mayo Clinic experience. *J Gastrointest Oncol*. 2018; (suppl 4S) [DOI: 10.21037/jgo.2018.07.05]

67 **Wang YC**, Wu TJ, Wu TH, Lee CF, Chou HS, Chan KM, Lee WC. The risk factors to predict acute rejection in liver transplantation. *Transplant Proc* 2012; **44**: 526-528 [PMID: 22410062 DOI: 10.1016/j.transproceed.2012.01.041]

68 **Liu M**, Guo W, Zhang S. Cancer immunotherapy in patients with new or recurrent malignancies after liver transplantation. *Int J Surg Oncol* (NY) 2017; **2**: e49 [PMID: 29302641 DOI: 10.1097/IJ9.0000000000000049]

69 **Ranganath HA**, Panella TJ. Administration of ipilimumab to a liver transplant recipient with unresectable metastatic melanoma. *J Immunother* 2015; **38**: 211 [PMID: 25962109 DOI: 10.1097/CJI.0000000000000077]

70 **Morales RE**, Shoushtari AN, Walsh MM, Grewal P, Lipson EJ, Carvajal RD. Safety and efficacy of ipilimumab to treat advanced melanoma in the setting of liver transplantation. *J Immunother Cancer* 2015; **3**: 22 [PMID: 26082835 DOI: 10.1186/s40425-015-0066-0]

71 **Kuo JC**, Lilly LB, Hogg D. Immune checkpoint inhibitor therapy in a liver transplant recipient with a rare subtype of melanoma: a

case report and literature review. *Melanoma Res* 2018; **28**: 61-64 [PMID: 29140833 DOI: 10.1097/CMR.0000000000000410]
72 **Blazar BR**, Carreno BM, Panoskaltsis-Mortari A, Carter L, Iwai Y, Yagita H, Nishimura H, Taylor PA. Blockade of programmed death-1 engagement accelerates graft-versus-host disease lethality by an IFN-gamma-dependent mechanism. *J Immunol* 2003; **171**: 1272-1277 [PMID: 12874215]
73 **Kittai AS**, Oldham H, Cetnar J, Taylor M. Immune Checkpoint Inhibitors in Organ Transplant Patients. *J Immunother* 2017; **40**: 277-281 [PMID: 28719552 DOI: 10.1097/CJI.0000000000000180]
74 **Hellman S**, Weichselbaum RR. Oligometastases. *J Clin Oncol* 1995; **13**: 8-10 [PMID: 7799047 DOI: 10.1200/JCO.1995.13.1.8]
75 **Niibe Y**, Hayakawa K. Oligometastases and oligo-recurrence: the new era of cancer therapy. *Jpn J Clin Oncol* 2010; **40**: 107-111 [PMID: 20047860 DOI: 10.1093/jjco/hyp167]
76 **Kornberg A**, Küpper B, Tannapfel A, Katenkamp K, Thrum K, Habrecht O, Wilberg J. Long-term survival after recurrent hepatocellular carcinoma in liver transplant patients: clinical patterns and outcome variables. *Eur J Surg Oncol* 2010; **36**: 275-280 [PMID: 19857941 DOI: 10.1016/j.ejso.2009.10.001]
77 **Sapisochin G**, Goldaracena N, Astete S, Laurence JM, Davidson D, Rafael E, Castells L, Sandroussi C, Bilbao I, Dopazo C, Grant DR, Lázaro JL, Caralt M, Ghanekar A, McGilvray ID, Lilly L, Cattral MS, Selzner M, Charco R, Greig PD. Benefit of Treating Hepatocellular Carcinoma Recurrence after Liver Transplantation and Analysis of Prognostic Factors for Survival in a Large Euro-American Series. *Ann Surg Oncol* 2015; **22**: 2286-2294 [PMID: 25472651 DOI: 10.1245/s10434-014-4273-6]
78 **Bodzin AS**, Lunsford KE, Markovic D, Harlander-Locke MP, Busuttil RW, Agopian VG. Predicting Mortality in Patients Developing Recurrent Hepatocellular Carcinoma After Liver Transplantation: Impact of Treatment Modality and Recurrence Characteristics. *Ann Surg* 2017; **266**: 118-125 [PMID: 27433914 DOI: 10.1097/SLA.0000000000001894]
79 **Fernandez-Sevilla E**, Allard MA, Selten J, Golse N, Vibert E, Sa Cunha A, Cherqui D, Castaing D, Adam R. Recurrence of hepatocellular carcinoma after liver transplantation: Is there a place for resection? *Liver Transpl* 2017; **23**: 440-447 [PMID: 28187493 DOI: 10.1002/lt.24742]
80 **Lee JG**, Kang CM, Park JS, Kim KS, Yoon DS, Choi JS, Lee WJ, Kim BR. The actual five-year survival rate of hepatocellular carcinoma patients after curative resection. *Yonsei Med J* 2006; **47**: 105-112 [PMID: 16502491 DOI: 10.3349/ymj.2006.47.1.105]
81 **Sommacale D**, Dondero F, Sauvanet A, Francoz C, Durand F, Farges O, Kianmanesh R, Belghiti J. Liver resection in transplanted patients: a single-center Western experience. *Transplant Proc* 2013; **45**: 2726-2728 [PMID: 24034033 DOI: 10.1016/j.transproceed.2013.07.032]
82 **Chok KSh**. Management of recurrent hepatocellular carcinoma after liver transplant. *World J Hepatol* 2015; **7**: 1142-1148 [PMID: 26052403 DOI: 10.4254/wjh.v7.i8.1142]
83 **Marangoni G**, Faraj W, Sethi H, Rela M, Muiesan P, Heaton N. Liver resection in liver transplant recipients. *Hepatobiliary Pancreat Dis Int* 2008; **7**: 590-594 [PMID: 19073403]
84 **Huang J**, Yan L, Wu H, Yang J, Liao M, Zeng Y. Is radiofrequency ablation applicable for recurrent hepatocellular carcinoma after liver transplantation? *J Surg Res* 2016; **200**: 122-130 [PMID: 26277218 DOI: 10.1016/j.jss.2015.07.033]
85 **Vivarelli M**, Guglielmi A, Ruzzenente A, Cucchetti A, Bellusci R, Cordiano C, Cavallari A. Surgical resection versus percutaneous radiofrequency ablation in the treatment of hepatocellular carcinoma on cirrhotic liver. *Ann Surg* 2004; **240**: 102-107 [PMID: 15213625]
86 **Sanuki N**, Takeda A, Kunieda E. Role of stereotactic body radiation therapy for hepatocellular carcinoma. *World J Gastroenterol* 2014; **20**: 3100-3111 [PMID: 24696597 DOI: 10.3748/wjg.v20.i12.3100]
87 **Sharabi AB**, Nirschl CJ, Kochel CM, Nirschl TR, Francica BJ, Velarde E, Deweese TL, Drake CG. Stereotactic Radiation Therapy Augments Antigen-Specific PD-1-Mediated Antitumor Immune Responses via Cross-Presentation of Tumor Antigen. *Cancer Immunol Res* 2015; **3**: 345-355 [PMID: 25527358 DOI: 10.1158/2326-6066.CIR-14-0196]
88 **Parker JJ**, Jones JC, Strober S, Knox SJ. Characterization of direct radiation-induced immune function and molecular signaling changes in an antigen presenting cell line. *Clin Immunol* 2013; **148**: 44-55 [PMID: 23649044 DOI: 10.1016/j.clim.2013.03.008]
89 **Gupta A**, Probst HC, Vuong V, Landshammer A, Muth S, Yagita H, Schwendener R, Pruschy M, Knuth A, van den Broek M. Radiotherapy promotes tumor-specific effector CD8+ T cells via dendritic cell activation. *J Immunol* 2012; **189**: 558-566 [PMID: 22685313 DOI: 10.4049/jimmunol.1200563]
90 **Ng J**, Dai T. Radiation therapy and the abscopal effect: a concept comes of age. *Ann Transl Med* 2016; **4**: 118 [PMID: 27127771 DOI: 10.21037/atm.2016.01.32]
91 **Cárdenes HR**, Price TR, Perkins SM, Maluccio M, Kwo P, Breen TE, Henderson MA, Schefter TE, Tudor K, Deluca J, Johnstone PA. Phase I feasibility trial of stereotactic body radiation therapy for primary hepatocellular carcinoma. *Clin Transl Oncol* 2010; **12**: 218-225 [PMID: 20231127 DOI: 10.1007/s12094-010-0492-x]
92 **Andolino DL**, Johnson CS, Maluccio M, Kwo P, Tector AJ, Zook J, Johnstone PA, Cardenes HR. Stereotactic body radiotherapy for primary hepatocellular carcinoma. *Int J Radiat Oncol Biol Phys* 2011; **81**: e447-e453 [PMID: 21645977 DOI: 10.1016/j.ijrobp.2011.04.011]
93 **Bujold A**, Massey CA, Kim JJ, Brierley J, Cho C, Wong RK, Dinniwell RE, Kassam Z, Ringash J, Cummings B, Sykes J, Sherman M, Knox JJ, Dawson LA. Sequential phase I and II trials of stereotactic body radiotherapy for locally advanced hepatocellular carcinoma. *J Clin Oncol* 2013; **31**: 1631-1639 [PMID: 23547075 DOI: 10.1200/JCO.2012.44.1659]
94 **Kang JK**, Kim MS, Cho CK, Yang KM, Yoo HJ, Kim JH, Bae SH, Jung DH, Kim KB, Lee DH, Han CJ, Kim J, Park SC, Kim YH. Stereotactic body radiation therapy for inoperable hepatocellular carcinoma as a local salvage treatment after incomplete transarterial chemoembolization. *Cancer* 2012; **118**: 5424-5431 [PMID: 22570179 DOI: 10.1002/cncr.27533]
95 **Wong SL**, Mangu PB, Choti MA, Crocenzi TS, Dodd GD 3rd, Dorfman GS, Eng C, Fong Y, Giusti AF, Lu D, Marsland TA, Michelson R, Poston GJ, Schrag D, Seidenfeld J, Benson AB 3rd. American Society of Clinical Oncology 2009 clinical evidence review on radiofrequency ablation of hepatic metastases from colorectal cancer. *J Clin Oncol* 2010; **28**: 493-508 [PMID: 19841322 DOI: 10.1200/JCO.2009.23.4450]
96 **Garrean S**, Hering J, Saied A, Helton WS, Espat NJ. Radiofrequency ablation of primary and metastatic liver tumors: a critical review of the literature. *Am J Surg* 2008; **195**: 508-520 [PMID: 18361927 DOI: 10.1016/j.amjsurg.2007.06.024]
97 **Rim CH**, Yang DS, Park YJ, Yoon WS, Lee JA, Kim CY. Effectiveness of high-dose three-dimensional conformal radiotherapy in hepatocellular carcinoma with portal vein thrombosis. *Jpn J Clin Oncol* 2012; **42**: 721-729 [PMID: 22689916 DOI: 10.1093/jjco/hys082]
98 **Xi M**, Zhang L, Zhao L, Li QQ, Guo SP, Feng ZZ, Deng XW, Huang XY, Liu MZ. Effectiveness of stereotactic body radiotherapy for hepatocellular carcinoma with portal vein and/or inferior vena cava tumor thrombosis. *PLoS One* 2013; **8**: e63864 [PMID: 23737955 DOI: 10.1371/journal.pone.0063864]
99 **Pompili M**, Mirante VG, Rondinara G, Fassati LR, Piscaglia F, Agnes S, Covino M, Ravaioli M, Fagiuoli S, Gasbarrini G, Rapaccini GL. Percutaneous ablation procedures in cirrhotic patients with hepatocellular carcinoma submitted to liver transplantation: Assessment of efficacy at explant analysis and of safety for tumor recurrence. *Liver Transpl* 2005; **11**: 1117-1126 [PMID: 16123960 DOI: 10.1002/lt.20469]
100 **Mazzaferro V**, Battiston C, Perrone S, Pulvirenti A, Regalia E, Romito R, Sarli D, Schiavo M, Garbagnati F, Marchianò A, Spreafico C, Camerini T, Mariani L, Miceli R, Andreola S. Radiofrequency ablation of small hepatocellular carcinoma in cirrhotic patients awaiting liver transplantation: a prospective study. *Ann Surg* 2004; **240**: 900-909 [PMID: 15492574]
101 **Ko HK**, Ko GY, Yoon HK, Sung KB. Tumor response to

transcatheter arterial chemoembolization in recurrent hepatocellular carcinoma after living donor liver transplantation. *Korean J Radiol* 2007; **8**: 320-327 [PMID: 17673843 DOI: 10.3348/kjr.2007.8.4.320]

102 **Zhou B**, Shan H, Zhu KS, Jiang ZB, Guan SH, Meng XC, Zeng XC. Chemoembolization with lobaplatin mixed with iodized oil for unresectable recurrent hepatocellular carcinoma after orthotopic liver transplantation. *J Vasc Interv Radiol* 2010; **21**: 333-338 [PMID: 20116286 DOI: 10.1016/j.jvir.2009.11.006]

103 **Salem R**, Lewandowski RJ, Mulcahy MF, Riaz A, Ryu RK, Ibrahim S, Atassi B, Baker T, Gates V, Miller FH, Sato KT, Wang E, Gupta R, Benson AB, Newman SB, Omary RA, Abecassis M, Kulik L. Radioembolization for hepatocellular carcinoma using Yttrium-90 microspheres: a comprehensive report of long-term outcomes. *Gastroenterology* 2010; **138**: 52-64 [PMID: 19766639 DOI: 10.1053/j.gastro.2009.09.006]

104 **Hwang S**, Kim YH, Kim DK, Ahn CS, Moon DB, Kim KH, Ha TY, Song GW, Jung DH, Kim HR, Park GC, Namgoong JM, Yoon SY, Jung SW, Park SI, Lee SG. Resection of pulmonary metastases from hepatocellular carcinoma following liver transplantation. *World J Surg* 2012; **36**: 1592-1602 [PMID: 22411088 DOI: 10.1007/s00268-012-1533-0]

105 **Aoki M**, Hatayama Y, Kawaguchi H, Hirose K, Sato M, Akimoto H, Miura H, Ono S, Takai Y. Stereotactic body radiotherapy for lung metastases as oligo-recurrence: a single institutional study. *J Radiat Res* 2016; **57**: 55-61 [PMID: 26494115 DOI: 10.1093/jrr/rrv063]

106 **Sahgal A**, Larson DA, Chang EL. Stereotactic body radiosurgery for spinal metastases: a critical review. *Int J Radiat Oncol Biol Phys* 2008; **71**: 652-665 [PMID: 18514775 DOI: 10.1016/j.ijrobp.2008.02.060]

107 **Chang EL**, Shiu AS, Mendel E, Mathews LA, Mahajan A, Allen PK, Weinberg JS, Brown BW, Wang XS, Woo SY, Cleeland C, Maor MH, Rhines LD. Phase I/II study of stereotactic body radiotherapy for spinal metastasis and its pattern of failure. *J Neurosurg Spine* 2007; **7**: 151-160 [PMID: 17688054 DOI: 10.3171/SPI-07/08/151]

108 **Owen D**, Laack NN, Mayo CS, Garces YI, Park SS, Bauer HJ, Nelson K, Miller RW, Brown PD, Olivier KR. Outcomes and toxicities of stereotactic body radiation therapy for non-spine bone oligometastases. *Pract Radiat Oncol* 2014; **4**: e143-e149 [PMID: 24890360 DOI: 10.1016/j.prro.2013.05.006]

109 **Ahmed KA**, Stauder MC, Miller RC, Bauer HJ, Rose PS, Olivier KR, Brown PD, Brinkmann DH, Laack NN. Stereotactic body radiation therapy in spinal metastases. *Int J Radiat Oncol Biol Phys* 2012; **82**: e803-e809 [PMID: 22330988 DOI: 10.1016/j.ijrobp.2011.11.036]

110 **Lee E**, Kim TG, Park HC, Yu JI, Lim DH, Nam H, Lee H, Lee JH. Clinical outcomes of stereotactic body radiotherapy for spinal metastases from hepatocellular carcinoma. *Radiat Oncol J* 2015; **33**: 217-225 [PMID: 26484305 DOI: 10.3857/roj.2015.33.3.217]

111 **Yoo GS**, Park HC, Yu JI, Lim DH, Cho WK, Lee E, Jung SH, Han Y, Kim ES, Lee SH, Eoh W, Park SJ, Chung SS, Lee CS, Lee JH. Stereotactic ablative body radiotherapy for spinal metastasis from hepatocellular carcinoma: its oncologic outcomes and risk of vertebral compression fracture. *Oncotarget* 2017; **8**: 72860-72871 [PMID: 29069831 DOI: 10.18632/oncotarget.20529]

P- Reviewer: Hoyos S, Kang KJ, Matsui K, Yao DF
S- Editor: Wang XJ **L- Editor**: A **E- Editor**: Huang Y

World Journal of Gastroenterology

Submit a Manuscript: http://www.f6publishing.com

World J Gastroenterol 2018 December 7; 24(45): 5095-5108

DOI: 10.3748/wjg.v24.i45.5095

ISSN 1007-9327 (print) ISSN 2219-2840 (online)

ORIGINAL ARTICLE

Basic Study

Effects of alkaline-electrolyzed and hydrogen-rich water, in a high-fat-diet nonalcoholic fatty liver disease mouse model

Karen Jackson, Noa Dressler, Rotem S Ben-Shushan, Ari Meerson, Tyler W LeBaron, Snait Tamir

Karen Jackson, Noa Dressler, Rotem S Ben-Shushan, Ari Meerson, Snait Tamir, Laboratory of Human Health and Nutrition Sciences, MIGAL-Galilee Research Institute, Kyriat Shmona 11016, Israel

Karen Jackson, Noa Dressler, Snait Tamir, Tel Hai College, Upper Galilee 12110, Israel

Tyler W LeBaron, Center of Experimental Medicine, Institute for Heart Research, Slovak Academy of Sciences, Bratislava 84005, Slovakia

Tyler W LeBaron, Molecular Hydrogen Institute, UT 48101, United States

ORCID number: Karen Jackson (0000-0001-5696-6224); Noa Dressler (0000-0002-7636-3110); Rotem S Ben-Shushan (0000-0003-1240-5630); Ari Meerson (0000-0002-5811-7952); Tyler W LeBaron (ID 0000-0001-9164-6728); Snait Tamir (0000-0002-7473-7369).

Author contributions: Jackson K designed and coordinated the research analyzed the data and wrote the paper; Dressler N performed the majority of experiments and analyzed the data; Ben-Shushan RS performed the perfusion, and in vitro experiments; Meerson A designed and analyzed the PCR data, LeBaron TW analyzed the data and wrote the paper; Tamir S analyzed the data and contributed to the writing of the final draft.

Supported by Tel Hai College Research funding Grant, No. 25-2-14-114.

Institutional review board statement: This study was reviewed and approved by the Research Committee of Migal Galilee Research Institute.

Institutional animal care and use committee statement: All Protocols were carried out according to relevant guidelines and regulations.

Conflict-of-interest statement: The authors declare no conflict of interest.

Data sharing statement: No additional data are available.

ARRIVE guidelines statement: The authors have read the ARRIVE guidelines, and the manuscript was prepared and revised according to the ARRIVE guidelines.

Manuscript source: Unsolicited manuscript

Correspondence author to: Karen Jackson, PhD, Senior Lecturer, Senior Researcher, Laboratory of Human Health and Nutrition Sciences, MIGAL-Galilee Research Institute, POB 831, Kyriat Shmona 11016, Israel. karen@migal.org.il
Telephone: +972-4-6953511
Fax: +972-4-6944980

Received: September 30, 2018
Peer-review started: September 30, 2018
First decision: October 23, 2018
Revised: October 31, 2018
Accepted: November 9, 2018
Article in press: November 9, 2018
Published online: December 7, 2018

Abstract

AIM

To identify the effect of hydrogen-rich water (HRW) and electrolyzed-alkaline water (EAW) on high-fat-induced non-alcoholic fatty acid disease in mice.

METHODS

Mice were divided into four groups: (1) Regular diet (RD)/regular water (RW); (2) high-fat diet (HFD)/RW;

(3) RD/EAW; and (4) HFD/EAW. Weight and body composition were measured. After twelve weeks, animals were sacrificed, and livers were processed for histology and reverse-transcriptase polymerase chain reaction. A similar experiment was performed using HRW to determine the influence and importance of molecular hydrogen (H_2) in EAW. Finally, we compared the response of hepatocytes isolated from mice drinking HRW or RW to palmitate overload.

RESULTS

EAW had several properties important to the study: (1) pH = 11; (2) oxidation-reduction potential of -495 mV; and (3) H_2 = 0.2 mg/L. However, in contrast to other studies, there were no differences between the groups drinking EAW or RW in either the RD or HFD groups. We hypothesized that the null result was due to low H_2 concentrations. Therefore, we evaluated the effects of RW and low and high HRW concentrations (L-HRW = 0.3 mg H_2/L and H-HRW = 0.8 mg H_2/L, respectively) in mice fed an HFD. Compared to RW and L-HRW, H-HRW resulted in a lower increase in fat mass (46% *vs* 61%), an increase in lean body mass (42% *vs* 28%), and a decrease in hepatic lipid accumulation ($P < 0.01$). Lastly, exposure of hepatocytes isolated from mice drinking H-HRW to palmitate overload demonstrated a protective effect from H_2 by reducing hepatocyte lipid accumulation in comparison to mice drinking regular water.

CONCLUSION

H_2 is the therapeutic agent in electrolyzed-alkaline water and attenuates HFD-induced nonalcoholic fatty liver disease in mice.

Key words: Hydrogen-rich-water; Nonalcoholic fatty liver disease; Alkaline water; Metabolic syndrome; Molecular hydrogen; High-fat diet

Core tip: In this work, we compared the effects of two functional waters: Electrolyzed alkaline water and Hydrogen-rich water in a high-fat-diet-induced nonalcoholic fatty liver disease (NAFLD) mouse model. Hydrogen-rich water (HRW) has potential for NAFLD treatment by attenuating hepatic lipid accumulation, inflammation, and CD36 expression. However, neither electrolyzed-alkaline water (EAW) nor HRW with a low H_2 concentration had protective effects on NAFLD. Additionally, we demonstrated that H_2 pretreatment has a protective effect by modifying gene expression. The results demonstrate that H_2 has a surprisingly positive impact in preventing NAFLD in mice and is also the key agent responsible in EAW for these benefits.

Jackson K, Dressler N, Ben-Shushan RS, Meerson A, LeBaron TW, Tamir S. Effects of alkaline-electrolyzed and hydrogen-rich water, in a high-fat-diet nonalcoholic fatty liver disease mouse model. *World J Gastroenterol* 2018; 24(45): 5095-5108 Available from: URL: http://www.wjgnet.com/1007-9327/full/v24/i45/5095.htm DOI: http://dx.doi.org/10.3748/wjg.v24.i45.5095

INTRODUCTION

Nonalcoholic fatty liver disease (NAFLD) is considered the hepatic expression of metabolic syndrome, and in most cases, it is associated with obesity, dyslipidemia, diabetes, and insulin resistance[1]. At present, NAFLD is considered the most common liver disease affecting 20%-30% of the Western World's population[1]. The spectrum of NAFLD ranges from simple, apparently benign, hepatic lipid accumulation (simple steatosis) to nonalcoholic steatohepatitis (NASH)[2]. NASH is characterized by inflammation and collagen deposition (fibrosis)[2] and may progress to hepatic tissue damage (cirrhosis)[3]. Generally, the disease remains in the steatotic stage, characterized by an excessive accumulation of triglycerides in the hepatocytes. However, in about 5% to 10% of cases, the disease will progress to NASH, and from there, 10%-25% will develop cirrhosis with about 1% of those patients progressing to hepatocellular carcinoma[4]. The disease's pathogenesis is complex and multifactorial and involves genetic and environmental factors, including altered gut microbiome as part of the multistep pathogenic NAFLD model[4]. Insulin resistance is a key factor in the disease onset resulting in increased hepatic *de novo* lipogenesis (DNL), adipose tissue lipolysis, and inhibition of free fatty acid (FFA) β-oxidation. The reaction of the liver to intracellular lipid buildup results in a cascade of events, including oxidative stress, mitochondrial and endoplasmic reticulum dysfunction, and inflammation[5].

Lifestyle changes that promote weight loss improve disease status; however, this is often difficult to maintain in the long term[6]. At present, there is no specific pharmacological treatment for this disease as most drugs indicated for NAFLD target secondary features of the disease such as obesity, dyslipidemia, and insulin resistance[7]. Due to the high prevalence and increasing NAFLD incidence coupled with the current treatment's ineffectiveness and health risks, the need for a simple and safe alternative is warranted. Regardless of the factors, NAFLD pathogenesis and progression are linked to excessive oxidative stress and inflammation, the attenuation of which may be a viable approach[8].

Hydrogen-rich and electrolyzed alkaline waters (HRW and EAW, respectively) have been reported as types of functional waters that may ameliorate various disease conditions[9]. EAW is produced *via* electrolysis of water. At the cathode (equation 1), water is reduced to hydrogen gas/molecular hydrogen (H_2) and hydroxide ions (OH^-). The OH^- ions cause an increase in the resulting water's pH making it more alkaline. At the anode (equation 2), water is oxidized to oxygen gas

(O_2) and protons (H^+). The increased hydrogen ion (H^+) concentration makes the water acidic. EAW units have a membrane that separates the cathode and anode compartments, without which the resulting pH would be neutral (equation 3).

Cathode reaction: $4H_2O$ (l) + $4e^-$ → $2H_2$ (g) + $4OH^-$ (aq) Equation 1

Anode reaction: $6H_2O$ (l) + $4e^-$ → + O_2 (g) + $4H_3O^+$ (aq) Equation 2

Overall reaction: $2H_2O$ (l) → $2H_2$ (g) + O_2 (g) Equation 3

EAW has been reported to have anti-obesity, anti-oxidant, anti-diabetic, and hepatoprotective effects[10-13]. However, the properties of EAW associated with these beneficial effects have been debated[11-14]. EAW exhibits a negative oxidation-reduction potential (ORP) due to the dissolved hydrogen gas and high pH[11], which is expected according to the Nernst equation. Nevertheless, H_2 is not recognized by some researchers/commercial companies as the principal therapeutic agent in EAW[15].

H_2 has recently been demonstrated to exert therapeutic benefits in animal and human clinical studies in ameliorating excessive inflammation and oxidative stress[16]. It was first confirmed to have therapeutic potential in animals for cancer (hyperbaric chamber)[17] and ischemia-reperfusion (inhalation)[18] in studies published in Science and Nature Medicine, respectively. H_2's potential therapeutic effects have now been confirmed in over 170 different human and animal-disease models and in essentially every organ of the human body[19]. H_2 is nonpolar, hydrophobic, and the smallest molecule, thus allowing it to quickly diffuse through cell membranes and reach the mitochondria, nucleus, endoplasmic reticulum, and other subcellular compartments[20]. These properties make it an attractive molecule for NAFLD treatment[21]. Although more research is needed to elucidate the molecular mechanism(s) and optimal dosing for H_2, preliminary animal and human studies are promising. Clinical studies of drinking hydrogen-rich water (HRW) have demonstrated beneficial effects in several diseases such as Parkinson's disease, type II diabetes, rheumatoid arthritis, mitochondrial myopathies, muscle fatigue, metabolic syndrome, hyperlipidemia, liver inflammation (hepatitis B) and others reviewed previously[19,22-30]. Clinical studies involving metabolic and liver conditions further support the potential benefits of hydrogen on NAFLD.

Several animal and cells studies concerning NAFLD and hydrogen therapy have been reported using different models. For example, one study[31] using hydrogen-rich saline in a NAFLD rat model induced with hyperglycemia and hyperlipidemia, found H_2 significantly lowered levels of oxidative stress and inflammation[31]. In another study using a methionine-choline-deficient diet-induced NASH model, ingestion of HRW significantly attenuated steatohepatitis to a degree comparable to the drug pioglitazone and suppressed hepatic tumorigenesis in a streptozotocin-induced NASH-related hepatocarcinogenic mouse model[32]. Similar positive effects of H_2 have also been reported in other studies[33,34]. In the present study, we used a different NAFLD animal model induced by a high-fat diet (HFD) which is more relevant to human physiology.

We aimed to determine the influence of both types of functional waters, EAW and HRW, on an HFD-induced-NAFLD model, and the importance of H_2 as a therapeutic factor in EAW. Furthermore, we investigated if pretreatment with HRW could protect cells from further exposure to a high-fat environment.

MATERIALS AND METHODS

Animal and animal care

Animal protocols were approved by the Israeli National Committee for Animal Ethics and Welfare. In all experiments, animals had *ad libitum* access to food and water.

Electrolyzed water on NAFLD

Forty-eight C57bl/6J young male mice (three weeks old, approximately 20 g) were obtained from Harlan Laboratories (Israel). The mice were randomly separated into conventional polycarbonate rodent cages (six animals per cage) and fed a regular diet (RD), which was a commercial purified control diet composed of 17% calories from fat, 23% calories from protein, and 60% calories from carbohydrates (TD 120455, Harlan Laboratories, United States). Conventional polycarbonate bottles with a stainless-steel cap were put on the top of each cage. Cages were maintained at 23 ℃ ± 1 ℃ and 40%-60% humidity under a 12:12 h light:dark cycle. During this time, animals were weighed twice a week to check that there were no differences in the initial growth rate.

After a 2-week acclimation period, mice were divided into four groups (n = 12) according to the type of diet and water: (1) RD/ Regular Water (RW); (2) RD/EAW; (3) HFD/RW; and (4) HFD/EAW. Mice were individually identified by ear punching. The HFD was a purified commercial diet for inducing obesity (TD 06414, Harlan Laboratories, United States) and was composed of 60.3% calories from fat, 21.3% from carbohydrates, and 18.4% from protein. Formula and specific components of both the RD and HFD are shown in Table 1.

EAW was prepared with a Water Ionizer Batch System (BTM-3000, BionTech, Korea). Commercial mineral water (initial pH 7.8) was electrolyzed continuously for 3 h, and the water at the cathode was collected (pH 11 ± 0.48, ORP of -495 ± 27 mV, H_2 ≈ 0.2 mg/L). The water was transferred to feeding bottles and added to the mice's cages. Fresh electrolyzed water was prepared twice a week.

Body weight was measured weekly at 9 AM before the morning feeding using an Ohaus Scout Pro 200 g scale (Nänikon Switzerland). Body composition: fat

Table 1 Composition of the regular and high-fat diet

Ingredients	Ingredient concentration (g/kg)	
	Regular diet	High fat diet
Casein	210.0	265.0
L-cystine	3.0	4.0
High amylose corn starch	500.0	-
Maltodextrin	100.0	160.0
Sucrose	39.14	90.0
Anhydrous milkfat	20.0	-
Lard	20.0	310.0
Soybean oil	20.0	30.0
Cellulose	35.0	65.5
Mineral mix, AIN-93G-MX (94046) (g/kg)	35.0	48.0
Calcium phosphate, dibasic	-	3.4
Vitamin mix, AIN-93-VX (94047)	15.0	21.0
Choline bitartrate	2.75	3.0
TBHQ, antioxidant	0.01	-
Protein (% by weight)	18.6	23.5
Carbohydrate (% by weight)	50.6	27.3
Fat (% by weight)	6.2	34.3

mass (FM), fat-free mass (FFM), and extracellular fluid were measured using time-domain nuclear magnetic resonance (Minispec Analyst AD; Bruker Optics, Silberstreifen, Germany) following a 12 h fast at the end of the acclimation phase and during the experiment at six and 12 wk.

At the end of the experimental period, animals were sacrificed using inhaled isofluorane, and livers were processed for histology and real-time polymerase chain reaction (RT-PCR).

Hydrogen-rich water on NAFLD

Twenty-Four C57bl/6J males (three weeks old, approximately 20 g) were obtained from Harlan Laboratories (Israel). Mice were separated into appropriate cages and fed a RD for two weeks. After this acclimation period, all animals were fed a HFD ad libitum. Mice were then divided into three groups according to the type of water: (1) Group 1 (control group) received regular water; (2) the second group received hydrogen-rich water at low concentration (L-HRW); and (3) the third group received hydrogen-rich water at high concentration (H-HRW). Mice were individually identified by ear punching. Body weight, food consumption, and fluid intake were measured weekly, and at the end of the experiment, livers were processed for histology, RT-PCR and quantification of total fat were done following the protocol by Roopchand *et al*[35].

Preparation and chemical properties of hydrogen-rich water

HRW was prepared using a sachet made of a net cloth containing metallic magnesium (Sigma, St. Louis, United States; 98% turnings) and small natural stones. The sachet was immersed in closed glass bottles containing cold water (4 ℃) that was previously acidified to pH 2.0 with 37% hydrochloride acid (Sigma). The water was vortexed for 1 h, during which time H_2 was produced according to the reaction: $Mg + 2H_2O \rightarrow Mg(OH)_2 + H_2$. The final pH of the solution reached ≈ 11.0 and contained dissolved hydrogen at a concentration of 1.2 mg/L. The solution was then diluted with regular water to make high (0.8 mg/L) and low (0.3 mg/L) concentrations of HRW each at a pH of approximately 8.0.

Each solution was transferred to mice-feeding bottles in which a new magnesium sachet was added. Due to the alkaline pH of the water, the amount of H_2 produced *via* the above reaction was minimal (the rate of escape ≈ rate of production) but was enough to maintain the low and high H_2 concentration for 24 h. Fresh HRW was produced every other day. The sachets kept in the feeding bottles were rinsed with 5% acetic acid followed by RW every time the water was changed. The H_2 concentration in water was measured daily.

Determination of hydrogen concentration in water

The hydrogen concentration in water was determined with H_2Blue (H_2Sciences Inc., United States), which is a redox titration reagent composed of methylene blue and a colloidal platinum catalyst[36].

Liver histology

After dissection, the liver was cut into small pieces, immersed in 4% paraformaldehyde at room temperature for 24 h, and then stored at 4 ℃ for 24 h. Samples were dehydrated with ethanol and cleared with xylene and embedded in paraffin. Five-micrometer sections were cut and stained with Hematoxylin and Eosin (HE). Pictures of 4-6 different fields per sample were taken under an Axiovert40-CFL (Zeiss, Germany) microscope equipped with a digital camera (AxioCam MRC, Germany).

Real-time polymerase chain reaction

Total RNA was extracted using Tri-Reagent (T-9424, SIGMA). One microgram of RNA from each sample was

Table 2 Primers used in this study

Gene marker	Full name	Primer sequence (5'-3')
β-*Actin*	Beta-actin	GCCCTGGACTTCGAGCAAGA
		TGCCAGGGTACATGGTGGTG
β-*2m*	Beta-2 microglobulin	TGCTTGTCTCAC TGACCGGCC
		TGGGGGTGAATTCAGTGTGAGCC
SOD2	Super oxide dismutase 2	ACAACAGGCCTTATTCCGCT
		CCCCAGTCATAGTGCTGCAA
SREBP-1c	Sterol regulatory element Binding protein	CACCCTGTAGGTCACCGTTT
		AGAACTCCCTGTCTCCGTCA
ACC1	Acetyl-CoA	GACAGAGGAAGATGGCGTCC
	Carboxylase	TACAACTTCTGCTCGCTGGG
TNF-α	Tumor necrosis	CGTCGTAGCAAACCACCAAG
	Factor-alpha	AGCAAATCGGCTGACGGTG
CRP	C-Reactive Protein	ACTGTGGGGCCAGATGCAAGC
		GGGGCTGAGTGTCCCACCAAC
CAT	Catalase	TCACTCAGGTGCGGACATTC
		TAGTCAGGGTGGACGTCAGT
IL-6	Interleukin-6	TCTATACCACTTCACAAGTCGGA
		GAATTGCCATTGCACAACTCTTT
Adipo	Adiponectin	GACGACACCAAAAGGGCTCA
		GAGGCCATCTCTGCCATCA
AdipoR2	Adiponectin	CTCTGACAGGATTTGGGGTCAA
	Receptor 2	GTGCCCTTTTCTGAGCCGTA

reverse transcribed into cDNA using the Verso cDNA Synthesis Kit (Thermo Fisher Scientific). Quantitative RT-PCR was performed in quadruplicate in 384-well plates using the ABI Prism® 7900HT sequence detection system (Applied Biosystems). Each well contained 2 μL of cDNA template (diluted X 20 after the RT reaction), 2.5 μL SYBR green (Bio-Rad, United States), and 0.25 μL each of both forward and reverse gene-specific primers at 10 μmol/L (primers are listed in Table 2). Beta-2 microglobulin (β2m) and β-Actin were used as endogenous reference genes for normalization. The thermal profile was 95 ℃ for 1 min followed by 40 amplification cycles of 95 ℃ for 15 s and 60 ℃ for 30 s. After that melting curve analysis was done. The resulting Ct values were used to determine the relative gene expression.

In vitro experiments

Hepatocytes from mice that drank H-HRW or RW were isolated by perfusion to test if consumption of H-HRW had a long-term effect.

Twelve C57bl/6J male mice (three weeks old) were obtained from Harlan Laboratories (Israel). Mice were divided into two groups: (1) One that drank HRW (0.8 mg/L) and (2) the second that drank RW; both groups were fed a regular diet. After four weeks, hepatocytes (one mouse from each group) were isolated using perfusion under anesthesia through the portal vein according to Zhang *et al*[37].

The primary hepatocytes were isolated through a two-step collagenase perfusion system as described in a previous report[38]. Isolated hepatocytes from each mouse were seeded in 6-well plates (10^6 cells/wells) for measuring gene expression, and in 12-well plates (200000 cells/well) for the steatosis assay in William's E medium (Sigma, St. Louis, United States) containing 10% fetal bovine serum (FBS) (Invitrogen, Carlsbad, United States). Cells obtained from each mouse were seeded in a different plate. After 3 h, the medium was replaced with fresh medium without FBS, and the plates were prepared for further processing.

Steatosis assay

Cells were exposed overnight to 0.3 mmol/L palmitate-BSA conjugate or BSA as a control (in quadruplicate). Preparation of the palmitate stock solution was carried out as described previously[39]. Briefly, 20-mM palmitate (Sodium Palmitate, SIGMA) stock solution was prepared in 0.01 mol/L NaOH by heating at 80 ℃. A 2 mmol/L FFA-free BSA (Sigma) solution was prepared in ddH_2O and maintained at 37 ℃ in a water bath. A 4 mmol/L FFA/1% BSA (5:1) solution was obtained by complexing the appropriate amount of palmitate stock solution to the BSA at 50 ℃ for another 15 min.

After overnight incubation with BSA-palmitate, the medium was removed, and cells were stained with Oil-Red-O to examine fat accumulation (steatosis)[40]. Plates were washed with cold phosphate-buffered saline and fixed in 4% paraformaldehyde for 1 h. After two changes of 70% ethanol, plates were rinsed in distilled water and stained for 30 min by Oil-Red-O and then placed to dry at room temperature. The stain collected by the cells was then extracted with 100% isopropanol. Steatosis was estimated according to the extracted oil red concentration (determined by measuring the absorbance at 520 nm). The steatosis percentage was determined by dividing the average OD value of experimental wells (treated with palmitate) by the average OD value of control cells (treated with BSA only) × 100. In each assay, two plates (HRW or RW)

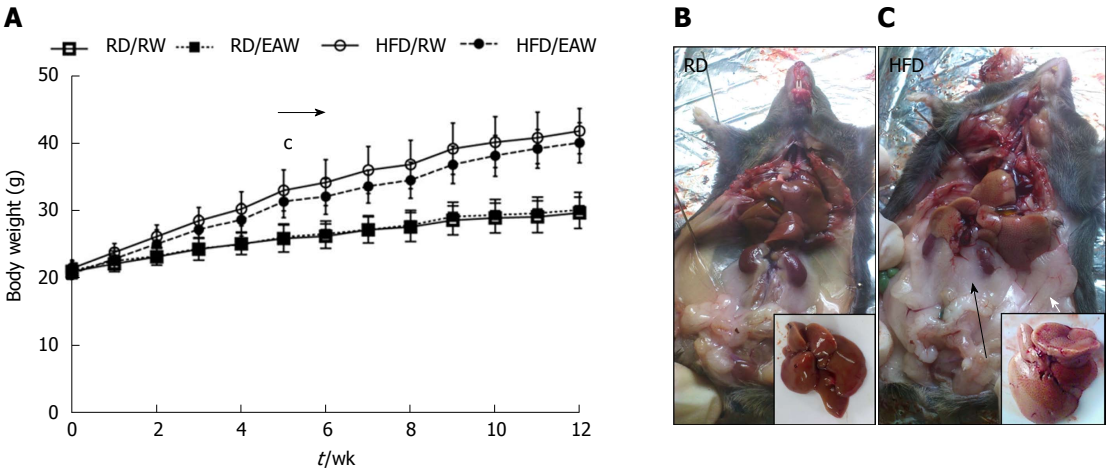

Figure 1 Effect of electrolyzed-alkaline water on body weight and composition. A: Body weight (n = 12, mean ± SD) °shows significant diference between high-fat and regular diets. Mann Whitney and Kruskal-Wallis °P < 0.001); B and C: Ventral view of dissected mice after 12 wk of the experiment. Black arrow: Retroperitoneal fat pads; white arrow epididymal fat pad. Insert: Fresh dissected liver. RW: Regular water; EAW: Electrolysed alkaline water; RD: Regular diet; HFD: High fat diet.

were processed in parallel.

Gene expression

Six-well plates containing 1 × 10^6 cells were used. The cells were exposed to 0.3 mmol/L bovine serum albumin-palmitate conjugate for 4 h, after which RNA was extracted from cells as described above.

Statistical analysis

Data are expressed as mean values ± SD. Data were analyzed by Kruskal-Wallis nonparametric test followed by a Mann-Whitney nonparametric test. A P-value ≤ 5% is considered statistically significant. The data were analyzed using the SPSS version 24 (SPSS Inc., Chicago, IL, United States). The statistical methods of this study were reviewed by Ms. Adi Sharabi-Nov of Tel -Hai Academic College.

RESULTS

Effect of EAW on body weight and composition

Water and food intake were measured for the entire group (n = 12) and calculated for each mouse once per week. As expected, mice fed an HFD showed a high-calorie intake when compared to mice fed chow (10.65 kcal/mouse/d *vs* 8.30 kcal/mouse/d, P < 0.01). Daily water intake was similar in mice drinking RW and EAW (2.49 mL/ mouse).

Mice fed an HFD had higher body weights compared to RD mice. Significant body weight differences were observed from the fifth week until the end of the experiment (Figure 1). At the end of 12 wk, the weight was 72% greater in HFD mice than in RD mice (P < 0.001). The differences in final body weight were due to an increase in fat mass. Larger retroperitoneal and epididymal fat pads were detected in HFD mice. The HFD also affected liver morphology. Livers from mice maintained on a regular diet were dark red/brown and showed a clear and homogeneous texture. Livers from mice fed an HFD were light brown and showed a heterogenic flocculent texture. There was no difference in the weight of mice drinking RW or EAW in either group.

Body composition measurements based on NMR are shown in Figure 2. After 12 wk on different diets, the mice fed a HFD contained more fat (21.7 g ± 2.5 g) than RD mice (8.1 g ± 1.7 g. (P < 0.001). However, FFM was similar in both groups (16.5 g ± 0.8 g and 15.1 g ± 1.2 g in RD and HFD, respectively). EAW did not affect body composition of mice in either the RD or the HFD group.

EAW water effects on liver histology

The HE stained sections from livers are shown in Figure 3. Most of the liver parenchyma of HFD mice (Figure 3C and D) was steatotic with many enlarged cells, which were distributed among the remaining normal parenchyma. The enlarged hepatocytes showed micro- and macrovesicular steatosis. RD-fed mice presented liver parenchyma with no signs of steatosis (Figure 3A and B). EAW water did not affect the liver histology in the RD group or the HFD group.

Effect of HRW on NAFLD development

To evaluate the impact of HRW on NAFLD, we used mice fed an HFD only. Mice were separated into three groups according to the type of water. Control group received RW, and experimental groups received HRW at either low (HRW-L, 0.3 mg/L) or high (HRW-H, 0.8 mg/L) concentration. After 12 wk, mice were sacrificed, and liver histology and gene expression were analyzed. Body weight and composition were measured throughout the experiment.

Water and food consumption

Average water consumption was significantly higher

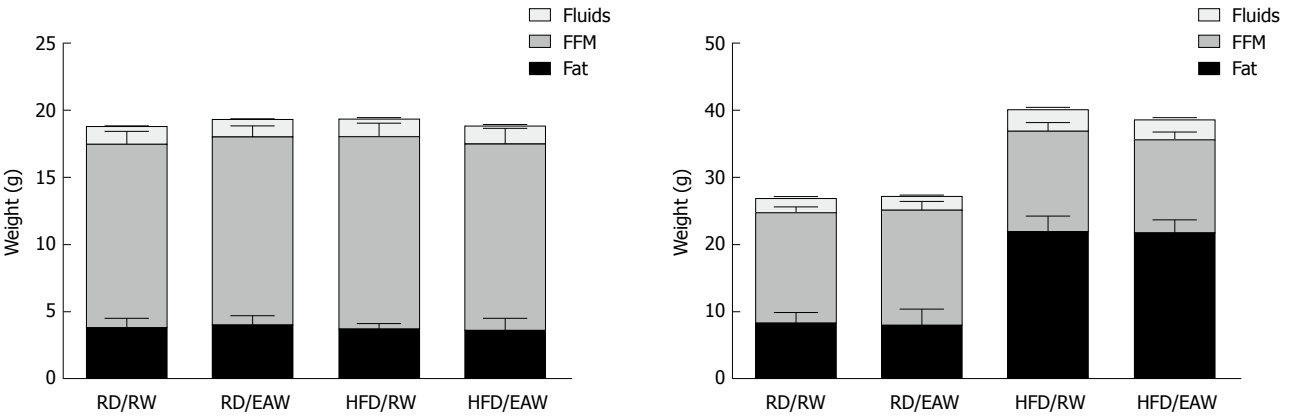

Figure 2 Body mass composition fat, free fatty mass and fluids of mice at different groups (n = 12) before the beginning of the experiment (up) and after 12 wk (down). Data are expressed as mean ± SD. Different letters show significant difference in fat content (Mann Whitney and Kruskal-Wallis $^{a}P < 0.05$). RD/RW: Regular diet/regular water; RD/EAW: Regular diet/electrolysed alkaline water; HFD/RW: High fat diet/regular water; HFD/EAW: High fat diet/electrolysed alkaline water.

for H-HRW group (8.83 mL/mouse/d) than for L-HRW group (3.66 mL/mouse/d), and control group (3.34 mL/mouse/d, P = 0.012). However, the differences in water consumption did not affect appetite and food consumption. All three groups had the same caloric intake consisting of 9.99 kcal/mouse/day for the control group, 9.38 kcal/mouse/day for L-HRW group, and 10.5 kcal/mouse/day H-HRW group (P = 0.505).

Body weight and body composition

All three groups gained weight during the experiment; however, the H-HRW gained less weight compared to the two other groups (P = 0.0567).

Body composition was significantly affected by HFD. As expected, the total body mass of the three groups increased, mainly due to the addition of fat mass. However, mice in the H-HRW group showed a smaller increase in fat tissue when compared to the other two groups (p = 0.002). At the end of the experiment, mice in the H-HRW group showed a body composition of 46% fat mass and 42% lean body mass, compared to 61% fat mass and 28% lean body mass of the control group. There were also no differences in body water content among the three groups (Figure 4). Since the body mass composition of mice in the L-HRW group was similar to the control group, no further analysis of the L-HRW group was performed.

Liver fat content and histology:

Mice that drank H-HRW water accumulated significantly (P < 0.01) less hepatic lipids (30.49 mg ± 4.3 mg/300 mg tissue) in comparison to mice that drank RW (48.24 mg ± 6.0 mg/300 mg tissue). This result is corroborated by the histological sections.

Figure 5 shows liver H&E sections of the control group and H-HRW group (two mice from each group, the heaviest and lightest). Each pair of pictures shows the livers of mice of the two different groups that reached a similar total weight. Figure 5A and B show livers of mice in the H-HRW group and control group that achieved final weights of 35.5 g and 35.9 g, respectively. The liver in the control group has visible steatosis, mainly at the periphery of the lobule. In contrast, the liver sections of the H-HRW group hardly developed fat inclusions. Figure 5C and D shows mice livers in the H-HRW group and control group weighing 40.0 g and 40.9 g, respectively. Although both livers are steatotic, the steatosis of the control group is visibly more pronounced. The hepatocytes show microvesicular steatosis at acinar zones 2 and 3; macrovesicular steatosis is most concentrated at zone 1. In contrast, the liver of H-HRW group is characterized by only mild steatosis, mainly at zone 1, and the beginning of microvesicular steatosis at zones 2 and 3.

NAFLD-related genes expression

The effect of HRW on the expression of several genes involved in NAFLD development compared to control is shown in Table 3. Acetyl CoA oxidase (ACOX), a gene related to lipid metabolism, was significantly up-regulated (P < 0.05), while others (such as carnitine palmitoyltransferase 1 (CPT1) and acetyl-CoA carboxylase), did not change significantly. HRW consumption did not alter the expression of the lipogenic enzymes SREBP1-c, fatty acid synthase (FAS) or acetyl-CoA carboxylase (ACC1). The most significant change was in the expression of CD36, which was markedly reduced in the H-HRW group (P = 0.028). Additionally, while the expression of adiponectin receptor 2 (AdipoR2) did not change significantly, a significant increase in adiponectin expression was detected (P = 0.022).

Genes related to oxidative stress [such as catalase (CAT) and superoxide dismutase (SOD)] did not change significantly; however, the inflammatory gene tumor necrosis factor (TNF)-α, but not interleukin (IL)-6 was significantly down-regulated. However, when the gene expression was measured after overloading with 0.3 mmol/L BSA-palmitate for 4 h, TNF-α and IL-6 were

Table 3 Expression of genes relevant to nonalcoholic fatty liver disease

Gene	RW		HRW		*P* value
	M	Sd	M	Sd	
IL-6	1.10	0.46	1.17	0.26	0.26
TNF-α	1.19[a]	0.36	0.68[b]	0.22	0.02
SREBP-1c	1.04	0.19	1.02	0.30	0.87
ACOX	1.04[a]	0.21	1.31[b]	0.25	0.04
CD36	1.06[a]	0.28	0.71[b]	0.06	0.02
CPT1	1.08	0.37	1.43	0.40	0.14
ACC2	1.12	0.50	1.05	0.23	0.64
ACC1	1.06	0.14	1.13	0.17	0.13
FAS	1.09	0.42	1.42	0.36	0.29
SOD	1.04	0.17	0.96	0.08	0.86
Cat	1.04	0.21	1.12	0.24	0.80
AdipoR2	1.01	0.22	1.14	0.28	0.23
Adipo	0.92[a]	0.29	1.32[b]	0.38	0.004

Each value is the average of 8 mice after normalization with keeping genes (β2m, β-actin). Statistically significant difference marked by different letters $P < 0.05$ (Kruskal-Wallis, Mann Whitney test). Regular water or hydrogen-rich water.

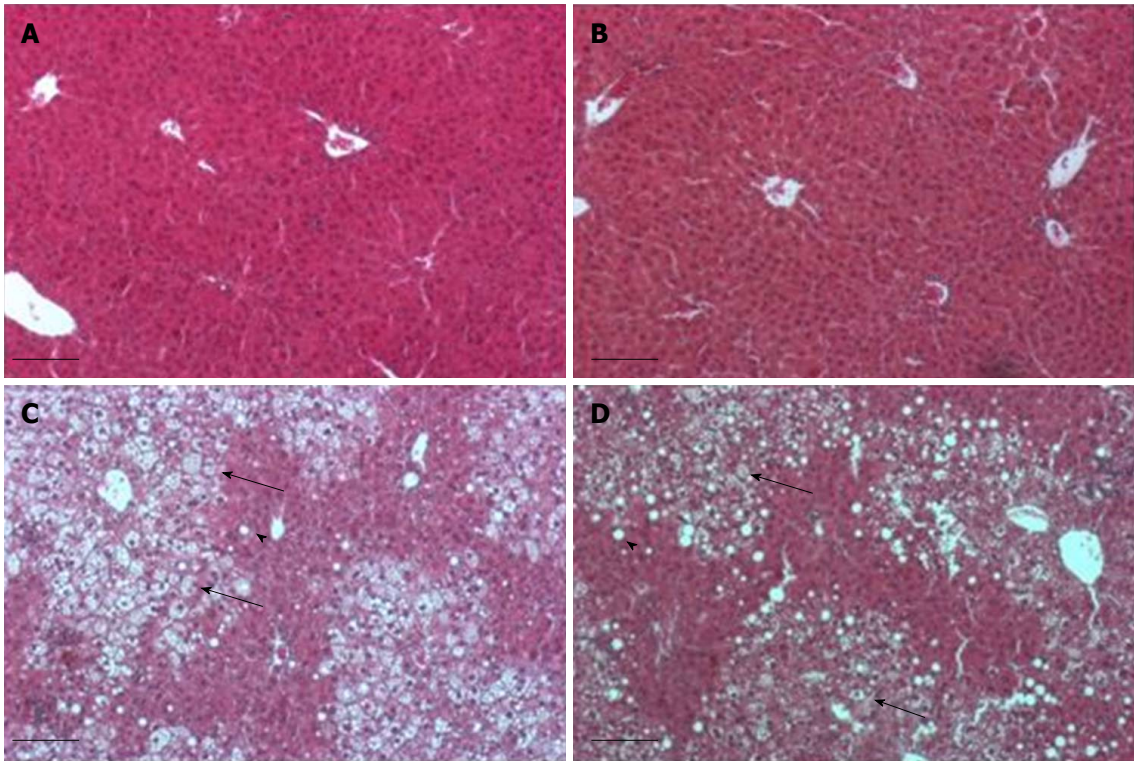

Figure 3 Histological sections stained by hematoxylin eosin of livers from mice fed regular diet and regular water (A), regular diet and electrolyzed alkaline water (B), high fat diet and regular water (C), high fat diet and electrolyzed alkaline water (D). Note the prominent steatosis in mice fed on high-fat diet. Microvesicular inclusions (big arrow), macrovesicular inclusion (small arrow).

both significantly down-regulated ($P = 0.036$ and $P = 0.002$, respectively) as shown in Table 4.

Long-term influence of HRW on hepatocytes

To investigate the long-term effects of HRW on hepatocytes, we extracted cells from different mice drinking either HRW or regular water and compared the fat accumulation after exposing them overnight to 0.3 mmol/L BSA-palmitate *in vitro*. There was less fat accumulation ($P = 0.057$) in the hepatocytes from the mice that drank HRW (44.0% ± 18.6%) compared to hepatocytes from mice that drank regular water (52.8% ± 20.9%).

DISCUSSION

The high prevalence of NAFLD and the lack of safe and effective treatments have resulted in the search for natural alternative methods. The claims of purported functional waters for human health have increased in

Table 4 Expression of genes relevant to nonalcoholic fatty liver disease from hepatocytes isolated from mice drinking regular water or hydrogen-rich water after palmitate overloading *in vitro*

	RW		HRW		
	M	Sd	M	Sd	*P* value
TNF-α	9.16[a]	1.90	5.71[b]	4.59	0.036
IL-6	3.2[a]	0.87	2.24[b]	0.64	0.002
CRP	0.96	0.28	1.20	0.34	0.065
SREBP-1c	0.96	0.12	1.05	0.19	0.196
ACC1	0.84	0.18	0.86	0.14	0.902
SOD	1.07	0.34	1.30	0.56	0.184
AdipoR2	0.80	0.08	0.78	0.18	1.000
Adipo	1.00	0.30	0.79	0.30	0.097

Each value is the average of hepatocytes obtained from 4 different mice after normalization with keeping genes (β2m, β-actin). Statistically significant difference marked by different letters (Kruskal-Wallis, Mann Whitney test).

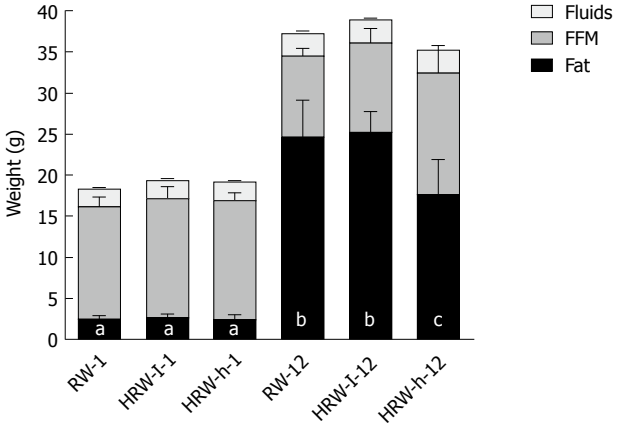

Figure 4 Body mass composition: Fat, fluids and free fatty mass at weeks 1 (first three columns) and 12 (last three columns), (*n* = 8). Data are expressed as mean ± SD. Different letters show a significant difference in fat content (Mann Whitney and Kruskal-Wallis $P < 0.05$). RW: Regular water; HRW-l: Hydrogen-rich water low concentration; HRW-h: Hydrogen-rich water high concentration).

recent years; however, many of these claims are not supported by the scientific literature. Therefore, our study used mice fed a HFD to determine and compare the potential effects of two claimed functional waters (EAW and HRW). We focused on the early stages of NAFLD, a disease associated with obesity and insulin resistance, which has become the leading cause of liver disease affecting adults and children worldwide.

As expected, mice fed a HFD gained significantly more weight (72%) as fat mass with accompanying liver steatosis compared to mice fed a RD. However, contrary to previous findings, using EAW[13], our results found no differences in body weight or liver histology between the regular water group and the EAW group. EAW was prepared by continuous electrolysis (3 h) to optimize its properties (such as pH, ORP, platinum nanoparticles) according to previous protocols[14,41,42]. The resulting water had a high stable pH (11) and a high negative ORP (-495 mV). However, the H_2 concentration in water was only 0.2 mg/L. In this way, mice drinking EAW received high alkaline water with a negative ORP but with only trace amounts of H_2. Due to the non-detectable differences between EAW and RW on body weight or liver parenchyma in either the RD or HFD groups, we did not perform any further analysis (such as gene expression or inflammatory markers).

In contrast to the H_2 concentration in EAW, our method for HRW preparation allowed us to maintain the H_2 concentration. However, L-HRW was also not efficient, but H-HRW was significantly effective at preventing the HFD-induced increase in fat tissue and hepatic lipid accumulation while increasing the amount of lean body mass compared to the control group. We also found that H-HRW significantly abolished the fat inclusions in liver sections, contained fewer triglycerides, and suppressed micro- and macrovesicular steatosis compared to the control. The suppression of fat gain by H-HRW may be attributed to hydrogen's ability to induce the hepatic hormone fibroblast growth factor-21 (FGF21), which causes an increase in energy expenditure[43]. Indeed, administration of FGF-21 can improve obesity and reverse hepatic steatosis[44]. In their study, H_2 water similarly attenuated HFD-induced fatty liver and weight gain in both wildtype and db/db mice. It also reduced hepatic oxidative stress[43].

To understand the mechanism by which H_2 affects NAFLD, we measured the expression of several essential genes related to the disease, including those genes related to oxidative stress, lipid metabolism, and inflammation. From the enzymes related to lipid metabolism, only peroxisomal fatty acyl-CoA oxidase (ACOX) showed significant differences. ACOX is one of the first enzymes in the metabolism of lipids and is a rate-limiting enzyme for beta-oxidation of very-long-chain fatty acids in peroxisomes. The participation of ACOX in suppressing NAFLD is essential. Fan *et al*[45] found that lack of ACOX expression in homozygous (ACOX-/-) mice resulted in liver steatosis, and Kohjima *et al*[46] found that in humans with NAFLD, its expression was increased two-fold, most likely to compensate for the increase in lipid accumulation. We found that mice that drank HRW showed a significant increase in ACOX expression, which would help enhance fatty acid

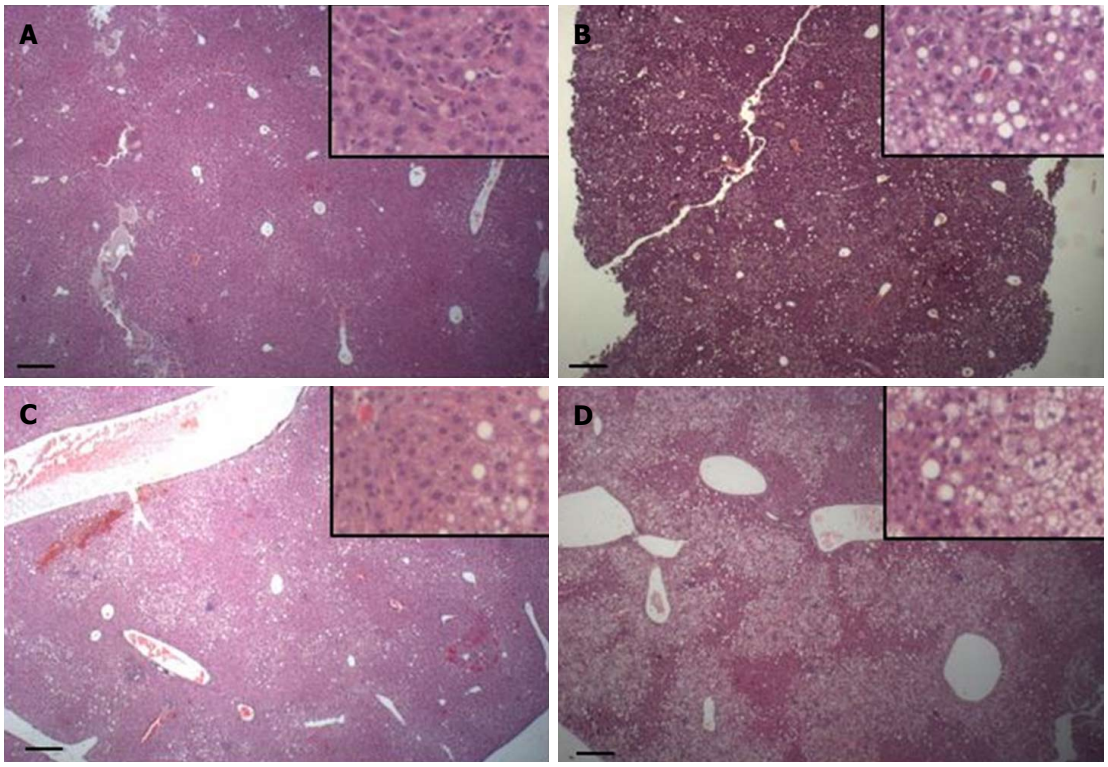

Figure 5 Histological sections of livers (HE) of mice fed a high-fat diet for 12 wk. A and C: Hydrogen-rich water (HRW) group; B and D: Regular water (RW) group. Each row shows sections of different mice that reached a similar weight at the end of the experiment. Note the pronounced steatosis in mice that drank RW in compare to mice of the same weight that drank HRW. Insert detail of each section. Bar = 200 μm HWR: Hydrogen-rich water; RW: Regular water.

oxidation, compared to the control group. The increase in ACOX expression is mediated by the transcription factor peroxisome proliferator-activated receptor[46], which can be upregulated by H_2[31,43].

Fatty acid translocase-36 (CD36), also known as FAT (fatty acid translocase), is a member of the scavenger receptor family and is involved in low-density lipoprotein, long chain fatty acid, and phospholipid oxidation[47]. CD36 expression in normal livers is relatively low; however, it was demonstrated that an increase in CD36 expression is related to a HFD, liver steatosis, and NAFLD. Wilson *et al*[48] showed that CD36 deletion in mice fed a HFD reduced their liver lipid contents and induced insulin resistance, while specific induction of CD36 transport in livers led to hepatomegaly and fatty liver[49]. In our study, HRW significantly caused downregulation of CD36 mRNA expression. Suppression of fatty acid uptake and lipid accumulation in Hep G2 cells overloaded with palmitate through CD36 downregulation at the protein level has been reported to have been induced by HRW[33]; however, contrary to our work, the downregulation was only detected at the protein but not the mRNA level[33].

HRW also influenced the expression of other genes related to *de novo* fatty acid synthesis (such as ACC1, FAS), which are upregulated in NAFLD, and the carnitine palmitoyltransferase 1 gene, which is usually downregulated in NAFLD[46]. Another factor affecting NAFLD is adiponectin, which is a peptide mainly released by adipocytes but also can be released by liver cells[50,51]. When adiponectin binds to its receptor (AipoR2) in the liver, it affects intracellular signaling (resulting in a decrease in *de novo* lipogenesis) and FFA influx by causing downregulation of CD36 expression and increase in FFA oxidation[52]. In addition to those metabolic effects, adiponectin also has anti-inflammatory actions *via* inhibition of TNF-α expression through the nuclear factor-κB pathway[53]. In our study, we found that mice that drank HRW showed an increase in the mRNA expression of adiponectin and a decrease in the mRNA expression of TNF-α. The reduction in TNF-α mRNA expression caused by H_2 in a similar model has been previously reported[32]. In a double-blinded, human crossover study, drinking HRW for eight weeks also increased adiponectin levels[23].

We did not detect an increase in the mRNA expression of the antioxidant enzymes SOD and CAT in the HFD groups that drank RW or HRW. However, NAFLD mice already have higher levels of SOD and CAT that are required to help neutralize the enhanced HFD-induced reactive oxygen species (ROS) production[46]. Although many H_2 studies have reported increased levels of these antioxidants *via* activation of the Nrf2 pathway (reviewed here[19]), in some cases, H_2 causes a decrease in their levels because it mitigates their need by attenuating the assault[54-58]. Thus, HRW may have attenuated some ROS by mitigating the HFD-induced damage, which reduced the need for higher antioxidant levels.

In the *in vitro* study, we checked for a residual effect resulting from drinking HRW that could be reflected in hepatocytes overloaded with palmitate *in vitro*. We compared the function of hepatocytes isolated from mice that were fed regular chow and drank HRW to mice that drank regular water. It has previously been demonstrated that hepatocytes respond to palmitate overload by increasing steatosis and cytokine production[59]. Interestingly, hepatocytes from mice that drank HRW showed less fat accumulation and significantly lower mRNA expression of the cytokines TNF-α and IL-6. Therefore, drinking HRW for four weeks before exposure to palmitate appeared to confer hepatocyte protection to palmitate overload *in vitro*, which may partly be explained by HRW's effects on pro-inflammatory cytokine gene expression. This residual effect was sustained for at least 24 h after animals were sacrificed. A similar result was demonstrated in hydrogen preconditioning of *ex vivo* lung grafts, in which it improved post-transplant graft function[60].

Our study demonstrates that the functional water, HRW, may have the potential for the prevention of NAFLD by attenuating HFD-induced increases in fatty tissues, lipid accumulation in the liver, inflammation, and CD36 expression. However, neither EAW nor L-HRW had beneficial protective effects. This result also confirmed the importance of H_2 as the therapeutic agent in these waters. Effectively, all three waters could be considered HRW at different concentrations. EAW still had a negative ORP due to the presence of H_2, whereas L-HRW only contained 0.3 mg/L, and H-HRW contained 0.8 mg/L. However, the mice in the H-HRW group drank nearly three times more water than L-HRW or control. Due to the higher volume of consumed water and higher concentration, the actual dose of H_2 per day in the H-HRW group would have been significantly more ($\approx$ eight times) than what was ingested in the L-HRW group. It is unknown why mice in the H-HRW group ingested nearly 3 times more water. Perhaps the magnesium/water reaction continued to elevate the pH after our initial measurements, which may then result in an increased thirst sensation. Acidic beverages are generally considered more satisfying to quench thirst than those of higher pH. Additionally, we demonstrated that H_2 pretreatment had a residual protective effect by modifying gene expression and conferring future cytoprotection. H_2 is already in use without any reports of known side effects. However, more research is needed to determine the benefits and optimal dosing to be recognized as a conventional therapy for the prevention and treatment for NAFLD.

ARTICLE HIGHLIGHTS

Research background

Nonalcoholic fatty liver disease (NAFLD) is a major growing metabolic health condition. Conventional pharmaceuticals and drugs are not effective in preventing or treating this disease condition. There is a deep interest in searching for novel, safe, and effective methods to prevent and treat NAFLD. For many years there have been many claims about healthy functional waters including alkaline ionized water, also known as electrolyzed reduced water. Some of those claims suggest it is beneficial for obesity and metabolic disturbances. However, there is a paucity of scientific data on this electrolyzed water, but significant noise and claims by commercial companies marketing and selling it. There are untenable claims about the benefits of high pH, alkaline water, or the oft claimed, albeit impossible, microclustering/structuring of the water. Strong claims have also been made regarding the water's negative oxidation-reduction potential. However, electrolysis of water does produce hydrogen gas at the cathode, and H_2 gas does produce a negative oxidation-reduction potential (ORP). Interestingly, biomedical investigations of molecular hydrogen have demonstrated that this small molecule does have therapeutic potential. Perhaps electrolyzed alkaline water does have beneficial effects, but they are not due to its high alkaline pH or other impossible properties, but due to the presence of dissolved H_2 gas produced during electrolysis. Additionally, molecular hydrogen may be an important molecule to combat against NAFLD.

Research motivation

We first wanted to examine if the claimed functional water, electrolyzed alkaline water, could exert therapeutic effects on a mouse model of NAFLD induced by a high-fat diet. We also wanted to compare these results to water with a similar and a greater concentration of molecular hydrogen. This would allow us to know if electrolyzed water has any beneficial effects on NAFLD, and the importance of molecular hydrogen in that water. Additionally, if molecular hydrogen was shown to be therapeutic as previous studies suggest, then it would add to the body of literature lending support for more research.

Research objectives

To determine the effects of H_2 water in preventing NAFLD development under an obesogenic diet. This is the first step to understanding the efficacy of this approach for preventing and treating the disease.

Research methods

In this research mice under an obesogenic high fat diet were used for developing NAFLD. Control mice ingested regular water while the experimental consumed two types of hydrogen-rich water produced in two different ways: *via* electrolysis with an alkaline water ionizer or *via* a chemical reaction between water and metallic magnesium. General parameters as food and water consumption, body weight and composition were measured during the experiment. In the end, livers were sampled for histology and gene expression measuring by means of RT-PCR. In the *in vitro* experiment hepatocytes obtained from mice drinking either regular water or H_2-rich water were exposed to a high-fat environment in order to check the residual protective effects of H_2-rich water.

Research results

This study demonstrated the positives effects of H_2-rich water on NAFLD. Mice fed a high-fat diet that were drinking H_2-rich water showed less weight gain, more lean body tissue, less steatosis, and better liver histology when compared to the control group. It was also demonstrated that electrolyzed water with a high pH, -ORP, but a low H_2 concentration did not result in any improvement. Hepatocytes derived from mice drinking H_2-rich water were more resilient to palmitate overload *in vitro* when compared to hepatocytes obtained from mice drinking regular water. H_2-rich water positively affected the expression of several NAFLD related genes. However, the mechanism of action of H_2-rich water needs further investigation.

Research conclusions

This study demonstrated that the H_2 dissolved in water is the therapeutic agent in functional waters since electrolyzed water with a high pH and a negative ORP did not show any effect on preventing the development of NAFLD. Apparently, H_2 works at a molecular level since it changed the expression of specific genes related to the disease. This study also demonstrates a long-term protective effect of H_2 in an *in vitro* experiment. Functional water rich in H_2 could be a preventive agent in NAFLD. The Therapeutic aspect of H_2 still need to be elucidated and the optimum dosage determined.

Research perspectives

H_2-rich water is already consumed by humans without any contraindication, which makes it a good candidate for future human clinical studies on NAFLD patients.

ACKNOWLEDGMENTS

We thank Adi Sharabi-Nov for assistance with statistical methods.

REFERENCES

1 **Paschos P**, Paletas K. Non alcoholic fatty liver disease and metabolic syndrome. *Hippokratia* 2009; **13**: 9-19 [PMID: 19240815]

2 **Ahmed M**. Non-alcoholic fatty liver disease in 2015. *World J Hepatol* 2015; **7**: 1450-1459 [PMID: 26085906 DOI: 10.4254/wjh.v7.i11.1450]

3 **Abd El-Kader SM**, El-Den Ashmawy EM. Non-alcoholic fatty liver disease: The diagnosis and management. *World J Hepatol* 2015; **7**: 846-858 [PMID: 25937862 DOI: 10.4254/wjh.v7.i6.846]

4 **Scalera A**, Tarantino G. Could metabolic syndrome lead to hepatocarcinoma via non-alcoholic fatty liver disease? *World J Gastroenterol* 2014; **20**: 9217-9228 [PMID: 25071314 DOI: 10.3748/wjg.v20.i28.9217]

5 **Xu X**, Lu L, Dong Q, Li X, Zhang N, Xin Y, Xuan S. Research advances in the relationship between nonalcoholic fatty liver disease and atherosclerosis. *Lipids Health Dis* 2015; **14**: 158 [PMID: 26631018 DOI: 10.1186/s12944-015-0141-z]

6 **Vilar-Gomez E**, Martinez-Perez Y, Calzadilla-Bertot L, Torres-Gonzalez A, Gra-Oramas B, Gonzalez-Fabian L, Friedman SL, Diago M, Romero-Gomez M. Weight Loss Through Lifestyle Modification Significantly Reduces Features of Nonalcoholic Steatohepatitis. *Gastroenterology* 2015; **149**: 367-378.e5; quiz e14-e15 [PMID: 25865049 DOI: 10.1053/j.gastro.2015.04.005]

7 **Dajani A**, AbuHammour A. Treatment of nonalcoholic fatty liver disease: Where do we stand? an overview. *Saudi J Gastroenterol* 2016; **22**: 91-105 [PMID: 26997214 DOI: 10.4103/1319-3767.178527]

8 **Takaki A**, Kawai D, Yamamoto K. Multiple hits, including oxidative stress, as pathogenesis and treatment target in non-alcoholic steatohepatitis (NASH). *Int J Mol Sci* 2013; **14**: 20704-20728 [PMID: 24132155 DOI: 10.3390/ijms141020704]

9 **Henry M**, Chambron J. Physico-Chemical, Biological and Therapeutic Characteristics of Electrolyzed Reduced Alkaline Water (ERAW). *Water* 2013; **5**(4): 2094-115 [DOI:10.3390/w5042094]

10 **Ignacio RM**, Kang TY, Kim CS, Kim SK, Yang YC, Sohn JH, Lee KJ. Anti-obesity effect of alkaline reduced water in high fat-fed obese mice. *Biol Pharm Bull* 2013; **36**: 1052-1059 [PMID: 23811554 DOI: 10.1248/bpb.b12-00781]

11 **Shirahata S**, Kabayama S, Nakano M, Miura T, Kusumoto K, Gotoh M, Hayashi H, Otsubo K, Morisawa S, Katakura Y. Electrolyzed-reduced water scavenges active oxygen species and protects DNA from oxidative damage. *Biochem Biophys Res Commun* 1997; **234**: 269-274 [PMID: 9169001 DOI: 10.1006/bbrc.1997.6622]

12 **Jin D**, Ryu SH, Kim HW, Yang EJ, Lim SJ, Ryang YS, Chung CH, Park SK, Lee KJ. Anti-diabetic effect of alkaline-reduced water on OLETF rats. *Biosci Biotechnol Biochem* 2006; **70**: 31-37 [PMID: 16428818 DOI: 10.1271/bbb.70.31]

13 **Tsai CF**, Hsu YW, Chen WK, Chang WH, Yen CC, Ho YC, Lu FJ. Hepatoprotective effect of electrolyzed reduced water against carbon tetrachloride-induced liver damage in mice. *Food Chem Toxicol* 2009; **47**: 2031-2036 [PMID: 19477216 DOI: 10.1016/j.fct.2009.05.021]

14 **Shirahata S**, Hamasaki T, Teruya K. Advanced research on the health benefit of reduced water. *Trends Food Sci Technol* 2012; **23**(2): 124-131 [DOI: 10.1016/j.tifs.2011.10.009]

15 **Hamasaki T**, Harada G, Nakamichi N, Kabayama S, Teruya K, Fugetsu B, Gong W, Sakata I, Shirahata S. Electrochemically reduced water exerts superior reactive oxygen species scavenging activity in HT1080 cells than the equivalent level of hydrogen-dissolved water. *PLoS One* 2017; **12**: e0171192 [PMID: 28182635 DOI: 10.1371/journal.pone.0171192]

16 **Slezák J**, Kura B, Frimmel K, Zálešák M, Ravingerová T, Viczenczová C, Okruhlicová Ľ, Tribulová N. Preventive and therapeutic application of molecular hydrogen in situations with excessive production of free radicals. *Physiol Res* 2016; **65** Suppl 1: S11-S28 [PMID: 27643933]

17 **Dole M**, Wilson FR, Fife WP. Hyperbaric hydrogen therapy: a possible treatment for cancer. *Science* 1975; **190**: 152-154 [PMID: 1166304]

18 **Ohsawa I**, Ishikawa M, Takahashi K, Watanabe M, Nishimaki K, Yamagata K, Katsura K, Katayama Y, Asoh S, Ohta S. Hydrogen acts as a therapeutic antioxidant by selectively reducing cytotoxic oxygen radicals. *Nat Med* 2007; **13**: 688-694 [PMID: 17486089 DOI: 10.1038/nm1577]

19 **Ichihara M**, Sobue S, Ito M, Ito M, Hirayama M, Ohno K. Beneficial biological effects and the underlying mechanisms of molecular hydrogen - comprehensive review of 321 original articles. *Med Gas Res* 2015; **5**: 12 [PMID: 26483953 DOI: 10.1186/s13618-015-0035-1]

20 **Ohta S**. Molecular hydrogen as a novel antioxidant: overview of the advantages of hydrogen for medical applications. *Methods Enzymol* 2015; **555**: 289-317 [PMID: 25747486 DOI: 10.1016/bs.mie.2014.11.038]

21 **Takaki A**, Kawai D, Yamamoto K. Molecular mechanisms and new treatment strategies for non-alcoholic steatohepatitis (NASH). *Int J Mol Sci* 2014; **15**: 7352-7379 [PMID: 24786095 DOI: 10.3390/ijms15057352]

22 **Yoritaka A**, Takanashi M, Hirayama M, Nakahara T, Ohta S, Hattori N. Pilot study of H_2 therapy in Parkinson's disease: a randomized double-blind placebo-controlled trial. *Mov Disord* 2013; **28**: 836-839 [PMID: 23400965 DOI: 10.1002/mds.25375]

23 **Kajiyama S**, Hasegawa G, Asano M, Hosoda H, Fukui M, Nakamura N, Kitawaki J, Imai S, Nakano K, Ohta M, Adachi T, Obayashi H, Yoshikawa T. Supplementation of hydrogen-rich water improves lipid and glucose metabolism in patients with type 2 diabetes or impaired glucose tolerance. *Nutr Res* 2008; **28**: 137-143 [PMID: 19083400 DOI: 10.1016/j.nutres.2008.01.008]

24 **Ishibashi T**, Sato B, Rikitake M, Seo T, Kurokawa R, Hara Y, Naritomi Y, Hara H, Nagao T. Consumption of water containing a high concentration of molecular hydrogen reduces oxidative stress and disease activity in patients with rheumatoid arthritis: an open-label pilot study. *Med Gas Res* 2012; **2**: 27 [PMID: 23031079 DOI: 10.1186/2045-9912-2-27]

25 **Ito M**, Ibi T, Sahashi K, Ichihara M, Ito M, Ohno K. Open-label trial and randomized, double-blind, placebo-controlled, crossover trial of hydrogen-enriched water for mitochondrial and inflammatory myopathies. *Med Gas Res* 2011; **1**: 24 [PMID: 22146674 DOI: 10.1186/2045-9912-1-24]

26 **Aoki K**, Nakao A, Adachi T, Matsui Y, Miyakawa S. Pilot study: Effects of drinking hydrogen-rich water on muscle fatigue caused by acute exercise in elite athletes. *Med Gas Res* 2012; **2**: 12 [PMID: 22520831 DOI: 10.1186/2045-9912-2-12]

27 **Nakao A**, Toyoda Y, Sharma P, Evans M, Guthrie N. Effectiveness of hydrogen rich water on antioxidant status of subjects with potential metabolic syndrome-an open label pilot study. *J Clin Biochem Nutr* 2010; **46**: 140-149 [PMID: 20216947 DOI: 10.3164/jcbn.09-100]

28 **Song G**, Li M, Sang H, Zhang L, Li X, Yao S, Yu Y, Zong C, Xue Y, Qin S. Hydrogen-rich water decreases serum LDL-cholesterol levels and improves HDL function in patients with potential metabolic syndrome. *J Lipid Res* 2013; **54**: 1884-1893 [PMID: 23610159 DOI: 10.1194/jlr.M036640]

29 **Xia C**, Liu W, Zeng D, Zhu L, Sun X, Sun X. Effect of hydrogen-

rich water on oxidative stress, liver function, and viral load in patients with chronic hepatitis B. *Clin Transl Sci* 2013; **6**: 372-375 [PMID: 24127924 DOI: 10.1111/cts.12076]

30 **Nicolson GL**, de Mattos GF, Settineri R, Costa C, Ellithorpe R, Rosenblatt S. Clinical Effects of Hydrogen Administration: From Animal and Human Diseases to Exercise Medicine. *Int J Clin Med* 2016; **7** [DOI: 10.4236/ijcm.2016.71005]

31 **Zhai X**, Chen X, Lu J, Zhang Y, Sun X, Huang Q, Wang Q. Hydrogen-rich saline improves non-alcoholic fatty liver disease by alleviating oxidative stress and activating hepatic PPARα and PPARγ. *Mol Med Rep* 2017; **15**: 1305-1312 [PMID: 28098910 DOI: 10.3892/mmr.2017.6120]

32 **Kawai D**, Takaki A, Nakatsuka A, Wada J, Tamaki N, Yasunaka T, Koike K, Tsuzaki R, Matsumoto K, Miyake Y, Shiraha H, Morita M, Makino H, Yamamoto K. Hydrogen-rich water prevents progression of nonalcoholic steatohepatitis and accompanying hepatocarcinogenesis in mice. *Hepatology* 2012; **56**: 912-921 [PMID: 22505328 DOI: 10.1002/hep.25782]

33 **Iio A**, Ito M, Itoh T, Terazawa R, Fujita Y, Nozawa Y, Ohsawa I, Ohno K, Ito M. Molecular hydrogen attenuates fatty acid uptake and lipid accumulation through downregulating CD36 expression in HepG2 cells. *Med Gas Res* 2013; **3**: 6 [PMID: 23448206 DOI: 10.1186/2045-9912-3-6]

34 **Hou C**, Wang Y, Zhu E, Yan C, Zhao L, Wang X, Qiu Y, Shen H, Sun X, Feng Z, Liu J, Long J. Coral calcium hydride prevents hepatic steatosis in high fat diet-induced obese rats: A potent mitochondrial nutrient and phase II enzyme inducer. *Biochem Pharmacol* 2016; **103**: 85-97 [PMID: 26774456 DOI: 10.1016/j.bcp.2015.12.020]

35 **Roopchand DE**, Carmody RN, Kuhn P, Moskal K, Rojas-Silva P, Turnbaugh PJ, Raskin I. Dietary Polyphenols Promote Growth of the Gut Bacterium Akkermansia muciniphila and Attenuate High-Fat Diet-Induced Metabolic Syndrome. *Diabetes* 2015; **64**: 2847-2858 [PMID: 25845659 DOI: 10.2337/db14-1916]

36 **Seo T**, Kurokawa R, Sato B. A convenient method for determining the concentration of hydrogen in water: use of methylene blue with colloidal platinum. *Med Gas Res* 2012; **2**: 1 [PMID: 22273079 DOI: 10.1186/2045-9912-2-1]

37 **Zhang W**, Sargis RM, Volden PA, Carmean CM, Sun XJ, Brady MJ. PCB 126 and other dioxin-like PCBs specifically suppress hepatic PEPCK expression via the aryl hydrocarbon receptor. *PLoS One* 2012; **7**: e37103 [PMID: 22615911 DOI: 10.1371/journal.pone.0037103]

38 **Klaunig JE**, Goldblatt PJ, Hinton DE, Lipsky MM, Trump BF. Mouse liver cell culture. II. Primary culture. *In Vitro* 1981; **17**: 926-934 [PMID: 7309042 DOI: 10.2307/4292596]

39 **Ricchi M**, Odoardi MR, Carulli L, Anzivino C, Ballestri S, Pinetti A, Fantoni LI, Marra F, Bertolotti M, Banni S, Lonardo A, Carulli N, Loria P. Differential effect of oleic and palmitic acid on lipid accumulation and apoptosis in cultured hepatocytes. *J Gastroenterol Hepatol* 2009; **24**: 830-840 [PMID: 19207680 DOI: 10.1111/j.1440-1746.2008.05733.x]

40 **Mehlem A**, Hagberg CE, Muhl L, Eriksson U, Falkevall A. Imaging of neutral lipids by oil red O for analyzing the metabolic status in health and disease. *Nat Protoc* 2013; **8**: 1149-1154 [PMID: 23702831 DOI: 10.1038/nprot.2013.055]

41 **Jun Y**, Teruya K, Katakura Y, Otsubo K, Morisawa S, Shirahata S. Suppression of invasion of cancer cells and angiogenesis by electrolyzed reduced water. *In Vitro Cell Dev-An* 2004; **40**: 79A

42 **Kinjo T**, Ye J, Yan H, Hamasaki T, Nakanishi H, Toh K, Nakamichi N, Kabayama S, Teruya K, Shirahata S. Suppressive effects of electrochemically reduced water on matrix metalloproteinase-2 activities and in vitro invasion of human fibrosarcoma HT1080 cells. *Cytotechnology* 2012; **64**: 357-371 [PMID: 22695858 DOI: 10.1007/s10616-012-9469-7]

43 **Kamimura N**, Nishimaki K, Ohsawa I, Ohta S. Molecular hydrogen improves obesity and diabetes by inducing hepatic FGF21 and stimulating energy metabolism in db/db mice. *Obesity* (Silver Spring) 2011; **19**: 1396-1403 [PMID: 21293445 DOI: 10.1038/oby.2011.6]

44 **Liu J**, Xu Y, Hu Y, Wang G. The role of fibroblast growth factor 21 in the pathogenesis of non-alcoholic fatty liver disease and implications for therapy. *Metabolism* 2015; **64**: 380-390 [PMID: 25516477 DOI: 10.1016/j.metabol.2014.11.009]

45 **Fan CY**, Pan J, Chu R, Lee D, Kluckman KD, Usuda N, Singh I, Yeldandi AV, Rao MS, Maeda N, Reddy JK. Hepatocellular and hepatic peroxisomal alterations in mice with a disrupted peroxisomal fatty acyl-coenzyme A oxidase gene. *J Biol Chem* 1996; **271**: 24698-24710 [PMID: 8798738]

46 **Kohjima M**, Enjoji M, Higuchi N, Kato M, Kotoh K, Yoshimoto T, Fujino T, Yada M, Yada R, Harada N, Takayanagi R, Nakamuta M. Re-evaluation of fatty acid metabolism-related gene expression in nonalcoholic fatty liver disease. *Int J Mol Med* 2007; **20**: 351-358 [PMID: 17671740]

47 **Silverstein RL**, Li W, Park YM, Rahaman SO. Mechanisms of cell signaling by the scavenger receptor CD36: implications in atherosclerosis and thrombosis. *Trans Am Clin Climatol Assoc* 2010; **121**: 206-220 [PMID: 20697562]

48 **Wilson CG**, Tran JL, Erion DM, Vera NB, Febbraio M, Weiss EJ. Hepatocyte-Specific Disruption of CD36 Attenuates Fatty Liver and Improves Insulin Sensitivity in HFD-Fed Mice. *Endocrinology* 2016; **157**: 570-585 [PMID: 26650570 DOI: 10.1210/en.2015-1866]

49 **Musso G**, Gambino R, Cassader M. Recent insights into hepatic lipid metabolism in non-alcoholic fatty liver disease (NAFLD). *Prog Lipid Res* 2009; **48**: 1-26 [PMID: 18824034 DOI: 10.1016/j.plipres.2008.08.001]

50 **Yoda-Murakami M**, Taniguchi M, Takahashi K, Kawamata S, Saito K, Choi-Miura NH, Tomita M. Change in expression of GBP28/adiponectin in carbon tetrachloride-administrated mouse liver. *Biochem Biophys Res Commun* 2001; **285**: 372-377 [PMID: 11444852 DOI: 10.1006/bbrc.2001.5134]

51 **Achari AE**, Jain SK. Adiponectin, a Therapeutic Target for Obesity, Diabetes, and Endothelial Dysfunction. *Int J Mol Sci* 2017; **18** [PMID: 28635626 DOI: 10.3390/ijms18061321]

52 **Polyzos SA**, Kountouras J, Zavos C, Tsiaousi E. The role of adiponectin in the pathogenesis and treatment of non-alcoholic fatty liver disease. *Diabetes Obes Metab* 2010; **12**: 365-383 [PMID: 20415685 DOI: 10.1111/j.1463-1326.2009.01176.x]

53 **Chen B**, Liao WQ, Xu N, Xu H, Wen JY, Yu CA, Liu XY, Li CL, Zhao SM, Campbell W. Adiponectin protects against cerebral ischemia-reperfusion injury through anti-inflammatory action. *Brain Res* 2009; **1273**: 129-137 [PMID: 19362080 DOI: 10.1016/j.brainres.2009.04.002]

54 **Xie K**, Yu Y, Huang Y, Zheng L, Li J, Chen H, Han H, Hou L, Gong G, Wang G. Molecular hydrogen ameliorates lipopolysaccharide-induced acute lung injury in mice through reducing inflammation and apoptosis. *Shock* 2012; **37**: 548-555 [PMID: 22508291 DOI: 10.1097/SHK.0b013e31824ddc81]

55 **Wang T**, Zhao L, Liu M, Xie F, Ma X, Zhao P, Liu Y, Li J, Wang M, Yang Z, Zhang Y. Oral intake of hydrogen-rich water ameliorated chlorpyrifos-induced neurotoxicity in rats. *Toxicol Appl Pharmacol* 2014; **280**: 169-176 [PMID: 24967689 DOI: 10.1016/j.taap.2014.06.011]

56 **Gopinath D**, Gurupriya VS, Aswathi PB, Anu G. Molecular Hydrogen Therapy: A major milestone in Medicine. *World J Pharm Pharma Scien* 2014; **3**: 1201-1205

57 **Yoon YS**, Sajo ME, Ignacio RM, Kim SK, Kim CS, Lee KJ. Positive Effects of hydrogen water on 2,4-dinitrochlorobenzene-induced atopic dermatitis in NC/Nga mice. *Biol Pharm Bull* 2014; **37**: 1480-1485 [PMID: 25177031]

58 **Ning Y**, Shang Y, Huang H, Zhang J, Dong Y, Xu W, Li Q. Attenuation of cigarette smoke-induced airway mucus production by hydrogen-rich saline in rats. *PLoS One* 2013; **8**: e83429 [PMID: 24376700 DOI: 10.1371/journal.pone.0083429]

59 **Chavez-Tapia NC**, Rosso N, Tiribelli C. Effect of intracellular

lipid accumulation in a new model of non-alcoholic fatty liver disease. *BMC Gastroenterol* 2012; **12**: 20 [PMID: 22380754 DOI: 10.1186/1471-230X-12-20]

60 **Noda K**, Shigemura N, Tanaka Y, Bhama J, D'Cunha J, Kobayashi H, Luketich JD, Bermudez CA. Hydrogen preconditioning during ex vivo lung perfusion improves the quality of lung grafts in rats. *Transplantation* 2014; **98**: 499-506 [PMID: 25121557 DOI: 10.1097/TP.0000000000000254]

P- Reviewer: Das U, Tarantino G, Xu CF **S- Editor**: Wang XJ
L- Editor: A **E- Editor**: Huang Y

World Journal of Gastroenterology

Submit a Manuscript: http://www.f6publishing.com

World J Gastroenterol 2018 December 7; 24(45): 5109-5119

DOI: 10.3748/wjg.v24.i45.5109

ISSN 1007-9327 (print) ISSN 2219-2840 (online)

ORIGINAL ARTICLE

Basic Study

Neonatal rhesus monkeys as an animal model for rotavirus infection

Na Yin, Feng-Mei Yang, Hong-Tu Qiao, Yan Zhou, Su-Qin Duan, Xiao-Chen Lin, Jin-Yuan Wu, Yu-Ping Xie, Zhan-Long He, Mao-Sheng Sun, Hong-Jun Li

Na Yin, Hong-Tu Qiao, Yan Zhou, Xiao-Chen Lin, Jin-Yuan Wu, Yu-Ping Xie, Mao-Sheng Sun, Hong-Jun Li, Department of Molecular Biology, Institute of Medical Biology, Chinese Academy of Medical Science and Peking Union Medical College, Kunming 650118, Yunnan Province, China

Feng-Mei Yang, Su-Qin Duan, Zhan-Long He, Primate Experimental Center of the Institute of Medical Biology, Chinese Academy of Medical Science and Peking Union Medical College, Kunming 650118, Yunnan Province, China

ORCID number: Na Yin (0000-0002-9816-2854); Feng-Mei Yang (0000-0002-7695-7453); Hong-Tu Qiao (0000-0002-6965-8391); Yan Zhou (0000-0002-1802-5244); Su-Qin Duan (0000-0002-7685-1691); Xiao-Chen Lin (0000-0003-4249-6879); Jin-Yuan Wu (0000-0001-6125-1821); Yu-Ping Xie (0000-0002-5696-2239); Zhan-Long He (0000-0002-7436-1509); Mao-Sheng Sun (0000-0002-8575-5079); Hong-Jun Li (0000-0001-6941-9852).

Author contributions: Yin N conceived the idea; Sun MS and Li HJ performed the experiments; Zhou Y, He ZL, and Li HJ contributed reagents and funds; Yang FM, Qiao HT, and Duan SQ performed the animal experiment; Wu JY performed all ELISA experiments; Zhou Y and Xie YP performed the viral RNA extraction and qRT-PCR assay experiments; Qiao HT and Lin XC performed the immunofluorescence experiments; Yin N, Yang FM, Zhou Y, and Li HJ drafted, read, corrected, and approved the manuscript; all authors reviewed the manuscript.

Supported by the CAMS Initiative for Innovative Medicine, No. 2016-I2M-1-019; National Natural Science Foundation of China, No. 31700154; Major Science and Technology Special Project of Yunnan Province (Biomedicine), No. 2018ZF006; Science and Technology Project of Yunnan Province-general program, No. 2016FB034; Science and Technology Innovation Team Project of Kunming, No. 2016-2-R-07674; the Project of National Nonprofit Scientific Institutes Basic Scientific Service Fee, No. 2016ZX310179-4; Science and Technology Project of Yunnan Province, Key New Product Development, No. 2014BC008.

Institutional review board statement: This study was reviewed and approved by the Institute of Medical Biology, Chinese Academy of Medical Science and Peking Union Medical College Institutional Review Board.

Institutional animal care and use committee statement: All procedures involving animals were reviewed and approved by the Institutional Animal Care and Use Committee (IACUC) of the Institute of Medical Biology, Chinese Academy of Medical Science and Peking Union Medical College.

Conflict-of-interest statement: The authors do not have a commercial or other association that might pose a conflict of interest.

Data sharing statement: No additional data are available.

ARRIVE guidelines statement: The manuscript was prepared and revised according to the ARRIVE guidelines.

Manuscript source: Unsolicited Manuscript

Correspondence author to: Hong-Jun Li, PhD, Academic Research, Department of Molecular Biology, Institute of Medical Biology, Chinese Academy of Medical Science and Peking Union Medical College, No. 935, Jiaoling Road, Kunming 650118, Yunnan Province, China. lihj6912@163.com
Telephone: +86-871-68225391
Fax: +86-871-68225391

Received: August 14, 2018
Peer-review started: August 15, 2018
First decision: October 10, 2018
Revised: October 22, 2018
Accepted: November 7, 2018

Article in press: November 7, 2018
Published online: December 7, 2018

Abstract

AIM

To establish a rotavirus (RV)-induced diarrhea model using RV SA11 in neonatal rhesus monkeys for the study of the pathogenic and immune mechanisms of RV infection and evaluation of candidate vaccines.

METHODS

Neonatal rhesus monkeys with an average age of 15-20 d and an average weight of 500 g ± 150 g received intragastric administration of varying doses of SA11 RV (10^7 PFUs/mL, 10^6 PFUs/mL, or 10^5 PFUs/mL, 10 mL/animal) to determine whether the SA11 strain can effectively infect these animals by observing their clinical symptoms, fecal shedding of virus antigen by ELISA, distribution of RV antigen in the organs by immunofluorescence, variations of viral RNA load in the organs by qRT-PCR, histopathological changes in the small intestine by HE staining, and apoptosis of small intestinal epithelial cells by TUNEL assay.

RESULTS

The RV monkey model showed typical clinical diarrhea symptoms in the 10^8 PFUs SA11 group, where we observed diarrhea 1-4 d post infection (dpi) and viral antigen shed in the feces from 1-7 dpi. RV was found in jejunal epithelial cells. We observed a viral load of approximately 5.85 × 10^3 copies per 100 mg in the jejunum at 2 dpi, which was increased to 1.09 × 10^5 copies per 100 mg at 3 dpi. A relatively high viral load was also seen in mesenteric lymph nodes at 2 dpi and 3 dpi. The following histopathological changes were observed in the small intestine following intragastric administration of SA11 RV: vacuolization, edema, and atrophy. Apoptosis in the jejunal villus epithelium was also detectable at 3 dpi.

CONCLUSION

Our results indicate that we have successfully established a RV SA11 strain diarrhea model in neonatal rhesus monkeys. Future studies will elucidate the mechanisms underlying the pathogenesis of RV infection, and we will use the model to evaluate the protective effect of candidate vaccines.

Key words: Rotavirus; Neonatal rhesus monkey; Animal model; Infection; Diarrhea

Core tip: Rotavirus (RV) is one of the main pathogens responsible for severe diarrhea in children under 5 years of age. Vaccine-induced immunity is an effective way to block RV disease. Nonhuman primates are the animals most closely related to humans and have advantages over non-primates as an animal model of RV diarrhea, so development of a nonhuman primate animal model of RV infection is needed to ensure the effectiveness and safety of these vaccines. Our current study has indicated that RV SA11 can lead to obvious diarrhea and pathological changes in the intestine of neonatal rhesus monkeys. The RV infection model we established is useful for us to further investigate the RV infection mechanism and the associated immune mechanisms in human infants and evaluate the cross protection of potential HRV vaccine candidates.

Yin N, Yang FM, Qiao HT, Zhou Y, Duan SQ, Lin XC, Wu JY, Xie YP, He ZL, Sun MS, Li HJ. Neonatal rhesus monkeys as an animal model for rotavirus infection. *World J Gastroenterol* 2018; 24(45): 5109-5119 Available from: URL: http://www.wjgnet.com/1007-9327/full/v24/i45/5109.htm DOI: http://dx.doi.org/10.3748/wjg.v24.i45.5109

INTRODUCTION

As the primary cause of severe acute gastroenteritis in infants and young children, rotavirus (RV) is one of the most important causes of pathogenicity worldwide[1]. RV infection can result in vomiting, fever, severe dehydration, diarrhea, and even death. Over 200000 infants and young children die each year due to RV infection worldwide, and low-income countries are disproportionately affected[2].

There are currently no specific drugs for the treatment of diarrhea caused by RV infection[3]; therefore, the development of safe and effective vaccines to control RV infection is particularly important[4-7]. Furthermore, an effective animal model of RV infection is needed to ensure the effectiveness and safety of these vaccines. Nonetheless, some progress has been made in the development of animal RV models, and have included gnotobiotic piglets, calves, lambs, suckling mice, and rabbits. While RV infection in calves and lambs results in mild clinical disease[8-10], gnotobiotic piglets are more susceptible to RV infection, since their immune system more closely resembles that of a human infant, and the period of susceptibility is very long[11-13]. However, breeding conditions for gnotobiotic piglets are quite strict and their cost is prohibitively high, restricting the study of RV infection in these animals. Suckling mice and rabbits have also been used to study RV infection[14-18] and they have strong reproductive abilities and are easy to maintain; however, these animal models have a distant evolutionary relationship with humans, which can limit the ability of data obtained from these animal models to improve the understanding of the pathogenesis of RV infection in humans. Therefore, developing models using non-human primates, the species more closely related to humans, is necessary[19-23].

The SA11 strain is a simian RV strain, obtained from an asymptomatic vervet monkey *in vitro*[24]. As described before, the SA11 strain can infect not only non-human primates, such as chimpanzee, macaque (cynomolgus monkey and rhesus monkey)[20,21], but also other non-primates, such as mice[14]. Petschow *et al*[25] inoculated five newborn cynomolgus monkeys with the simian RV strain SA11, and detected SA11 in feces of three monkeys for up to 2 d after inoculation. In this study, we infected the neonatal rhesus monkeys with RV SA11 through oral gavage to establish an RV diarrhea model. Our data indicated that 10^8 plaque forming units (PFUs) of SA11 can infect intestinal villous epithelial cells in neonatal rhesus monkeys, and result in obvious pathological changes in the small intestine as well as clinical symptoms including diarrhea. Together, these findings indicate that the neonatal rhesus monkey could be used as an animal model for RV infection, providing a powerful tool for further study of the pathogenesis of RV and the associated immune mechanisms in human infants and evaluation of RV vaccines.

MATERIALS AND METHODS

Ethics statement and experimental animals

The experimental animals in this study were provided by the Primate Experimental Center of the Institute of Medical Biology, Chinese Academy of Medical Sciences. A total of 12 healthy neonatal rhesus monkeys with an average age of 15-20 d and an average weight of 500 g ± 150 g were randomly divided into three experimental groups and a control group, each with three monkeys. The experimental animal procedures were performed in accordance with the guidelines of the Institutional Animal Care and Use Committee (IACUC) of the Institute of Medical Biology, Chinese Academy of Medical Sciences. A neutralizing antibody test was conducted to confirm that the monkeys did not have antibodies against RV SA11 prior to the study. All of the animals were housed in a separate incubator one week before the initiation of the experiment.

Neutralization test

The activated RVs were adjusted to 1000 PFUs/100 μL in serum-free MEM. The serum samples were diluted from 1:10 to 1:1280 in 100 μL serum-free MEM. The diluted RVs and serum samples were mixed with each and incubated at 37 ℃ for 1 h. The mixtures were transferred to the 96-well plates covered with a confluent monolayer of MA104 cells and were cultured at 37 ℃ for 5 d. The cultures were completely transferred to the wells of the ELISA plate coated with a goat anti-RV polyclonal antibody (Millipore, AB1129) and blocked with 3% (w/v) BSA (Biosharp, BS043D). The cultures were inoculated at 37 ℃ for 1 h. A rabbit anti-RV polyclonal antibody (prepared by the Department of Molecular Biology, Institute of Medical Biology, Chinese Academy of Medical Science and Peking Union Medical College) conjugated with horseradish peroxidase (HRP) was used to detect RV antigen at a dilution of 1:2000 (v/v) in PBS at 37 ℃ for 1 h. All ELISA plates were developed using TMB (TIANGEN, PA107-01) to generate a colorimetric reaction and terminated with 2 mol/L H_2SO_4. The absorbance was read on a universal microplate reader (El × 800, Bio-Tek, United States) at 450 nm and 630 nm. A serum specimen was determined to be positive if the OD value was less than or equal to two times the average OD value of the negative control. The neutralization titers were defined as the highest dilution.

Cells and virus

MA104 cells were maintained in MEM supplemented with 10% fetal bovine serum (Gibco, 16000-044) and grown to a confluent monolayer in roller bottles (850 cm^2) (CORNING, 430849). The RV strain used in this study was standard strain SA11 (G3P[2]) that was originally isolated from a monkey. Prior to infection, SA11 was activated with 20 μg/mL trypsin (Gibco, 15090-046) at 37 ℃ for 45 min. Infected cultures were harvested by freezing at -20 ℃ and thawing at room temperature, followed by centrifugation at 8873 *g* for 20 min. The harvested virus titer reached 10^7 PFUs/mL[26].

Inoculation of neonatal rhesus monkeys with SA11

The neonatal rhesus monkeys were inoculated with varying doses of RV SA11 (10^8/10^7/10^6 PFUs/monkey) or 10 mL medium without serum *via* oral gavage (Supplementary Table 1). After the infection, each neonatal rhesus monkey was housed alone in the incubator.

Fecal sample collection and processing

From 0 to 14 d post infection (dpi), the infected neonatal rhesus monkeys were monitored once daily for clinical signs, such as mental status, weight, body temperature, and hair, and diarrhea situation. The fecal samples were collected in a fecal collector by gently pressing the abdomen of the neonatal rhesus monkeys every day. According to the color, hardness, and quantity of the feces, diarrhea was scored from 1 to 4 points[11,15], and > 2 points were considered to be indicative of diarrhea. The fecal sample was suspended in 10% (s/v) cold PBS, followed by centrifugation at 8873 *g* for 20 min, after which the supernatant was collected and stored at -80 ℃ for the subsequent study. At 2 and 3 dpi, one monkey that was infected with 10^8 PFUs of SA11 or medium without serum was killed by electric shock with anesthesia. Two aliquots of each tissue sample, including the heart, liver, spleen, lung, kidney, intestine (duodenum, jejunum, and ileum), and brain, were harvested. One sample was stored in liquid nitrogen and the other was fixed in 10% formalin.

Detection of RV antigen shedding in feces by ELISA

The wells of the ELISA plate were coated with a goat anti-RV polyclonal antibody (Millipore, AB1129) diluted

at 1:1000 (v/v) in carbonate-bicarbonate buffer overnight at 4 ℃. Then, the plates were blocked with 3% (w/v) BSA (Biosharp, BS043D) in PBS at 37 ℃ for 2 h. The fecal samples (100 μL/well) were serially two-fold diluted (dilution range from 1:2 to 1:4096) and incubated at 37 ℃ for 1 h. After washing, a rabbit anti-RV polyclonal antibody conjugated with HRP was used to detect RV antigen at a dilution of 1:2000 (v/v) in PBS at 37 ℃ for 1 h. All of the ELISA plates were developed using TMB (TIANGEN, PA107-01) to generate a colorimetric reaction and terminated with 2 mol/L H_2SO_4. A sample was determined to be positive if the OD value was greater than or equal to two times the average OD value of the negative control.

Histopathological and immunofluorometric assays

The small intestine was fixed in 10% (v/v) formalin in PBS, dehydrated in 70% (v/v) graded ethanol series, and embedded in paraffin before being sectioned at the 4.0 μm thickness for further hematoxylin and eosin staining. Histopathological observation of the small intestine was performed by light microscopy. For immunofluorescence microscopy, tissue sections were deparaffinized in xylene and hydrated through graded ethanol, followed by adding 0.03% (v/v) hydrogen peroxide solution. Antigen retrieval was performed with 0.01 mol/L sodium citrate (pH 6.0). The glass slides were blocked with normal goat serum (BOSTER, SA1006) at a 1:10 dilution for 20 min. Next, the glass slides were incubated with a goat anti-RV polyclonal antibody (prepared by the Department of Molecular Biology, Institute of Medical Biology, Chinese Academy of Medical Science and Peking Union Medical College) at a 1:500 dilution at 37 ℃ for 90 min. The glass slides were incubated with an FITC-labeled rabbit anti-goat IgG antibody (Jackson ImmunoResearch, 705-095-147) at a 1:1000 dilution at 37 ℃ for 60 min. After incubation, the glass slides detected under a fluorescence microscope.

Viral RNA extraction and qRT-PCR assay

Viral RNA was isolated from fresh tissue of experimental animals with Trizol (Ambion, 15596026). Trizol (1 mL) was added to 50-100 mg of fresh tissue and the sample was grinded on the ice with an electric grinder. The homogenized sample was incubated for 5-10 min at room temperature. Chloroform (0.2 mL) was added to the homogenized samples. The tube was shaken vigorously by hands for 15 s and incubated for 15 min at room temperature. Next, the tube was centrifuged at 12000 rpm for 15 min at 4 ℃ and the aqueous phase was transferred to a clean tube. Isopropyl alcohol (0.5 mL) was added to the tubes. Then, the tube was incubated for 10 min at room temperature and centrifuged at 12000 rpm for 10 min at 4 ℃. The supernatant was removed and the RNA was washed with 1 mL of 75% ethanol. The tube was centrifuged at 12000 rpm for 5 min at 4 ℃, and RNA was washed again and dried for 5-10 min at room temperature. Finally, RNA was completely dissolved in 30 μL of RNase-free water and stored at -70 ℃.

At the same time, viral RNA was isolated from venous blood samples using the QIAamp Viral RNA Mini Kit, according to the manufacture's protocol (Qiagen, 52904).

RT-PCR assays were performed using the TransScript II Probe One-Step qRT-PCR SuperMix (TRANS, AQ321-01) in the Real-Time System (CFX96, BIO-RAD, United States). The reaction system included 5 μL of RNA template, forward primer at 20 nm, reverse primer at 20 nm, FAM-labeled probe at 20 nm, and E-mix in a total reaction volume of 20 μL. The sequences for the primers were as follows: forward primer, 5'-GTTGTCATCTATGCATAACCCTC-3'; reverse primer, 5'-ACATAACGCCCCTATAGCCA-3'; FAM-labeled probe, 5'-ATGAGCACAATAGTTAAAAGCTAACACTGTCAA-3'. The following protocol was used for all of the RT-PCR: 5 min at 50 ℃; 30 s at 94 ℃; followed by 40 cycles of 94 ℃ for 5 s and 60 ℃ for 30 s. A standard reference curve was obtained by measurement of standard virus RNA. According to the standard reference curve, the viral load was quantified in each sample.

Detection of apoptosis of small intestine epithelial cells

We detected cell apoptosis in the small intestine of the infected neonatal rhesus monkeys using the TUNEL Bright Green Apoptosis Detection Kit (Vazyme, A112-03), according to the manufacturer's protocol. The analysis of apoptosis was performed by fluorescence microscopy.

RESULTS

Clinical symptoms in SA11-infected neonatal rhesus monkeys

Neonatal rhesus monkeys received intragastric administration of $10^8/10^7/10^6$ PFUs of SA11 or medium without serum. Only the 10^8 PFUs group showed significantly characteristic symptoms, and all of the neonatal rhesus monkeys in that group showed obvious clinical symptoms including depression, dull hair color, lethargy, weakened activity, and diarrhea between 1 and 3 dpi. On day 1, monkeys infected with 10^8 PFUs of SA11 developed diarrhea that was flocculent or watery (Table 1). On day 2 and 3, significant fecal pollution was observed around the anus, and diarrhea symptoms were the most serious. On day 4, obvious symptom relief was observed, physiological characteristics began to improve, diarrhea stopped gradually, and animals recovered to normal excreta. In the 10^7 PFUs group, only one monkey developed severe diarrhea at 1 dpi. None of the neonatal rhesus monkeys infected with 10^6 PFUs of RV or medium without serum developed obvious clinical symptoms of RV infection, and other physiological characteristics, including body temperature and body weight, did not change significantly from 0-4 dpi in the experimental group compared to the control

Table 1 Diarrhea scores of the neonatal rhesus monkeys from 1 d post infection to 4 d post infection

Dose (PFUs)	Monkey ID	Diarrhea score[1]				Mean diarrhea score[2]				Percentage with diarrhea (%)[3]			
		1 dpi	2 dpi	3 dpi	4 dpi	1 dpi	2 dpi	3 dpi	4 dpi	1 dpi	2 dpi	3 dpi	4 dpi
10^8	17020	4	4	3	2								
	17011	3	4	4	-	3.67	4	3.5	-	100	100	100	-
	17015	4	4	-	-								
10^7	17018	2	0	0	1								
	17003	2	0	0	1	2.67	0.67	0.33	1	100	33.3	0	0
	17001	4	2	1	1								
10^6	17008	0	2	0	1								
	17012	0	1	2	0	0	1.33	1	0.33	0	33.3	33.3	0
	17016	0	1	1	0								
0	17006	0	0	0	0								
	17002	0	0	0	-	0.33	0	0	-	0	0	0	-
	17004	1	0	-	-								

[1]0 was considered failure to collect feces by gently pressing the abdomen of the neonatal rhesus monkeys (we collected feces from the bottom of the incubator); [2]Mean diarrhea score: The sum of all diarrhea or not-diarrhea scores/n (n = the number of total samples); [3]Percentage with diarrhea (%): The number of diarrhea monkeys/the total number of monkeys in this group. 1 was considered no diarrhea (brown hard feces); 2 was considered common diarrhea (soft feces); 3 was considered severe diarrhea(loose feces); 4 was considered very severe diarrhea (watery feces). -: The monkey was sacrificed for histological analysis.

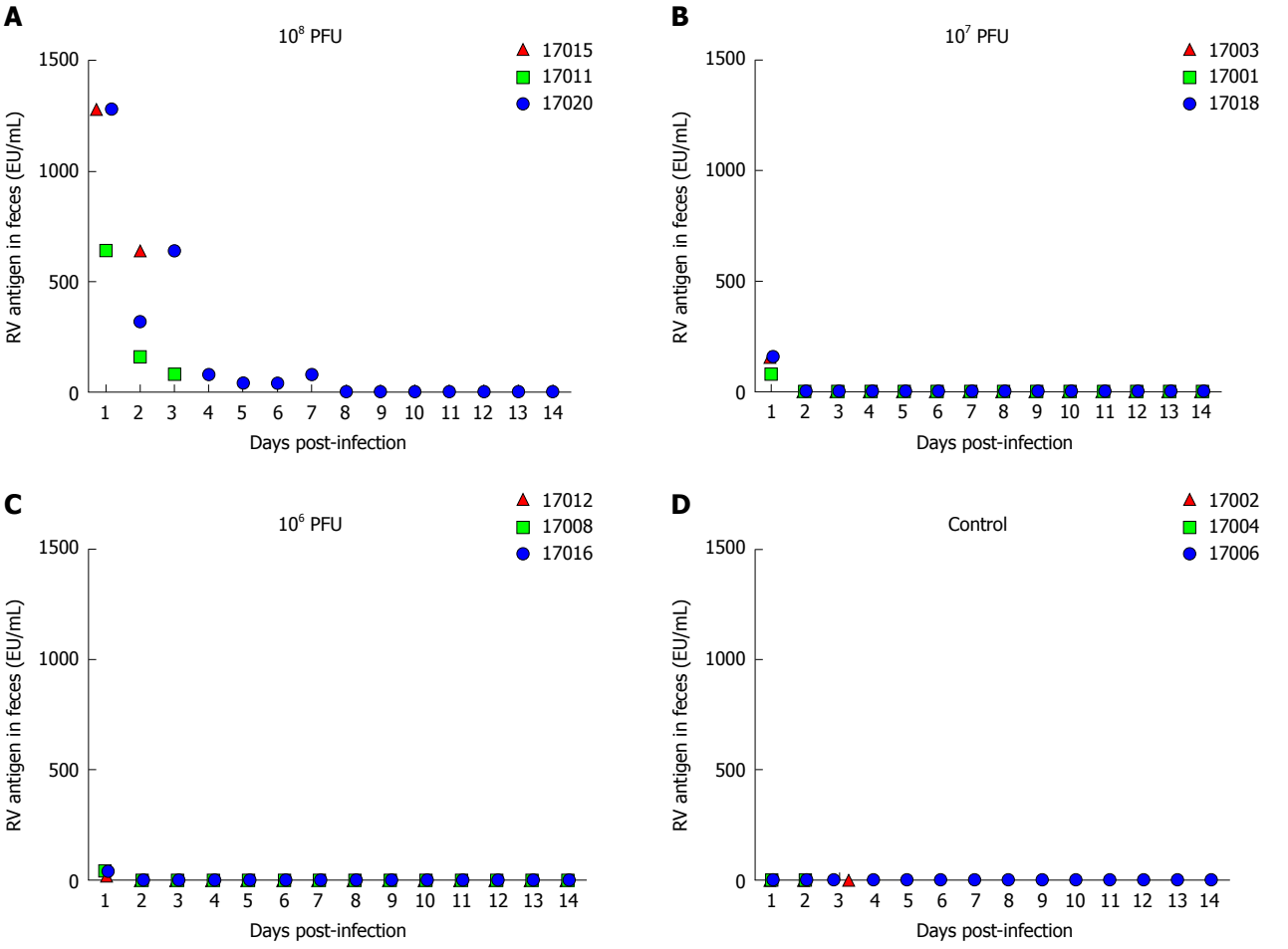

Figure 1 Rotavirus antigen shedding in feces of neonatal rhesus monkeys inoculated with SA11 or medium without serum from 0 dpi to 14 dpi. A: 10 mL of 10^8 PFUs of SA11; B: 10 mL of 10^7 PFUs of SA11; C: 10 mL of 10^6 PFUs of SA11; D: 10 mL of medium without serum. PFUs: Plaque forming units.

group (Supplementary Figure 1).

RV shedding in feces of SA11-infected neonatal rhesus monkeys

RV is transmitted through the fecal-oral route[27]. RV primarily infects human or animal small intestinal villous epithelial cells[28], and is expulsed through feces *in vivo*. The viral shedding observed in the feces reflects the replication and infection level of the virus in the body. We evaluated fecal viral shedding by ELISA in neonatal

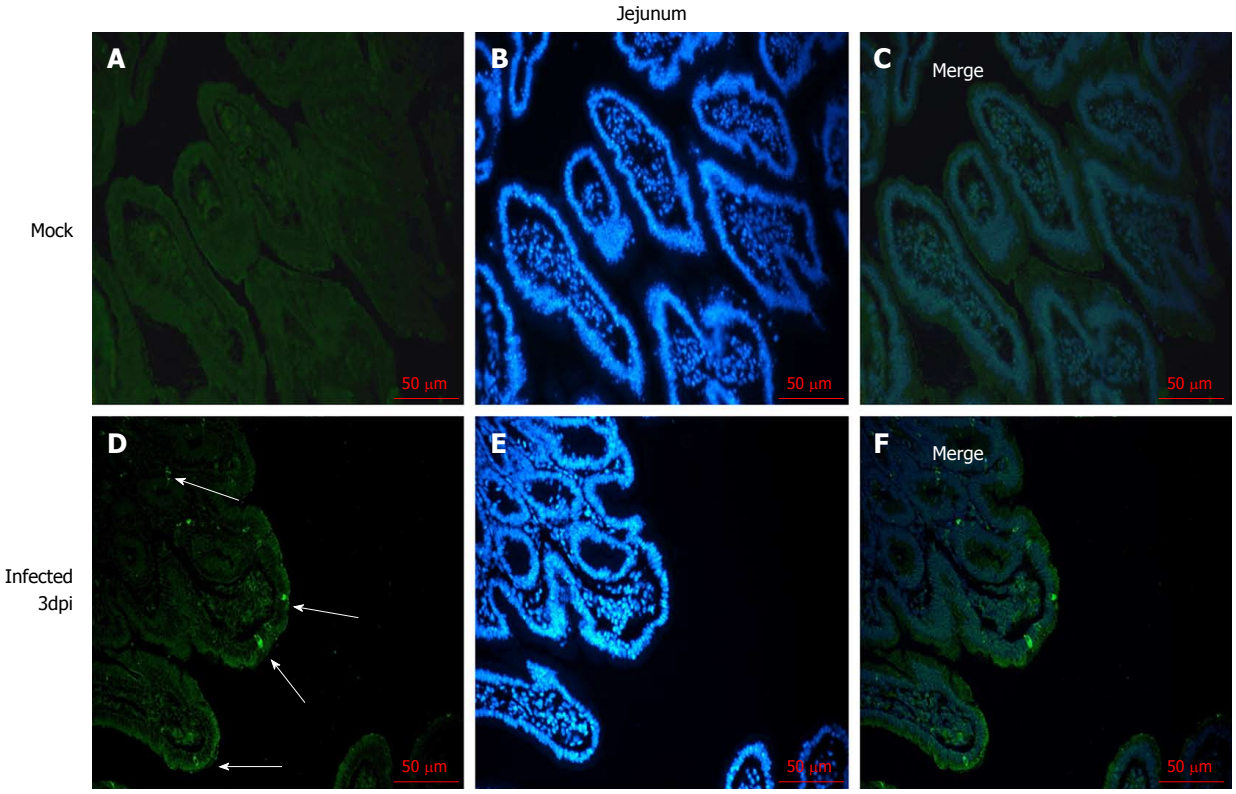

Figure 2 Immunofluorescence of rotavirus antigen in the jejunum of neonatal rhesus monkeys inoculated with SA11 or medium without serum. A-C: The jejunum of neonatal rhesus monkeys inoculated with medium without serum at 3 dpi; D-F: Jejunum of neonatal rhesus monkeys inoculated with 10^8 PFUs of SA11/monkey at 3 dpi. The glass slides were incubated with goat anti-rotavirus (RV) polyclonal antibody and then incubated with rabbit anti-goat IgG antibody labeled with FITC (green). Cell nuclei are shown with DAPI staining (blue). White arrows indicate representative RV-positive cells. Magnification, × 20. Bar: 50 μm.

rhesus monkeys receiving either SA11 or medium without serum. Neonatal rhesus monkeys infected with 10^8 PFUs of SA11 virus shed antigen beginning at 1 dpi and it lasted for 7 days (Figure 1). A small amount of virus antigen was shed in the feces of neonatal rhesus monkeys infected with 10^7 PFUs or 10^6 PFUs of SA11 strain at 1 dpi, and no virus antigen was detected in the control group (Figure 1).

Distribution of RV antigen in the jejunum of SA11-infected neonatal rhesus monkeys

The distribution of RV in the jejunum was detected by immunofluorescence to confirm that the RV infects villus epithelial cells in the small intestine. RV antigen was detected in the jejunal epithelial cells in the 10^8 PFUs of SA11-infected neonatal rhesus monkeys at 3 dpi. No RV antigen was detected in the jejunal epithelial cells in the control group (Figure 2).

Viral load variations in the tissues of SA11-infected neonatal rhesus monkeys

The viral load variations in various organs of the monkeys infected by 10^8 PFUs of SA11 were detected by qRT-PCR at 2 and 3 dpi to understand the transmission and distribution of RV across the various organs. We observed a viral load of approximately 5.85 × 10^3 copies per 100 mg in the jejunum at 2 dpi, which was increased to 1.09 × 10^5 copies per 100 mg at 3 dpi (Figure 3). A relatively high viral load of 9.9 × 10^6 copies per 100 mg was seen in the mesenteric lymph nodes at 2 dpi, but was decreased to 2.42 × 10^6 copies per 100 mg at 3 dpi (Figure 3). A viral load of 1.02 × 10^5 copies per 100 mg in the kidney was detected at 2 dpi, but no viral load was detected in the kidney at 3 dpi (Figure 3). No virus was detected in the heart, liver, spleen, lung, or brain (Supplementary Table 2). We also collected blood samples at 12 h post infection (hpi), 24 hpi, 48 hpi, and 72 hpi, and detected no viral load.

Histopathological changes in the small intestine of SA11-infected neonatal rhesus monkeys

We examined the small intestine of the infected neonatal rhesus monkeys at 2 dpi and 3 dpi to confirm whether RV infection causes histopathological changes, and found inflation and swelling in the small intestine of some infected animals. We collected the tissues (duodenum, jejunum, and ileum) and examined the small intestine by HE staining. We found obvious pathological changes in the small intestinal tissues in the RV SA11 group compared to negative controls, including vacuolization, edema, atrophy, and breakage of the small intestinal villus cells, as well as an absence of obvious inflammatory cell infiltration (Figure 4).

Apoptosis of jejunal epithelial cells increases during SA11 infection

We used the TUNEL method to detect apoptosis of jejunal epithelial cells after SA11 infection. Apoptotic

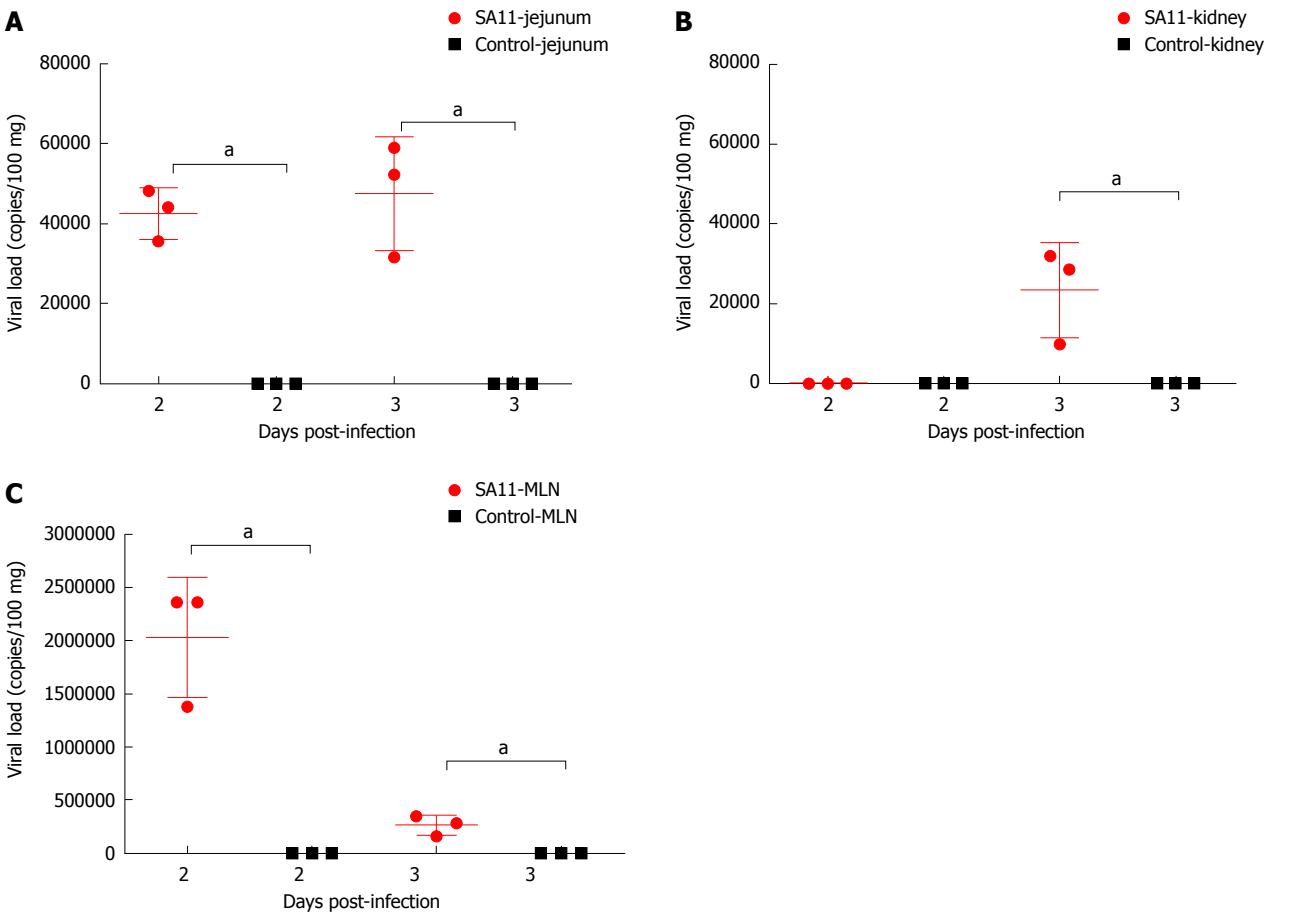

Figure 3 Comparison of viral load in different organs of neonatal rhesus monkeys inoculated with SA11 or medium without serum. A: Viral load in the jejunum of neonatal rhesus monkeys inoculated with SA11 or medium without serum at 2 dpi and 3 dpi; B: Viral load in kidney of neonatal rhesus monkeys inoculated with SA11 or medium without serum at 2 dpi and 3 dpi; C: Viral load in the mesenteric lymph nodes of neonatal rhesus monkeys inoculated with SA11 or medium without serum at 2 dpi and 3 dpi. Data are expressed as the mean ± SD, $n = 3$, $^{a}P < 0.01$.

cells were not observed in the mock infection group (Figure 4). In infected animals, apoptosis of jejunal epithelial cells was not increased at 2 dpi (Figure 4), but at 3 dpi, apoptosis of the upper jejunal villus epithelial cells increased significantly, with apoptotic cells arranged in clusters along the villus top and some apoptotic cells detached from the jejunal villi (Figure 4).

DISCUSSION

A RV diarrhea model is crucial for the study of the pathogenic and immune protection mechanisms of RV infection and vaccine development. Various models have been used to study RV infection; however, these animal models are evolutionarily distant from humans and cannot simulate the process of RV infection in human infants. Therefore, a nonhuman primate RV diarrhea model is needed for the study of human RV infection.

RV infection is age-restricted[17]. We inoculated rhesus monkeys of various ages (15-20 d, 60 d, 120 d, and 1 year) with the same dose of SA11 strain in previous studies. Monkeys with an average age of 15-20 d were more sensitive to the SA11 strain and presented obvious clinical symptoms.

The SA11 is one of classic RVs that several study have used to model infection of newborn animals. They showed that 5×10^6 PFUs infection of newborn mice with 5×10^6 PFUs of RV and infection of newborn rats with 10^8 PFUs could induce obvious diarrhea[29,30]. In our present study, we used different doses of SA11 virus to infect neonatal rhesus monkeys based on our calculation of its median diarrhea dose (DD_{50}; $10^{7.47}$ PFUs/kg), and observed the most obvious symptoms in animals receiving 10^8 PFUs ($3.38DD_{50}$) of the virus. This dose was consistent with that used in newborn mice, after equal conversion of body weight/metering. The clinical symptoms of RV-infected human infants include fever, vomiting, and diarrhea, with the clinical symptoms lasting for 7-14 d[31]. We observed a similar time course in the neonatal rhesus monkeys infected with SA11. Compared to the clinical symptoms observed in RV-infected infants, neonatal rhesus monkeys infected with SA11 suffered from diarrhea only. This symptom developed at 1 dpi, and the most serious diarrhea was observed from 2-3 dpi, which was alleviated and improved from 4 dpi. Viral shedding in the feces occurred from 1-7 dpi, and was the highest at 1 to 3 dpi. RV can cause weight loss in suckling mice during the early stages of infection[32]; however,

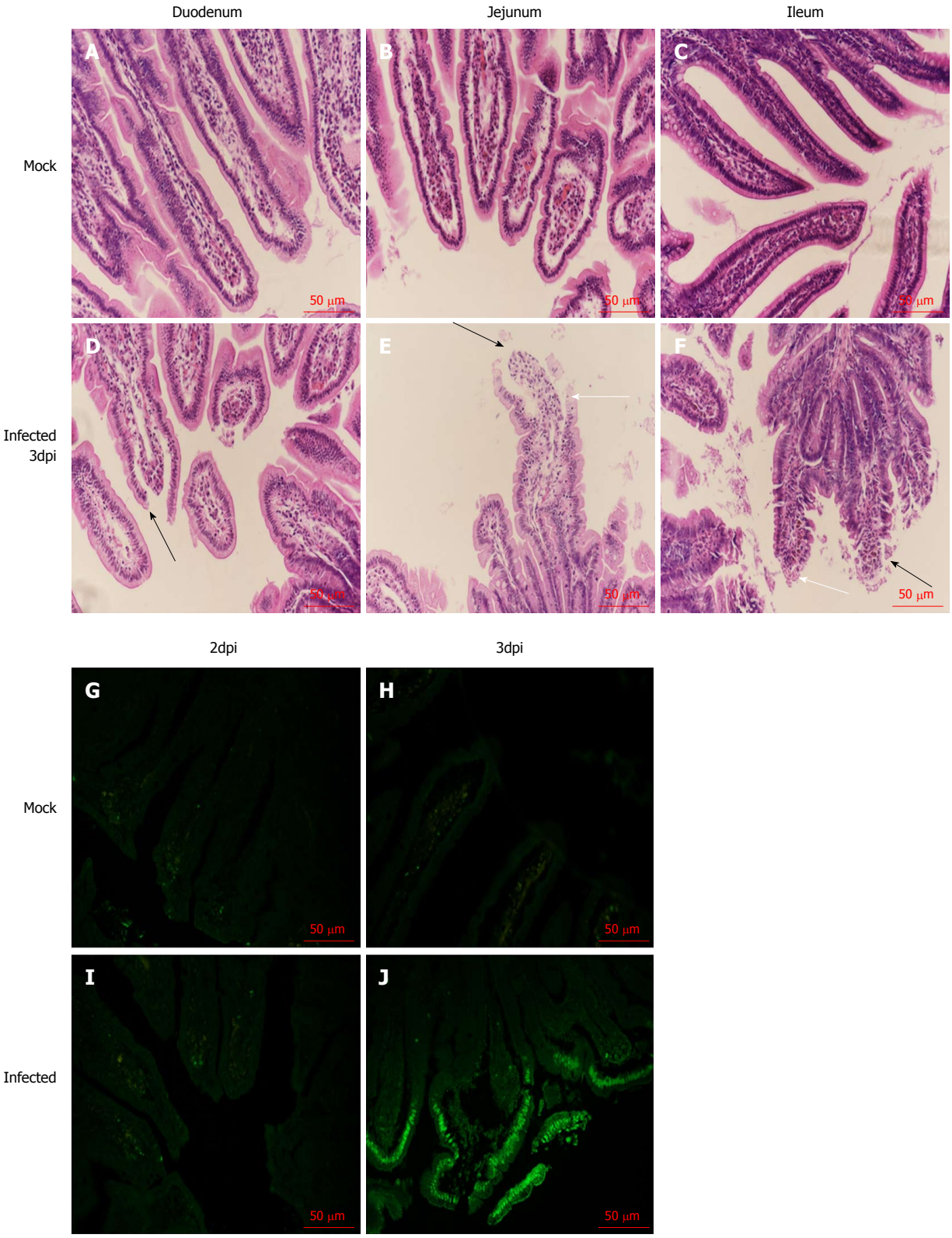

Figure 4 Histopathological changes and apoptosis in the small intestine of neonatal rhesus monkeys infected with SA11 or medium without serum. A: The duodenum of neonatal rhesus monkeys infected with medium without serum at 3 dpi; B: The jejunum of neonatal rhesus monkeys infected with medium without serum at 3 dpi; C: The ileum of neonatal rhesus monkeys infected with medium without serum at 3 dpi; D: The duodenum of neonatal rhesus monkeys infected with 10^8 PFUs of SA11 at 3 dpi; E: The jejunum of neonatal rhesus monkeys infected with 10^8 PFUs of SA11 at 3 dpi; F: The ileum of neonatal rhesus monkeys infected with 10^8 PFUs of SA11 at 3 dpi; histopathological changes in the small intestinal tissues including vacuolization (white arrow), edema, atrophy, and breakage of the small intestinal villus cells (black arrow); G-J: Apoptosis of jejunal epithelial cells during SA11 infection detected by TUNEL assay; G: Inoculated with medium without serum at 2 dpi; H: Inoculated with medium without serum at 3 dpi; I: Inoculated with 10^8 PFUs of SA11 at 2 dpi; J: Inoculated with 10^8 PFUs of SA11 at 3 dpi; the numbers of apoptotic jejunal villus epithelial cells increased significantly at 3 dpi. Magnification: × 20. Bar: 50 μm.

the weight of the neonatal rhesus monkeys infected with SA11 was not significantly lower than that of the negative control group in this study. RV infection in human infants can also cause serious dehydration and even death in the absence of aggressive hydration. However, no monkeys died during these experiments, which may be related to the sensitivity of the virus strain or the immune state of the monkey. RV infection can cause viremia and results in lesions to the liver, gallbladder, respiratory system, nervous system, and urinary system[33]. The occurrence of viremia depends on the virus strain and the immune state of the host[34,35]. RV escapes the gastrointestinal tract through the blood and lymphatic system. Previous reports have detected RV in the blood of some children infected with RV in the clinic[36-38], but no RV was found in the blood following infection in the current study. Furthermore, we determined the viral load of RV in the organs of the infected monkeys at 2 and 3 dpi. Our data showed that a viral RNA load of 1.02×10^5 copies per 100 mg in the kidney was detected at 2 dpi and a relatively high viral load was seen in the mesenteric lymph nodes at 2 dpi. Therefore, we speculate that RV SA11 is capable of escaping from the intestine and transmitted to the kidney *via* the mesenteric lymph nodes. A mechanism of the extra-intestinal spread of RV has been discussed in a report of a neonatal mouse model of RV[39]. Rhesus rotavirus (RRV) and reassortant R7 rotavirus (R7 RV) can spread from the intestine to the terminal ileum, mesenteric lymph nodes, and peripheral tissues. Previous studies suggested that the transmission capacity of RV in the neonatal mouse was related to the NSP3 and VP6 regions[40], and whether they facilitate RV transmission in monkeys remains to be examined.

Diarrhea is one of the most typical symptoms of RV infection. Early studies have shown that RV infection leads to shortened intestinal villi and loss of epithelial cells at the top of the villus[28]. In the current study, a large amount of vacuolization, cell edema, and intestinal villus atrophy, and various degrees of breakage occurred in the villus cells of neonatal rhesus monkeys infected with SA11. Apoptosis of small intestinal epithelial cells is also a cause of diarrhea[41], and apoptosis has been observed in RV-infected HT-29 cells[42-45]. We analyzed the apoptosis of small intestinal epithelial cells after infection, and observed apoptosis in the apical layer of the intestinal villus epithelial cells.

In conclusion, our results indicate that we have successfully established a RV SA11 strain diarrhea model in neonatal rhesus monkeys. The RV infection model we established was useful for us to further investigate the RV infection mechanism and evaluate the cross protection of potential HRV vaccine candidates[29,46].

ARTICLE HIGHLIGHTS

Research background

Rotavirus (RV) is one of the main pathogens responsible for severe diarrhea in children under 5 years of age. There are currently no specific drugs for the treatment of diarrhea caused by RV infection. Therefore, the development of safe and effective vaccines to control RV infection is particularly important. An effective animal model of RV infection is needed to ensure the effectiveness and safety of these vaccines.

Research motivation

Nonhuman primates are the animals most closely related to humans and have advantages over non-primates as an animal model of RV diarrhea, so development of a nonhuman primate animal model of RV infection is needed to ensure the effectiveness and safety of RV candidate vaccines.

Research objectives

To establish a monkey model of RV infection.

Research methods

Neonatal rhesus monkeys with an average age of 15-20 d and an average weight of 500 g ± 150 g received intragastric administration of varying doses of SA11 RV to determine whether the SA11 strain can effectively infect these animals by observing their clinical symptoms, fecal shedding of virus antigen by ELISA, distribution of RV antigen in the organs by immunofluorescence, variations of viral RNA load in the organs by qRT-PCR, histopathological changes in the small intestine by HE staining, and apoptosis of small intestinal epithelial cells by TUNEL assay.

Research results

The RV monkey model showed typical clinical diarrhea symptoms in the 10^8 PFUs SA11 group, where we observed diarrhea 1-4 d post infection (dpi) and viral antigen shed in the feces from 1-7 dpi. RV was found in jejunal epithelial cells. We observed a viral load of approximately 5.85×10^3 copies per 100 mg in the jejunum at 2 dpi, which was increased to 1.09×10^5 copies per 100 mg at 3 dpi. A relatively high viral load was also seen in the mesenteric lymph nodes at 2 dpi and 3 dpi. The following histopathological changes were observed in the small intestine following intragastric administration of SA11 RV: vacuolization, edema, and atrophy. Apoptosis of the jejunal villus epithelium was also detectable at 3 dpi.

Research conclusions

We successfully established a RV SA11 strain diarrhea model in neonatal rhesus monkeys.

Research perspectives

The monkey model of RV infection is useful for us to further investigate the RV infection mechanism and evaluate the protection of potential HRV vaccine candidates.

ACKNOWLEDGMENTS

We thank Jia-Hong Gao for making paraffin sections.

REFERENCES

1 **Crawford SE**, Ramani S, Tate JE, Parashar UD, Svensson L, Hagbom M, Franco MA, Greenberg HB, O'Ryan M, Kang G, Desselberger U, Estes MK. Rotavirus infection. *Nat Rev Dis Primers* 2017; **3**: 17083 [PMID: 29119972 DOI: 10.1038/nrdp.2017.83]

2 **Tate JE**, Burton AH, Boschi-Pinto C, Parashar UD; World Health Organization–Coordinated Global Rotavirus Surveillance Network. Global, Regional, and National Estimates of Rotavirus Mortality in Children <5 Years of Age, 2000-2013. *Clin Infect Dis* 2016; **62** Suppl 2: S96-S105 [PMID: 27059362 DOI: 10.1093/cid/civ1013]

3 **Leung AK**, Robson WL. Acute gastroenteritis in children: role of anti-emetic medication for gastroenteritis-related vomiting. *Paediatr Drugs* 2007; **9**: 175-184 [PMID: 17523698]

4 **Burnett E**, Jonesteller CL, Tate JE, Yen C, Parashar UD. Global Impact of Rotavirus Vaccination on Childhood Hospitalizations and Mortality From Diarrhea. *J Infect Dis* 2017; **215**: 1666-1672 [PMID:

28430997 DOI: 10.1093/infdis/jix186]
5 **Lepage P**, Vergison A. Impact of rotavirus vaccines on rotavirus disease. *Expert Rev Anti Infect Ther* 2012; **10**: 547-561 [PMID: 22702319 DOI: 10.1586/eri.12.39]
6 **Madhi SA**, Cunliffe NA, Steele D, Witte D, Kirsten M, Louw C, Ngwira B, Victor JC, Gillard PH, Cheuvart BB, Han HH, Neuzil KM. Effect of human rotavirus vaccine on severe diarrhea in African infants. *Malawi Med J* 2016; **28**: 108-114 [PMID: 27895844]
7 **Wang CM**, Chen SC, Chen KT. Current status of rotavirus vaccines. *World J Pediatr* 2015; **11**: 300-308 [PMID: 26454434 DOI: 10.1007/s12519-015-0038-y]
8 **Reynolds DJ**, Hall GA, Debney TG, Parsons KR. Pathology of natural rotavirus infection in clinically normal calves. *Res Vet Sci* 1985; **38**: 264-269 [PMID: 2989988]
9 **Archambault D**, Morin G, Elazhary Y, Roy RS. Study of virus excretion in feces of diarrheic and asymptomatic calves infected with rotavirus. *Zentralbl Veterinarmed B* 1990; **37**: 73-76 [PMID: 2161171]
10 **Snodgrass DR**, Ferguson A, Allan F, Angus KW, Mitchell B. Small intestinal morphology and epithelial cell kinetics in lamb rotavirus infections. *Gastroenterology* 1979; **76**: 477-481 [PMID: 218864]
11 **Li JT**, Wei J, Guo HX, Han JB, Ye N, He HY, Yu TT, Wu YZ. Development of a human rotavirus induced diarrhea model in Chinese mini-pigs. *World J Gastroenterol* 2016; **22**: 7135-7145 [PMID: 27610023 DOI: 10.3748/wjg.v22.i31.7135]
12 **Desselberger U**, Huppertz HI. Immune responses to rotavirus infection and vaccination and associated correlates of protection. *J Infect Dis* 2011; **203**: 188-195 [PMID: 21288818 DOI: 10.1093/infdis/jiq031]
13 **Saif LJ**, Ward LA, Yuan L, Rosen BI, To TL. The gnotobiotic piglet as a model for studies of disease pathogenesis and immunity to human rotaviruses. *Arch Virol Suppl* 1996; **12**: 153-161 [PMID: 9015112]
14 **Ciarlet M**, Conner ME, Finegold MJ, Estes MK. Group A rotavirus infection and age-dependent diarrheal disease in rats: a new animal model to study the pathophysiology of rotavirus infection. *J Virol* 2002; **76**: 41-57 [PMID: 11739670]
15 **Boshuizen JA**, Reimerink JH, Korteland-van Male AM, van Ham VJ, Koopmans MP, Büller HA, Dekker J, Einerhand AW. Changes in small intestinal homeostasis, morphology, and gene expression during rotavirus infection of infant mice. *J Virol* 2003; **77**: 13005-13016 [PMID: 14645557]
16 **Du J**, Lan Z, Liu Y, Liu Y, Li Y, Li X, Guo T. Detailed analysis of BALB/c mice challenged with wild type rotavirus EDIM provide an alternative for infection model of rotavirus. *Virus Res* 2017; **228**: 134-140 [PMID: 27932206 DOI: 10.1016/j.virusres.2016.12.001]
17 **Ciarlet M**, Gilger MA, Barone C, McArthur M, Estes MK, Conner ME. Rotavirus disease, but not infection and development of intestinal histopathological lesions, is age restricted in rabbits. *Virology* 1998; **251**: 343-360 [PMID: 9837799 DOI: 10.1006/viro.1998.9406]
18 **Ciarlet M**, Estes MK, Conner ME. Simian rhesus rotavirus is a unique heterologous (non-lapine) rotavirus strain capable of productive replication and horizontal transmission in rabbits. *J Gen Virol* 2000; **81**: 1237-1249 [PMID: 10769066 DOI: 10.1099/0022-1317-81-5-1237]
19 **McNeal MM**, Sestak K, Choi AH, Basu M, Cole MJ, Aye PP, Bohm RP, Ward RL. Development of a rotavirus-shedding model in rhesus macaques, using a homologous wild-type rotavirus of a new P genotype. *J Virol* 2005; **79**: 944-954 [PMID: 15613323 DOI: 10.1128/JVI.79.2.944-954.2005]
20 **Kalter SS**, Heberling RL, Rodriguez AR, Lester TL. Infection of baboons (Papio cynocephalus) with rotavirus (SA11). *Dev Biol Stand* 1983; **53**: 257-261 [PMID: 6307781]
21 **Soike KF**, Gary GW, Gibson S. Susceptibility of nonhuman primate species to infection by simian rotavirus SA-11. *Am J Vet Res* 1980; **41**: 1098-1103 [PMID: 6254409]
22 **Majer M**, Behrens F, Weinmann E, Mauler R, Maass G, Baumeister HG, Luthardt T. Diarrhea in newborn cynomologus monkeys infected with human rotavirus. *Infection* 1978; **6**: 71-72 [PMID: 206515]
23 **Wyatt RG**, Sly DL, London WT, Palmer AE, Kalica AR, Van Kirk DH, Chanock RM, Kapikian AZ. Induction of diarrhea in colostrum-deprived newborn rhesus monkeys with the human reovirus-like agent of infantile gastroenteritis. *Arch Virol* 1976; **50**: 17-27 [PMID: 816334]
24 **MALHERBE H**, HARWIN R. The cytopathic effects of vervet monkey viruses. *S Afr Med J* 1963; **37**: 407-411 [PMID: 13932505]
25 **Petschow BW**, Litov RE, Young LJ, McGraw TP. Response of colostrum-deprived cynomolgus monkeys to intragastric challenge exposure with simian rotavirus strain SA11. *Am J Vet Res* 1992; **53**: 674-678 [PMID: 1326241]
26 **Smith EM**, Estes MK, Graham DY, Gerba CP. A plaque assay for the simian rotavirus SAII. *J Gen Virol* 1979; **43**: 513-519 [PMID: 225432 DOI: 10.1099/0022-1317-43-3-513]
27 **Mayanskiy NA**, Mayanskiy AN, Kulichenko TV. [Rotavirus infection: epidemiology, pathology, vaccination]. *Vestn Ross Akad Med Nauk* 2015; 47-55 [PMID: 26027271]
28 **Lundgren O**, Svensson L. Pathogenesis of rotavirus diarrhea. *Microbes Infect* 2001; **3**: 1145-1156 [PMID: 11709295]
29 **Offit PA**, Clark HF, Kornstein MJ, Plotkin SA. A murine model for oral infection with a primate rotavirus (simian SA11). *J Virol* 1984; **51**: 233-236 [PMID: 6328042]
30 **Guerin-Danan C**, Meslin JC, Lambre F, Charpilienne A, Serezat M, Bouley C, Cohen J, Andrieux C. Development of a heterologous model in germfree suckling rats for studies of rotavirus diarrhea. *J Virol* 1998; **72**: 9298-9302 [PMID: 9765478]
31 **Karampatsas K**, Osborne L, Seah ML, Tong CYW, Prendergast AJ. Clinical characteristics and complications of rotavirus gastroenteritis in children in east London: A retrospective case-control study. *PLoS One* 2018; **13**: e0194009 [PMID: 29565992 DOI: 10.1371/journal.pone.0194009]
32 **Salim AF**, Phillips AD, Walker-Smith JA, Farthing MJ. Sequential changes in small intestinal structure and function during rotavirus infection in neonatal rats. *Gut* 1995; **36**: 231-238 [PMID: 7883222]
33 **Ramig RF**. Pathogenesis of intestinal and systemic rotavirus infection. *J Virol* 2004; **78**: 10213-10220 [PMID: 15367586 DOI: 10.1128/JVI.78.19.10213-10220.2004]
34 **Fenaux M**, Cuadras MA, Feng N, Jaimes M, Greenberg HB. Extraintestinal spread and replication of a homologous EC rotavirus strain and a heterologous rhesus rotavirus in BALB/c mice. *J Virol* 2006; **80**: 5219-5232 [PMID: 16699002 DOI: 10.1128/JVI.02664-05]
35 **Crawford SE**, Patel DG, Cheng E, Berkova Z, Hyser JM, Ciarlet M, Finegold MJ, Conner ME, Estes MK. Rotavirus viremia and extraintestinal viral infection in the neonatal rat model. *J Virol* 2006; **80**: 4820-4832 [PMID: 16641274 DOI: 10.1128/JVI.80.10.4820-4832.2006]
36 **Chitambar SD**, Tatte VS, Dhongde R, Kalrao V. High frequency of rotavirus viremia in children with acute gastroenteritis: discordance of strains detected in stool and sera. *J Med Virol* 2008; **80**: 2169-2176 [PMID: 19040295 DOI: 10.1002/jmv.21338]
37 **Chiappini E**, Azzari C, Moriondo M, Galli L, de Martino M. Viraemia is a common finding in immunocompetent children with rotavirus infection. *J Med Virol* 2005; **76**: 265-267 [PMID: 15834882 DOI: 10.1002/jmv.20351]
38 **Huang XL**, Chen J, Yu YP, Chen LQ, Li ZY, Zhao ZY. [Viraemia and extraintestinal involvement after rotavirus infection]. *Zhejiang Da Xue Xue Bao Yi Xue Ban* 2006; **35**: 69-75 [PMID: 16470924]
39 **Mossel EC**, Ramig RF. A lymphatic mechanism of rotavirus extraintestinal spread in the neonatal mouse. *J Virol* 2003; **77**: 12352-12356 [PMID: 14581572]
40 **Mossel EC**, Ramig RF. Rotavirus genome segment 7 (NSP3) is a determinant of extraintestinal spread in the neonatal mouse. *J Virol* 2002; **76**: 6502-6509 [PMID: 12050363]
41 **Bhowmick R**, Halder UC, Chattopadhyay S, Chanda S, Nandi S, Bagchi P, Nayak MK, Chakrabarti O, Kobayashi N, Chawla-Sarkar M. Rotaviral enterotoxin nonstructural protein 4 targets mitochondria for activation of apoptosis during infection. *J Biol*

Chem 2012; **287**: 35004-35020 [PMID: 22888003 DOI: 10.1074/jbc.M112.369595]
42 **Goodarzi Z**, Soleimanjahi H, Arefian E, Saberfar E. The effect of bovine rotavirus and its nonstructural protein 4 on ER stress-mediated apoptosis in HeLa and HT-29 cells. *Tumour Biol* 2016; **37**: 3155-3161 [PMID: 26427658 DOI: 10.1007/s13277-015-4097-4]
43 **Superti F**, Ammendolia MG, Tinari A, Bucci B, Giammarioli AM, Rainaldi G, Rivabene R, Donelli G. Induction of apoptosis in HT-29 cells infected with SA-11 rotavirus. *J Med Virol* 1996; **50**: 325-334 [PMID: 8950690 DOI: 10.1002/(SICI)1096-9071(199612)50:43.0.CO;2-A]
44 **Frias AH**, Jones RM, Fifadara NH, Vijay-Kumar M, Gewirtz AT. Rotavirus-induced IFN-β promotes anti-viral signaling and apoptosis that modulate viral replication in intestinal epithelial cells. *Innate Immun* 2012; **18**: 294-306 [PMID: 21733977 DOI: 10.1177/1753425911401930]
45 **Chaïbi C**, Cotte-Laffitte J, Sandré C, Esclatine A, Servin AL, Quéro AM, Géniteau-Legendre M. Rotavirus induces apoptosis in fully differentiated human intestinal Caco-2 cells. *Virology* 2005; **332**: 480-490 [PMID: 15680413 DOI: 10.1016/j.virol.2004.11.039]
46 **Torres A**, Ji-Huang L. Diarrheal response of gnotobiotic pigs after fetal infection and neonatal challenge with homologous and heterologous human rotavirus strains. *J Virol* 1986; **60**: 1107-1112 [PMID: 3023662]

P- Reviewer: Krishnan T, Mesquita J **S- Editor**: Wang XJ
L- Editor: Wang TQ **E- Editor**: Huang Y

World Journal of Gastroenterology

Submit a Manuscript: http://www.f6publishing.com

World J Gastroenterol 2018 December 7; 24(45): 5120-5130

DOI: 10.3748/wjg.v24.i45.5120

ISSN 1007-9327 (print) ISSN 2219-2840 (online)

ORIGINAL ARTICLE

Basic Study

Glucocorticoid receptor regulates expression of microRNA-22 and downstream signaling pathway in apoptosis of pancreatic acinar cells

Qiang Fu, Chuan-Jiang Liu, Xu Zhang, Zhen-Sheng Zhai, Yu-Zhu Wang, Ming-Xing Hu, Xian-Ling Xu, Hong-Wei Zhang, Tao Qin

Qiang Fu, Chuan-Jiang Liu, Xu Zhang, Zhen-Sheng Zhai, Yu-Zhu Wang, Ming-Xing Hu, Xian-Ling Xu, Hong-Wei Zhang, Tao Qin, Department of Hepatobiliary and Pancreatic Surgery, People's Hospital of Zhengzhou University (Henan Provincial People's Hospital), School of Medicine, Zhengzhou University, Zhengzhou 450003, Henan Province, China

ORCID number: Qiang Fu (0000-0002-9457-2434); Chuan-Jiang Liu (0000-0001-6766-554X); Xu Zhang (0000-0001-6553-1214); Zhen-Sheng Zhai (0000-0002-2997-5026); Yu-Zhu Wang (0000-0002-7504-6033); Ming-Xing Hu (0000-0001-6262-460X); Xian-Ling Xu (0000-0001-6288-9472); Hong-Wei Zhang (0000-0002- 3848-9222); Tao Qin (0000-0002-1303-9217).

Author contributions: Fu Q and Zhang X performed the majority of experiments; Zhang HW and Qin T designed the research and provided financial support for this work; Liu CJ conducted the experimental analysis; Wang YZ provided vital reagents; Hu MX and Xu XL analyzed sequencing data and developed analysis tools; Fu Q and Qin T wrote the paper.

Supported by National Natural Science Foundation of China, No. 31671440.

Institutional review board statement: This study was reviewed and approved by the Ethics Committee of People's Hospital of Zhengzhou University (Henan Provincial People's Hospital).

Conflict-of-interest statement: We declare that we have no financial and personal relationships with other people or organizations that can inappropriately influence our work, and there is no professional or other personal interest of any nature or kind in any products, service and/or company that could be construed as influencing the position presented in, or the review of, the manuscript.

Data sharing statement: No additional data are available.

ARRIVE guidelines statement: The manuscript has been revised according to the ARRIVE guidelines.

Manuscript source: Unsolicited manuscript

Corresponding author to: Tao Qin, MD, PhD, Doctor, Professor, Department of Hepatobiliary and Pancreatic Surgery, People's Hospital of Zhengzhou University (Henan Provincial People's Hospital), School of Medicine, Zhengzhou University, No. 7, Weiwu Road, Zhengzhou 450003, Henan Province, China. m18937638396@163.com
Telephone: +86-371-65580368
Fax: +86-371-65580368

Received: September 5, 2018
Peer-review started: September 5, 2018
First decision: October 24, 2018
Revised: November 12, 2018
Accepted: November 13, 2018
Article in press: November 13, 2018
Published online: December 7, 2018

Abstract

AIM

To elucidate the underlying mechanism that microRNA-22 (miR-22) promotes the apoptosis of rat pancreatic acinar cells (AR42J) and the elements that regulate the expression of miR-22.

METHODS

One hundred nanomoles per liter of caerulein (Cae) was administrated to induce the apoptosis of AR42J cells and the apoptosis rate was detected by flow cytometry analysis. An amylase assay kit was used to measure the amylase expression level in the supernatant. Quantitative real-time PCR (qRT-PCR) was adopted to measure miR-22 expression. We used online tools to predict the potential transcription promoter of miR-22 and the binding sites, which was further identified by using luciferase reporter analysis, chromatin immunoprecipitation (ChIP) and ChIP-qPCR assays. Then, a mimic of miR-22, Nr3c1 plasmid encoding the glucocorticoid receptor (GR), and si-Nr3c1 were used to transfect AR42J cells, respectively. The mRNA expression of miR-22, Nr3c1, and Erb-b2 receptor tyrosine kinase 3 (ErbB3) was confirmed by qRT-PCR and the apoptosis rate of AR42J cells was detected by flow cytometry analysis. Western blot was used to detect the expression of ErbB3, GR, PI3k, PI3k-p85α, Akt, p-Akt, Bad, Bax, Bcl-xl, Bcl-2, and cleaved caspase3.

RESULTS

After inducing apoptosis of AR42J cells *in vitro*, the expression of miR-22 was significantly increased by 2.20 ± 0.26 and 4.19 ± 0.54 times, respectively, at 3 h and 6 h in comparison with the control group. As revealed by qRT-PCR assay, the expression of miR-22 was 78.25 ± 6.61 times higher in the miR-22 mimic group relative to the miRNA control group, accompanied with an obviously increased acinar cell apoptosis rate (32.53 ± 1.15 *vs* 18.07 ± 0.89, P = 0.0006). The upregulation of miR-22 could suppress its target gene, ErbB3, and the phosphorylation of PI3k and Akt. Furthermore, we predicted the potential transcription promoter of miR-22 and the binding sites using online tools. Luciferase reporter analysis and site-directed mutagenesis indicated that the binding site (GACAGCCATGTACA) of the GR, which is encoded by the Nr3c1 gene. Downregulation of the expression of GR could upregulate the expression of miR-22, which further promoted the apoptosis of AR42J cells.

CONCLUSION

GR transcriptionally represses the expression of miR-22, which further promotes the apoptosis of pancreatic acinar cells by downregulating the downstream signaling pathway.

Key words: MicroRNA-22; Apoptosis; Pancreatic acinar cells; Erb-b2 receptor tyrosine kinase 3; Glucocorticoid receptor

Core tip: The severity of acute pancreatitis (AP) is inversely related to the rate of apoptosis of pancreatic acinar cells. MicroRNA-22 (miR-22) might promote caerulein-induced apoptosis of pancreatic acinar cells (AR42J) *via* down-regulating the expression of its target gene, Erb-b2 receptor tyrosine kinase 3 (ErbB3) and the PI3k/Akt signaling pathway. Glucocorticoid receptor transcriptionally repressed the expression of miR-22 by binding to the miR-22 promoter transcription start site. The upregulation of miR-22 expression resulting from silencing Nr3c1 contributed to the apoptosis of AR42J cells.

Fu Q, Liu CJ, Zhang X, Zhai ZS, Wang YZ, Hu MX, Xu XL, Zhang HW, Qin T. Glucocorticoid receptor regulates expression of microRNA-22 and downstream signaling pathway in apoptosis of pancreatic acinar cells. *World J Gastroenterol* 2018; 24(45): 5120-5130 Available from: URL: http://www.wjgnet.com/1007-9327/full/v24/i45/5120.htm DOI: http://dx.doi.org/10.3748/wjg.v24.i45.5120

INTRODUCTION

Acute pancreatitis (AP), which has had high morbidity and mortality rates in recent years, is characterized by acute inflammatory changes in the pancreas and destruction of the acinar cells[1]. Until now, the pathogenesis of AP has remained unclear. Two patterns of pancreatic acinar cell death (apoptosis and necrosis) are involved in AP[2]. Apoptosis is a physiological and programmed form of cell death, and it is thought to be the best method of cell death[3]. The relationship between apoptosis and AP has been extensively investigated, and it has been demonstrated that the severity of AP is inversely related to the rate of apoptosis[4].

MicroRNAs (miRNAs), noncoding small RNAs that are 18 to 24 nucleotides in length, play essential roles in various physiological and pathological processes in animals and plants[5]. By binding to the 3′ untranslated region (UTR) of their target mRNA molecules, miRNAs can downregulate target gene expression and block the translation of mRNA at the posttranscriptional level[6,7]. Recently, many studies have shown that miRNAs are essential to different cellular processes, regulating almost 80% of genes in processes such as development, proliferation, apoptosis, metabolism, and morphogenesis in multiple cell types under physiological and pathological conditions[8,9].

Our previous study showed that microRNA-22 (miR-22) is important in the process of pancreatic acinar cell apoptosis. The upregulation of miR-22 promotes the apoptosis of pancreatic acinar cells induced by tumor necrosis factor alpha (TNF-α). We demonstrated the role of miR-22 in promoting cell apoptosis by repressing its target gene, Erb-b2 receptor tyrosine kinase 3 (ErbB3). However, the underlying mechanism has not been fully elucidated[10]. Currently, most miRNA studies have focused on the regulation of downstream target gene expression, and there have been few studies on upstream miRNA transcription factors[11]. An intergenic

miRNA has its own independent transcription start site (TSS), while an intragenic miRNA is generally transcribed with its cohost gene[12]. MiR-22, an exonic miRNA, has its own host gene promoter[13].

In this study, we elucidated the downstream signaling pathways that miR-22 regulates in pancreatic acinar cell apoptosis. Furthermore, we identified the transcriptional promoter of miR-22 and verified its function in pancreatic acinar cell apoptosis.

MATERIALS AND METHODS

MiR-22 mimic, Nr3c1 plasmid encoding the glucocorticoid receptor and si-Nr3c1 construct

The mimic of miR-22, Nr3c1 plasmid encoding the glucocorticoid receptor (GR), and si-Nr3c1 were designed and chemically synthesized by RiboBio (Guangzhou, China).

Cell culture and transfection

The pancreatic acinar cell line AR42J (American Type Culture Collection, United States) was cultured in Dulbecco's modified Eagle's medium (DMEM)-F12 (Gibco, United States) containing 20% fetal bovine serum (Gibco, United States) in a humidified incubator. AR42J cells (1×10^6/well) were seeded in 6-well plates 12 h before transfection. The cells were transfected with the Nr3c1 plasmid encoding the GR (100 nmol/L) with Lipofectamine ™ 2000 (Invitrogen, United States). The cells were transfected with the miR-22 mimic (100 nmol/L) and si-Nr3c1 (50 nmol/L) using transfection reagents (RiboBio, Guangzhou, China). After transfection for 48 h, the AR42J cells were collected for the next experiment.

Amylase detection

AR42J cells at 5×10^5/well were seeded into 6-well plates and incubated with DMEM-F12 containing 100 nmol/L caerulein (Cae) for 24 h. The supernatant was collected. An amylase assay kit (Jiancheng Bio, Nanjing, China) was used to measure the amylase expression level in the supernatant, following the manufacturer's instructions.

Flow cytometry analysis of apoptosis

AR42J cells were harvested after treatment with 100 nmol/L Cae for 24 h. Then, the apoptosis rate of AR42J cells was dectected using Annexin V-APC apoptosis kit (KeyGEN Bio, China) according to the manufacturer's instructions.

Quantitative reverse-transcription polymerase chain reaction

Total RNA was extracted and reverse-transcribed into cDNA using PrimeScript RT Master Mix (Takara, Japan). qRT-PCR was performed using the SYBR Premix Ex TaqTM kit (Takara, Japan). The expression levels of miR-22, ErbB3, and Nr3c1 relative to the expression level of GAPDH were determined using the $2^{-\Delta\Delta CT}$ method. The specific primer sequences are as follows: ErbB3 (forward), 5′-TCTGCATTAAAGTCATCGAGGAC-3′ and ErbB3 (reverse), 5′-CAGCCGTACAATGTGGGCAT-3′; Nr3c1 (forward), 5′-CTTGAGAAACTTACACCTCGATGACC-3′ and Nr3c1 (reverse), 5′-AGCAGTAGGTAAGGAGATTCTCAACC-3′; and GAPDH (forward), 5′-TCTCTGCTCCTCCCTGTTCT-3′ and GAPDH (reverse), 5′-TACGGCCAAATCCGTTCACA-3′. The miR-22 primer was designed and synthesized by RiboBio (Guangzhou, China).

Western blot analysis

Total protein from cultured AR42J cells was extracted according to the manufacturer's instructions (Beyotime Bio, Wuhan, China). Forty micrograms of protein of each sample was loaded and separated on a 12% SDS polyacrylamide gel and electrophoretically transferred onto PVDF membranes (Millipore, United States). Then the membranes were incubated with anti-rat monoclonal Bad, Bax, Bcl-xl, Cleaved-Caspase3, PI3k, Akt, p-Akt, GR, (CST, United States), Bcl-2, PI3k-p85α, and ErbB3 antibodies (Santa Cruz Bio, United States) or the anti-β-actin antibody (CST, United States) at 4 ℃ overnight, and subsequently HRP-labeled secondary antibodies (1:5000) at 37 ℃ for 2 h; then the signals were visualized with an electrochemiluminescence kit (Pierce, Rockford, IL, United States).

Transcription factor search

The potential miR-22 transcriptional promoter and binding sites were predicted using the online tools (http://www.genomatix.de/; http://jaspar.binf.ku.dk/cgi-bin/jaspar_db.pl; and http://www.gene-regulation.com). The transcriptional promoter with the highest score was chosen for further analysis.

Luciferase reporter assay

AR42J cells were seeded in 24-well plates and, after 24 h, transfected with 100 ng Nr3c1 control plasmid (Nr3c1-NC) or the Nr3c1 plasmid encoding the GR (Nr3C1-OE), together with 50 nmol/L miR-22 promoter plasmid (miR-22 promoter) contained by psiCHECKTM-2 vector (RiboBio, China) with Lipofectamine™ 2000 (Invitrogen, United States); cells transfected with only the miR-22 promoter control plasmid (miR-22 promoter NC) served as the control group. Binding site mutations were generated with mutagenic primers using a MutanBEST Kit (Takara). The mutant miR-22 promoter plasmids (miR-22 promoter mut1 and miR-22 promoter mut2) were cotransfected with Nr3c1-OE. The luciferase activity was measured 48 h after transfection.

Chromatin immunoprecipitation (ChIP) and ChIP-qPCR assays

ChIP assays were performed following the instructions provided with the ChIP assay kit (Beyotime, Wuhan, China). First, the chromatin in AR42J cells was cross-linked with 1% formaldehyde for 10 min at 37 ℃, and then the cells were washed three times with cold PBS. The cells were collected, lysed, and sonicated.

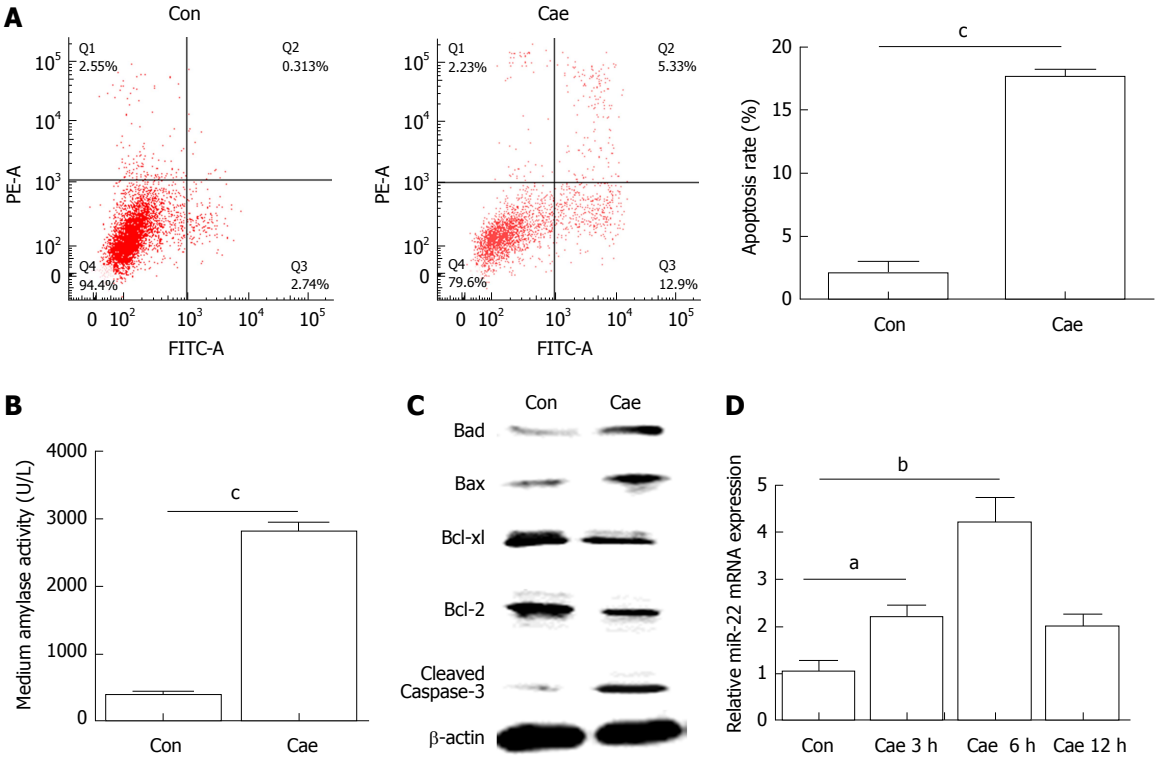

Figure 1 The apoptosis rate and levels of amylase, apoptosis-associated proteins, and microRNA-22 in caerulein-induced AR42J cells. A: The apoptosis rate of AR42J cells after incubation with caerulein for 24 h; B: Amylase levels in the medium; C: Western blot analysis of the levels of apoptosis-associated proteins in AR42J cells; D: MicroRNA-22 levels in AR42J cells. Data were obtained from three independent experiments performed in triplicate and are shown as the mean ± SD. $^{a}P < 0.05$, $^{b}P < 0.01$, $^{c}P < 0.001$ *vs* control group. Cae: Caerulein; miR-22: MicroRNA-22.

The nuclear lysates were sonicated, and an equal amount of chromatin was immunoprecipitated at 4 ℃ overnight with 3 μg of GR and IgG anti-rat monoclonal antibody (CST, United States). The immunoprecipitated products were collected after incubation on protein A + G-coated magnetic beads; then, the beads were washed, and the bound chromatin was eluted in ChIP elution buffer. The protein was digested with proteinase K for 4 h at 45 ℃. The DNA was purified using a DNA purification kit (Beyotime). The DNA fragments of the GR binding sites in the miR-22 promoter were designed and synthesized by RiboBio (Guangzhou, China). After immunoprecipitation, the GR binding site was evaluated using qPCR and normalized to the total chromatin. Total chromatin was used as the input. IgG and a non-specific GR binding site (Nbs) were used as controls. The primers used to amplify the DNA fragments of the GR binding sites in the miR-22 promoter were also designed and synthesized by RiboBio (Guangzhou, China). The ChIP-qPCR conditions were based on a three-step method.

Statistical analysis

The results are expressed as the mean ± SD from at least three separate experiments. Statistical analyses were performed using SPSS 22.0 software, and comparisons were made using Student's *t*-tests and one-way ANOVA. $^{a}P < 0.05$, $^{b}P < 0.01$, and $^{c}P < 0.001$ was considered statistically significant.

RESULTS

Cae induced apoptosis of AR42J cells

Flow cytometry was used to detect apoptosis of AR42J cells. As shown in Figure 1A, the apoptosis rate of AR42J cells increased significantly after treatment with 100 nmol/L Cae for 24 h. The amylase level in the medium was higher compared with that in the control group (Figure 1B). Compared with the control cells, the Cae-treated cells had increased protein expression levels of Bad, Bax, and cleaved caspase-3 and significantly decreased protein expression levels of Bcl-2 and Bcl-xl (Figure 1C). The expression of miR-22 was confirmed by qRT-PCR. As shown in Figure 1D, the expression level of miR-22 was higher in AR42J cells exposed to Cae for 3 h and 6 h than in the control cells.

Upregulation of miR-22 promotes the apoptosis of AR42J cells by suppressing the PI3k/Akt signaling pathway

AR42J cells were transfected with the miR-22 mimic as described. The expression of miR-22 was significantly elevated in the cells transfected with the mimic compared with the miRNA NC cells (Figure 2A). As shown in Figure 2B and C, the mRNA and protein expression levels of ErbB3, the target gene of miR-22, were significantly lower in cells overexpressing miR-22 than in the control cells. After AR42J cells were induced with Cae, the apoptosis rate, amylase level, and the protein expression

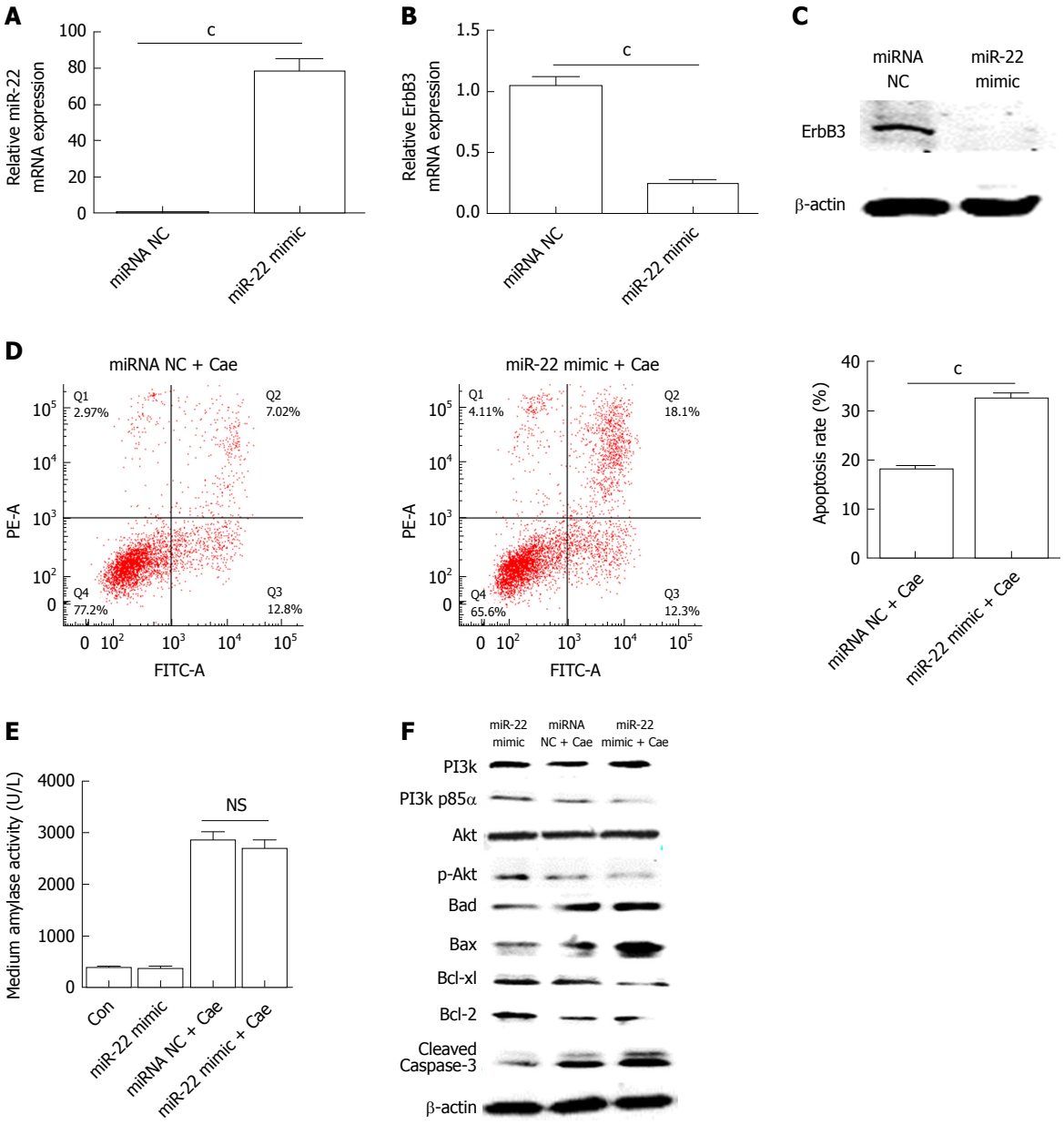

Figure 2 Upregulation of microRNA-22 promotes the apoptosis of AR42J cells by suppressing the PI3k/Akt signaling pathway. A: MicroRNA-22 expression level; B: Erb-b2 receptor tyrosine kinase 3 (ErbB3) mRNA expression level; C: ErbB3 protein expression level; D: The apoptosis rate of AR42J cells induced with caerulein (Cae) after transfection; E: Amylase levels in the medium; F: Western blot analysis of the levels of PI3k, p-PI3k, Akt, p-Akt, and apoptosis-associated proteins in AR42J cells. Data were obtained from three independent experiments performed in triplicate and are shown as the mean ± SD. $^{NS}P > 0.05$, $^{c}P < 0.001$ *vs* miRNA NC or miRNA NC + Cae groups. ErbB3: Erb-b2 receptor tyrosine kinase 3; Cae: Caerulein; miRNA: MicroRNA; miR-22: MicroRNA-22.

levels of PI3k, p-PI3k, Akt, p-Akt, and apoptosis-associated protein were detected. The apoptosis rate in the miR-22 mimic + Cae group was significantly higher than that in the miRNA NC + Cae group (Figure 2D), while the amylase level did not differ significantly between the two groups (Figure 2E). Compared with the miRNA NC cells, cells with upregulated miR-22 had higher expression levels of Bad, Bax, and activated caspase-3. The expression levels of the proteins that promoted cellular proliferation were clearly reduced in the miR-22 mimic + Cae group. In addition, the upregulation of miR-22 significantly reduced the phosphorylation of PI3k and Akt induced by Cae.

Prediction and verification of the transcription factor of miR-22

Using online programs, we predicted the transcription factor and binding sites of the miR-22 promoter. The possible transcription factors are shown in Figure 3A, of which Nr3c1 had the highest score. The 5'-flanking region of miR-22 was cloned into the Xba1-site of the pGL3-luciferase reporter vector, and the empty pGL3-luciferase reporter was used as a control group. The results showed that overexpression of Nr3c1 led to a significant decrease in luciferase activity compared with that of the Nr3c1 NC + miR-22 promoter group (Figure 3B). We further identified the binding sites of Nr3c1

A

Nr3c1 (GR)	C/EBP-α	AR
C/EBP-β	HNF3-β	CBF
C/EBP-δ	DBP	T3R-α
Sp3	USF-1	NF-1
Sp1	Nkx2-1	SRF
c-Fos	AP-1	USF2

Nr3c1 (GR)	Score 208.6	$P < 0.001$

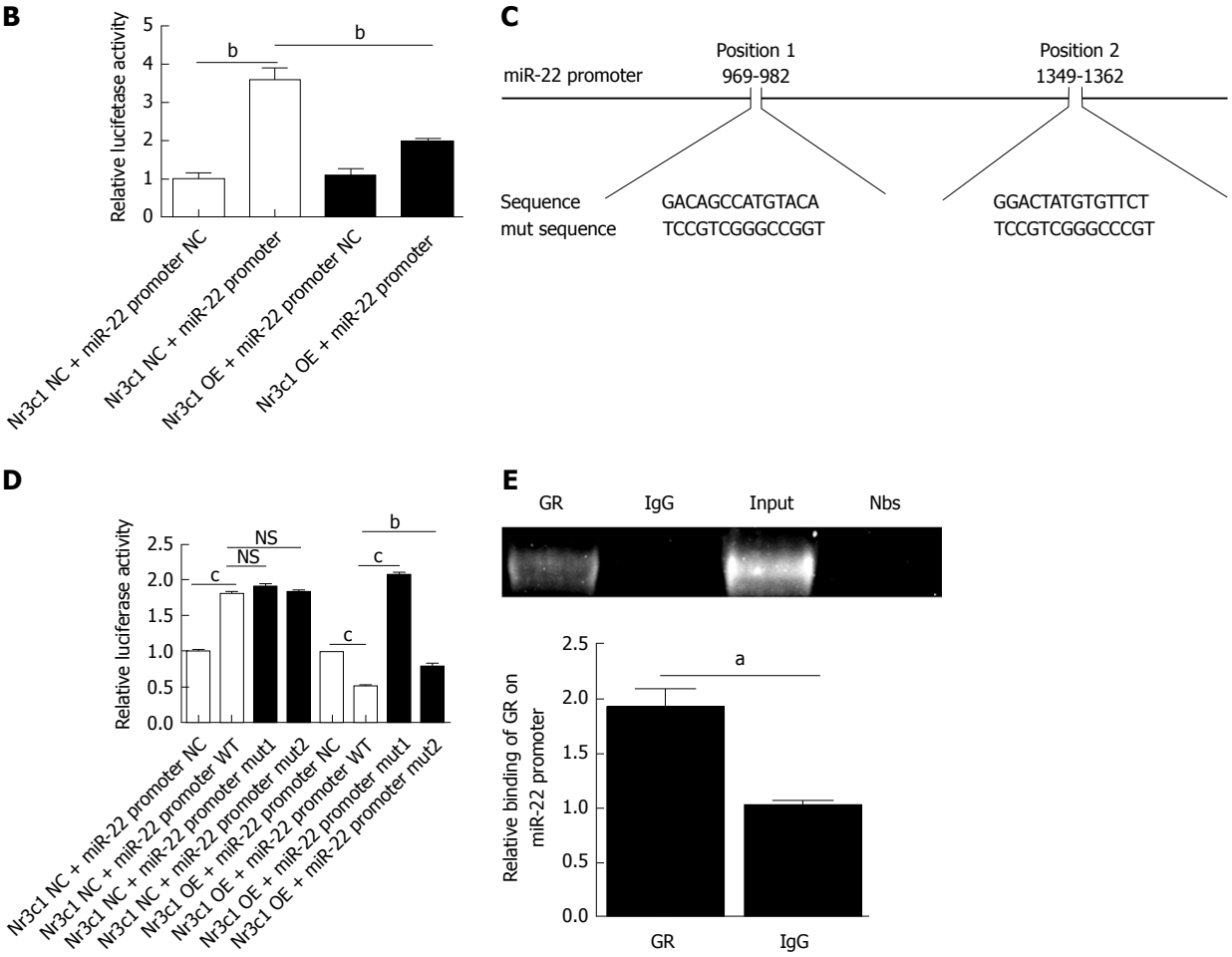

Figure 3 Prediction of the transcription factors of microRNA-22 and the luciferase reporter. A: The possible transcription factors of microRNA-22 (miR-22) were predicted, of which Nr3c1 had the highest score; B: The luciferase reporter expression after the overexpression of Nr3c1; C: The predicted glucocorticoid receptor binding sites within the miR-22 promoter and the mutant versions generated by site mutagenesis are shown; D: The luciferase reporter expression after mutagenesis. MiR-22 promoter NC, mut 1, or mut 2 plasmid was co-transfected with Nr3c1 NC or Nr3c1 OE plasmid into AR42J cells, respectively. Dual luciferase reporter assays were performed 48 h after transfection; E: Results of the chromatin immunoprecipitation (ChIP) assay and ChIP-qPCR. Data were obtained from three independent experiments performed in triplicate and are shown as the mean ± SD. $^{NS}P > 0.05$, $^{a}P < 0.05$, $^{b}P < 0.01$, $^{c}P < 0.001$ *vs* Nr3c1 NC + miR-22 promoter NC, Nr3c1 NC + miR-22 promoter, Nr3c1 NC + miR-22 promoter WT, Nr3c1 OE + miR-22 promoter NC, Nr3c1 OE + miR-22 promoter WT or IgG groups. ChIP: Chromatin immunoprecipitation; GR: Glucocorticoid receptor; mut: Mutagenesis; OE: Overexpression; miR-22: MicroRNA-22.

using TF search software. To determine the functional importance of Nr3c1 binding sites in the miR-22 promoter, site-directed mutagenesis was performed. The base sequences of the predicted binding sites and mutated sequences are shown in Figure 3C. The luciferase reporter results demonstrated that compared with the wild-type group, the group with the mutated first binding site had significantly higher luciferase activity, while the group with the mutated second binding site had activity that was significantly higher than that of the wild-type but not as high as that of the group with the mutated first binding site (Figure 3D), indicating that Nr3c1 might bind to the first site (GACAGCCATGTACA) to regulate miR-22 promoter activity. Furthermore, ChIP analysis was performed in AR42J cells to determine whether GR bound to the miR-22 promoter. As shown in Figure 3E, the ChIP and ChIP-qPCR assays showed that GR interacted with the miR-22 promoter within the

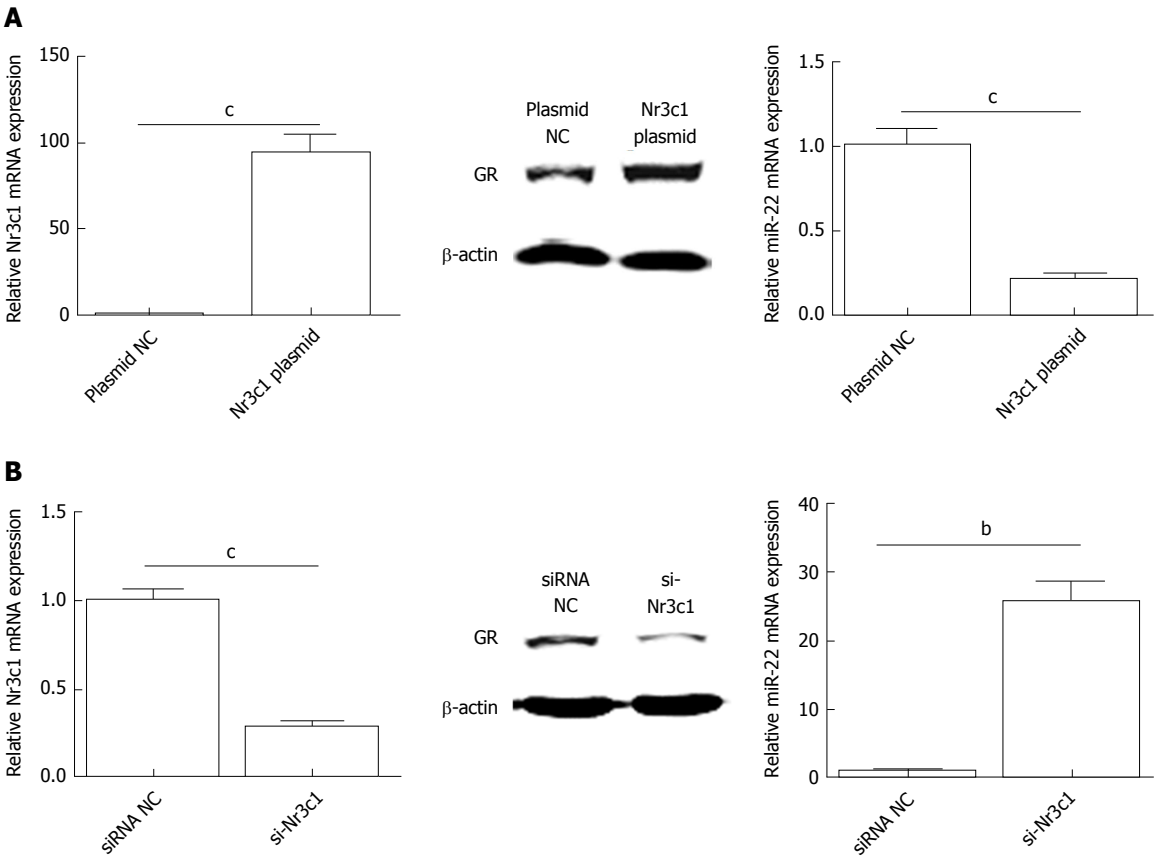

Figure 4 Expression of Nr3c1 mRNA, glucocorticoid receptor protein, and microRNA-22 level after transfection. A: The levels of Nr3c1 mRNA, GR protein, and miR-22 after transfection with Nr3c1 plasmid; B: The levels of Nr3c1 mRNA, glucocorticoid receptor protein, and miR-22 after transfection with si-Nr3c1. Data were obtained from three independent experiments in triplicate and are shown as the mean ± SD. $^{b}P < 0.01$, $^{c}P < 0.001$ *vs* plasmid NC or siRNA NC groups. GR: Glucocorticoid receptor; miR-22: MicroRNA-22.

GACAGCCATGTACA site.

Nr3c1 regulates the expression of miR-22

To investigate the influence of Nr3c1 on the expression of miR-22, the Nr3c1 plasmid encoding the GR and si-Nr3c1 were used to regulate the expression of Nr3c1. As shown in Figure 4A, overexpression of Nr3c1 significantly reduced miR-22 expression compared with that of the control. In contrast, si-Nr3c1 downregulated the expression levels of Nr3c1 mRNA and the GR protein, which promote the expression of miR-22 (Figure 4B).

Si-Nr3c1 promotes the apoptosis of AR42J cells

Downregulation of Nr3c1 promoted the expression of miR-22. The genes involved in the pathway downstream of miR-22 that promoted apoptosis were detected. As shown in Figure 5A and B, the mRNA and protein expression levels of ErbB3 were significantly lower when miR-22 was upregulated than in the control. After AR42J cells were induced with Cae, the apoptosis rate increased significantly (Figure 5C). However, the amylase level was not significantly different between the two groups (Figure 5D). As shown in Figure 5E, the expression levels of p-PI3k and p-Akt were clearly lower in the cells transfected with si-Nr3c1 than in the siRNA NC group. Downregulation of Nr3c1 increased the expression of Bad, Bax, and activated caspase-3, while Bcl-2 and Bcl-xl protein expression levels were obviously reduced. Together, these data suggest that downregulation of Nr3c1 promoted the expression of miR-22 and the apoptosis of AR42J cells.

DISCUSSION

Some studies have demonstrated that miR-22 plays important roles in regulating the expression levels of its target genes and that it is associated with various diseases, such as autoimmune diseases, cardiovascular diseases, emphysema, and cancer[14-18]. Our previous results showed that the expression of miR-22 is clearly higher in acute edema pancreatitis (AEP) *in vivo*. Elevating miR-22 expression using a miR-22 mimic could promote the activity of activated caspase-3 and the rate of apoptosis of pancreatic acinar cells (AR42J) induced with TNF-α *in vitro*. Moreover, the target genes of miR-22 were predicted by bioinformatics, and the luciferase reporter gene confirmed that ErbB3 was the target gene of miR-22[10]. Furthermore, we identified the signaling pathway by which miR-22 regulates the apoptosis of AR42J cells. The results demonstrated that miR-22 represses the expression of its target gene ErbB3. ErbB3, which belongs to the ErbB family, can be

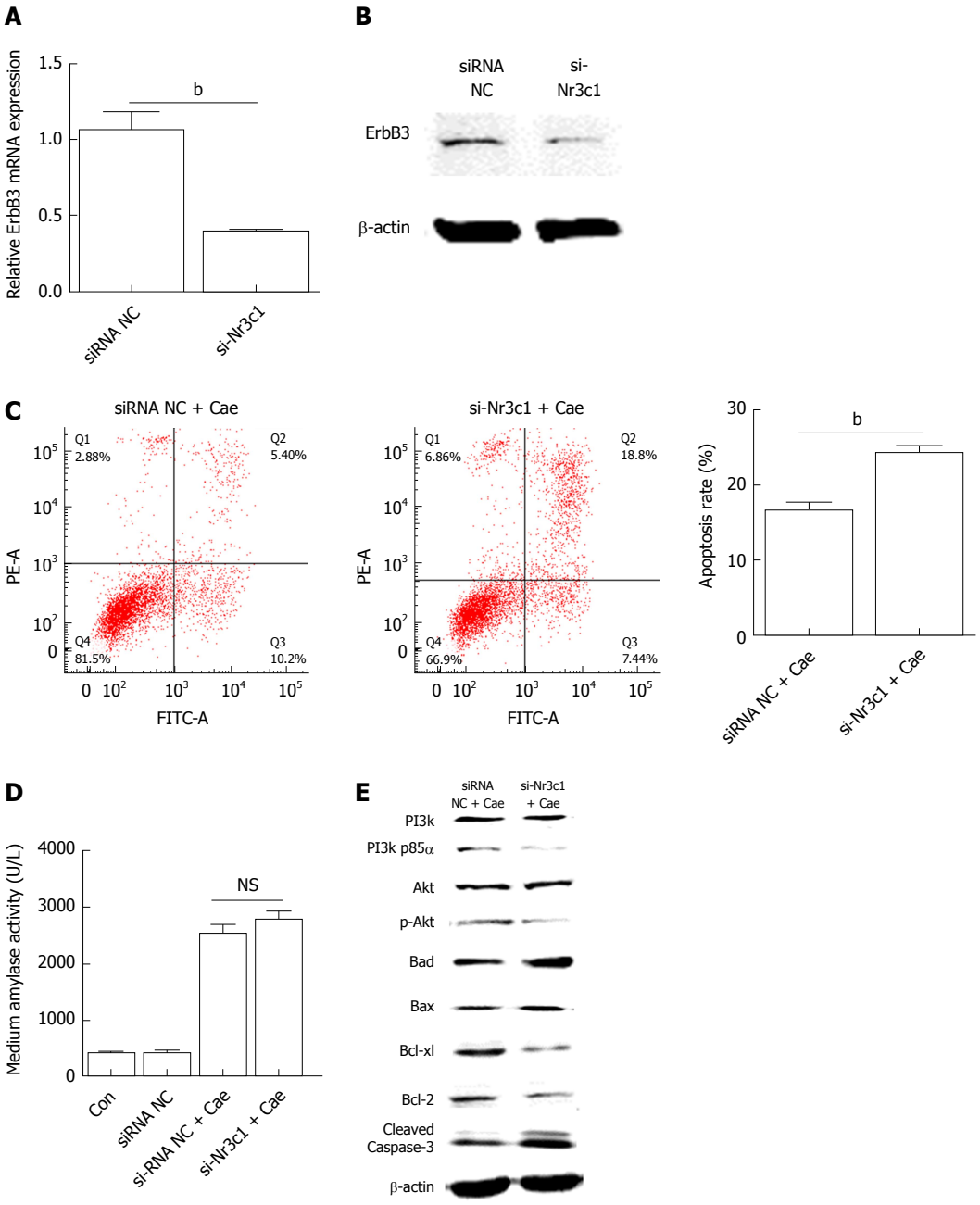

Figure 5 Down-regulation of Nr3c1 by using si-Nr3c1 promotes the apoptosis of AR42J cells by suppressing the PI3k/Akt signaling pathway. A: Erb-b2 receptor tyrosine kinase 3 (ErbB3) mRNA expression level; B: ErbB3 protein level; C: The apoptosis rate of AR42J cells after the effect of caerulein for 24 h; D: Amylase level in medium; E: Western blot analysis for p-PI3k, p-Akt, and apoptosis associated proteins in AR42J cells. Data were obtained from three independent experiments in triplicate and are shown as the mean ± SD. $^{b}P < 0.01$ *vs* siRNA NC groups. ErbB3: Erb-b2 receptor tyrosine kinase 3; Cae: Caerulein; miR-22: MicroRNA-22.

transactivated by forming heterodimers with other ErbB family members, especially ErbB2. ErbB3 lacks intrinsic kinase activity and cannot autophosphorylate due to the evolutionary acquisition of several changes within the kinase domain[19,20].

Among the members of the ErbB family, ErbB3 has the highest affinity for PI3k because of its six YXXM motifs that can directly bind to the p85 regulatory subunit of PI3k after tyrosine phosphorylation of ErbB3[21,22]. Therefore, the activation of ErbB3 results in a strong activation of the PI3k/Akt signaling pathway[23]. The activation of the PI3k/Akt signaling pathway can lead to apoptosis resistance in cancers such as ovarian, thyroid, breast, hepatic, cervical, prostate, lung, pancreatic, and colon cancers. Many studies have demonstrated that inhibiting the activation of PI3k/Akt may lead to cell apoptosis[24-31]. Our results showed that miR-22 could upregulate the expression of genes that promote apoptosis and reduce the expression of genes that promote proliferation by suppressing the phosphorylation of PI3k and Akt in Cae-induced apoptosis, which results in promoting the activity of caspase 3. Caspases are

a family of cysteine proteases that are present in the cytosol as inactive proenzymes, and they become activated when apoptosis is initiated, playing essential roles in various stages of apoptosis[32]. MiR-22 might promote the apoptosis of AR42J cells by repressing the PI3k/Akt pathway *via* inhibition of its target gene, ErbB3.

Transcription factors are a group of proteins that bind to a specific sequence at the 5'-end of a gene to ensure that the target gene is expressed at a specific time, in a specific location, and with a specific intensity. In fact, transcriptional regulators play pivotal roles during developmental and pathophysiological processes[33,34]. MiR-22, which belongs to the category of intergenic miRNAs, has its own independent transcription factors. Recent studies have shown that the transcription factors of miR-22 include Jak3, STAT3, STAT5, and FosB. FosB promotes the expression of miR-22, while Jak3, STAT3, and STAT5 are transcriptional repressors[35,36]. In this study, to identify the miR-22 transcription factor involved in regulating the apoptosis of pancreatic acinar cells, we first predicted the transcription factor and TSS. The prediction results showed that Nr3c1 might be a transcription factor regulating miR-22. Nr3c1 is a vital GR gene; it can receive stimulation from glucocorticoids and then influence downstream transcription factors by changing the protein configuration, thereby playing an indispensable role in gene regulation[37]. We cloned the 5' flanking regions of miR-22 and analyzed the promoter regions. The first site (GACAGCCATGTACA) demonstrated the highest promoter activity, as measured by the luciferase reporter assay. The results of the site-directed mutagenesis and ChIP-qPCR confirmed that Nr3c1 binds to the miR-22 core promoter. The upregulation of miR-22 expression resulting from silencing Nr3c1 contributed to the apoptosis of AR42J cells. Apoptosis is a physiological and programmed form of cell death, which is considered the best method of cell death. It is characterized by cell shrinkage, nuclear chromatin condensation, and the retention of organelles[38]. The severity of AP is inversely related to the degree of apoptosis, suggesting that apoptosis may be a teleologically beneficial response to acinar cell injury in general and especially in AP[39].

In conclusion, our results indicated that GR transcriptionally repressed the expression of miR-22 by binding to the miR-22 promoter TSS. Downregulating the expression of GR could promote the expression of miR-22. The upregulation of miR-22 promoted Cae-induced apoptosis of AR42J cells by targeting ErbB3 and further suppressed the PI3k/Akt signaling pathway. The upregulation of miR-22 might have therapeutic potential for AP.

ARTICLE HIGHLIGHTS

Research background

The severity of acute pancreatitis (AP) is inversely related to the rate of apoptosis of pancreatic acinar cells. Our previous study showed that microRNA-22 (miR-22) promotes the apoptosis of pancreatic acinar cells by targeting Erb-b2 receptor tyrosine kinase 3 (ErbB3). However, the underlying mechanism has not been fully elucidated, and the elements that regulate the expression of miR-22 remain unclear.

Research motivation

The downstream signaling pathways that miR-22 regulates pancreatic acinar cell apoptosis have not been fully elucidated. Besides, miR-22 is an exonic microRNA and has its own host gene promoter. In this study, we identified the transcriptional promoter of miR-22 and verified their functions in pancreatic acinar cell apoptosis.

Research objectives

This research aimed to elucidate the underlying mechanism that miR-22 promotes the apoptosis of rat pancreatic acinar cells (AR42J) and identify the transcriptional promoter of miR-22.

Research methods

MiR-22 promoted the apoptosis of AR42J cells by targeting the ErbB3 gene, and the downstream signaling pathway (PI3k/Akt signaling pathway) was identified using caerulein (Cae)-induced apoptosis of AR42J cells. Furthermore, we predicted the potential transcription promoter of miR-22 and the binding sites using online tools. Luciferase reporter analysis and site-directed mutagenesis indicated the binding site of the glucocorticoid receptor (GR). The binding of GR to the miR-22 promoter in cell culture was identified by a chromatin immunoprecipitation assay.

Research results

The results of this study indicated that GR transcriptionally repressed the expression of miR-22 by binding to the miR-22 promoter transcription start site. Downregulation of the expression of GR could upregulate the expression of miR-22. The upregulation of miR-22 promoted the Cae-induced apoptosis of AR42J by targeting ErbB3 and further suppressing the PI3k/Akt signaling pathway.

Research conclusions

GR transcriptionally repressed the expression of miR-22 and downregulation of the expression of GR could upregulate the expression of miR-22, which further promoted the Cae-induced apoptosis of AR42J cells.

Research perspectives

This study found that GR transcriptionally repressed the expression of miR-22, which might be a target to regulate the expression of miR-22. The further research is to explore the treatment measures for AP by using drugs targeting GR in *in vitro* cell models and *in vivo* AP models.

REFERENCES

1 **Pan LL**, Li J, Shamoon M, Bhatia M, Sun J. Recent Advances on Nutrition in Treatment of Acute Pancreatitis. *Front Immunol* 2017; **8**: 762 [PMID: 28713382 DOI: 10.3389/fimmu.2017.00762]

2 **Mareninova OA**, Sung KF, Hong P, Lugea A, Pandol SJ, Gukovsky I, Gukovskaya AS. Cell death in pancreatitis: caspases protect from necrotizing pancreatitis. *J Biol Chem* 2006; **281**: 3370-3381 [PMID: 16339139 DOI: 10.1074/jbc.M511276200]

3 **Fuchs Y**, Steller H. Live to die another way: modes of programmed cell death and the signals emanating from dying cells. *Nat Rev Mol Cell Biol* 2015; **16**: 329-344 [PMID: 25991373 DOI: 10.1038/nrm3999]

4 **Bhatia M**. Apoptosis versus necrosis in acute pancreatitis. *Am J Physiol Gastrointest Liver Physiol* 2004; **286**: G189-G196 [PMID: 14715516 DOI: 10.1152/ajpgi.00304.2003]

5 **Khan S**, Ansarullah, Kumar D, Jaggi M, Chauhan SC. Targeting microRNAs in pancreatic cancer: microplayers in the big game. *Cancer Res* 2013; **73**: 6541-6547 [PMID: 24204026 DOI: 10.1158/0008-5472.CAN-13-1288]

6 **Fabian MR**, Sonenberg N, Filipowicz W. Regulation of mRNA translation and stability by microRNAs. *Annu Rev Biochem* 2010; **79**: 351-379 [PMID: 20533884 DOI: 10.1146/annurev-

biochem-060308-103103]
7 **Bartel DP**. MicroRNAs: genomics, biogenesis, mechanism, and function. *Cell* 2004; **116**: 281-297 [PMID: 14744438 DOI: 10.1016/S0092-8674(04)00045-5]
8 **Mahmoudi E**, Cairns MJ. MiR-137: an important player in neural development and neoplastic transformation. *Mol Psychiatry* 2017; **22**: 44-55 [PMID: 27620842 DOI: 10.1038/mp.2016.150]
9 **Bartel DP**. MicroRNAs: target recognition and regulatory functions. *Cell* 2009; **136**: 215-233 [PMID: 19167326 DOI: 10.1016/j.cell.2009.01.002]
10 **Qin T**, Fu Q, Pan YF, Liu CJ, Wang YZ, Hu MX, Tang Q, Zhang HW. Expressions of miR-22 and miR-135a in acute pancreatitis. *J Huazhong Univ Sci Technolog Med Sci* 2014; **34**: 225-233 [PMID: 24710937 DOI: 10.1007/s11596-014-1263-7]
11 **Berindan-Neagoe I**, Monroig Pdel C, Pasculli B, Calin GA. MicroRNAome genome: a treasure for cancer diagnosis and therapy. *CA Cancer J Clin* 2014; **64**: 311-336 [PMID: 25104502 DOI: 10.3322/caac.21244]
12 **He C**, Li Z, Chen P, Huang H, Hurst LD, Chen J. Young intragenic miRNAs are less coexpressed with host genes than old ones: implications of miRNA-host gene coevolution. *Nucleic Acids Res* 2012; **40**: 4002-4012 [PMID: 22238379 DOI: 10.1093/nar/gkr1312]
13 **Rodriguez A**, Griffiths-Jones S, Ashurst JL, Bradley A. Identification of mammalian microRNA host genes and transcription units. *Genome Res* 2004; **14**: 1902-1910 [PMID: 15364901 DOI: 10.1101/gr.2722704]
14 **Wang B**, Yao Q, Xu D, Zhang JA. MicroRNA-22-3p as a novel regulator and therapeutic target for autoimmune diseases. *Int Rev Immunol* 2017; **36**: 176-181 [PMID: 28471251 DOI: 10.1080/08830185.2017.1281272]
15 **Huang ZP**, Wang DZ. miR-22 in Smooth Muscle Cells: A Potential Therapy for Cardiovascular Disease. *Circulation* 2018; **137**: 1842-1845 [PMID: 29685931 DOI: 10.1161/CIRCULATIONAHA.118.033042]
16 **Brusselle GG**, Bracke KR. MicroRNA miR-22 drives T(H)17 responses in emphysema. *Nat Immunol* 2015; **16**: 1109-1110 [PMID: 26482970 DOI: 10.1038/ni.3295]
17 **Mansini AP**, Lorenzo Pisarello MJ, Thelen KM, Cruz-Reyes M, Peixoto E, Jin S, Howard BN, Trussoni CE, Gajdos GB, LaRusso NF, Perugorria MJ, Banales JM, Gradilone SA. MicroRNA (miR)-433 and miR-22 dysregulations induce histone-deacetylase-6 overexpression and ciliary loss in cholangiocarcinoma. *Hepatology* 2018; **68**: 561-573 [PMID: 29406621 DOI: 10.1002/hep.29832]
18 **Jiang X**, Hu C, Arnovitz S, Bugno J, Yu M, Zuo Z, Chen P, Huang H, Ulrich B, Gurbuxani S, Weng H, Strong J, Wang Y, Li Y, Salat J, Li S, Elkahloun AG, Yang Y, Neilly MB, Larson RA, Le Beau MM, Herold T, Bohlander SK, Liu PP, Zhang J, Li Z, He C, Jin J, Hong S, Chen J. miR-22 has a potent anti-tumour role with therapeutic potential in acute myeloid leukaemia. *Nat Commun* 2016; **7**: 11452 [PMID: 27116251 DOI: 10.1038/ncomms11452]
19 **Pellat A**, Vaquero J, Fouassier L. Role of ErbB/HER family of receptor tyrosine kinases in cholangiocyte biology. *Hepatology* 2017; Epub ahead of print [PMID: 28671339 DOI: 10.1002/hep.29350]
20 **Yarden Y**, Sliwkowski MX. Untangling the ErbB signalling network. *Nat Rev Mol Cell Biol* 2001; **2**: 127-137 [PMID: 11252954 DOI: 10.1038/35052073]
21 **Soltoff SP**, Carraway KL 3rd, Prigent SA, Gullick WG, Cantley LC. ErbB3 is involved in activation of phosphatidylinositol 3-kinase by epidermal growth factor. *Mol Cell Biol* 1994; **14**: 3550-3558 [PMID: 7515147 DOI: 10.1128/mcb.14.6.3550]
22 **Kim HH**, Sierke SL, Koland JG. Epidermal growth factor-dependent association of phosphatidylinositol 3-kinase with the erbB3 gene product. *J Biol Chem* 1994; **269**: 24747-24755 [PMID: 7929151]
23 **Hennessy BT**, Smith DL, Ram PT, Lu Y, Mills GB. Exploiting the PI3K/AKT pathway for cancer drug discovery. *Nat Rev Drug Discov* 2005; **4**: 988-1004 [PMID: 16341064 DOI: 10.1038/nrd1902]
24 **Chen C**, Chang YC, Lan MS, Breslin M. [Corrigendum] Leptin stimulates ovarian cancer cell growth and inhibits apoptosis by increasing cyclin D1 and Mcl-1 expression via the activation of the MEK/ERK1/2 and PI3K/Akt signaling pathways. *Int J Oncol* 2016; **49**: 847 [PMID: 27279381 DOI: 10.3892/ijo.2016.3564]
25 **Mazumdar M**, Adhikary A, Chakraborty S, Mukherjee S, Manna A, Saha S, Mohanty S, Dutta A, Bhattacharjee P, Ray P, Chattopadhyay S, Banerjee S, Chakraborty J, Ray AK, Sa G, Das T. Targeting RET to induce medullary thyroid cancer cell apoptosis: an antagonistic interplay between PI3K/Akt and p38MAPK/caspase-8 pathways. *Apoptosis* 2013; **18**: 589-604 [PMID: 23329180 DOI: 10.1007/s10495-013-0803-0]
26 **Yuan L**, Wang J, Xiao H, Xiao C, Wang Y, Liu X. Isoorientin induces apoptosis through mitochondrial dysfunction and inhibition of PI3K/Akt signaling pathway in HepG2 cancer cells. *Toxicol Appl Pharmacol* 2012; **265**: 83-92 [PMID: 23026832 DOI: 10.1016/j.taap.2012.09.022]
27 **Kim MS**, Kim JH, Bak Y, Park YS, Lee DH, Kang JW, Shim JH, Jeong HS, Hong JT, Yoon DY. 2,4-bis (p-hydroxyphenyl)-2-butenal (HPB242) induces apoptosis via modulating E7 expression and inhibition of PI3K/Akt pathway in SiHa human cervical cancer cells. *Nutr Cancer* 2012; **64**: 1236-1244 [PMID: 23163851 DOI: 10.1080/01635581.2012.718405]
28 **Harashima N**, Inao T, Imamura R, Okano S, Suda T, Harada M. Roles of the PI3K/Akt pathway and autophagy in TLR3 signaling-induced apoptosis and growth arrest of human prostate cancer cells. *Cancer Immunol Immunother* 2012; **61**: 667-676 [PMID: 22038398 DOI: 10.1007/s00262-011-1132-1]
29 **Zhou L**, Luan H, Liu Q, Jiang T, Liang H, Dong X, Shang H. Activation of PI3K/Akt and ERK signaling pathways antagonized sinomenine-induced lung cancer cell apoptosis. *Mol Med Rep* 2012; **5**: 1256-1260 [PMID: 22367396 DOI: 10.3892/mmr.2012.798]
30 **Hu W**, Shen T, Wang MH. Cell cycle arrest and apoptosis induced by methyl 3,5-dicaffeoyl quinate in human colon cancer cells: Involvement of the PI3K/Akt and MAP kinase pathways. *Chem Biol Interact* 2011; **194**: 48-57 [PMID: 21872580 DOI: 10.1016/j.cbi.2011.08.006]
31 **Roy SK**, Srivastava RK, Shankar S. Inhibition of PI3K/AKT and MAPK/ERK pathways causes activation of FOXO transcription factor, leading to cell cycle arrest and apoptosis in pancreatic cancer. *J Mol Signal* 2010; **5**: 10 [PMID: 20642839 DOI: 10.1186/1750-2187-5-10]
32 **Budihardjo I**, Oliver H, Lutter M, Luo X, Wang X. Biochemical pathways of caspase activation during apoptosis. *Annu Rev Cell Dev Biol* 1999; **15**: 269-290 [PMID: 10611963 DOI: 10.1146/annurev.cellbio.15.1.269]
33 **Niwa H**. The principles that govern transcription factor network functions in stem cells. *Development* 2018; **145** [PMID: 29540464 DOI: 10.1242/dev.157420]
34 **Omatsu Y**, Nagasawa T. The critical and specific transcriptional regulator of the microenvironmental niche for hematopoietic stem and progenitor cells. *Curr Opin Hematol* 2015; **22**: 330-336 [PMID: 26049754 DOI: 10.1097/MOH.0000000000000153]
35 **Sibbesen NA**, Kopp KL, Litvinov IV, Jønson L, Willerslev-Olsen A, Fredholm S, Petersen DL, Nastasi C, Krejsgaard T, Lindahl LM, Gniadecki R, Mongan NP, Sasseville D, Wasik MA, Iversen L, Bonefeld CM, Geisler C, Woetmann A, Odum N. Jak3, STAT3, and STAT5 inhibit expression of miR-22, a novel tumor suppressor microRNA, in cutaneous T-Cell lymphoma. *Oncotarget* 2015; **6**: 20555-20569 [PMID: 26244872 DOI: 10.18632/oncotarget.4111]
36 **Ahmad HM**, Muiwo P, Muthuswami R, Bhattacharya A. FosB regulates expression of miR-22 during PMA induced differentiation of K562 cells to megakaryocytes. *Biochimie* 2017; **133**: 1-6 [PMID: 27889568 DOI: 10.1016/j.biochi.2016.11.005]
37 **Palma-Gudiel H**, Córdova-Palomera A, Leza JC, Fañanás L. Glucocorticoid receptor gene (NR3C1) methylation processes as mediators of early adversity in stress-related disorders causality: A critical review. *Neurosci Biobehav Rev* 2015; **55**: 520-535 [PMID: 26073068 DOI: 10.1016/j.neubiorev.2015.05.016]
38 **Kiraly G**, Simonyi AS, Turani M, Juhasz I, Nagy G, Banfalvi

G. Micronucleus formation during chromatin condensation and under apoptotic conditions. *Apoptosis* 2017; **22**: 207-219 [PMID: 27783174 DOI: 10.1007/s10495-016-1316-4]

39 **Kaiser AM**, Saluja AK, Sengupta A, Saluja M, Steer ML. Relationship between severity, necrosis, and apoptosis in five models of experimental acute pancreatitis. *Am J Physiol* 1995; **269**: C1295-C1304 [PMID: 7491921 DOI: 10.1152/ajpcell.1995.269.5.C1295]

P- Reviewer: Demonacos C, Gonzalez A, Mendez I **S- Editor**: Ma RY
L- Editor: Wang TQ **E- Editor**: Bian YN

World Journal of Gastroenterology

Submit a Manuscript: http://www.f6publishing.com

World J Gastroenterol 2018 December 7; 24(45): 5131-5143

DOI: 10.3748/wjg.v24.i45.5131

ISSN 1007-9327 (print) ISSN 2219-2840 (online)

ORIGINAL ARTICLE

Basic Study

Abdominal paracentesis drainage ameliorates severe acute pancreatitis in rats by regulating the polarization of peritoneal macrophages

Ruo-Hong Liu, Yi Wen, Hong-Yu Sun, Chun-Yu Liu, Yu-Fan Zhang, Yi Yang, Qi-Lin Huang, Jia-Jia Tang, Can-Chen Huang, Li-Jun Tang

Ruo-Hong Liu, Yi Wen, Hong-Yu Sun, Chun-Yu Liu, Yi Yang, Qi-Lin Huang, Can-Chen Huang, Li-Jun Tang, PLA Center of General Surgery and Pancreatic Injury and Repair Key Laboratory of Sichuan Province, Chengdu Military General Hospital, Chengdu 610083, Sichuan Province, China

Ruo-Hong Liu, Yi Wen, Li-Jun Tang, Third Military Medical University (Army Medical University), Chongqing 400037, China

Yu-Fan Zhang, Jiaotong Hospital Affiliated with the Sichuan Provincial People's Hospital, Chengdu 611730, Sichuan Province, China

Jia-Jia Tang, Department of Ultrasound, Chinese Academy of Medical Sciences and Peking Union Medical College Hospital, Beijing 100032, China

ORCID number: Ruo-Hong Liu (0000-0003-0885-8397); Yi Wen (0000-0001-9801-0853); Hong-Yu Sun (0000-0002-8587-0499); Chun-Yu Liu (0000-0002-4768-0459); Yu-Fan Zhang (0000-0002-3015-4962); Yi Yang (0000-0002-0189-6246); Qi-Lin Huang (0000-0002-0819-4829); Jia-Jia Tang (0000-0001-6036-6133); Can-Chen Huang (0000-0002-5598-4225); Li-Jun Tang (0000-0001-6000-9515).

Author contributions: Liu RH, Wen Y and Sun HY contributed equally to this work; Liu RH and Wen Y performed the majority of the experiments; Liu CY and Huang CC contributed to the animal experiments; Yang Y and Huang QL helped with the in vitro experiments; Zhang YF and Tang JJ contributed to data collection and manuscript preparation; Liu RH and Sun HY drafted the manuscript; and Tang LJ revised and approved the manuscript.

Supported by the National Natural Science Foundation of China, No. 81772001, No. 8177071311 and No. 81502696; the National Clinical Key Subject of China, No. 41792113; the Technology Plan Program of Sichuan Province, No. 2015SZ0229, No. 2018JY0041 and No. 18YYJC0442; and the Science and Technology Development Plan of Sichuan Province, No. 2016YJ0023.

Institutional animal care and use committee statement: All animal protocols were approved by the Animal Welfare Committee of Chengdu Military General Hospital, Chengdu, China (No. A20170312004).

Conflict-of-interest statement: The authors declare that there are no conflicts of interest related to this study.

Data sharing statement: No additional data are available.

ARRIVE guidelines statement: In the manuscript, the ARRIVE guidelines were adopted.

Manuscript source: Unsolicited manuscript

Correspondence author to: Li-Jun Tang, MD, PhD, Chief Doctor, PLA Center for General Surgery and Pancreatic Injury and the Repair Key Laboratory of Sichuan Province, Chengdu Military General Hospital, No. 270, Tianhui Road, Rongdu Avenue, Jinniu, Chengdu 610083, Sichuan Province, China. tanglj2016@163.com
Telephone: +86-28-86570265

Received: September 27, 2018
Peer-review started: September 27, 2018
First decision: October 14, 2018
Revised: October 20, 2018

Accepted: November 9, 2018
Article in press: November 9, 2018
Published online: December 7, 2018

Abstract

AIM

To investigate the role of peritoneal macrophage (PM) polarization in the therapeutic effect of abdominal paracentesis drainage (APD) on severe acute pancreatitis (SAP).

METHODS

SAP was induced by 5% Na-taurocholate retrograde injection in Sprague-Dawley rats. APD was performed by inserting a drainage tube with a vacuum ball into the lower right abdomen of the rats immediately after the induction of SAP. To verify the effect of APD on macrophages, PMs were isolated and cultured in an environment, with the peritoneal inflammatory environment simulated by the addition of peritoneal lavage in complete RPMI 1640 medium. Hematoxylin and eosin staining was performed. The levels of pancreatitis biomarkers amylase and lipase as well as the levels of inflammatory mediators in the blood and peritoneal lavage were determined. The polarization phenotypes of the PMs were identified by detecting the marker expression of M1/M2 macrophages *via* flow cytometry, qPCR and immunohistochemical staining. The protein expression in macrophages that had infiltrated the pancreas was determined by Western blot.

RESULTS

APD treatment significantly reduced the histopathological scores and levels of amylase, lipase, tumor necrosis factor-α and interleukin (IL)-1β, indicating that APD ameliorates the severity of SAP. Importantly, we found that APD treatment polarized PMs towards the M2 phenotype, as evidenced by the reduced number of M1 macrophages and the reduced levels of pro-inflammatory mediators, such as IL-1β and L-selectin, as well as the increased number of M2 macrophages and increased levels of anti-inflammatory mediators, such as IL-4 and IL-10. Furthermore, in an *in vitro* study wherein peritoneal lavage from the APD group was added to the cultured PMs to simulate the peritoneal inflammatory environment, PMs also exhibited a dominant M2 phenotype, resulting in a significantly lower level of inflammation. Finally, APD treatment increased the proportion of M2 macrophages and upregulated the expression of the anti-inflammatory protein Arg-1 in the pancreas of SAP model rats.

CONCLUSION

These findings suggest that APD treatment exerts anti-inflammatory effects by regulating the M2 polarization of PMs, providing novel insights into the mechanism underlying its therapeutic effect.

Key words: Abdominal paracentesis drainage; Peritoneal macrophages; Polarization; Severe acute pancreatitis

Core tip: In the present study, we provided evidence for the first time that abdominal paracentesis drainage (APD) ameliorates inflammation in rats with severe acute pancreatitis (SAP) by regulating peritoneal macrophage M2 polarization. The important findings are that: (1) by removing pancreatitis-associated ascitic fluids, APD could improve the inflammatory environment of the peritoneal cavity; (2) the improved environment in the peritoneal cavity could polarize peritoneal macrophages towards the M2 phenotype; and (3) APD could promote M2 polarization of macrophages in the pancreas of SAP model rats. These findings provide new insights into the mechanisms underlying the effectiveness of APD, which may advance the clinical use of APD to benefit patients with SAP.

Liu RH, Wen Y, Sun HY, Liu CY, Zhang YF, Yang Y, Huang QL, Tang JJ, Huang CC, Tang LJ. Abdominal paracentesis drainage ameliorates severe acute pancreatitis in rats by regulating the polarization of peritoneal macrophages. *World J Gastroenterol* 2018; 24(45): 5131-5143 Available from: URL: http://www.wjgnet.com/1007-9327/full/v24/i45/5131.htm DOI: http://dx.doi.org/10.3748/wjg.v24.i45.5131

INTRODUCTION

Severe acute pancreatitis (SAP) is a lethal inflammatory condition that is frequently accompanied by many complications, such as systemic inflammatory response syndrome (SIRS) and multiple organ dysfunction syndrome (MODS), which lead to a high risk of death in SAP patients. To date, the mortality rate for SAP remains high at 30%[1]. The key issue is that there is no effective strategy for controlling the activated inflammatory cascade and restoring immune homeostasis during SAP. Numerous studies have suggested that pancreatitis-associated ascitic fluids (PAAF) play an important role in the pathogenesis of SAP because they contain tumor necrosis factors, interleukins, endotoxins and other substances[2-4]. Our previous studies suggested that abdominal paracentesis drainage (APD) ameliorates SAP in patients safely and effectively by removing PAAF[5-7]. However, the mechanism underlying APD treatment remains poorly understood.

Macrophages are the main inflammatory cells implicated in the initiation and progression of the early stage of SAP[8,9]. They can be polarized into the following two different functional phenotypes in response to the microenvironment: classically activated macrophages (M1) or alternatively activated macrophages (M2). M1 macrophages produce pro-inflammatory cytokines,

including interleukin (IL)-1β, IL-6 and tumor necrosis factor (TNF)-α, while the M2 phenotype produces anti-inflammatory cytokines, such as IL-10[10]. Macrophages can also transition between the M1 and M2 phenotypes in response to certain signals[11,12]. Therefore, the polarization of macrophages towards the M2 phenotype has emerged as an interesting strategy to control the progression of inflammation[13]. Among the macrophages associated with SAP, peritoneal macrophages (PMs) are known to play a crucial role in the progression from local to systemic inflammation. PMs widely interact with PAAF, and the function of PMs is regulated by PAAF[14]. Although the activation of macrophages is tightly associated with the severity of SAP, whether APD can change the polarization state of PMs by removing PAAF in rats with SAP is uncertain.

Based on the above considerations, in the present study, we sought to determine the polarization phenotypes of PMs and the corresponding inflammatory response in a rat model of SAP following APD treatment. Our study offers new insights into the mechanism by which APD treatment ameliorates SAP.

MATERIALS AND METHODS

Experimental animals

The animal protocol was designed to minimize pain or discomfort to the animals. Adult male Sprague-Dawley rats weighing 200-250 g were purchased from Chengdu Dossy Experimental Animals Co., Ltd. (Chengdu, China). All rats were housed and fed in a pathogen-free facility under 12-h day and night cycles throughout the experiment. Animal experiments were performed according to the guidelines of the Animal Welfare Committee of Chengdu Military General Hospital.

In vivo experiments

Eighteen rats were divided into the following three equal groups according to a random number table: an SAP group, an APD group and a sham operation group (SHAM). Pancreatitis was induced in the SAP and APD groups by retrograde injection of 5% Na-taurocholate (0.1 mL/100 g body weight, Sigma, United States)[15] *via* the pancreatic duct using a syringe pump. In the APD group, a drainage tube with a vacuum ball was inserted into the lower right abdomen immediately after pancreatitis was induced[16]. Rats in the sham group did not receive any operation except opening and closure of the abdomen. Anesthesia was performed with an anesthesia machine using isoflurane (RWD Life Science, Shenzhen, China). Rats were sacrificed 12 h after the model was established. Blood samples were collected, and pancreatic tissues were harvested. According to previously described methods[17], PMs were isolated by peritoneal lavage after the ascetic fluid of SAP rats was drained.

Pancreatic histological analysis

The pancreas was dissected along the pancreatic duct, and a 0.5 cm × 0.5 cm sample was fixed in 4% paraformaldehyde solution. After being embedded in paraffin, the samples were cut into 4-μm thick sections and stained with hematoxylin and eosin (HE). Then, the slides were observed under an optical microscope, and the histopathology was scored using a previously described scoring system[18]. The scores were averaged for five individual slides from every pancreas.

Enzyme-linked immunosorbent assay

Enzyme-linked immunosorbent assays (ELISAs) were performed with the serum samples from each group using commercial rat-specific kits for amylase, lipase, IL-1β and TNF-α (Dakewe Biotech Co., Ltd. Shenzhen, China) according to the supplier's specifications.

Cell isolation

The ascetic fluid in the abdomen of SAP rats or the residual liquid in APD rats was drained followed by intraperitoneal injection of 20 mL of precooled PBS solution. After 5 minutes of abdominal kneading, 15 mL of lavage fluid containing peritoneal cells was transferred into the anticoagulant tube *via* a syringe. The cells were washed with PBS, resuspended in RPMI-1640 (Gibco, CA, United States) with 20% fetal bovine serum (Gibco, CA, United States) and cultured at 37 ℃ in 5% CO_2 for 1 h. The adherent cells were used in the subsequent experiments.

Flow cytometry

To detect the polarization phenotype of the macrophages in the abdomen, the PMs were analyzed by flow cytometry. PMs were washed with staining buffer (1% BSA in PBS containing 0.01% NaN_3, Thermo Fisher, United States) and incubated with 10% mouse serum for 20 min on ice. Subsequently, the cells were incubated with reagents from the LIVE/DEAD™ Fixable Dead Cell Stain Kit (Thermo Fisher, United States), FITC-conjugated anti-CD163 (Bio-Rad, United States), and PE-conjugated anti-CD86 (BD Biosciences, United States) at the manufacturer's recommended dilution for 40 min on ice. For intracellular staining, the cells were fixed and permeabilized with fixation buffer from a Fixation/Permeabilization Solution Kit (BD Biosciences, United States) for 1 h at 4 ℃ in the dark, washed with permeabilization buffer and incubated with Alexa-Flour647-conjugated anti-CD68 (Bio-Rad, United States) antibody in permeabilization buffer for 1 h at 4 ℃ in the dark. The samples were then washed and resuspended in permeabilization buffer and analyzed with a FACS Canto II system (BD Biosciences). The results were analyzed with BD FACS DIVA software (BD Biosciences, United States).

RNA isolation and qPCR

Total RNA from the abovementioned PMs was extracted using a commercial RNA extraction kit (Axygen, United States). The RNA was quantified by measuring the absorbance at 260 nm and 280 nm using a

spectrophotometer (NanoDrop Technologies, United States). cDNA was synthesized from a 100-ng RNA sample using the Primescript^{RT} reagent kit with a gDNA eraser (Takara, Tokyo, Japan) and stored at -80 ℃.

Real-time quantitative PCR was performed with a CFX96 Real-Time PCR Detection System using the SYBR Green Master Mix (Bio-Rad, United States). The primers used were as follows: INOS forward, 5′-CAGCCCTCAGAGTACAACGAT-3′ and reverse, 5′-CAGCAGGCACACGCAATGAT-3′; CD206 forward, 5′-ATTCCGGTCGCTGTTCAACT-3′ and reverse, 5′-AACGGAGATGGCGCTTAGAG-3′; TNF-α forward, 5′-CGTCGTAGCAAACCACCAAG-3′ and reverse, 5′-CACAGAGCAATGACTCCAAAG-3′; CD163 forward, 5′-CAACCGATGCTCAGGAAGAG-3′ and reverse, 5′-GATGGCACTTCCACATCCAA-3′. GAPDH was used as a reference gene, and the primers for GAPDH were the commercial Rat GAPDH Endogenous Reference Gene Primers (BBI Life Science, China).

Luminex assay

The concentrations of IL-1β, CXCL2, IL-4, IL-10 and TNF-α in the lavage fluid were determined by Luminex assays. A premixed commercial kit was used according to the manufacturer's recommendation (RD, United States). The assays were performed using the Luminex X-200 System (Luminex Corp, United States).

Immunofluorescence staining

The distribution of the two phenotypes of macrophages in the pancreas was assayed by immunofluorescence staining. Pancreatic tissues were washed with PBS twice, fixed with 4% paraformaldehyde for 24 h and dehydrated in a 30% sucrose solution. Then, the tissues were embedded in Tissue Freezing Medium and cut into 7-μm thick sections. The slides were washed with PBS and permeabilized with 0.1% Triton X-100. Subsequently, the slides were incubated with goat serum at 37 ℃ for 30 min. The samples were stained by incubation with Alexa-Flour647-conjugated anti-CD68 (Bio-Rad, United States) and FITC-conjugated anti-CD163 (Bio-Rad, United States) or Alexa-Flour647-conjugated anti-CD68 and PE-conjugated anti-CD86 (BD Biosciences, United States) at the manufacturer's recommended dilution at 4 ℃ overnight; then, the samples were stained with DAPI to visualize the nuclei. The distribution of the two phenotypes of macrophages in the pancreas was examined by laser scanning confocal microscopy.

Western blot analysis

Pancreatic tissues were dissociated in a commercial lysis buffer kit containing protease inhibitor and phenylmethylsulfonyl fluoride (PMSF) (Solarbio Science & Technology Co., Ltd, China) using a homogenizer. The tissue lysates were centrifuged at 12000 rpm for 30 min at 4 ℃, and the supernatant was collected for analysis. The protein concentration was measured using a commercial BCA protein assay kit (Solarbio Science and Technology Co., Ltd, China) according to the manufacturer's instructions. Proteins were mixed into the premixed protein sample buffer (Bio-Rad, United States) at equal concentrations and heated for 10 min at 100 ℃ to denature the protein. Electrophoresis was performed on 10% or 8% SDS-polyacrylamide gels followed by transferring the protein onto a PVDF membrane. After blocking with 5% nonfat milk in TBS solution for 1 h at room temperature, the blots were incubated in the following primary antibodies overnight at 4 ℃: mouse anti-Arg1 (1:200, Santa Cruz, United States), mouse anti-CD163 (1:200, Bio-Rad, United States), mouse anti-CD86 (1:200, BD Biosciences, United States), mouse anti-NOS2 (Santa Cruz, United States), and mouse anti-GAPDH (Thermo Fisher, United States). Afterwards, the blots were incubated with goat anti-mouse horseradish peroxidase (HRP)-conjugated secondary antibody (1:5000, Abcam, United Kingdom) for 1 h at room temperature. Then, the blots were developed using the enhanced chemiluminescence (ECL) method (Merck Milipore, Germany) in a bioimaging system (UVP, United Kingdom).

In vitro experiments

Primary cultured PMs were isolated from an additional ten rats as described above, washed with PBS and resuspended in RPMI-1640 (Gibco, CA, United States) with 20% fetal bovine serum (Gibco, CA, United States). All cells were plated at 1 × 10^6 cells per well in a 6-well plate and then cultured at 37 ℃ in 5% CO_2 for 3 d; adherent cells were identified as macrophages. Flow cytometry was used to identify the purity of the clones.

To test the effect of the abdominal inflammatory environment on PMs, primary cultured PMs were treated with medium containing 10% lavage fluid from SAP and APD rats separately for 12 h, and PBS was used as a control. The polarization phenotypes of the primary cultured PMs were determined by flow cytometry as mentioned above.

Statistical analysis

Statistical analyses were performed using SPSS 18.0 (SPSS Inc., United States), and the data are reported as the mean ± SD. Data were compared by Student's *t*-tests or one-way ANOVA followed by the SNK test for multiple comparisons, and nonparametrically distributed variables were compared by the Mann-Whitney test. $P < 0.05$ was considered statistically significant.

RESULTS

Therapeutic effects of APD on SAP in rats

The SAP rat model induced by Na-taurocholate retrograde injection (Figure 1A) is a stable animal model that has many similarities to the clinical manifestations of SAP in humans. To simulate the APD treatment, a drainage tube was inserted into the lower right abdomen of SAP

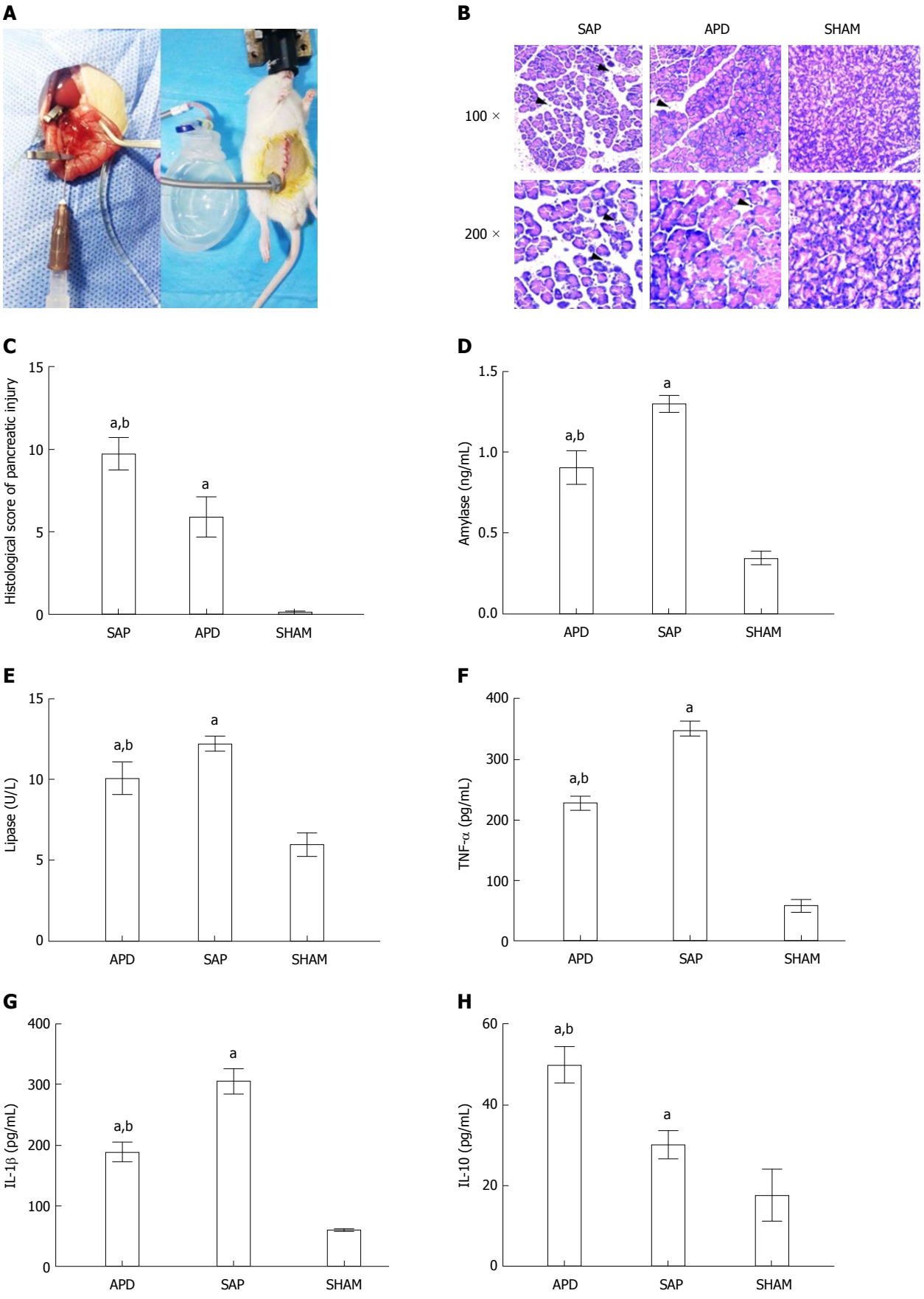
A
B
SAP
APD
SHAM
100 ×
200 ×
C
Histological score of pancreatic injury
15
10
5
0
a,b
a
SAP
APD
SHAM
D
Amylase (ng/mL)
1.5
1.0
0.5
0.0
a,b
a
APD
SAP
SHAM
E
Lipase (U/L)
15
10
5
0
a,b
a
APD
SAP
SHAM
F
TNF-α (pg/mL)
400
300
200
100
0
a,b
a
APD
SAP
SHAM
G
IL-1β (pg/mL)
400
300
200
100
0
a,b
a
APD
SAP
SHAM
H
IL-10 (pg/mL)
60
40
20
0
a,b
a
APD
SAP
SHAM

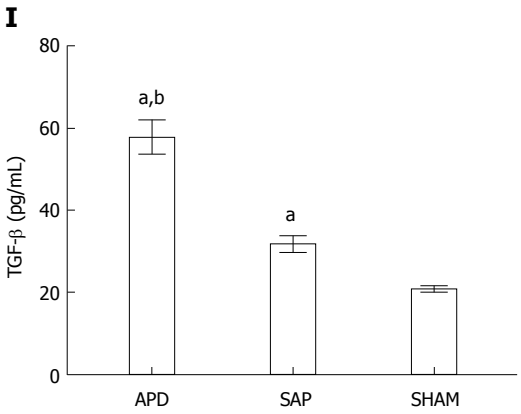

Figure 1 Abdominal paracentesis drainage ameliorates severe acute pancreatitis in a rat model. A: Model establishment. Retrograde injection of Na-taurocholate (left) and a rat after abdominal paracentesis drainage (APD) treatment (right); B and C: Histopathological analysis of the pancreas. Comprehensive disruption of the pancreatic structure with widespread infiltration of leukocytes, acinar cell vacuolization and necrosis was observed in severe acute pancreatitis (SAP) rats; localized leukocyte infiltration and relatively intact acinar structure were observed in APD rats; D-I: Plasma levels of amylase, lipase, tumor necrosis factor-α, interleukin (IL)-1β, IL-10 and transforming growth factor-β, respectively. Data indicate the mean ± SD of six mice (C-I). $^{a}P < 0.05$ *vs* sham, $^{b}P < 0.05$ *vs* SAP.

rats (Figure 1A). Histologically, apparent morphological damage in the form of acinar cell necrosis and inflammatory infiltration was observed in rats with SAP, while the tissue damage was significantly reduced in the APD treatment group (Figure 1B). This result was supported by the lower histopathological score in the APD group than in the SAP group (Figure 1C).

Subsequently, we measured the serum amylase and lipase levels, as they are known biomarkers of SAP. As shown in Figure 1, the APD group showed lower levels of amylase and lipase when compared with the SAP group (Figure 1D and E). In the APD and SAP groups, the concentrations of amylase and lipase were 0.906 ± 0.102 ng/mL *vs* 1.302 ± 0.052 ng/mL and 10.118 ± 1.019 U/L *vs* 12.251 ± 0.458 U/L, respectively.

Pro-inflammatory cytokines, such as TNF-α and IL-1β, are known to induce systemic inflammation in SAP. Compared with SAP rats, in APD rats, the levels of TNF-α and IL-1β were significantly lower, while the levels of the anti-inflammatory cytokines IL-10 and transforming growth factor-β were higher (Figure 1F-H), reflecting an amelioration of systematic inflammation in APD rats.

These results suggest that APD treatment could exert a protective role against the progression of SAP, as supported by the observed improved tissue damage and reduced systematic inflammation.

APD polarizes PMs towards the M2 phenotype in the peritoneal cavity

PMs play important roles in the progression of SAP. To assess the direct effect of APD on PMs, we first investigated the polarization phenotypes of the PMs in each group by flow cytometry. CD68 was used as a marker of all macrophages; CD68+CD86+ macrophages were identified as M1 macrophages, while CD68+CD163+ cells were identified as M2 macrophages. Flow cytometry plots revealed a significantly lower proportion of M1 PMs in APD rats compared to SAP rats, while a slight increase occurred in the proportion of M2 PMs (Figure 2B). Meanwhile, the M1/M2 ratio tended to be lower in the APD group than in the SAP group (Figure 2 B).

To further confirm the polarization phenotype of PMs at the genetic level, the expression of the M1-associated gene iNOS and the M2-associated gene CD206 was determined by qPCR. As expected, the expression of CD206 gene increased in the APD group, while it was inhibited in the SAP group. Although the expression of the iNOS gene was upregulated in both groups, it increased markedly in the SAP group (Figure 2E). These data indicate that APD treatment polarized PMs towards the M2 phenotype in the peritoneal cavity of SAP model rats.

APD reduces the levels of pro-inflammatory cytokines and increases the levels of anti-inflammatory cytokines in the peritoneal cavity

APD treatment drained the PAAF from SAP rats, thus altering the inflammatory environment of the peritoneal cavity. To compare the inflammatory environments in SAP and APD rats, we measured the production of representative pro-inflammatory and anti-inflammatory cytokines in the peritoneal lavage of each group by Luminex (Figure 3). The protein levels of the pro-inflammatory mediators IL-1β and L-selectin were significantly lower in APD rats than in SAP rats, while the levels of the anti-inflammatory cytokines IL-4 and IL-10 were increased. Although there were no significant differences in the levels of the pro-inflammatory cytokines IL-6 and CXCL2, the mean levels of these cytokines were greater in SAP rats than in APD rats. These results indicate that APD treatment promoted anti-inflammatory cytokine production and inhibited pro-inflammatory cytokine production.

PMs are polarized to the M2 phenotype in the simulated peritoneal inflammatory environment of APD rats in vitro

The phenotypes of PMs depend on the inflammatory

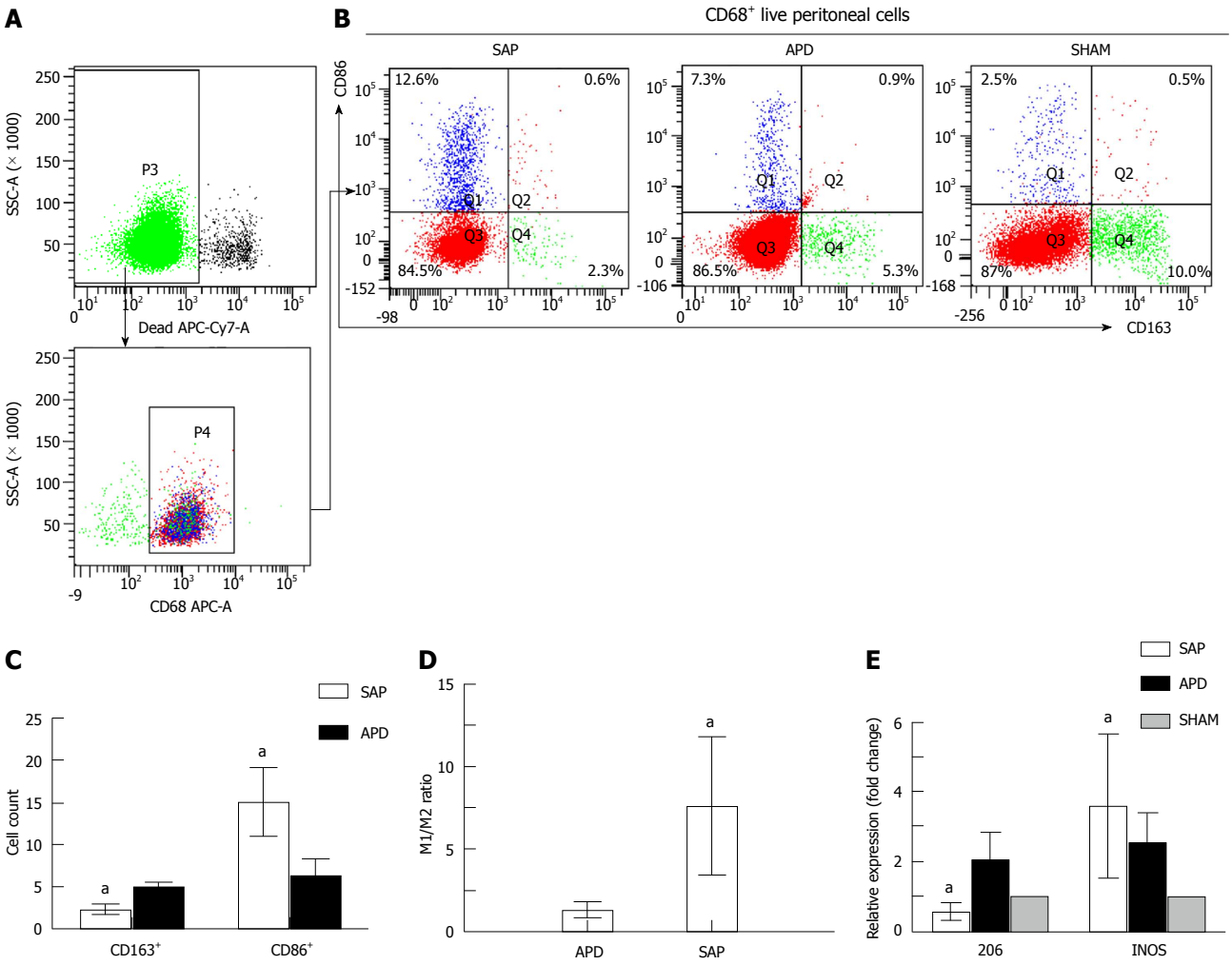

Figure 2 Different polarized phenotypes of peritoneal macrophages in each group. A: Gating strategy for the peritoneal macrophage population; B-D: Representative dot plot (B) and the percentages (C) and M1/M2 ratio (D) of CD68+CD86+ (M1) cells and CD68+CD163+ (M2) cells in each group; E: Relative expression levels of CD206 and iNOS gene in peritoneal cells measured by real-time PCR and normalized to GAPDH mRNA. The data represent at least three independent experiments (A-B) or indicate the mean ± SD of six mice (E). $^{a}P < 0.05$ *vs* abdominal paracentesis drainage.

environment. To investigate whether the peritoneal inflammatory environment affects PMs polarization *in vitro,* we simulated this environment by adding peritoneal lavage from the SAP and APD groups to primary cultured PMs. PBS was used as a negative control. Then, the PMs were evaluated by flow cytometry. The dot plot of FCM (Figure 4) indicated that the number of M2 macrophages increased slightly in PMs cultured in the APD environment, while no increase was found in cells cultured in the SAP environment. Although the numbers of M1 macrophages rose in both groups, they increased dramatically in the SAP environment. These data indicate that the altered peritoneal inflammatory environment induced by APD treatment enhanced M2 macrophage polarization in PMs.

APD promotes M2 polarization of macrophages in the pancreases of SAP rats

Given that macrophages are associated with intra-pancreatic injury during SAP, we evaluated the effect of APD on the polarization response of macrophages in the pancreas by immunofluorescence staining and Western blot. As shown in Figure 5A, the number of M2 macrophages clearly increased, while the number of M1 macrophages decreased in the pancreas of APD rats compared with SAP rats. The morphological changes were confirmed by Western blot (Figure 5B). The pancreatic levels of M2-associated proteins Arg-1 and CD163 were higher in APD rats than in SAP rats. In contrast, the levels of M1-associated proteins iNOS and CD86 were lower in APD rats than in SAP rats. The data show that APD could promote M2 polarization of macrophages in the pancreas of SAP rats.

Based on the above findings, a schematic model was proposed to elucidate the possible mechanism responsible for the beneficial effects of APD on SAP (Figure 6). Once SAP occurs, the inflammatory cells are activated following acinar cell injury and exudate full of pro-inflammatory mediators collects in the peritoneal cavity, which can polarize the PMs towards the M1 phenotype and lead to the overexpression of pro-inflammatory mediators by PMs. By removing the PAAF,

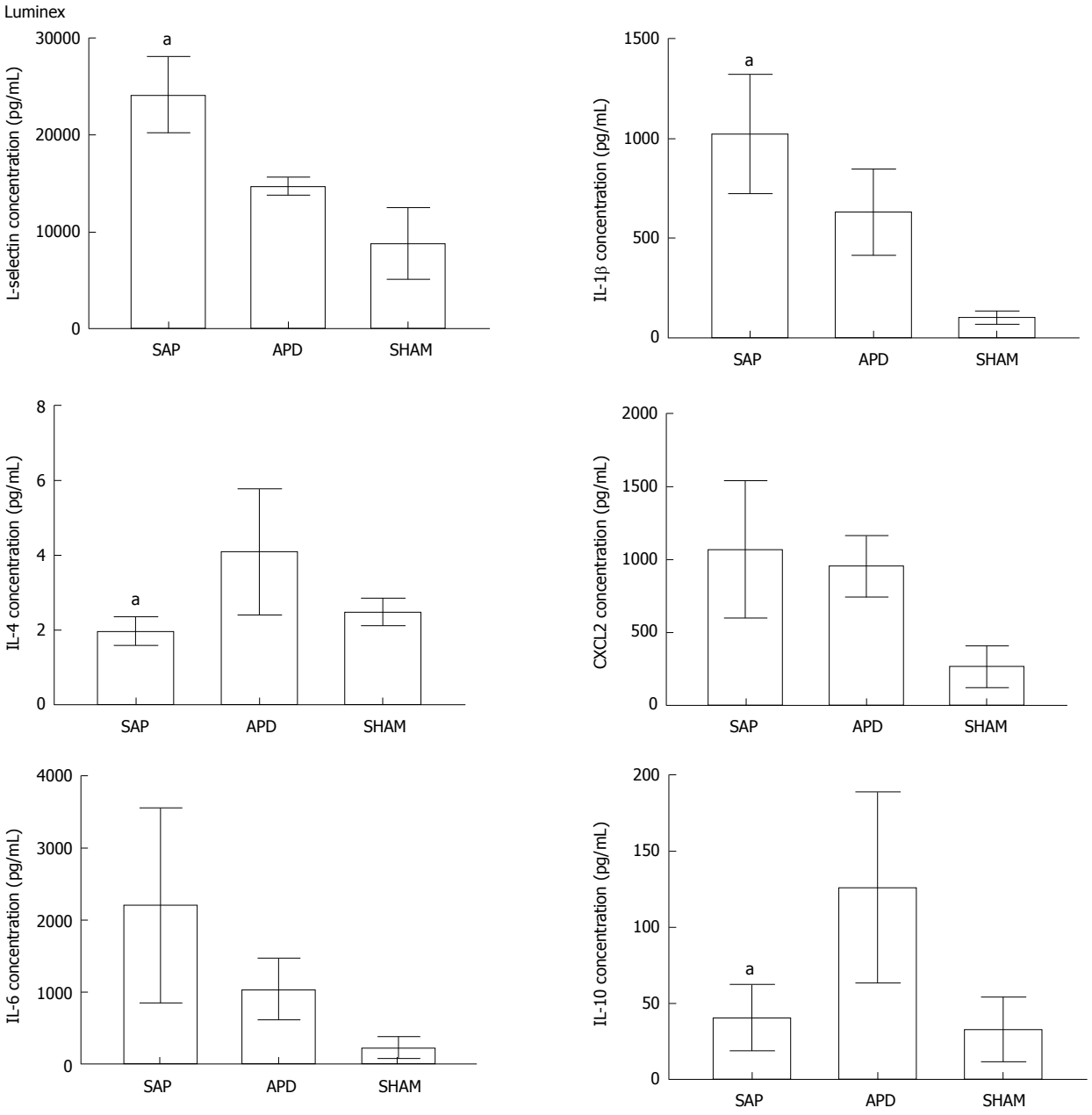

Figure 3 Abdominal paracentesis drainage alters the inflammatory environment in the peritoneal cavity. Protein levels in peritoneal lavage were measured by Luminex. The results reflect the mean ± SD obtained from six animals in each group. [a]*P* < 0.05 *vs* abdominal paracentesis drainage.

APD could improve the inflammatory environment of the peritoneal cavity and thus regulate M2 polarization of PMs in the peritoneal cavity. Meanwhile, APD could also promote M2 polarization of macrophages in pancreatic tissues. These events could upregulate the expression of anti-inflammatory cytokines, which ultimately ameliorate pancreatic injury.

DISCUSSION

In the present study, we provided evidence for the first time that APD ameliorates inflammation in rats with SAP by regulating PM M2 polarization. The important findings are that: (1) by removing PAAF, APD can improve the inflammatory environment of the peritoneal cavity; (2) the improved environment in the peritoneal cavity can polarize PMs towards the M2 phenotype; and (3) APD can promote M2 polarization of macrophages in the pancreas of SAP rats. These findings provide new insight into the mechanisms underlying the effectiveness of APD in the treatment of SAP, which may advance the clinical use of APD to benefit patients with SAP.

APD treatment before percutaneous catheter drainage has been proven to exert a beneficial effect on patients with SAP in our serial reports. Here, we demonstrated that APD treatment ameliorates the levels of inflammatory factors, including TNF-α, IL-1β and IL-6, in the serum and ascitic fluid of patients and rats with SAP[16]. Consistent with these results, in this paper, we found that APD not only decreased the levels of pro-

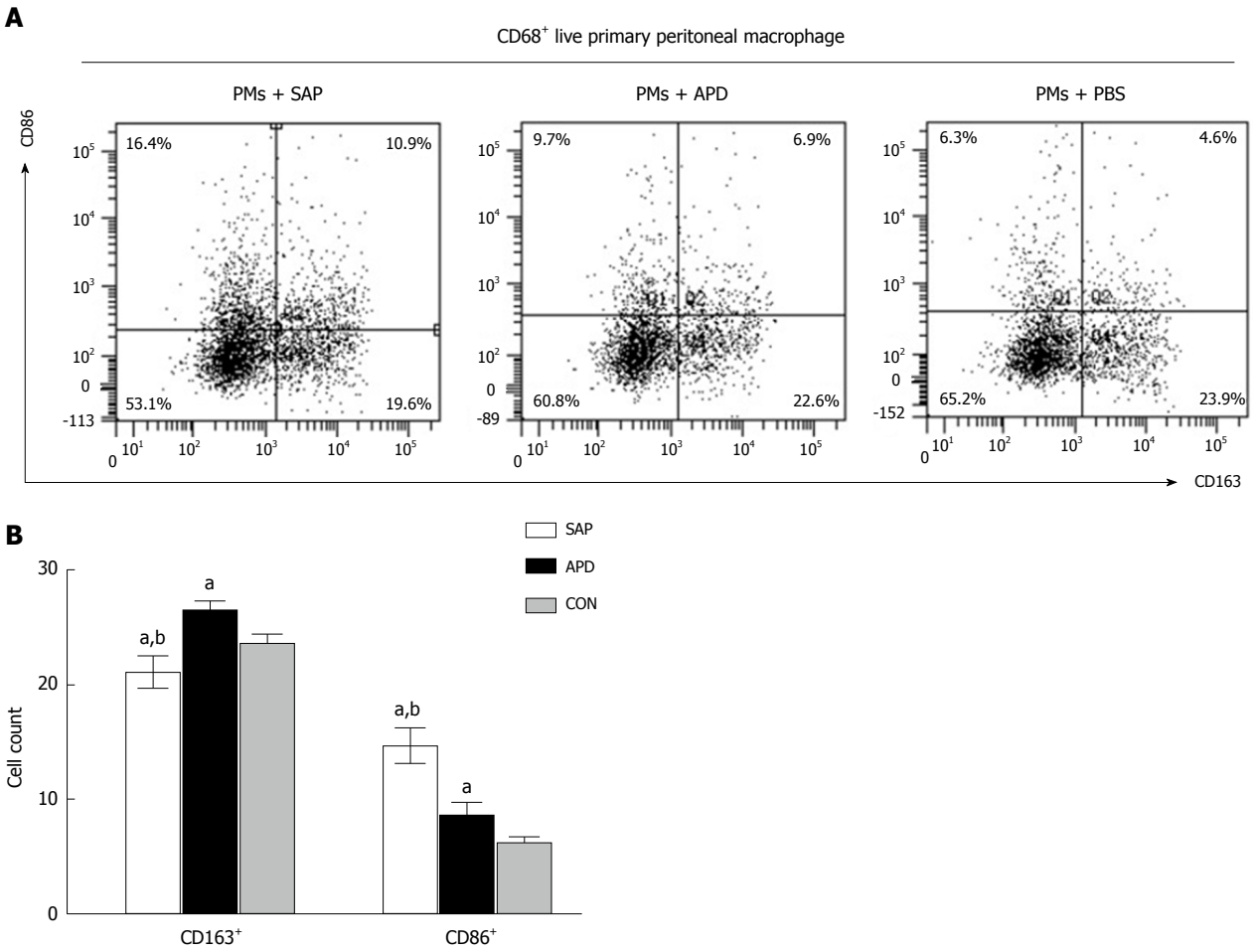

Figure 4 ***In vitro*** **simulated peritoneal inflammatory environment of abdominal paracentesis drainage rats changes the polarized phenotype of peritoneal macrophages.** Primary peritoneal macrophages were cultured in medium simulating different inflammatory environments. The percentages of $CD86^+$ and $CD163^+$ cells were measured by flow cytometry. The data are representative of at least three independent experiments. $^aP < 0.05$ *vs* CON, $^bP < 0.05$ *vs* abdominal paracentesis drainage.

inflammatory cytokines, such as IL-1β, and the adhesion molecule L-selectin but also increased the levels of anti-inflammatory cytokines, such as IL-4 and IL-10. This is in line with the findings of a recent study by Zhu and colleagues[19] in which it was shown that the levels of pro-inflammatory cytokines in ascites, including IL-1β, IL-6, IL-8 and TNF-α, decreased after early-stage drainage of the PAAF, while the level of the anti-inflammatory cytokine IL-10 increased significantly. Similar results were also reported by Souza[20], and these two studies suppose M2 macrophages as causative factors.

As is known, macrophages will acquire distinct functional phenotypes when responding to environmental cues. Because APD improves the inflammatory environment of the peritoneal cavity, we speculated that APD may influence the activation state of PMs. In fact, our results indicate that the proportion of M1 PMs in APD rats decreased significantly while the proportion of M2 PMs increased slightly when compared with the proportions in SAP rats. From a recent point of view, it has been suggested that macrophages do not exist as distinct M1 or M2 phenotypes but rather as a continuum of overlapping functional states, and the transition between the M1 to M2 phenotype is a dynamic process[10]. Therefore, we calculated the M1/M2 ratio to reflect the dynamic balance of macrophage polarization. The results indicate that the M1/M2 ratios in SAP rats and APD rats were 7.286 ± 4.22 *vs* 1.278 ± 0.481, respectively. Although M1 polarization was dominant in both groups, there was a trend to skew the balance towards the M2 phenotype in the APD group.

The mechanism by which APD polarizes PMs towards an M2 phenotype in the peritoneal cavity remains unknown; however, based on the above findings, we infer that APD might eliminate the comprehensively inflammatory environment, which provides an environment suitable for the survival of M2 macrophages and enhances the M2 polarization of PMs. The increase in the number of M2 macrophages in turn leads to the production of anti-inflammatory cytokines. To validate the effect of APD on the polarization of macrophages, lavage from each group was used to treat the primary cultured PMs. Consistent with the *in vivo* experiments, the number of M2 PMs increased in the APD group.

Studies have shown that polarizing macrophages towards the M2 phenotype ameliorates many chronic

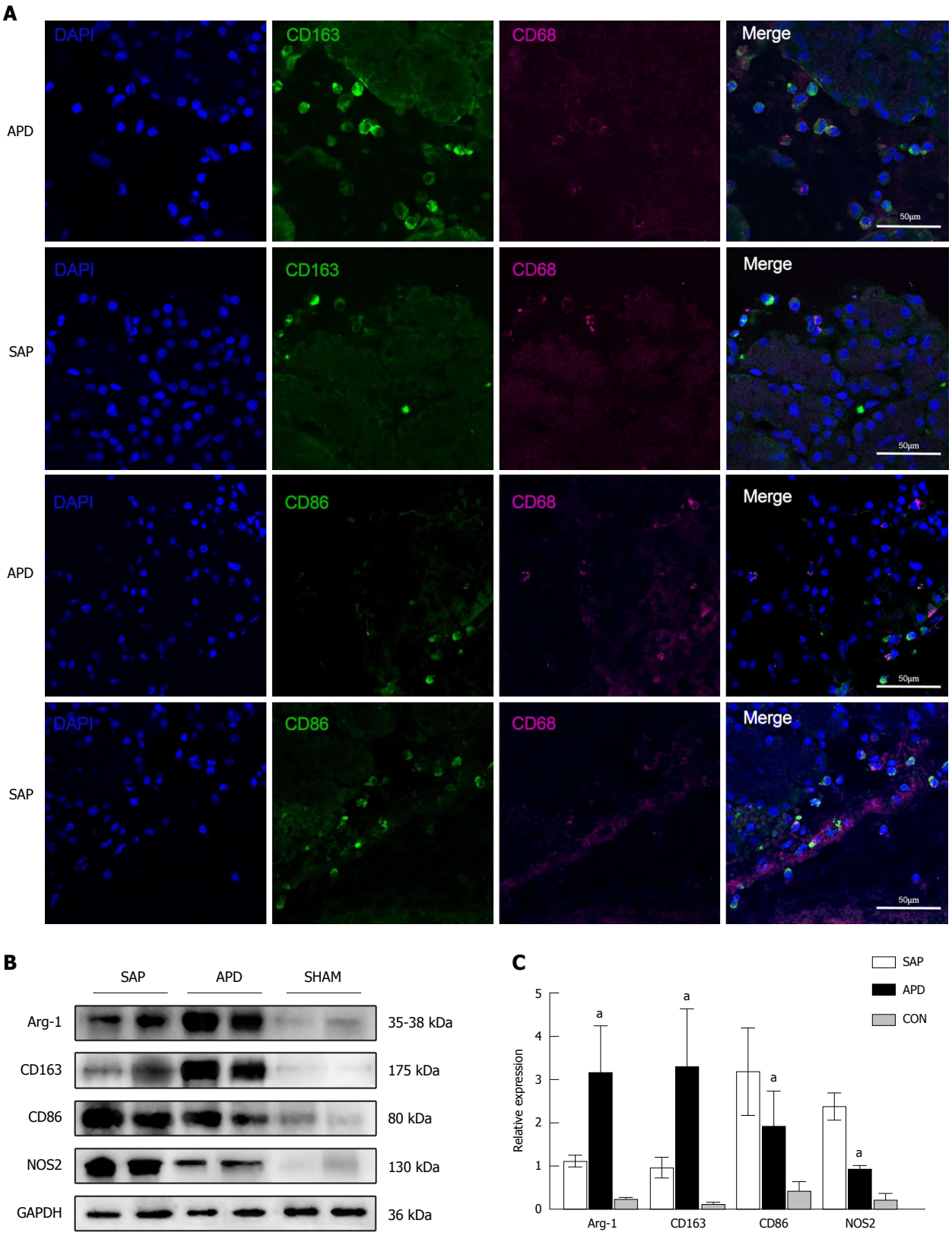

Figure 5 Number of M2 macrophages increases in the pancreas of abdominal paracentesis drainage rats and exerts anti-inflammatory effects. A: Pancreatic tissues from each group were stained with DAPI (blue), CD163 (green in upper two panels), CD86 (green in lower two panels) and CD68 (infrared represented by carmine). Representative images are shown; B and C: Protein levels of Arg-1, CD163, CD86 and iNOS in the pancreatic tissues of each group were measured by Western blot, and the relative expression of these proteins was normalized to GAPDH. Data are representative of at least three independent experiments. $^{a}P < 0.05$ *vs* severe acute pancreatitis.

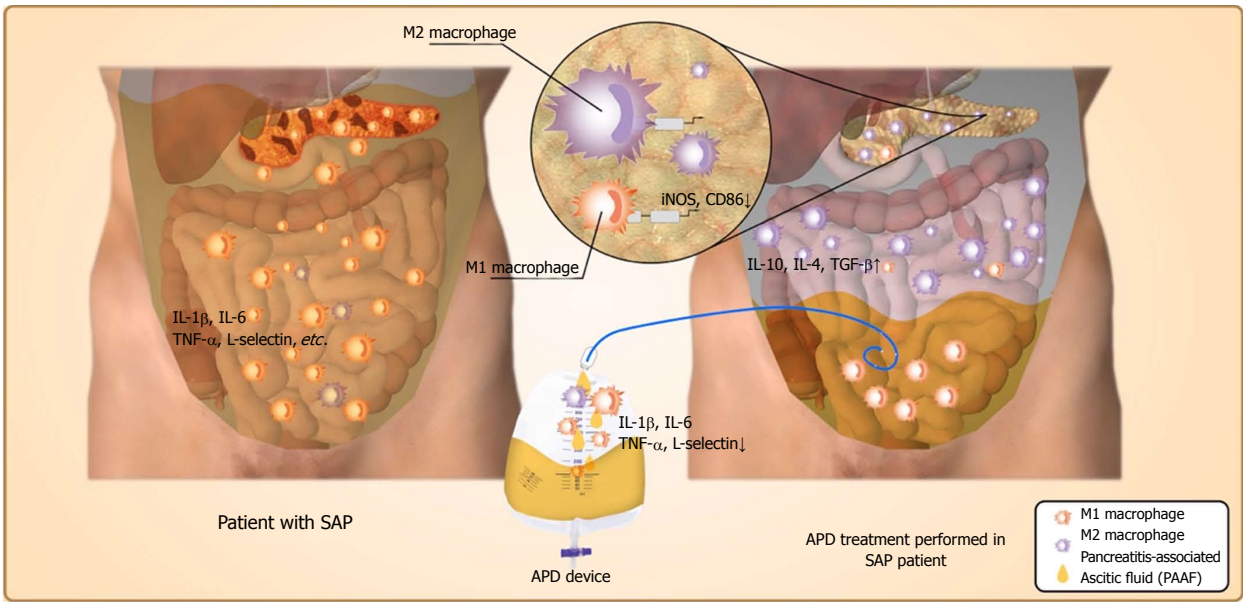

Figure 6 Possible mechanisms responsible for the beneficial effects of abdominal paracentesis drainage on severe acute pancreatitis. Once severe acute pancreatitis (SAP) occurs, the inflammatory cells are activated following acinar cell injuries and exudate full of pro-inflammatory mediators collects in the peritoneal cavity, which can polarize the peritoneal macrophages (PMs) towards the M1 phenotype and lead to the overexpression of pro-inflammatory mediators by PMs. By removing the pancreatitis-associated ascitic fluids, abdominal paracentesis drainage (APD) could improve the inflammatory environment of the peritoneal cavity, thus promoting M2 polarization of PMs in the peritoneal cavity. Meanwhile, APD could also promote M2 polarization of macrophages in pancreatic tissues. These events could upregulate the expression of anti-inflammatory cytokines, which ultimately ameliorate pancreatic injury. APD: Abdominal paracentesis drainage; SAP: Severe acute pancreatitis.

inflammation and autoimmune diseases[21], such as SLE[22], rheumatoid arthritis[23] and colitis[24]. Many methods have been used to induce M2 polarization[25]. However, most of the reports are *in vitro* experiments, and the therapeutic effect of M2 macrophages on acute inflammatory disease[26] is rarely reported. Although Xu *et al*[27] induced M2 polarization in primary cultured liver macrophages from rats with acute pancreatitis, they did not report any therapeutic effect of these cells in SAP. One possible reason is that large amounts of pro-inflammatory cytokines are released when the inflammatory cascade is activated, which overwhelmingly skews the M1/M2 balance towards M1 polarization *in vivo*. Our successful induction of the M2 polarization of PMs in SAP rats *in vivo* is a new attempt to utilize the advantages of M2 macrophages to ameliorate acute inflammatory diseases.

In addition, our findings demonstrate that the number of M2 macrophages also increased in the pancreas of SAP rats; however, only trace amounts of macrophages in the peripheral blood and bone marrow were polarized (data not shown). The data imply that the increase in the number of M2 macrophages in the pancreas is independent of the number of CD68+CD163+ cells in the peripheral blood and bone marrow. In our analysis, M2 macrophages may have migrated from the peritoneal cavity to the pancreas and regulated the immune responses in the pancreas of SAP rats. PMs have been reported to selectively migrate to the specific sites of inflammation in a colitis rat model[21], indicating that PMs could directly migrate to the focal zone in the peritoneal cavity. Moreover, the protein level of Arg-1, which is a key modulator in regulating T-lymphocyte functions and maintaining immunological tolerance[28], also increased. However, whether the M2 macrophages in the pancreas are PMs migrating from the peritoneal cavity still needs to be proven.

In conclusion, our findings suggest that APD treatment exerts anti-inflammatory effects to ameliorate SAP by regulating PM M2 polarization, thereby increasing the number of M2 macrophages and Arg-1 protein levels in the pancreas; these findings provide novel insights into the mechanisms underlying the therapeutic effect of APD.

ARTICLE HIGHLIGHTS

Research background

Severe acute pancreatitis (SAP) is a highly lethal disease with limited therapeutic options and is characterized by a critical systemic inflammatory response. Pancreatitis-associated ascitic fluids (PAAF) play an important role in the pathogenesis of SAP because of the pro-inflammatory mediators the PAAF contain. Our previous studies suggested that APD ameliorates SAP by removing the PAAF. However, the mechanism underlying the success of APD treatment remains poorly understood. In the present study, we aimed to explore the possible mechanism by which APD ameliorates SAP.

Research motivation

The key issue in treating SAP is to control the activated inflammatory cascade and restore immune homeostasis. Peritoneal macrophages (PMs), crucial inflammatory cells in the abdominal cavity, are implicated in the initiation and progression of SAP in the early stage, and the function of PMs is regulated by the PAAF. In this study, we found that APD treatment exerts anti-inflammatory effects by regulating the M2 polarization of PMs, providing novel insights into

the mechanisms underlying the therapeutic effect of APD.

Research objectives

The aim of this study was to determine the polarization phenotypes of PMs and the corresponding inflammatory responses in a rat model of SAP following APD treatment and to explore the possible mechanism by which APD treatment ameliorates SAP.

Research methods

The effect of APD on the polarization response of PMs was determined in an SAP rat model induced by 5% Na-taurocholate retrograde injection and in a peritoneal inflammatory environment simulated by adding peritoneal lavage to culture medium *in vitro*. HE staining and measurement of the levels of amylase, lipase, and inflammatory mediators were performed. The M1/M2 phenotype ratio of PMs was identified by flow cytometry and RT-PCR. The distribution of macrophages and their protein expression in the pancreas were determined by immunofluorescence staining and Western blot.

Research results

APD treatment ameliorates SAP by significantly reducing the pathological scores and the levels of amylase, lipase, tumor necrosis factor-α, and interleukin (IL)-1β. Importantly, APD treatment polarizes PMs towards the M2 phenotype and increases the anti-inflammatory mediators IL-4 and IL-10 in the peritoneal lavage. Furthermore, PMs exhibited a trend towards the M2 phenotype in a simulated peritoneal inflammatory environment *in vitro*. Finally, APD treatment increased the number of M2 macrophages and upregulated the expression of the anti-inflammatory protein Arg-1 in the pancreas of SAP rats.

Research conclusions

APD treatment exerts anti-inflammatory effects by regulating the M2 polarization of PMs, providing novel insights into the mechanisms underlying its therapeutic effect.

Research perspectives

Our study provided evidence for the first time that APD ameliorates inflammation in rats with SAP by regulating PM M2 polarization. However, solid evidence that APD polarizes PMs to the M2 phenotype and the underlying molecular mechanism still need to be explored. Furthermore, future research should focus on the effect of M2 macrophages on immune homeostasis restoration and tissue repair in the injured pancreas.

REFERENCES

1 **Forsmark CE**, Vege SS, Wilcox CM. Acute Pancreatitis. *N Engl J Med* 2016; **375**: 1972-1981 [PMID: 27959604 DOI: 10.1056/NEJMra1505202]

2 **Wang J**, Xu P, Hou YQ, Xu K, Li QH, Huang L. Pancreatitis-associated ascitic fluid induces proinflammatory cytokine expression in THP-1 cells by inhibiting anti-inflammatory signaling. *Pancreas* 2013; **42**: 855-860 [PMID: 23774701 DOI: 10.1097/MPA.0b013e318279fe5c]

3 **Takeyama Y**, Nishikawa J, Ueda T, Hori Y, Yamamoto M, Kuroda Y. Involvement of peritoneal macrophage in the induction of cytotoxicity due to apoptosis in ascitic fluid associated with severe acute pancreatitis. *J Surg Res* 1999; **82**: 163-171 [PMID: 10090825 DOI: 10.1006/jsre.1998.5535]

4 **Gutierrez PT**, Folch-Puy E, Bulbena O, Closa D. Oxidised lipids present in ascitic fluid interfere with the regulation of the macrophages during acute pancreatitis, promoting an exacerbation of the inflammatory response. *Gut* 2008; **57**: 642-648 [PMID: 18203805 DOI: 10.1136/gut.2007.127472]

5 **Liu L**, Yan H, Liu W, Cui J, Wang T, Dai R, Liang H, Luo H, Tang L. Abdominal Paracentesis Drainage Does Not Increase Infection in Severe Acute Pancreatitis: A Prospective Study. *J Clin Gastroenterol* 2015; **49**: 757-763 [PMID: 26053169 DOI: 10.1097/MCG.0000000000000358]

6 **Liu WH**, Ren LN, Chen T, Liu LY, Jiang JH, Wang T, Xu C, Yan HT, Zheng XB, Song FQ, Tang LJ. Abdominal paracentesis drainage ahead of percutaneous catheter drainage benefits patients attacked by acute pancreatitis with fluid collections: a retrospective clinical cohort study. *Crit Care Med* 2015; **43**: 109-119 [PMID: 25251762 DOI: 10.1097/CCM.0000000000000606]

7 **Liu L**, Liu W, Yan H, Cui J, Zhou J, Wang T, Tang L. Abdominal Paracentesis Drainage Does Not Bring Extra Risk to Patients With Severe Acute Pancreatitis. *J Clin Gastroenterol* 2016; **50**: 439 [PMID: 26890331 DOI: 10.1097/MCG.0000000000000488]

8 **Mikami Y**, Takeda K, Shibuya K, Qiu-Feng H, Shimamura H, Yamauchi J, Egawa S, Sunamura M, Yagi H, Endo Y, Matsuno S. Do peritoneal macrophages play an essential role in the progression of acute pancreatitis in rats? *Pancreas* 2003; **27**: 253-260 [PMID: 14508132 DOI: 10.1097/00006676-200310000-00011]

9 **Mayerle J**, Dummer A, Sendler M, Malla SR, van den Brandt C, Teller S, Aghdassi A, Nitsche C, Lerch MM. Differential roles of inflammatory cells in pancreatitis. *J Gastroenterol Hepatol* 2012; **27** Suppl 2: 47-51 [PMID: 22320916 DOI: 10.1111/j.1440-1746.2011.07011.x]

10 **Murray PJ**. Macrophage Polarization. *Annu Rev Physiol* 2017; **79**: 541-566 [PMID: 27813830 DOI: 10.1146/annurev-physiol-022516-034339]

11 **Zhou D**, Huang C, Lin Z, Zhan S, Kong L, Fang C, Li J. Macrophage polarization and function with emphasis on the evolving roles of coordinated regulation of cellular signaling pathways. *Cell Signal* 2014; **26**: 192-197 [PMID: 24219909 DOI: 10.1016/j.cellsig.2013.11.004]

12 **Labonte AC**, Tosello-Trampont AC, Hahn YS. The role of macrophage polarization in infectious and inflammatory diseases. *Mol Cells* 2014; **37**: 275-285 [PMID: 24625576 DOI: 10.14348/molcells.2014.2374]

13 **Atri C**, Guerfali FZ, Laouini D. Role of Human Macrophage Polarization in Inflammation during Infectious Diseases. *Int J Mol Sci* 2018; **19** [PMID: 29921749 DOI: 10.3390/ijms19061801]

14 **Satoh A**, Shimosegawa T, Masamune A, Fujita M, Koizumi M, Toyota T. Ascitic fluid of experimental severe acute pancreatitis modulates the function of peritoneal macrophages. *Pancreas* 1999; **19**: 268-275 [PMID: 10505757 DOI: 10.1097/00006676-199910000-00007]

15 **Aho HJ**, Koskensalo SM, Nevalainen TJ. Experimental pancreatitis in the rat. Sodium taurocholate-induced acute haemorrhagic pancreatitis. *Scand J Gastroenterol* 1980; **15**: 411-416 [PMID: 7433903]

16 **Chen GY**, Dai RW, Luo H, Liu WH, Chen T, Lin N, Wang T, Luo GD, Tang LJ. Effect of percutaneous catheter drainage on pancreatic injury in rats with severe acute pancreatitis induced by sodium taurocholate. *Pancreatology* 2015; **15**: 71-77 [PMID: 25455348 DOI: 10.1016/j.pan.2014.10.005]

17 **Pineda-Torra I**, Gage M, de Juan A, Pello OM. Isolation, Culture, and Polarization of Murine Bone Marrow-Derived and Peritoneal Macrophages. *Methods Mol Biol* 2015; **1339**: 101-109 [PMID: 26445783 DOI: 10.1007/978-1-4939-2929-0_6]

18 **Schmidt J**, Rattner DW, Lewandrowski K, Compton CC, Mandavilli U, Knoefel WT, Warshaw AL. A better model of acute pancreatitis for evaluating therapy. *Ann Surg* 1992; **215**: 44-56 [PMID: 1731649]

19 **Zhu L**, Lu J, Yang J, Sun P. Early-phase peritoneal drainage and lavage in a rat model of severe acute pancreatitis. *Surg Today* 2016; **46**: 371-378 [PMID: 25893772 DOI: 10.1007/s00595-015-1172-9]

20 **Souza LJ**, Coelho AM, Sampietre SN, Martins JO, Cunha JE, Machado MC. Anti-inflammatory effects of peritoneal lavage in acute pancreatitis. *Pancreas* 2010; **39**: 1180-1184 [PMID: 20683217 DOI: 10.1097/MPA.0b013e3181e664f2]

21 **Funes SC**, Rios M, Escobar-Vera J, Kalergis AM. Implications of macrophage polarization in autoimmunity. *Immunology* 2018; **154**: 186-195 [PMID: 29455468 DOI: 10.1111/imm.12910]

22 **Schaper F**, de Leeuw K, Horst G, Bootsma H, Limburg PC, Heeringa P, Bijl M, Westra J. High mobility group box 1 skews macrophage polarization and negatively influences phagocytosis

of apoptotic cells. *Rheumatology* (Oxford) 2016; **55**: 2260-2270 [PMID: 27632996 DOI: 10.1093/rheumatology/kew324]
23 **Quero L**, Hanser E, Manigold T, Tiaden AN, Kyburz D. TLR2 stimulation impairs anti-inflammatory activity of M2-like macrophages, generating a chimeric M1/M2 phenotype. *Arthritis Res Ther* 2017; **19**: 245 [PMID: 29096690 DOI: 10.1186/s13075-017-1447-1]
24 **Liu T**, Ren J, Wang W, Wei XW, Shen GB, Liu YT, Luo M, Xu GC, Shao B, Deng SY, He ZY, Liang X, Liu Y, Wen YZ, Xiang R, Yang L, Deng HX, Wei YQ. Treatment of dextran sodium sulfate-induced experimental colitis by adoptive transfer of peritoneal cells. *Sci Rep* 2015; **5**: 16760 [PMID: 26565726 DOI: 10.1038/srep16760]
25 **Tran TH**, Rastogi R, Shelke J, Amiji MM. Modulation of Macrophage Functional Polarity towards Anti-Inflammatory Phenotype with Plasmid DNA Delivery in CD44 Targeting Hyaluronic Acid Nanoparticles. *Sci Rep* 2015; **5**: 16632 [PMID: 26577684 DOI: 10.1038/srep16632]
26 **Işik A**, Firat D, İdiz UO. Nüks/komplike ve akut olgularda yaklaşımlar. *Turkiye Klinikleri Journal of General Surgery Special Topics* 2018; **11**: 112-114
27 **Xu L**, Yang F, Lin R, Han C, Liu J, Ding Z. Induction of m2 polarization in primary culture liver macrophages from rats with acute pancreatitis. *PLoS One* 2014; **9**: e108014 [PMID: 25259888 DOI: 10.1371/journal.pone.0108014]
28 **Bronte V**, Serafini P, Mazzoni A, Segal DM, Zanovello P. L-arginine metabolism in myeloid cells controls T-lymphocyte functions. *Trends Immunol* 2003; **24**: 302-306 [PMID: 12810105 DOI: 10.1016/S1471-4906(03)00132-7]

P- Reviewer: Isik AR, Smyrniotis V **S- Editor**: Wang XJ
L- Editor: Wang TQ **E- Editor**: Huang Y

World Journal of Gastroenterology

Submit a Manuscript: http://www.f6publishing.com

World J Gastroenterol 2018 December 7; 24(45): 5144-5153

DOI: 10.3748/wjg.v24.i45.5144

ISSN 1007-9327 (print) ISSN 2219-2840 (online)

ORIGINAL ARTICLE

Retrospective Cohort Study

Pelvic exenterations for primary rectal cancer: Analysis from a 10-year national prospective database

Gianluca Pellino, Sebastiano Biondo, Antonio Codina Cazador, José María Enríquez-Navascues, Eloy Espín-Basany, Jose Vicente Roig-Vila, Eduardo García-Granero, on behalf of the Rectal Cancer Project

Gianluca Pellino, Eduardo García-Granero, Colorectal Unit, Hospital Universitario y Politecnico La Fe, University of Valencia, Valencia 46026, Spain

Sebastiano Biondo, Department of General and Digestive Surgery, Colorectal Unit, Bellvitge University Hospital, University of Barcelona and IDIBELL, L'Hospitalet de Llobregat, Barcelona 08907, Spain

Antonio Codina Cazador, Department of General and Digestive Surgery--Colorectal Unit, Josep Trueta University Hospital, Girona 17001, Spain

José María Enríquez-Navascues, General and Digestive Surgery Department, Donostia University Hospital, Donostia 20014, Spain

Eloy Espín-Basany, Department of General Surgery, Colorectal Surgery Unit, Hospital Valle de Hebron, Autonomous University of Barcelona, Barcelona 08035, Spain

Jose Vicente Roig-Vila, Unit of Coloproctology, Hospital Vithas-Nisa 9 de Octubre, Valencia 46015, Spain

ORCID number: Gianluca Pellino (0000-0002-8322-6421); Sebastiano Biondo (0000-0002-7374-0371); Antonio Codina Cazador (0000-0003-3040-2716); José María Enríquez-Navascues (0000-0002-6486-1489); Eloy Espín-Basany (0000-0003-3784-1359); Jose Vicente Roig-Vila (0000-0002-8433-140X); Eduardo García-Granero (0000-0003-2657-6852).

Author contributions: Pellino G and García-Granero E designed the research; Pellino G, Biondo S, Codina Cazador A, Enríquez-Navascues JM, Espín-Basany E and Roig-Vila JV performed the research; Pellino G and García-Granero E analyzed the data; Pellino G, Biondo S, Codina Cazador A, Enríquez-Navascues JM, Espín-Basany E, Roig-Vila JV and García-Granero E wrote the paper and critically revised the manuscript for important intellectual content.

Institutional review board statement: The study was approved by the institutional review board.

Informed consent statement: Patients were not required to give informed consent to the study because the analysis used anonymous data that were obtained retrospectively.

Conflict-of-interest statement: All the authors declare no conflict of interest related to the manuscript.

Data sharing statement: Data will not be shared.

STROBE statement: The study adheres to STROBE Guidelines.

Manuscript source: Invited manuscript

Correspondence author to: Eduardo García-Granero, MD, PhD, Professor, Department of Surgery, University of Valencia, C/Pizarro 5 2-2, Valencia 46004, Spain. eggranero@telefonica.net
Telephone: +34-96-1244000
Fax: +34-96-3868864

Received: October 13, 2018
Peer-review started: October 15, 2018
First decision: October 23, 2018
Revised: November 5, 2018
Accepted: November 16, 2018
Article in press: November 16, 2018
Published online: December 7, 2018

Abstract

AIM

To identify short-term and oncologic outcomes of pelvic exenterations (PE) for locally advanced primary

rectal cancer (LAPRC) in patients included in a national prospective database.

METHODS

Few studies report on PE in patients with LAPRC. For this study, we included PE for LAPRC performed between 2006 and 2017, as available, from the Rectal Cancer Registry of the Spanish Association of Surgeons [Asociación Española de Cirujanos (AEC)]. Primary endpoints included procedure-associated complications, 5-year local recurrence (LR), disease-free survival (DFS) and overall survival (OS). A propensity-matched comparison with patients who underwent non-exenterative surgery for low rectal cancers was performed as a secondary endpoint.

RESULTS

Eight-two patients were included. The mean age was 61.8 ± 11.5 years. More than half of the patients experienced at least one complication. Surgical site infections were the most common complication (abdominal wound 18.3%, perineal closure 19.4%). Thirty-three multivisceral resections were performed, including two hepatectomies and four metastasectomies. The long-term outcomes of the 64 patients operated on before 2013 were assessed. The five-year LR was 15.6%, the distant recurrence rate was 21.9%, and OS was 67.2%, with a mean survival of 43.8 mo. R+ve resection increased LR [hazard ratio (HR) = 5.58, 95%CI: 1.04-30.07, P = 0.04]. The quality of the mesorectum was associated with DFS. Perioperative complications were independent predictors of shorter survival (HR = 3.53, 95%CI: 1.12-10.94, P = 0.03). In the propensity-matched analysis, PE was associated with better quality of the specimen and tended to achieve lower LR with similar OS.

CONCLUSION

PE is an extensive procedure, justified if disease-free margins can be obtained. Further studies should define indications, accreditation policy, and quality of life in LAPRC.

Key words: Pelvic exenteration; Advanced rectal cancer; Colorectal surgery; Complication; Outcome

Core tip: Pelvic exenteration (PE) for locally advanced primary rectal cancer (LAPRC) is associated with high rates of perioperative adverse events, but the survival benefit obtained when R-ve margins are achieved outweighs this risk. In low LAPRC, PE achieved better pathologic outcomes, resulting in a trend towards reduced LR compared with non-exenterative procedures.

Pellino G, Biondo S, Codina Cazador A, Enríquez-Navascues JM, Espín-Basany E, Roig-Vila JV, García-Granero E, on behalf of the Rectal Cancer Project. Pelvic exenterations for primary rectal cancer: Analysis from a 10-year national prospective database. *World J Gastroenterol* 2018; 24(45): 5144-5153 Available from: URL: http://www.wjgnet.com/1007-9327/full/v24/i45/5144.htm DOI: http://dx.doi.org/10.3748/wjg.v24.i45.5144

INTRODUCTION

Colorectal cancer is the fourth cause of cancer-related death in United States[1]. A recent analysis of the SEER programme concerning age-specific annual percent change in incidence rates from 2000 to 2013 showed that the incidence of rectal cancer and advanced disease has slightly decreased, but it is less than that of colon cancer[2]. Five-year survival is influenced by tumour stage, ranging from 90% in cancer confined to the primary site and 71% in those with local node involvement to 14% in Stage IV[3]. One-third of newly diagnosed rectal cancers in the United Kingdom will be locally advanced at the time of diagnosis, accounting for more than 4600 cases of cancer per year[4,5].

Recent advances in the multimodal management of patients with rectal cancer invading local structures have led to an increase in the rate of patients amenable to receive surgery along the anatomical planes after neoadjuvant treatment. Nevertheless, a relatively high number of patients might still be found with tumours invading surrounding organs[4].

Pelvic exenteration (PE) is a technically demanding procedure involving "*en-bloc*" excision of the rectum and adjacent invaded organs, aiming at obtaining disease-free resection margins. Over time, contraindications to such a demolitive approach have been gradually reduced as a result of perioperative patient conditioning, increased surgical experience, and postoperative multidisciplinary management[5-7]. Surgery beyond the total mesorectal excision (TME) plane and involving sacrifice of other pelvic organs for locally recurrent or advanced rectal cancer has been analogous to a "sarcoma-like" procedure[6,8-10], during which several surgical teams and specialties need to be involved. PE for rectal cancer brings higher risks of complications, ranging from 25% to 42%[5,8,11], with studies reporting higher rates when PE for other-than-rectal cancers is included[12]. The high incidence of complications is downplayed by the survival benefits obtained by excision of the pelvic mass with microscopically negative margins (R0)[7,8,12-14]. Few studies have focused on the outcomes of PE in locally advanced primary rectal cancer (LAPRC), although an increasing number of patients are being offered this extensive procedure. A recent study of the PelvEx Collaborative found that the median life expectancy after curative PE for LAPRC surpasses 40 mo, but median survival after resections with macroscopically involved margins drops to less than one year[14].

As part of a national quality improvement programme in the treatment of rectal cancer, the Spanish Association of Surgeons ["Asociación Española de Cirujanos" (AEC)] started an online database[15] in which all primary rectal

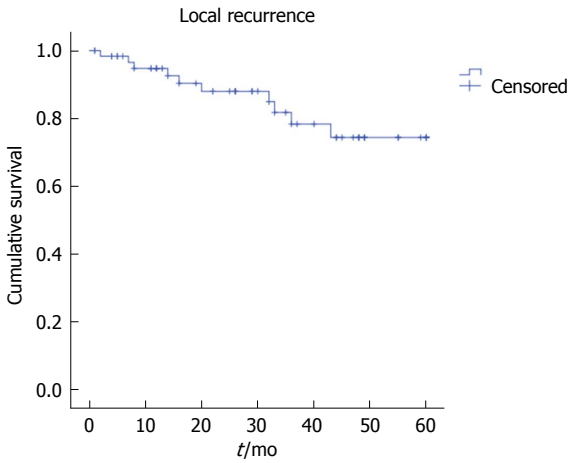

Figure 1 Overall local recurrence after pelvic exenteration for locally advanced primary rectal cancer.

cancers were prospectively included on a voluntary basis. Data on patients undergoing PE were also recoded.

The aims of this study are to assess the short- and long-term outcomes of PE for primary LAPRC in patients included in the AEC registry and to compare the oncologic results of PE with a matched group of patients treated with non-exenterative TME during the study timeframe.

MATERIALS AND METHODS

This study complies with the STROBE statement for observational studies[16] (Flowchart in Supplementary Figure 1; checklist available as uploaded STROBE Statement). In 2006, the AEC established a national audit project to improve the outcomes of rectal cancer surgery. The project was named "Viking" because it was inspired by the project from Norway[17] and followed the same principles[18]. Between 2006 and 2017, 105 Spanish hospitals joined the online registry, with over 18000 patients included. The aim of this study was to assess morbidity and long-term outcomes of PE for LAPRC.

Inclusion and exclusion criteria

We included patients who underwent PE for LAPRC between 2006 and 2017. The patients were only included if they underwent surgery with curative intent. For the survival analysis, only patients with a minimum follow up of 5 years were evaluated.

The patients who were unfit for surgery, those who underwent palliative surgery, those diagnosed with other malignancies besides colonic malignancies, and those with unsatisfactory information were excluded from the analysis.

Endpoints and definitions

The primary aims of this study were: (1) short-term morbidity and mortality of PE for LAPRC; (2) overall 5-year local recurrence (LR), disease-free survival (DFS), and overall survival (OS). Secondary outcomes included oncologic outcomes after PE compared with patients in the registry who underwent TME for distal rectal cancer surgery during the same timeframe, with a propensity-matched analysis.

The online database allows the investigators to classify the type of intervention performed. Only "PE" interventions were included in the analysis and consisted of either posterior (removal of rectum, internal genital organs in female) or total (removal of rectum and bladder, in male and female). Indications for surgery and perioperative management were not standardized before starting the study, although most centres followed the agreed-upon criteria[19].

Thirty-day complications were collected, and the responsible collaborator at each centre updated the data on oncologic outcome yearly[18,20].

Specimen assessment and reporting have been previously described[18,20,21]. Briefly, margins were considered tumour-free if no microscopic involvement was seen at pathology. The circumferential resection margin was considered involved if cancer cells were found 1 mm or less from the margin[20]. The quality of the mesorectum and abdominoperineal excision was scored using three grades as described by others[20-23].

LR was defined as a mass near or at the same place as the original tumour, after a period of time in which the tumour was not detected. LR was included only if an imaging exam proved the recurrence combined with raised CEA.

DFS was defined as time to develop a distant disease relapse that was not present or suspected at primary surgery. Distant metastases included para-aortic and inguinal nodes.

OS was defined as time to death for any reason.

Detailed definitions and scope of the registry have been previously reported[15,18,20] (http://www.aecirujanos.es/images/stories/recursos/secciones/coloproctologia/2015/proyecto_vikingo/documentos/definiciones_proyecto_vikingo.pdf).

For the secondary aims, the group that was propensity matched with PE included all patients from the database with low rectal cancer who underwent TME surgery with abdominoperineal excision, extralevator abdominoperineal excision, and low anterior resection between March 2006 and December 2013.

Statistical analysis

Continuous variables are reported as the means ± standard deviations (SD), and categorical variables are reported as the numbers with percentages (%).

For the secondary aims, the propensity-matched analysis for complications was carried out based on the following variables: American Society of Anesthesiologists' (ASA) score, neoadjuvant treatment, and pT stage. Only patients with cancer of the lower third of the rectum (0-6 cm from anal verge) who underwent curative TME surgery were included.

Categorical variables were compared with Fisher's exact test and Chi square test as appropriate, whereas

Table 1 Demographic, preoperative, and surgical details for 82 pelvic exenterations *n* (%)

Variable	Value
Age, yr	61.8 (11.5)
Gender	
Male	54 (65.9)
Female	28 (34.1)
ASA score	
I	3 (3.7)
II	42 (51.2)
III	33 (40.2)
IV	4 (4.9)
Obstruction	5 (6.1)
MR T	
T3	13 (15.9)
T4	56 (68.3)
Missing	13 (15.9)
MR N	
N0	11 (13.4)
N1	24 (29.3)
N2	35 (42.7)
Missing	12 (14.6)
Sphincters involved	22 (26.8)
Metastasis at presentation	7 (8.5)
Neoadjuvant treatment	59 (72)
Long course RT	3 (5)
Long course CRT	41 (69.5)
CxT	4 (6.8)
Short Course RT	4 (6.8)
CxT followed by RT	7 (11.9)
Adjuvant treatment	54 (65.9)
CRT	6 (11.1)
CT	48 (88.9)
Perioperative transfusions, *n*	3.4 (2)
Anastomosis	15 (18.3)
Synchronous metastasis resected	4 (6.8)

Data are expressed as number of patients (%) or median (25-75 percentiles). ASA: American Society of Anaesthesiologists; CRT: Chemoradiation therapy; CxT: Chemotherapy; MR: Magnetic resonance; RT: Radiotherapy.

continuous variables were compared with Mann-Whitney *U* test.

Kaplan-Meier survival curves were generated to assess 5-year survival, and log rank test was used for comparisons when applicable. Cox regression analysis was used to identify predictors of LR, DFS, and OS, including the following variables: resection margin status, quality of mesorectum, neoadjuvant treatment, adjuvant treatment, and perioperative complications. The results are reported as hazard ratio (HR) with 95% confidence intervals (95%CI). HR > 1 is associated with increased risk. Patients lost at follow up were classified as censored.

P values < 0.05 were considered statistically significant. The Statistical Package for Social Sciences (SPSS version 24.0.0; IBM SPSS statistics, IBM Corporation, Armonk, NY) was used for the descriptive analyses.

RESULTS

We analysed data on 82 patients undergoing PE for LAPRC in 33 hospitals, with a mean number of procedures per hospital of 2.5 ± 3.1 overall.

Baseline patient characteristics and surgical details

Demographics and perioperative features are summarized in Table 1. The mean age of the patients was 61.8 ± 11.5 years, 65.9% were men, 34.1% were women, and 45.1% were classified as ASA ≥ III. Most patients were staged as MRcT4 [T4 with magnetic resonance (MR)] and had extensive nodal involvement. The tumour was located in the proximal third of the rectum (15-11 cm) in 18 (22%) patients, in the middle third (10-7 cm) in 31 (37.8%) patients, and in the distal third (6-0 cm) in 33 (40.2%) patients. Seven patients underwent PE with concomitant distant metastases. Neoadjuvant treatment was offered to 72% of patients and included radiotherapy in 93% of them. No data were available concerning time to surgery after treatment.

Fifty-four (65.9%) patients received postoperative chemotherapy, which was associated with radiotherapy in 6 (11.1%). An anastomosis was attempted in 15 patients. In the latter group, eight patients received preoperative radiotherapy and postoperative treatment was given in nine, including radiotherapy in two.

Thirty-three multivisceral resections were performed, including two hepatectomies and four metastasectomies. One liver lesion was treated with radiofrequency ablation. One patient received peritonectomy.

Primary aim: Short-term outcomes and pathology

Perioperative death rates did not exceed 2.5%. More than half of the patients experienced at least one complication, and 10% required reoperation. Intra-abdominal septic complications occurred in 10% of the patients.

Surgical site infections affected the abdominal wound in 18.3% and the perineal closure in 19.4% of those who did not receive an anastomosis. Short-term outcomes are reported Table 2.

Table 3 depicts pathological outcomes. Most cancers were pT4b (36.6%), with significant reduction of cN2 rate in favour of pN0 (40.2%) and pN1 (20.7%). The mean number of isolated nodes was well over 12 and rarely harboured cancer (in 25.6%). Nineteen patients (23.2%) received R+ve resection - one with both circumferential and distal margins affected.

Twenty percent of patients did not have any response to preoperative neoadjuvant treatment, one patient had complete pathological response (1.7%), and the remaining patients had a different spectrum of response (detailed in Table 3). The quality of mesorectum was classified as "good" (complete)[20-23] in 74.4% of patients.

Primary aim: Recurrence and survival

For the purpose of long-term outcomes, we excluded 18 patients who received PE after 2013, thereby analysing 64 patients.

The five-year LR was 15.6%, the distant recurrence

Table 2 Short-term outcomes *n* (%)

Variable	Value
Complications, any	45 (54.9)
Reoperation	8 (9.8)
Perioperative death	2 (2.4)
Sepsis	4 (4.9)
Abdominal Surgical Site Infection	15 (18.3)
Abdominal hernia	2 (2.4)
Perineal Wound Complications	13/67 (19.4)
Intra-abdominal septic complications	8 (9.8)
Injury to hollow viscera	2 (2.4)
Ileus	9 (11)
Urinary tract complications	9 (11)
Pulmonary complications	8 (9.8)
Neurological complications	2 (2.4)
Multiorgan failure	2 (2.4)
CVC infection	2 (2.4)
Acute kidney failure	2 (2.4)

Data are expressed as number of patients (%) or median (25-75 percentiles). CVC: Central venous catheter.

Table 3 Pathological outcomes and survival *n* (%)

Variable	Value
pT	
Tx	2 (2.4)
T0	1 (1.2)
T2	2 (2.4)
T3a,b	6 (7.3)
T3c,d	13 (15.9)
T4a	27 (32.9)
T4b	30 (36.6)
Missing	1 (1.2)
pN	
Nx	25 (30.5)
N0	33 (40.2)
N1	17 (20.7)
N2	6 (7.3)
Missing	1 (1.2)
Nodes isolated	15.5 (10.6)
Positive nodes	1.1 (0.4)
Resection margins involved	19 (23.2)
Response to neoadjuvant treatment (*n* = 59)	
Complete	1 (1.7)
Islands of tumour cells	1 (1.7)
Predominantly fibrotic	20 (33.9)
Predominantly tumour nests	21 (35.6)
No response	12 (20.3)
Missing	4 (6.8)
Quality of mesorectum[20-23]	
Good/complete	61 (74.4)
Partially good/near complete	9 (11)
Bad/incomplete	8 (9.8)
Missing	4 (4.9)

Data are expressed as number of patients (%) or median (25-75 percentiles).

rate was 21.9%, and OS was 67.2%, with a mean survival of 43.8 mo (Figures 1-3). Oncologic outcomes tended to be worse in pN+ patients in all dimensions, although these differences did not reach statistical significance.

The Cox regression analysis identified R+ve resection to increase the risk of LR (HR = 5.58, 95%CI: 1.04-30.07, P = 0.04), and partially good or bad quality mesorectum to predict shorter DFS (HR = 4.37, 95%CI: 1.02-18.65, P = 0.04, and HR = 6.29, 95%CI: 1.2-32.94, P = 0.03, respectively). Perioperative complications were independent predictors of shorter survival (HR = 3.53, 95%CI: 1.12-10.94, P = 0.03).

Secondary aims: Propensity-matched sub-analyses in lower rectum

The propensity match analysis identified 51 patients who received either PE (n = 26) or non exenterative TME (n = 25) for primary adenocarcinoma of the lower rectum. Patient characteristics are summarized in Table 4. TME patients more frequently received an anastomosis (3.8% *vs* 80%, PE *vs* TME, P < 0.001) and were less likely to need transfusions (P = 0.035). PE was associated with better quality of the specimen, consisting of fewer R+ve resections and higher rates of good quality mesorectum.

LR tended to be lower in patients who received PE compared with TME (P = 0.34) (Supplementary Figure 2), with comparable OS (P = 0.96) (Supplementary Figure 3).

DISCUSSION

The present study showed good survival following PE for LAPRC in a cohort of patients included in a national prospective database. The procedure brings a significant risk of complications, occurring in 50% of patients, and non-negligible perioperative death rates. Pathological outcomes and long-term survival justify such extensive operations. Negative resection margins were achieved in 76.8% of patients and were associated with reduced rates of LR. Complications impaired 5-year survival. Comparing patients who underwent PE *vs* TME for low rectal cancer, PE showed a trend towards better specimen quality and lower rates of R+ve resection and tended to have longer LR-free intervals.

Since the first description of PE for gynaecologic cancer in 1948[6,24], the procedure has been adopted with increasing success rates in patients with rectal cancer[8,12-14,25-27]. The PE of colorectal interest involves "*en bloc*" resection of the cancer and of the surrounding structures/organs, namely, the rectum, distal colon, internal reproductive organs, draining lymph in posterior PE (also known as composite resections) or bladder, lower ureters, rectum, distal colon, sacrum, reproductive organs, draining lymph nodes and peritoneum in total PE[6,28].

Perioperative complications in our study were in line with rates reported in the literature. A systematic review[29] with 23 studies found that postoperative complications ranged between 37% and 100% (median 57%) and that perioperative mortality ranged between 0% and 25% (median 2.2%) after PE for LAPRC and recurrent cancer. The studies including all types of pelvic malignancies reported a complication rate as

Table 4 Propensity-matched analysis *n* (%)

	Pelvic exenteration *n* = 26	Non-exenterative total mesorectal excision *n* = 25	*P* value
Male	18 (58.1)	13 (52)	0.208
Age at surgery	63.1 ± 8.6	62.3 ± 13.7	0.794
ASA score			0.957
I	1 (3.8)	1 (4)	
II	11 (42.3)	11 (44)	
III	12 (46.2)	12 (48)	
IV	2 (7.7)	1 (4)	
Obstruction	1 (3.8)	0	0.322
Neoadjuvant treatment	21 (80.8)	21 (84)	0.762
Adjuvant treatment	19 (73.1)	21 (84)	0.343
Anastomosis	1 (3.8)	20 (80)	< 0.001[a]
T Stage			0.913
pT3a,b	1 (3.8)	1 (4)	
pT3c,d	6 (23.1)	6 (24)	
pT4a	7 (26.9)	7 (28)	
pT4b	11 (42.3)	11 (44)	
pTx	1 (3.8)	0	
Resection margins involved	5 (19)	7 (28)	0.426
Perforation	2 (7.7)	4 (16)	0.357
Transfusions	2.6 ± 2.4	1.12 ± 2.4	0.035[a]
Quality of the mesorectum[20-23]			0.351
Good/Complete	16 (69.6)	13 (52)	
Partially good/Nearly complete	4 (17.4)	8 (32)	
Bad/Incomplete	3 (13)	4 (16)	

[a]*P*: statistically significant. ASA: American Society of Anaesthesiologists.

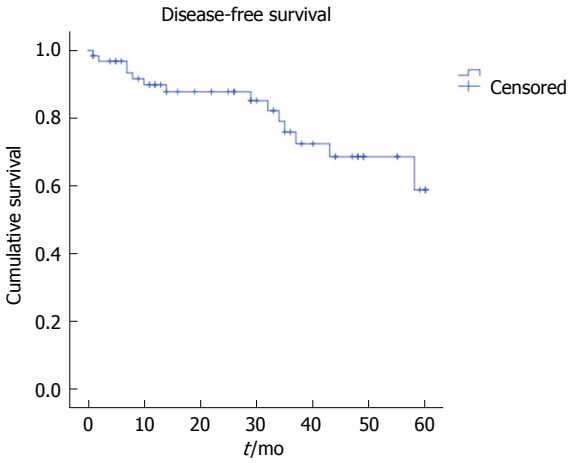

Figure 2 Overall disease-free survival after pelvic exenteration for locally advanced primary rectal cancer.

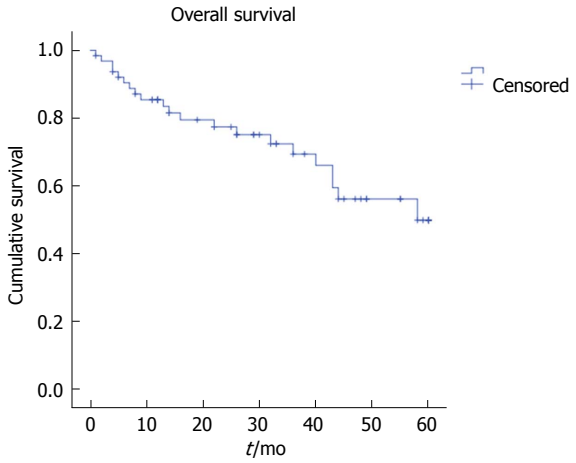

Figure 3 Overall survival after pelvic exenteration for locally advanced primary rectal cancer.

high as 64%[6]. In more recent series, complications occurred in 27.7% to 42.2% of patients who underwent PE for LAPRC[5,11,13,26]. Irrespective of ASA score, the rate of patients developing serious complications might be similar to that observed after TME anterior resection[11,30]. In our series, the rate of patients who developed complications needing reintervention was 10%. Surgeons willing to set up units dedicated to PE need to be prepared to long postoperative stays and significant morbidity, even in experienced hands[19]; early diagnosis and proactive management will be important to reduce their effects. Hsu *et al*[31] have discarded any influence of perioperative complications on survival after LAPRC surgery, but in our series, complications were independently associated with shorter life expectancy (HR = 3.53, 95%CI: 1.12-10.94, *P* = 0.03). These findings need to be carefully evaluated in the context of surgeon-specific outcomes[32] and learning curves associated with PE[33], and any attempt should be made to reduce complications, *e.g.*, being very selective in performing anastomosis and including a dedicated anaesthetist in the multidisciplinary team to allow for patient optimization[5,19,30].

The rate of R+ve resection in our study was similar to other reports but likely improvable. Combined with the quality of the excised specimen, it represents a reliable surrogate marker for LR and survival after PE[6,7,8,25]. The number of lymph nodes harvested in

specimens from patients who underwent neoadjuvant treatment is matter of debate in the vast majority of cases, and the PelvEx collaborative found it to be significantly associated with survival[13]. The mean number of nodes isolated from the specimen was higher than 12, which is the minimum acceptable number for TME. However, in this series, the effect on oncologic outcome was less obvious when comparing pN+ and pN- patients. Given the importance of pT and pN status in colorectal cancer[34], this issue needs to be further investigated in LAPRC. We confirmed that R status was an independent predictor of LR, which was impaired by five-fold in the event of positive resection margins. Statistical significance was maintained even if we observed a wide CI; cautious interpretation is needed, but the clinical relevance is unquestioned. Kontovounisios *et al*[5] analysed the performance of dedicated PE MDT at a single unit, and they achieved an R0 rate of 93% by the last year of their report. Interestingly, there was an inverse relation between the number of referrals (increasing over time) and the relative number of procedures performed (decreasing). This outcome resulted from better patient selection and better surgical timing in the context of multidisciplinary treatment. Other series reported rates of R+ve resections similar to the one in our analysis[11,13].

OS after PE for LAPRC is intertwined with the radicality of resection and recurrence[8,13]. The largest international, prospective study on PE for LAPRC included 1291 patients from 14 countries and showed a median 5-year survival of 43 months. The rate of patients who were alive at 5-year follow up from our database was 67.2%, which is at or above the upper limit of the ranges reported in the literature[6,12,26,30]. Reasons that could justify this finding include surgery probably not being offered to patients who might have been operated on in other centres with a more aggressive policy, *e.g.*, patients with pelvic bone involvement. According to the beyond TME collaborative[19], only poor performance status/medically unfit patients, bilateral sciatic nerve involvement and circumferential bone involvement should be considered absolute contraindications to surgery. A more conservative approach in patients from the database appears to be a reasonable option. Another reason could be early referral to hospitals with dedicated units. Lastly, individual investigators might have decided not to include patients with more complex disease and predictable poorer outcomes.

The ideal management of patients with LAPRC arising in the lower rectum is still a matter of debate. Given the excellent results in terms of tumour clearance and quality of life achieved with TME, mutilating approaches such as PE are deemed overtreatment in many patients. However, this part of the rectum is associated with higher rates of complications, and optimizing the outcomes of surgery for LAPRC of the lower third is still matter of research[35,36]. After adjusting two groups of patients with a propensity-matched analysis, we observed a trend towards better specimen quality and increased LR-free intervals with similar OS. These findings need further evaluation and should be considered when planning future studies on PE or involving low rectal cancers.

Limitations

This study has several limitations, and our findings should be interpreted with caution. Voluntary inclusion of patients in registries might account for a selection bias, even if they are prospective. The analysis covered a 10-year timeframe and included patients operated on different centres. Multidisciplinary patient management is crucial in PE[5], and variability between hospitals could not be removed. However, there are no universally agreed-upon guidelines to indicate or contraindicate PE in LAPRC, despite the latest available beyond-TME Collaborative position paper, which advocated the need for further research on the topic as a matter of priority[19]. No validation of the data was planned. LR was diagnosed by raising CEA associated with imaging proving recurrence, and this might have underestimated the actual incidence. Quality of life was not available in this study. Health-related quality of life and social function are of paramount importance in patients who are candidates for PE and should be considered an important endpoint of LARC surgery. The stressful experience that patients and families go through after receiving a diagnosis and when they are forced to face an advanced and aggressive disease is made even more difficult when the perspectives of the necessity of a definitive stoma (sometimes more than one) are considered. However, no dedicated questionnaires or assessments have been proposed and validated in this group of patients and should therefore be considered a research priority.

This study has strengths. Limited series of PE for LAPRC have been reported, and the findings described herein represent the second largest study with 5-year follow up available after the PelvEx Collaborative study. We suggested that patients with LAPRC of the lower third might benefit from a more aggressive surgical approach, and future studies could be designed to confirm the survival advantage in this group of patients. Some centres advocated PE in patients with liver metastases. The numbers were too small to conduct sub-analyses, and results could be misleading. Interestingly, distant metastases are usually a contraindication to PE in most referral centres[5]. As per the available position paper, LAPRC with metastases amenable to resection could benefit from PE, on the condition that a dedicated MDT agrees to the indication. In agreement with the statements of the beyond TME Collaborative[19], the outcomes of PE should be separately reported, and our manuscript only included this homogeneous group of patients.

PE is an extensive procedure with significant rate of perioperative adverse events. The analysis of a national database on LAPRC treated with PE over 10 years confirmed the survival benefit of the procedure, which overwhelms the morbidity and mortality associated with it. The rates of LR, DFS and OS were in line with

most of the reported studies, but any effort should be made to improve these results (*e.g.*, *via* centralization, adherence to prospective registries and auditing, dedicated training). Disease-free resection margins (R0) comprise the aim of surgery, as they predict LR. PE should be carried out in dedicated units under the care of MDT to reduce or promptly treat complications, which impair long-term survival.

Compared with non-exenterative TME surgery, PE was associated with longer disease-free intervals and achieved similar OS in patients with LAPRC for low rectal cancer.

Further studies are needed to clarify patient selection pathways and referral centre accreditation policies, and to assess quality of life after PE.

ARTICLE HIGHLIGHTS

Research background

Colorectal cancer is the fourth cause of death caused by cancer according to reports from the United States. Up to 33% of rectal cancers might present as locally advanced, requiring multidisciplinary approaches. Pelvic exenteration (PE) combined with multimodal treatment has resulted in increased survival in this population of patients, but there remains a need for further reports in the literature concerning the management of patients with primary locally advanced rectal cancer.

Research motivation

Previous studies suggested that an aggressive approach, with surgery combined with other treatment modalities, might confer good outcome in terms of tumour clearance and survival in locally advanced primary rectal cancer (LAPRC). Few reports have been published detailing the outcome of nationwide databases.

Research objectives

This study aimed to investigate the outcome of PE for primary rectal cancer in patients included in the National Spanish Association of Surgeons Rectal Cancer Registry.

Research methods

This is a retrospective, observational study drafted according to the STROBE statement. Patients who underwent PE for LAPRC between 2006 and 2017 and who were registered in the Spanish Registry of Rectal Cancer of the Spanish Association of Surgeons were included if surgery was performed with curative intent and if 5-year follow up had been completed.

Short-term morbidity and mortality of the procedure and 5-year oncologic outcome represented the primary aims of this study. Secondary aims included a comparison of outcomes with a matched group of patients from the registry who underwent non-exenterative surgery for low rectal cancer during the same time frame.

Research results

PE were associated with perioperative mortality in approximately 2.5% of patients, and perioperative morbidity was common. More than 50% of patients had at least one complication, which required reoperation in 10%. Up to 10% of patients suffered from intra-abdominal septic complication. Wound-associated complications at the perineum were common, almost reaching 20%. The rate of resections with margins that involved tumours was 23%, and good quality of the mesorectum was achieved in 74% of specimens.

Oncologic outcome was acceptable, with good life expectancy provided a free-free resection margin had been achieved. An involved margin was independently associated with increased risk of local recurrence [hazard ratio (HR) = 5.58, 95%CI: 1.04-30.07, P = 0.04]. Survival was impaired by perioperative complications [HR = 3.53, 95%CI: 1.12-10.94, P = 0.03].

In terms of comparison with non-exenterative procedures, the latter were associated with fewer blood transfusions (P = 0.035) and more anastomoses (P < 0.001). However, resections with involved margins were less common after PE.

Research conclusions

PE is an extensive procedure with a significant rate of perioperative adverse events. However, our analysis of patients with LAPRC treated with this procedure over 10 years confirmed that the survival benefits justify an aggressive attitude, provided that oncologic clearance is achievable. These procedures must be performed in a dedicated unit, and patients be managed under the care of multidisciplinary teams.

Research perspectives

An aggressive attitude could confer a significant survival gain in carefully selected patients with LAPRC. The use of national and International registries is of great value to monitor the performance of centres dealing with PE and internal auditing; therefore, their use should be encouraged.

ACKNOWLEDGMENTS

The authors would like to thank Hector Ortiz for coordinating the Rectal Cancer Project (Viking) and this manuscript. We thank all the collaborators in Rectal Cancer (Viking) Project.

Collaborators list of Rectal Cancer (Viking) Project

Raúl Adell Carceller (Hospital de Vinaroz), Juan Guillermo Ais Conde (Hospital de Segovia), Evelio Alonso Alonso (Complejo Asistencial de Burgos), Antonio Amaya Cortijo (Hospital San Juan de Dios del Aljarafe de Sevilla), Antonio Arroyo Sebastian (Hospital General Universitario de Elche), Pedro Barra Baños (Hospital General Reina Sofía de Murcia), Ricard Batlle Solé (Hospital de Santa María de Lleida), Juan C Bernal Sprekelsen (Hospital de Requena), Sebastiano Biondo (Hospital Universitari de Bellvitge), Francisco J Blanco Gonzalez (Hospital La Ribera, Alzira), Santiago Blanco (Hospital de Reus), J Bollo (Hospital Universitari de la Santa Creu i Sant Pau de Barcelona), Nieves Cáceres Alvarado (Complejo Hospitalario de Vigo Xeral + Meixoeiro), Ignasi Camps Ausas (Hospital Universitari Germans Trias i Pujol de Badalona), Ramon Cantero Cid (Hospital Infanta Sofía de Madrid), José Antonio Carmona Saez (Hospital Nuestra Señora de Sonsoles de Ávila), Enrique Casal Nuñez (Complejo Hospitalario de Vigo Xeral + Meixoeiro), Luis Cristobal Capitán Morales (Hospital Virgen Macarena de Sevilla), Guillermo Carreño Villarreal (Hospital de Cabueñes de Gijón), Jesús Cifuentes Tebar (Hospital General de Albacete), Miguel Á Ciga Lozano (Hospital Virgen del Camino-Complejo Hospitalario de Navarra), Antonio Codina Cazador (Hospital Universitari de Girona Dr. Josep Trueta), Juan de Dios Franco Osorio (Hospital General de Jerez), María de la Vega Olías (Hospital Puerto Real de Cádiz), Mario de Miguel Velasco (Hospital Virgen del Camino-Complejo Hospitalario de Navarra), Sergio Rodrigo del Valle (Hospital General Rafael Mendez de Murcia), José G Díaz Mejías (Hospital Nuestra Señora de la Candelaria de Tenerife), José M Díaz Pavón (Hospital Virgen del Rocío de Sevilla), Javier Die Trill (Hospital Universitario Ramón y Cajal de Madrid), José L Dominguez Tristancho (Hospital de Mérida), Paula Dujovne Lindenbaum (Hospital Universitario Fundación

Alcorcón), José Errasti Alustiza (Hospital Txagorritxu de Vitoria), Alejandro Espí Macias (Hospital Clínico Universitario de Valencia), Eloy Espín Basany (Hospital Universitari Vall d'Hebron de Barcelona), Rafael Estévan Estévan (Instituto Valenciano de Oncología IVO), Alfredo M Estevez Diz (Hospital Policlínico Povisa de Vigo), Luis Flores (Hospital Clínico y Provincial de Barcelona), Domenico Fraccalvieri (Hospital Universitari de Bellvitge), Alessandro Garcea (Hospital Torrevieja Salud UTE), Mauricio García Alonso (Hospital Clínico San Carlos de Madrid), Miguel Garcia Botella (Hospital General Universitario de Valencia), Maria José García Coret (Hospital General Universitario de Valencia), Alfonso García Fadrique (Instituto Valenciano de Oncología IVO), José M García García (Hospital de Cruces), Jacinto García García (Complejo Asistencial de Salamanca), Eduardo García-Granero (Hospital Universitario y Politécnico La Fe de Valencia), Jesús Á Garijo Alvarez (Hospital de Torrejón), José Gomez Barbadillo (Hospital Universitario Reina Sofía de Córdoba), Fernando Gris (Hospital Universitari Joan XXIII de Tarragona), Verónica Gumbau (Hospital General Universitario de Valencia), Javier Gutierrez (Complejo Hospitalario de Jaén), Pilar Hernandez Casanovas (Hospital Universitari de la Santa Creu i Sant Pau de Barcelona), Daniel Huerga Alvarez (Hospital Universitario de Fuenlabrada), Ana M Huidobro Piriz (Complejo Hospitalario de Palencia), Francisco Javier Jimenez Miramón (Hospital Universitario de Getafe), Ana Lage Laredo (Hospital Nuestra Señora del Rosell), Alberto Lamiquiz Vallejo (Hospital de Cruces), Félix Lluis Casajuana (Hospital General Universitario de Alicante), Manuel López Lara (Hospital Espíritu Santo de Santa Coloma de Gramanet), Juan A Lujan Mompean (Hospital Virgen de la Arrixaca), María Victoria Maestre (Hospital Virgen del Rocío de Sevilla), Eva Martí Martínez (Hospital Dr. Peset de Valencia), M Martinez (Hospital Universitari de la Santa Creu i Sant Pau de Barcelona), Javier Martinez Alegre (Hospital Infanta Sofía de Madrid), Gabriel Martínez Gallego (Complejo Hospitalario de Jaén), Roberto Martinez Pardavila (Onkologika de San Sebastian), Olga Maseda Díaz (Hospital Xeral de Lugo), Mónica Millan Schediling (Hospital Universitari Joan XXIII de Tarragona), Benito Mirón (Hospital Clínico Universitario San Cecilio de Granada), José Monzón Abad (Hospital Miguel Servet de Zaragoza), José A Múgica Martinera (Hospital Donostia), Francisco Olivet Pujol (Hospital Universitari de Girona Dr. Josep Trueta), Mónica Orelogio Orozco (Hospital General Juan Ramón Jimenez de Huelva), Luis Ortiz de Zarate (Consorci Sanitari Integral - Hospital General de L'Hospitalet y Hospital Moisés Broggi), Rosana Palasí Gimenez (Hospital Universitario y Politécnico La Fe de Valencia), Natividad Palencia García (Hospital de Henares, Coslada), Pablo Palma Carazo (Hospital Universitario Virgen de las Nieves), Alberto Parajo Calvo (Complejo Hospitalario de Ourense), Jesús Paredes Cotore (Hospital Clínico Universitario de Santiago de Compostela), Carlos Pastor Idoate (Fundación Jimenez Díaz), Miguel Pera Roman (Hospital del Mar de Barcelona), Francisco Pérez Benítez (Hospital Clínico Universitario San Cecilio de Granada), José A Pérez García (Hospital Virgen del Puerto de Plasencia), Marta Piñol Pascual (Hospital Universitari Germans Trias i Pujol de Badalona), Isabel Prieto Nieto (Hospital Universitario La Paz de Madrid), Ricardo Rada Morgades (Hospital General Juan Ramón Jimenez de Huelva), Mónica Reig Pérez (Hospital San Juan de Dios del Aljarafe de Sevilla), Ángel Reina Duarte (Hospital Torrecárdenas de Almería), Didac Ribé Serrat (Hospital General de Granollers), Xavier Rodamilans (Hospital de Santa María de Lleida), María D Ruiz Carmona (Hospital de Sagunto), Marcos Rodriguez Martin (Hospital Gregorio Marañón de Madrid), Francisco Romero Aceituno (Hospital San Pedro de Alcántara de Cáceres), Jesús Salas Martínez (Complejo Hospitalario de Badajoz), Ginés Sánchez de la Villa (Hospital General Rafael Mendez de Murcia), Inmaculada Segura Jimenez (Hospital Universitario Virgen de las Nieves), José Enrique Sierra Grañon (Hospital Universitario Arnau de Vilanova de Lleida), Amparo Solana Bueno (Hospital de Manises), Albert Sueiras Gil (Hospital de Viladecans), Teresa Torres Sanchez (Hospital Dr. Peset de Valencia), Natalia Uribe Quintana (Hospital Arnau de Vilanova de Valencia), Javier Valdés Hernández (Hospital Virgen Macarena de Sevilla), Fancesc Vallribera (Hospital Universitari Vall d'Hebron de Barcelona), Vicent Viciano Pascual (Hospital Lluis Alcanyis de Xàtiva).

REFERENCES

1 **US Cancer Statistics Working Group**. United States Cancer Statistics: 1999-2014 Incidence and Mortality Web-based Report. Atlanta: US Department of Health and Human Services, Centers for Disease Control and Prevention and National Cancer Institute; 2017. Accessed March 2, 2018 Available from: URL: https://nccd.cdc.gov/USCSDataViz/rdPage.aspx

2 **Siegel RL**, Miller KD, Fedewa SA, Ahnen DJ, Meester RGS, Barzi A, Jemal A. Colorectal cancer statistics, 2017. *CA Cancer J Clin* 2017; **67**: 177-193 [PMID: 28248415 DOI: 10.3322/caac.21395]

3 SEER Cancer Stat Facts: Colorectal Cancer. National Cancer Institute. Accessed March 2, 2018 Available from: URL: http://seer.cancer.gov/statfacts/html/colorect.html

4 **MERCURY Study Group**. Diagnostic accuracy of preoperative magnetic resonance imaging in predicting curative resection of rectal cancer: prospective observational study. *BMJ* 2006; **333**: 779 [PMID: 16984925 DOI: 10.1136/bmj.38937.646400.55]

5 **Kontovounisios C**, Tan E, Pawa N, Brown G, Tait D, Cunningham D, Rasheed S, Tekkis P. The selection process can improve the outcome in locally advanced and recurrent colorectal cancer: activity and results of a dedicated multidisciplinary colorectal cancer centre. *Colorectal Dis* 2017; **19**: 331-338 [PMID: 27629565 DOI: 10.1111/codi.13517]

6 **Brown KGM**, Solomon MJ, Koh CE. Pelvic Exenteration Surgery: The Evolution of Radical Surgical Techniques for Advanced and Recurrent Pelvic Malignancy. *Dis Colon Rectum* 2017; **60**: 745-754 [PMID: 28594725 DOI: 10.1097/DCR.0000000000000839]

7 **Simillis C**, Baird DL, Kontovounisios C, Pawa N, Brown G, Rasheed S, Tekkis PP. A Systematic Review to Assess Resection Margin Status After Abdominoperineal Excision and Pelvic Exenteration for Rectal Cancer. *Ann Surg* 2017; **265**: 291-299 [PMID: 27537531 DOI: 10.1097/SLA.0000000000001963]

8 **Selvaggi F**, Fucini C, Pellino G, Sciaudone G, Maretto I, Mondi I, Bartolini N, Caminati F, Pucciarelli S. Outcome and prognostic factors of local recurrent rectal cancer: a pooled analysis of 150 patients. *Tech Coloproctol* 2015; **19**: 135-144 [PMID: 25384359 DOI: 10.1007/s10151-014-1241-x]

9 **Harji DP**, Griffiths B, McArthur DR, Sagar PM. Surgery for recurrent rectal cancer: higher and wider? *Colorectal Dis* 2013; **15**: 139-145 [PMID: 22564242 DOI: 10.1111/j.1463-1318.2012.03076.x]

10 **Koh CE**, Solomon MJ, Brown KG, Austin K, Byrne CM, Lee P, Young JM. The Evolution of Pelvic Exenteration Practice at a Single Center: Lessons Learned from over 500 Cases. *Dis Colon Rectum* 2017; **60**: 627-635 [PMID: 28481857 DOI: 10.1097/DCR.0000000000000825]

11 **Rottoli M**, Vallicelli C, Boschi L, Poggioli G. Outcomes of pelvic exenteration for recurrent and primary locally advanced rectal cancer. *Int J Surg* 2017; **48**: 69-73 [PMID: 28987560 DOI: 10.1016/j.ijsu.2017.09.069]

12 **Garcia-Granero A**, Biondo S, Espin-Basany E, González-Castillo A, Valverde S, Trenti L, Gil-Moreno A, Kreisler E. Pelvic exenteration with rectal resection for different types of malignancies at two tertiary referral centres. *Cir Esp* 2018; **96**: 138-148 [PMID: 29229359 DOI: 10.1016/j.ciresp.2017.11.001]

13 **PelvEx Collaborative**. Surgical and Survival Outcomes Following Pelvic Exenteration for Locally Advanced Primary Rectal Cancer: Results from an International Collaboration. *Ann Surg* 2017; Epub ahead of print [PMID: 28938268 DOI: 10.1097/SLA.0000000000002528]

14 **PelvEx Collaborative**. Factors affecting outcomes following pelvic exenteration for locally recurrent rectal cancer. *Br J Surg* 2018; **105**: 650-657 [PMID: 29529336 DOI: 10.1002/bjs.10734]

15 **Ortiz H**, Codina A. Rectal cancer project of the Spanish Association of Surgeons (Viking project): Past and future. *Cir Esp* 2016; **94**: 63-64 [PMID: 26772740 DOI: 10.1016/j.ciresp.2015.11.009]

16 **von Elm E**, Altman DG, Egger M, Pocock SJ, Gøtzsche PC, Vandenbroucke JP; STROBE Initiative. Strengthening the Reporting of Observational Studies in Epidemiology (STROBE) statement: guidelines for reporting observational studies. *BMJ* 2007; **335**: 806-808 [PMID: 17947786 DOI: 10.1136/bmj.39335.541782.AD]

17 **Wibe A**, Møller B, Norstein J, Carlsen E, Wiig JN, Heald RJ, Langmark F, Myrvold HE, Søreide O; Norwegian Rectal Cancer Group. A national strategic change in treatment policy for rectal cancer--implementation of total mesorectal excision as routine treatment in Norway. A national audit. *Dis Colon Rectum* 2002; **45**: 857-866 [PMID: 12130870]

18 **Biondo S**, Ortiz H, Lujan J, Codina-Cazador A, Espin E, Garcia-Granero E, Kreisler E, de Miguel M, Alos R, Echeverria A. Quality of mesorectum after laparoscopic resection for rectal cancer - results of an audited teaching programme in Spain. *Colorectal Dis* 2010; **12**: 24-31 [PMID: 19175653 DOI: 10.1111/j.1463-1318.2008.01720.x]

19 **Beyond TME Collaborative**. Consensus statement on the multidisciplinary management of patients with recurrent and primary rectal cancer beyond total mesorectal excision planes. *Br J Surg* 2013; **100**: 1009-1014 [PMID: 23754654 DOI: 10.1002/bjs.9192]

20 **Ortiz H**, Ciga MA, Armendariz P, Kreisler E, Codina-Cazador A, Gomez-Barbadillo J, Garcia-Granero E, Roig JV, Biondo S; Spanish Rectal Cancer Project. Multicentre propensity score-matched analysis of conventional versus extended abdominoperineal excision for low rectal cancer. *Br J Surg* 2014; **101**: 874-882 [PMID: 24817654 DOI: 10.1002/bjs.9522]

21 **García-Granero E**, Faiz O, Muñoz E, Flor B, Navarro S, Faus C, García-Botello SA, Lledó S, Cervantes A. Macroscopic assessment of mesorectal excision in rectal cancer: a useful tool for improving quality control in a multidisciplinary team. *Cancer* 2009; **115**: 3400-3411 [PMID: 19479978 DOI: 10.1002/cncr.24387]

22 **Quirke P**, Steele R, Monson J, Grieve R, Khanna S, Couture J, O'Callaghan C, Myint AS, Bessell E, Thompson LC, Parmar M, Stephens RJ, Sebag-Montefiore D; MRC CR07/NCIC-CTG CO16 Trial Investigators; NCRI Colorectal Cancer Study Group. Effect of the plane of surgery achieved on local recurrence in patients with operable rectal cancer: a prospective study using data from the MRC CR07 and NCIC-CTG CO16 randomised clinical trial. *Lancet* 2009; **373**: 821-828 [PMID: 19269520 DOI: 10.1016/S0140-6736(09)60485-2]

23 **Nagtegaal ID**, van de Velde CJ, van der Worp E, Kapiteijn E, Quirke P, van Krieken JH; Cooperative Clinical Investigators of the Dutch Colorectal Cancer Group. Macroscopic evaluation of rectal cancer resection specimen: clinical significance of the pathologist in quality control. *J Clin Oncol* 2002; **20**: 1729-1734 [PMID: 11919228 DOI: 10.1200/JCO.2002.07.010]

24 **Brunschwig A**. Complete excision of pelvic viscera for advanced carcinoma; a one-stage abdominoperineal operation with end colostomy and bilateral ureteral implantation into the colon above the colostomy. *Cancer* 1948; **1**: 177-183 [PMID: 18875031]

25 **Heriot AG**, Byrne CM, Lee P, Dobbs B, Tilney H, Solomon MJ, Mackay J, Frizelle F. Extended radical resection: the choice for locally recurrent rectal cancer. *Dis Colon Rectum* 2008; **51**: 284-291 [PMID: 18204879 DOI: 10.1007/s10350-007-9152-9]

26 **Bhangu A**, Ali SM, Darzi A, Brown G, Tekkis P. Meta-analysis of survival based on resection margin status following surgery for recurrent rectal cancer. *Colorectal Dis* 2012; **14**: 1457-1466 [PMID: 22356246 DOI: 10.1111/j.1463-1318.2012.03005.x]

27 **Nielsen MB**, Rasmussen PC, Lindegaard JC, Laurberg S. A 10-year experience of total pelvic exenteration for primary advanced and locally recurrent rectal cancer based on a prospective database. *Colorectal Dis* 2012; **14**: 1076-1083 [PMID: 22107085 DOI: 10.1111/j.1463-1318.2011.02893.x]

28 **Loughrey MB McManus DT**. Pelvic Exenteration Specimens. In: Eds Allen D, Cameron R. Histopathology Specimens. London: Springer, 2013 [doi:10.1007/978-0-85729-673-3_35]

29 **Yang TX**, Morris DL, Chua TC. Pelvic exenteration for rectal cancer: a systematic review. *Dis Colon Rectum* 2013; **56**: 519-531 [PMID: 23478621 DOI: 10.1097/DCR.0b013e31827a7868]

30 **Coleman MP**, Forman D, Bryant H, Butler J, Rachet B, Maringe C, Nur U, Tracey E, Coory M, Hatcher J, McGahan CE, Turner D, Marrett L, Gjerstorff ML, Johannesen TB, Adolfsson J, Lambe M, Lawrence G, Meechan D, Morris EJ, Middleton R, Steward J, Richards MA; ICBP Module 1 Working Group. Cancer survival in Australia, Canada, Denmark, Norway, Sweden, and the UK, 1995-2007 (the International Cancer Benchmarking Partnership): an analysis of population-based cancer registry data. *Lancet* 2011; **377**: 127-138 [PMID: 21183212 DOI: 10.1016/S0140-6736(10)62231-3]

31 **Hsu TW**, Chiang FF, Chen MC, Wang HM. Pelvic exenteration for men with locally advanced rectal cancer: a morbidity analysis of complicated cases. *Asian J Surg* 2011; **34**: 115-120 [PMID: 22208686 DOI: 10.1016/j.asjsur.2011.08.002]

32 **García-Granero E**, Navarro F, Cerdán Santacruz C, Frasson M, García-Granero A, Marinello F, Flor-Lorente B, Espí A. Individual surgeon is an independent risk factor for leak after double-stapled colorectal anastomosis: An institutional analysis of 800 patients. *Surgery* 2017; **162**: 1006-1016 [PMID: 28739093 DOI: 10.1016/j.surg.2017.05.023]

33 **Georgiou PA**, Bhangu A, Brown G, Rasheed S, Nicholls RJ, Tekkis PP. Learning curve for the management of recurrent and locally advanced primary rectal cancer: a single team's experience. *Colorectal Dis* 2015; **17**: 57-65 [PMID: 25204543 DOI: 10.1111/codi.12772]

34 **Baguena G**, Pellino G, Frasson M, Roselló S, Cervantes A, García-Granero A, Giner F, García-Granero E. Prognostic impact of pT stage and peritoneal invasion in locally advanced colon cancer. Dis Colon Rectum 2018; In press

35 **Dayal S**, Moran B. LOREC: the English Low Rectal Cancer National Development Programme. *Br J Hosp Med* (Lond) 2013; **74**: 377-380 [PMID: 24159637]

36 **Sahnan K**, Pellino G, Adegbola SO, Tozer PJ, Chandrasinghe P, Miskovic D, Hompes R, Warusavitarne J, Lung PFC. Development of a model of three-dimensional imaging for the preoperative planning of TaTME. *Tech Coloproctol* 2018; **22**: 59-63 [PMID: 29188460 DOI: 10.1007/s10151-017-1724-7]

P- Reviewer: El-Hussuna A, Jurado M **S- Editor**: Ma RY
L- Editor: A **E- Editor**: Huang Y

World Journal of Gastroenterology

Submit a Manuscript: http://www.f6publishing.com

World J Gastroenterol 2018 December 7; 24(45): 5154-5166

DOI: 10.3748/wjg.v24.i45.5154

ISSN 1007-9327 (print) ISSN 2219-2840 (online)

ORIGINAL ARTICLE

Retrospective Study

Clinicopathological parameters predicting recurrence of pT1N0 esophageal squamous cell carcinoma

Li-Yan Xue, Xiu-Min Qin, Yong Liu, Jun Liang, Hua Lin, Xue-Min Xue, Shuang-Mei Zou, Mo-Yan Zhang, Bai-Hua Zhang, Zhou-Guang Hui, Zi-Tong Zhao, Li-Qun Ren, Yue-Ming Zhang, Xiu-Yun Liu, Yan-Ling Yuan, Jian-Ming Ying, Shu-Geng Gao, Yong-Mei Song, Gui-Qi Wang, Sanford M Dawsey, Ning Lu

Li-Yan Xue, Xue-Min Xue, Shuang-Mei Zou, Li-Qun Ren, Xiu-Yun Liu, Yan-Ling Yuan, Jian-Ming Ying, Ning Lu, Department of Pathology, National Cancer Center/National Clinical Research Center for Cancer/Cancer Hospital, Chinese Academy of Medical Sciences and Peking Union Medical College, Beijing 100021, China

Xiu-Min Qin, Yong Liu, Yue-Ming Zhang, Gui-Qi Wang, Department of Endoscopy, National Cancer Center/National Clinical Research Center for Cancer/Cancer Hospital, Chinese Academy of Medical Sciences and Peking Union Medical College, Beijing 100021, China

Jun Liang, Zhou-Guang Hui, Department of Radiation Oncology, National Cancer Center/National Clinical Research Center for Cancer/Cancer Hospital, Chinese Academy of Medical Sciences and Peking Union Medical College, Beijing 100021, China

Hua Lin, Department of Medical Record, National Cancer Center/National Clinical Research Center for Cancer/Cancer Hospital, Chinese Academy of Medical Sciences and Peking Union Medical College, Beijing 100021, China

Mo-Yan Zhang, Bai-Hua Zhang, Shu-Geng Gao, Department of Thoracic Surgery, National Cancer Center/National Clinical Research Center for Cancer/Cancer Hospital, Chinese Academy of Medical Sciences and Peking Union Medical College, Beijing 100021, China

Zi-Tong Zhao, Yong-Mei Song, State Key Laboratory of Molecular Oncology, National Cancer Center/National Clinical Research Center for Cancer/Cancer Hospital, Chinese Academy of Medical Sciences and Peking Union Medical College, Beijing 100021, China

Li-Yan Xue, Center for Cancer Precision Medicine, Cancer Hospital, Chinese Academy of Medical Sciences and Peking Union Medical College, Beijing 100021, China

Bai-Hua Zhang, The 2nd Department of Thoracic Surgery, Hunan Cancer Hospital, The Affiliated Cancer Hospital of Xiangya School of Medicine, CSU, Changsha 410006, Hunan Province, China

Li-Qun Ren, Department of Pathology, Chengde Medical College, Chengde 067000, Hebei Province, China

Sanford M Dawsey, Metabolic Epidemiology Branch, Division of Cancer Epidemiology and Genetics, National Cancer Institute, Bethesda, MD 20892, United States

ORCID number: Li-Yan Xue (0000-0001-5185-0126); Xiu-Min Qin (0000-0002-1651-073X); Yong Liu (0000-0003-3848-1682); Jun Liang (0000-0003-0309-0163); Hua Lin (0000-0002-8167-3017); Xue-Min Xue (0000-0002-7842-6883); Shuang-Mei Zou (0000-0001-8539-6291); Mo-Yan Zhang (0000-0001-8475-3824); Bai-Hua Zhang (0000-0001-9712-9043); Zhou-Guang Hui (0000-0002-7189-4692); Zi-Tong Zhao (0000-0001-9279-0924); Li-Qun Ren (0000-0003-0565-0881); Yue-Ming Zhang (0000-0001-9167-0824); Xiu-Yun Liu (0000-0002-3592-2684); Yan-Ling Yuan (0000-0003-3205-8664); Jian-Ming Ying (0000-0002-7301-4118); Shu-Geng Gao (0000-0003-1888-2622); Yong-Mei Song (0000-0002-7789-0158); Gui-Qi Wang (0000-0001-7767-1564); Sanford M Dawsey (0000-0003-2185-0533); Ning Lu (0000-0002-3937-024X).

Author contributions: Xue LY and Lu N designed the study and drafted the manuscript; Qin XM, Liu Y, Lin H, and Zhang BH collected the follow-up data; Xue LY and Xue XM performed statistical analyses; Xue LY, Zou SM, and Ren LQ reviewed the pathologic slides; Liu XY and Yuan YL did the immunohistochemistry; Dawsey SM, Liang J, Zhang MY, Hui ZG, Zhao ZT, Zhang YM, Ying JM, Gao SG, Song YM, and Wang GQ made critical revision of the manuscript for important intellectual content.

Supported by the National Natural Science Foundation of China, No. 81402463; CAMS Innovation Fund for Medical Sciences (CIFMS), No. 2016-I2M-1-001 and No. 2016-I2M-3-005; and the Non-profit Central Research Institute Fund of Chinese Academy of Medical Sciences, No. 2016ZX310178 and No. 2017PT32001.

Institutional review board statement: This study was reviewed and approved by the Ethics Committee of the National Cancer Center/National Clinical Research Center for Cancer/Cancer Hospital, Chinese Academy of Medical Sciences and Peking Union Medical College.

Informed consent statement: Patients were not required to give informed consent to the study because the analysis used anonymous clinicopathological data, and the study was exempted from informed consent requirement.

Conflict-of-interest statement: All authors declare no conflicts of interest related to this article.

Data sharing statement: No additional data are available.

Manuscript source: Unsolicited manuscript

Correspondence author to: Ning Lu, MD, Chief Doctor, Department of Pathology, National Cancer Center/National Clinical Research Center for Cancer/Cancer Hospital, Chinese Academy of Medical Sciences and Peking Union Medical College, Beijing 100021, China. nlu03@126.com
Telephone: +86-10-87788435
Fax: +86-10-67702630

Received: August 31, 2018
Peer-review started: September 2, 2018
First decision: October 14, 2018
Revised: October 22, 2018
Accepted: November 13, 2018
Article in press: November 13, 2018
Published online: December 7, 2018

Abstract

AIM

To identify the clinicopathological characteristics of pT1N0 esophageal squamous cell carcinoma (ESCC) that are associated with tumor recurrence.

METHODS

We reviewed 216 pT1N0 thoracic ESCC cases who underwent esophagectomy and thoracoabdominal two-field lymphadenectomy without preoperative chemoradiotherapy. After excluding those cases with clinical follow-up recorded fewer than 3 mo and those who died within 3 mo of surgery, we included 199 cases in the current analysis. Overall survival and recurrence-free survival were assessed by the Kaplan-Meier method, and clinicopathological characteristics associated with any recurrence or distant recurrence were evaluated using univariate and multivariate Cox proportional hazards models. Early recurrence (≤ 24 mo) and correlated parameters were assessed using univariate and multivariate logistic regression models.

RESULTS

Forty-seven (24%) patients had a recurrence at 3 to 178 (median, 33) mo. The 5-year recurrence-free survival rate was 80.7%. None of 13 asymptomatic cases had a recurrence. Preoperative clinical symptoms, upper thoracic location, ulcerative or intraluminal mass macroscopic tumor type, tumor invasion depth level, basaloid histology, angiolymphatic invasion, tumor thickness, submucosal invasion thickness, diameter of the largest single tongue of invasion, and complete negative aberrant p53 expression were significantly related to tumor recurrence and/or recurrence-free survival. Upper thoracic tumor location, angiolymphatic invasion, and submucosal invasion thickness were independent predictors of tumor recurrence (Hazard ratios = 3.26, 3.42, and 2.06, $P < 0.001$, $P < 0.001$, and $P = 0.002$, respectively), and a nomogram for predicting recurrence-free survival with these three predictors was constructed. Upper thoracic tumor location and angiolymphatic invasion were independent predictors of distant recurrence. Upper thoracic tumor location, angiolymphatic invasion, submucosal invasion thickness, and diameter of the largest single tongue of invasion were independent predictors of early recurrence.

CONCLUSION

These results should be useful for designing optimal individual follow-up and therapy for patients with T1N0 ESCC.

Key words: Esophageal squamous cell carcinoma; Tumor recurrence; Lymph node negative esophageal cancer; Recurrence-free survival; Clinicopathological parameters

Core tip: Recurrences of pT1N0 esophageal squamous cell carcinoma (ESCC) after esophagectomy are usually metachronous regional lymph node or distant metastases. We analyzed 199 thoracic pT1N0 ESCC cases who underwent esophagectomy and thoracoabdominal two-field lymphadenectomy. Forty-seven (24%) patients had a recurrence during 3 to 178 (median, 33) mo. Upper thoracic tumor location, angiolymphatic invasion, and submucosal invasion thickness were independent predictors of tumor recurrence, and a nomogram for predicting recurrence-free survival with these three predictors was constructed. These results should be useful for designing optimal individual follow-up and therapy for patients with T1N0 ESCC.

Xue LY, Qin XM, Liu Y, Liang J, Lin H, Xue XM, Zou SM, Zhang MY, Zhang BH, Hui ZG, Zhao ZT, Ren LQ, Zhang YM, Liu XY, Yuan YL, Ying JM, Gao SG, Song YM, Wang GQ,

Dawsey SM, Lu N. Clinicopathological parameters predicting recurrence of pT1N0 esophageal squamous cell carcinoma. *World J Gastroenterol* 2018; 24(45): 5154-5166 Available from: URL: http://www.wjgnet.com/1007-9327/full/v24/i45/5154.htm DOI: http://dx.doi.org/10.3748/wjg.v24.i45.5154

INTRODUCTION

Esophageal squamous cell carcinoma (ESCC) is one of the most common fatal malignancies worldwide, and is especially common in East Asia, including China and Japan. The prognosis of superficial (T1) ESCC is poor, compared with T1 gastric or colorectal cancer. The long longitudinally arranged collecting channels and plexuses of lymphatics in the esophageal submucosa account for the clinical observation that T1 esophageal cancer can metastasize not only to the mediastinal lymph nodes, but also to the cervical and abdominal lymph nodes far distant from the primary tumor, and to distant organs as well[1-3].

The presence of metastasis is the most important prognostic factor for ESCC. The unfavorable prognosis of patients with T1 ESCC is largely due to high rates of both synchronous and metachronous metastases. Recurrences of T1 ESCC after esophagectomy are usually metachronous regional lymph node or distant metastases, and are only infrequently due to anastomotic recurrences. When recurrence occurs, the prognosis is similar in patients who were node-negative or node-positive at the time of the original surgery[4]. Therefore, patients found to have a high risk of recurrence after esophagectomy need additional chemoradiotherapy. However, only a few studies have evaluated the clinicopathological characteristics associated with an increased risk of a postoperative recurrence in pT1N0 ESCC patients. These studies have shown that invasion depth of the primary tumor, lymphovascular invasion, histologic grade, and tumor length are associated with a high risk of recurrence[5-8]. No previous studies have separately evaluated the clinicopathological characteristics that are associated with distant recurrence or early recurrence in pT1N0 ESCC patients.

We previously reviewed 271 T1 ESCC esophagectomy cases, and established a set of clinicopathological and immunohistochemical indicators to identify patients with a high risk of synchronous regional lymph node metastasis[9]. However, recurrence was observed in quite a few pT1N0 ESCC cases. Thus, the identification of pT1N0 cases at high risk for recurrence is a very important and challenging aspect of the clinical management of these patients, to ensure appropriate use and maximum benefit of additional therapies. In the present study, we followed 199 pT1N0 thoracic ESCC cases in our original esophagectomy case series and investigated the clinicopathological characteristics that were associated with recurrence, distant recurrence, and early recurrence, in order to provide clues to optimal individual therapy.

MATERIALS AND METHODS

Patients and surgical procedures

Two hundred and sixteen pT1N0 thoracic ESCC patients received esophagectomy with thoracoabdominal lymphadenectomy, without preoperative chemoradiotherapy, at National Cancer Center/National Clinical Research Center for Cancer/Cancer Hospital, Chinese Academy of Medical Sciences and Peking Union Medical College, between February 1990 and January 2004. After excluding those cases with clinical follow-up recorded fewer than 3 mo (n = 12) and those who died within 3 mo of surgery (operative death, n = 5), we included 199 cases in the current analysis.

For lesions in the upper third of the thoracic segment, a three-phase abdominothoracic McKeown resection was generally performed through a right thoracotomy. For lesions in the middle and lower thirds, esophagectomy was performed on the left side using a single-incision Sweet approach. The tumor location was defined by the position of the center of the largest invasive lesion of each case (continuous invasive tongues were considered as one invasive lesion, but discontinuous invasive tongues separated by normal or dysplastic mucosa were considered as multiple invasive lesions). This study was approved by the Institutional Review Board of the National Cancer Center/National Clinical Research Center for Cancer/Cancer Hospital, Chinese Academy of Medical Sciences and Peking Union Medical College (NCC 2014 G-47), and interpretation of anonymized data was exempted from review by the Office of Human Subject Research Protection of the NIH.

Macroscopic tumor types

Macroscopic tumor types were defined as we previously described[9]. Briefly, we classified the lesions into six types, occult type (Paris classification 0-IIb), erosive type (Paris classification 0-IIc or 0-IIa + IIc), papillary type (Paris classification 0-Ip), plaque-like type (Paris classification 0-Is or 0-IIa), ulcerative type (Paris classification 0-III or 0-III + I), and intraluminal mass (fungating) type (Paris classification 0-Ip)[10,11]. The difference between the papillary type and the intraluminal mass type is that the largest diameter is < 3 cm and ≥ 3 cm, respectively[9].

Standard histopathological variables

All histopathological variables were first reviewed and graded independently by three pathologists (LX, SZ, and LR), and discordant cases were reviewed jointly until a consensus was reached. For the patients with multicentric esophageal carcinomas, the histopathological factors for the lesion with the greatest invasion depth were evaluated[9].

Maximum depth of invasion was classified into five levels: m2 (lamina propria mucosae), m3 (muscularis

mucosae), sm1, sm2, and sm3 (superficial, middle, and deep thirds of the submucosa, respectively). Degree of differentiation was classified as well, moderate, poor, basaloid or spindle cell/sarcomatoid[12].

Measured histopathological variables

Tumor thickness (from the surface to the deepest invasive front of cancer nests), submucosal invasion thickness (from the bottom of the muscularis mucosae to the deepest invasive front of the cancer nests), and the diameter of the largest single tongue of invasion were measured microscopically. Submucosal invasion thickness was measured in submucosal cases, and defined as 0 in mucosal cases.

In our previous study[9], 3000 μm for tumor thickness, 2000 μm for submucosal invasion thickness, and 2 cm for the diameter of the largest single tongue of invasion were found to be the best cut points for predicting lymph node metastasis. Thus, we also used these cut points for categorizing these measurements in this study.

Tissue microarray construction and immunohistochemistry

Details of the tissue microarray construction and the immunohistochemical staining and scoring for Cyclin D1, EGFR, and VEGF have been described previously[9]. We rescored p53 expression into three groups: weak or patchy (wild type), complete loss (nonsense, frameshift, or splice-site mutation type), and diffuse and strong (missense mutation type). The latter two groups were considered as aberrant p53 expression[13]. In the present study, the correlation between the expression levels of these four markers and tumor recurrence was further analyzed in the pT1N0 cases.

Follow-up

Follow-up and mortality data were mainly gathered from clinical notes. Patients were evaluated at return visits every 3 mo during the first 2 years after treatment, every 6 mo for the following 3 years, and annually thereafter according to hospital policy. At each visit, physical examination, endoscopic examination, and CT scan of the cervix, chest and abdomen were performed. Suspicious recurrences were biopsied. Confirmation of recurrence required imaging or pathological evaluation. Information about tumor recurrence was updated every time the patient came for a follow-up visit. For those patients who did not come for a follow-up visit, data were gathered by phone calls, and/or mail contact with patients or their next of kin. The patients were followed for a median of 72 mo and a maximum period of 263 mo.

Overall survival time was recorded as the number of months from the date of surgery to the date when death occurred, or to the time of last follow-up, at which point, the data were censored. Recurrence-free survival time was recorded as the number of months from the date of surgery to the date when recurrence occurred, or to the time of last follow-up, at which point, the data were censored.

Four cases underwent radiotherapy after esophagectomy, due to upper resection margins being involved by high grade dysplasia or as part of a randomized clinical trial.

Statistical analysis

Continuous variables such as age, tumor thickness, and submucosal invasion thickness were analyzed after categorization.

Overall and recurrence-free survival rates were calculated and survival curves were constructed using the Kaplan-Meier method, with significance evaluated by the log-rank test. The associations between clinicopathological characteristics and any recurrence or distant recurrence were determined using univariate Cox proportional hazards analysis. A backward stepwise multivariate Cox proportional hazards analysis was applied for factors achieving a significance level of 0.05 in univariate analysis. Hazard ratios (HRs) with 95% confidence intervals (CIs) were reported.

The associations between clinicopathological parameters and early recurrence (≤ 24 mo after surgery) were evaluated similarly, except using logistic regression analysis.

All the above statistical analyses were performed using SPSS 16.0 for Windows (SPSS, Chicago, IL, United States), with a significance level of 0.05 on two-tailed *P*-values.

A nomogram based on independent predictors for the recurrence-free survival identified by multivariate Cox proportional hazards analysis was constructed using the rms package in R 3.4.2 software.

RESULTS

Clinicopathological features

The clinicopathological features of the 199 pT1N0 ESCC patients are shown in Table 1. Seventy-one percent of the patients were men. The average age was 56 years, the median age was 57 years, and the age range was 34-77 years. Seventy-two percent of the tumors were found in the middle thoracic region. For all of the 199 patients, a total of 3197 lymph nodes (median, 14) were dissected.

Overall survival and recurrence-free survival

The 5-year and 10-year overall survival rates were 81.4% and 76.4%, respectively (Figure 1). Forty-seven (24%) patients had documented recurrences. These recurrences occurred during 3-178 mo, with a median of 33 mo. The 5-year and 10-year recurrence-free survival rates were 80.7% and 71.9%, respectively (Figure 1). Mediastinal lymph nodes (21 patients, 11%) were the most frequent site of recurrence, followed by cervical lymph nodes (19 patients, 10%, with 8 left, 10 right, and 1 bilateral) (Table 2).

Table 1 Summary of clinical, endoscopic, and histopathological characteristics of the 199 pT1N0 esophageal squamous cell carcinoma patients *n* (%)

Characteristic		Patients
Clinical variable		
Sex	Male	142 (71)
	Female	57 (29)
Age (yr)	< 60	121 (61)
	≥ 60	78 (39)
Symptoms	No	13 (7)
	Yes	186 (93)
Endoscopic variable		
Tumor location	Upper thoracic	31 (16)
	Middle thoracic	143 (72)
	Lower thoracic	25 (13)
Tumor size (measured endoscopically)	< 2 cm	59 (30)
	≥ 2 cm	140 (70)
Macroscopic tumor type	Erosive	73 (37)
	Papillary	26 (13)
	Plaque-like	79 (40)
	Ulcerative	9 (5)
	Intraluminal mass	12 (6)
Standard histopathological variable		
Tumor invasion depth level	m2	21 (11)
	m3	26 (13)
	sm1	18 (9)
	sm2	45 (23)
	sm3	89 (45)
Degree of differentiation	Well	39 (20)
	Moderate	76 (38)
	Poor	56 (28)
	Basaloid	19 (10)
	Spindle cell/sarcomatoid	9 (5)
Angiolymphatic invasion	No	172 (86)
	Yes	27 (14)
Multicentric invasive lesions	No	183 (92)
	Yes	16 (8)
Number of lymph nodes dissected	< 14	90 (45)
	≥ 14	109 (55)
Measured histopathological variables		
Tumor thickness	< 3000 μm	85 (43)
	≥ 3000 μm	114 (57)
Submucosal invasion thickness	0	47 (24)
	0-2000 μm	85 (43)
	≥ 2000 μm	67 (34)
Diameter of the largest single tongue of invasion	< 2 cm	134 (67)
	≥ 2 cm	65 (33)
Immunohistochemical staining[1]		
P53	Complete loss	50 (39)
	Weak, patchy	41 (32)
	Diffuse, strong	37 (29)
Cyclin D1	-	38 (30)
	1+	39 (31)
	2+	49 (39)
EGFR	-	52 (41)
	1+	44 (34)
	2+	32 (25)
VEGF	-	54 (44)
	1+	34 (28)
	2+	35 (28)

[1]Available in tissue microarray cases.

Analysis of factors predicting tumor recurrence

Using the Kaplan-Meier method, preoperative clinical symptoms, tumor location, macroscopic tumor type, tumor invasion depth level, degree of differentiation, angiolymphatic invasion, tumor thickness, submucosal invasion thickness, and diameter of the largest single tongue of invasion were significantly associated with recurrence-free survival ($P < 0.05$) (Table 3).

In univariate Cox regression, upper thoracic tumor location, ulcerative or intraluminal mass macroscopic

Table 2 Sites of recurrence in the 199 pT1N0 esophageal squamous cell carcinoma patients *n* (%)

Site of recurrence	Total patients with recurrence	Patients by tumor location			Patients by macroscopic tumor type	
		Upper thoracic (*n* = 31)	Middle thoracic (*n* = 143)	Lower thoracic (*n* = 25)	Ulcerative or intraluminal (*n* = 21)	Erosive, papillary, or plaque-like (*n* = 178)
Local-regional recurrences[1]	33 (17)	15 (48)	14 (10)	4 (16)	8 (38)	25 (14)
Anastomosis	3 (2)	3 (10)	0	0	2 (10)	1 (1)
Cervical node	19 (10)	10 (32)	7 (5)	2 (8)	4 (19)	15 (8)
Mediastinal node	21 (11)	9 (29)	9 (6)	3 (12)	8 (38)	13 (7)
Abdominal node	0	0	0	0	0	0
Distant recurrences[1]	16 (8)	5 (16)	8 (6)	3 (12)	4 (19)	12 (7)
Lung	7 (4)	2 (6)	5 (3)	0	1 (5)	6 (3)
Liver	2 (1)	1 (3)	0	1 (4)	0	2 (1)
Bone	6 (3)	0	4 (3)	2 (8)	2 (10)	4 (2)
Brain	1 (0)	1 (3)	0	0	0	1 (1)
Pleura	3 (2)	2 (6)	1 (1)	0	1 (5)	2 (1)
Distant node	0	0	0	0	0	0
Multiple site recurrences	15 (8)	7 (23)	6 (4)	2 (8)	5 (24)	10 (6)
Mediastinal node and bone	2 (1)	0	1 (1)	1 (4)	1 (5)	1 (1)
Mediastinal node, cervical node, and bone	1 (1)	0	0	1 (4)	0	1 (1)
Mediastinal node, pleura, and bone	1 (1)	0	1 (1)	0	0	1 (1)
Mediastinal node and cervical node	3 (1)	2 (6)	1 (1)	0	1 (5)	2 (1)
Cervical node and lung	1 (1)	0	1 (1)	0	0	1 (1)
Mediastinal node, cervical node, and anastomosis	1 (1)	1 (3)	0	0	1 (5)	0
Mediastinal node, cervical node, anastomosis, and pleura	1 (1)	1 (3)	0	0	1 (5)	0
Mediastinal node, cervical node, and lung	2 (1)	1 (3)	1 (1)	0	1 (5)	1 (1)
Cervical node, bone, and lung	1 (1)	0	1 (1)	0	0	1 (1)
Mediastinal node, liver, and lung	1 (1)	1 (3)	0	0	0	1 (1)
Mediastinal node and brain	1 (1)	1 (3)	0	0	0	1 (1)
Unknown sites	10 (5)	1 (3)	8 (6)	1 (4)	1 (5)	9 (5)
Total recurrences	47 (24)	16 (52)	25 (17)	6 (24)	10 (48)	37 (21)

[1]Including the patients with multiple site recurrences.

tumor type, invasion depth level, basaloid histology, angiolymphatic invasion, tumor thickness, submucosal invasion thickness, diameter of the largest single tongue of invasion, and complete loss of p53 expression were significantly associated with tumor recurrence ($P < 0.05$) (Table 3). In multivariate Cox regression, upper thoracic tumor location, angiolymphatic invasion, and submucosal invasion thickness were independent significant predictors of recurrence (Table 4).

A nomogram for predicting tumor recurrence with these three independent significant predictors is shown in Figure 2. The nomogram had a concordance index of 0.752.

Analysis of factors predicting distant tumor recurrence

Sixteen cases had well-documented distant recurrences. The lung (7 patients, 4%) was the most frequent site of distant recurrence, followed by the bone (6 patients, 3%) (Table 2). The time to distant recurrence ranged from 3-192 mo, with a median of 39 mo.

In univariate Cox regression, upper thoracic tumor location, ulcerative or intraluminal mass macroscopic tumor type, basaloid histology, and angiolymphatic invasion were significantly associated with distant recurrence ($P < 0.05$). In multivariate Cox regression, upper thoracic tumor location and angiolymphatic invasion were independent predictors of distant recurrence (Table 5).

Analysis of factors predicting early tumor recurrence

Among the 47 cases with recurrences, 18 (38%) had early recurrences (≤ 24 mo after surgery).

In univariate logistic regression, upper thoracic tumor location, ulcerative or intraluminal mass macroscopic tumor type, angiolymphatic invasion, tumor invasion depth level, tumor thickness, submucosal invasion thickness, and diameter of the largest single tongue of invasion were significantly associated with early recurrence ($P < 0.05$). Multivariate logistic regression showed that upper thoracic tumor location, angiolymphatic invasion, submucosal invasion thickness, and diameter of the largest single tongue of invasion were independent predictors of early recurrence (Table 6).

DISCUSSION

We previously analyzed pT1 ESCC esophagectomy cases to identify predictors of synchronous regional

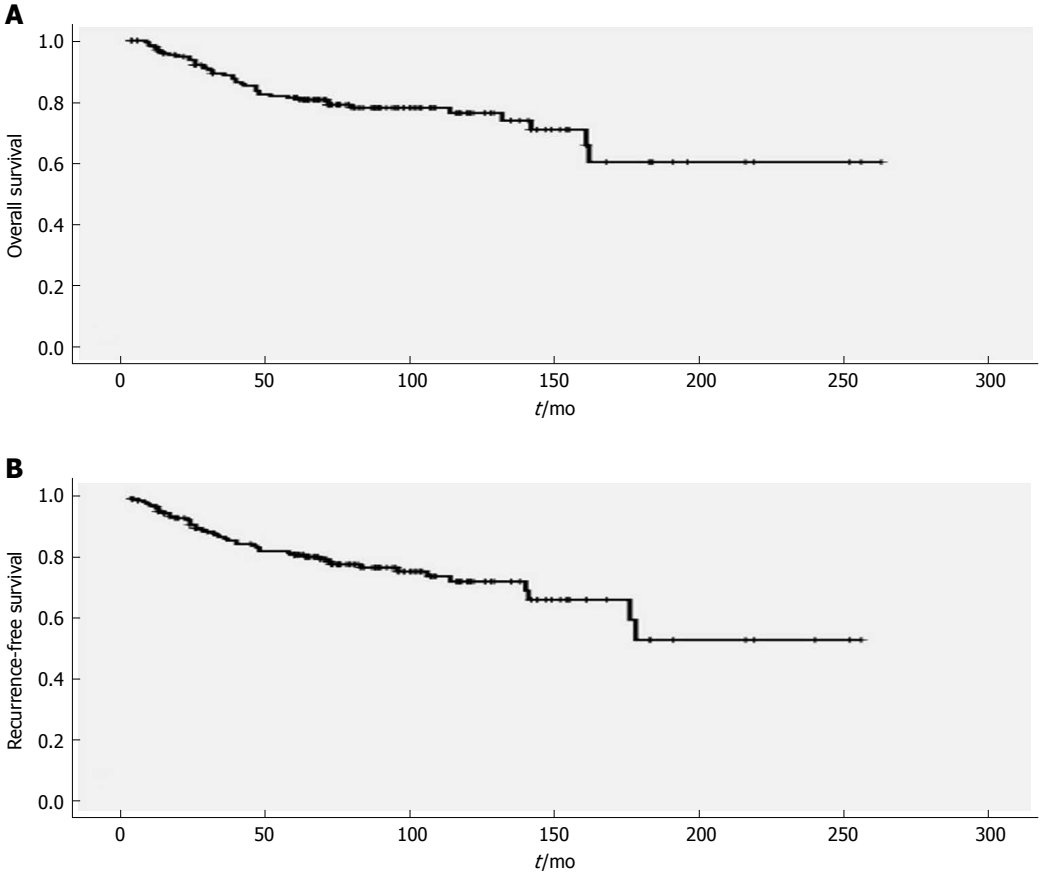

Figure 1 Survival curves of patients with pT1N0 esophageal squamous cell carcinoma. A: Overall survival curve. The 5-year and 10-year overall survival rates were 81.4% and 76.4%, respectively. B: Recurrence-free survival curve. The 5-year and 10-year recurrence-free survival rates were 80.7% and 71.9%, respectively.

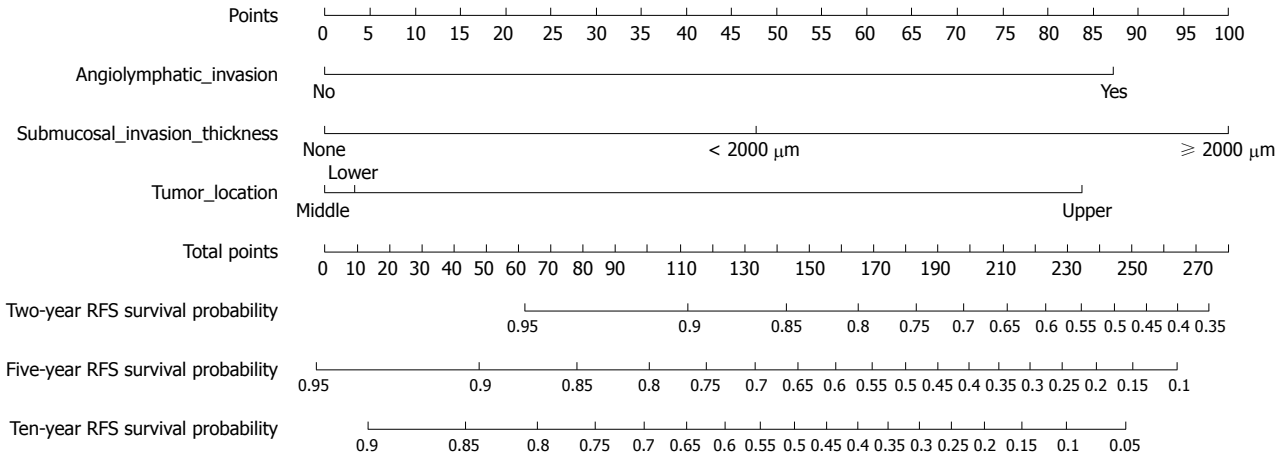

Figure 2 Nomogram for predicting the probability of recurrence-free survival of pT1N0 esophageal squamous cell carcinoma. The nomogram has eight rows. The first row is the point assignment for each variable. For each individual patient, each variable is assigned a point value in accordance with the clinicopathological characteristics (rows 2-4, angiolymphatic invasion, submucosal invasion thickness, and tumor location) by delineating a vertical line between the exact variable value and the point assignment line. Thereafter, the Total Points (row 5) can be obtained by summing all of the assigned points for the three variables. Finally, the probability of 2-, 5-, and 10-year RFS (recurrence-free survival) can be predicted by drawing a vertical line between the Total Points and the probability rows (rows 6-8, respectively).

lymph node metastatsis[5]. In the present study, we followed the pT1N0 thoracic ESCC cases further, for a median of 6 years, and investigated the risk of tumor recurrence and parameters predicting tumor recurrence. We studied the cases before 2004 when the endoscopic resection had not been performed yet in our hospital.

Consistent with our previous observation that all asymptomatic cases had no lymph node metastases, these cases also had no recurrence in our follow-up period. ESCC has a very good prognosis if detected when

Table 3 Relationship of clinicopathological parameters with recurrence-free survival and tumor recurrence in the 199 pT1N0 esophageal squamous cell carcinoma patients *n* (%)

Parameter		Total	Recurrences	Kaplan-Meier analysis			Univariate Cox proportional hazards analysis			
				5-yr RFS (%)	10-yr RFS (%)	*P*-value	HR	95%CI	Global *P*	*P*-for-trend
Clinical variable										
Sex	Male	142	33 (23)	81	71.6	0.97	1			
	Female	57	14 (25)	80	72.7		1.011	0.54-1.89	0.97	
Age (yr)	< 60	121	28 (23)	79.2	74.1	0.6	1			
	≥ 60	78	19 (24)	82.9	66.4		1.17	0.65-2.10	0.6	
Symptoms	No	13	0	100	100	0.03	1			
	Yes	186	47 (25)	79.2	69.8		23.54	0.28-2017	0.16	
Endoscopic variable										
Tumor location	Upper thoracic	31	15 (48)	55.9	44.7	< 0.001	3.46	1.83-6.54	< 0.001	
	Middle thoracic	143	26 (18)	85.2	78.5		1			
	Lower thoracic	25	6 (24)	86.5	65.4		1.49	0.61-3.63	0.38	
Tumor size	< 2 cm	59	16 (27)	79.3	69.7	0.53	1			
(endoscopically)	≥ 2 cm	140	31 (22)	81.2	73		0.82	0.45-1.51	0.53	
Macroscopic	Erosive	73	12 (16)	87.2	78	0.001	1			
tumor type	Papillary	26	4 (15)	90.2	90.2		0.98	0.32-3.06	0.98	
	Plaque-like	79	21 (27)	75.8	68.6		1.64	0.81-3.25	0.13	
	Ulcerative	9	6 (67)	53.3	26.7		6.06	2.26-16.26	< 0.001	
	Intraluminal mass	12	4 (33)	74.1	49.4		3.94	1.26-12.32	0.02	
Standard histopathological variable										
Tumor invasion depth	m2	21	1 (5)	94.1	94.1	0.04	1.52	1.14-1.97		0.004
level	m3	26	3 (12)	96.2	88.1					
	sm1	18	4 (22)	81.4	81.4					
	sm2	45	11 (25)	83.8	74.8					
	sm3	89	28 (31)	70.6	58.6					
Degree of	Well	39	10 (26)	79.5	65	0.02	1			
differentiation	Moderate	76	15 (20)	84.7	82		0.73	0.33-1.63	0.44	
	Poor	56	13 (23)	80.7	67.8		0.92	0.40-2.11	0.92	
	Basaloid	19	8 (42)	58.3	35		2.88	1.13-7.38	0.03	
	Spindle cell/ sarcomatoid	9	1 (11)	88.9	88.9		0.54	0.07-4.21	0.55	
Angiolymphatic	No	172	33 (19)	84.6	75.3	< 0.001	1			
invasion	Yes	27	14 (52)	55.4	49.9		3.48	1.85-6.52	< 0.001	
Multicentric invasive	No	183	45 (25)	80.2	70.9	0.42	1			
lesions	Yes	16	2 (13)	86.5	86.5		0.56	0.14-2.32	0.42	
Number of lymph	< 14	90	24 (27)	72.7	70.2	0.25	1			
nodes dissected	≥ 14	109	23 (21)	87.2	73.8		0.72	0.41-1.27	0.26	
Measured histopathological variable										
Tumor thickness	< 3000 μm	85	13 (15)	90	79.3	0.005	1			
	≥ 3000 μm	114	34 (30)	73.2	65.7		2.41	1.27-4.56	0.007	
Submucosal	0	47	4 (9)	95.5	90.5	0.001	2.24	1.44-3.46		< 0.001
invasion thickness	1-2000 μm	85	19 (22)	82.8	74.4					
	≥ 2000 μm	67	24 (36)	67.4	56.4					
Diameter of the	< 2 cm	134	27 (20)	85.5	75.7	0.008	1			
largest single tongue of invasion	≥ 2 cm	65	20 (31)	70.1	64.1		2.15	1.20-3.85	0.01	
Immunohistochemical staining[1]										
P53	Complete loss	50	19 (38)	64.8	59.5	0.33	2.43	1.02-5.79	0.045	
	Weak, patchy	41	7 (17)	81.8	81.8		1			
	Diffuse, strong	37	12 (33)	88.6	78.2		1.88	0.74-4.77	0.19	
Cyclin D1	-	38	14 (37)	71.3	56.4	0.88	0.93	0.64-1.36		0.72
	1+	39	11 (28)	80.7	73.7					
	2+	49	14 (29)	68.7	68.7					
EGFR	-	52	13 (25)	82.9	75.6	0.27	1.15	0.78-1.69		0.49
	1+	44	17 (39)	65.6	51.3					
	2+	32	9 (28)	70.2	68					
VEGF	-	54	15 (28)	76	67.3	0.59	1.05	0.72-1.54		0.79
	1+	34	12 (35)	74.1	59.6					
	2+	35	10 (29)	72.2	72.2					

[1]Available in tissue microarray cases. HR: Hazard ratio; CI: Confidence interval; 5-yr RFS: 5-year recurrence free survival; 10-yr RFS: 10-year recurrence free survival; NA: Not associated.

Table 4 Multivariate Cox proportional hazard models for tumor recurrence in the 199 pT1N0 esophageal squamous cell carcinoma patients

Parameter		HR	95%CI	Global *P*	*P*-for-trend
Tumor location	Upper thoracic	3.26	1.70-6.27	< 0.001	
	Middle thoracic	1			
	Lower thoracic	1.05	0.43-2.59	0.91	
Angiolymphatic invasion		3.42	1.80-6.52	< 0.001	
Submucosal invasion thickness		2.06	1.30-3.27		0.002

HR: Hazard ratio; CI: Confidence interval.

it is asymptomatic. This can be achieved by appropriate screening programs. However, few studies have analyzed the impact of symptoms on the prognosis of ESCC. Wang *et al*[14] observed the natural progression of untreated superficial ESCCs identified by screening in a high-risk area. Most of the patients were asymptomatic. It took a long time to progress from an early to an advanced stage, and most survived for over 5 years. Wang *et al*[15] also reported a 30-year experience with esophagectomy for superficial ESCCs identified in large-scale mass screenings in high-risk areas. Most patients were asymptomatic, and had a low recurrence rate. Natsugoe *et al*[16] also reported that asymptomatic esophageal carcinoma patients had a lower stage and a better prognosis.

Proximal tumors are known to have a more advanced stage, a lower resection rate, fewer R0 resections, more cervical and tracheobronchial lymph node metastases, and a poorer prognosis[17,18]. The 7th and 8th editions of the American Joint Committee on Cancer (AJCC) staging system include tumor location as a staging factor for T2-3N0M0 ESCC cases and T3N0M0 ESCC cases, respectively[19,20]. Few studies have focused on T1 proximal tumors. We found that the patients with upper thoracic tumors had much higher frequencies of cervical and mediastinal lymph node recurrences than other patients (Table 2), and these proximal tumors were significantly associated with an increased risk for any recurrence (Table 3), distant recurrence (Table 5), and early recurrence (Table 6). One reason for a higher frequency of cervical and mediastinal lymph node recurrences in upper thoracic cases is the characteristics of the lymphatic channels draining this area[1,2]. We also found that tumor thickness was greater in upper thoracic tumors (data not shown), which may be another reason. Upper thoracic tumor location was also one of the independent risk factors for any recurrence, distant recurrence, and early recurrence.

We need to say that the fact that most (33/37 = 89%) of the patients in whom the locations of the recurrences were recorded had recurrences in the cervical and/or mediastinal lymph nodes raises the question of whether (macroscopic or microscopic) tumor was present at the time of surgery and could have been removed if a three-field lymph node dissection (including the cervical lymph nodes) or a more extensive two-field lymph node dissection (including more mediastinal lymph nodes) had been done. In Japan, standard treatment for clinically submucosal ESCC is esophagectomy with three-field lymphadenectomy[21]. It is not yet known whether all patients would benefit from cervical lymphadenectomy, which often results in more severe complications. The optimal extent of lymph node dissection in esophagectomies is an ongoing discussion among surgeons, and our data can contribute to this discussion.

There is a macroscopic tumor type which looks like a large mushroom or a big polyp, and is commonly pedunculated. It belongs to the Paris classification 0-Ip[10,11], but it is different from other common 0-Ip cases. It can be called the intraluminal mass (fungating) type[9]. Most tumors of this type are spindle cell/sarcomatoid, basaloid, or poorly differentiated squamous cell carcinoma. Our previous study found that patients with ulcerative or intraluminal tumors had a high risk of lymph node metastasis[9]. We have now shown that they also have a significantly higher rate of recurrence.

In the current analysis, angiolymphatic invasion was significantly associated with tumor recurrence, distant recurrence, and early recurrence. We relied on HE staining to evaluate angiolymphatic invasion, and immunohistochemistry for endothelial cells was not routinely performed, in keeping with standard practice. Huang *et al*[8] reported that angiolymphatic invasion could act as a prognostic and staging factor in T1-3N0M0 ESCC.

In our previous study, patients with basaloid histology had a moderate risk of synchronous lymph node metastasis[9]. However, in the current study they had a high risk of recurrence, especially distant recurrence. Zhang *et al*[22] retrospectively analyzed 142 cases of basaloid ESCC, and found that the first site of recurrence was distant in 39 (54.9%) cases, distant plus loco-regional in 24 (33.8%) cases, and loco-regional alone in 8 (11.3%) cases. They concluded that basaloid ESCC frequently progresses *via* hematogenous metastasis rather than lymph node metastasis[22]. Saito *et al*[23] also reported that differentiated components of ESCC were most often found in sites of lymph node metastases, whereas basaloid components predominated in sites of hematogenous metastases. Thus, control of the hematogenous spread of basaloid components may lead to improved outcomes in these patients. Indeed, there is a case report of surgical intervention helping a basaloid

Table 5 Relationship between clinicopathological parameters and distant tumor recurrence in the 189 informative patients[1]

Univariate Cox proportional hazards analysis							
Parameter		**Total**	**Distant recurrences (%)**	**HR**	**95%CI**	**Global *P***	***P*-for-trend**
Clinical variables							
Sex	Male	136	14 (10)	1			
	Female	53	2 (4)	0.33	0.07-1.44	0.14	
Age (yr)	< 60	118	8 (7)	1			
	≥ 60	71	8 (11)	2.18	0.79-6.02	0.13	
Symptoms	No	13	0	1			
	Yes	176	16 (9)	23.59	0.01-40030	0.41	
Endoscopic variables							
Tumor location	Upper thoracic	30	5 (17)	3.56	1.15-11.07	0.03	
	Middle thoracic	135	8 (6)	1			
	Lower thoracic	24	3 (13)	2.37	0.63-8.94	0.2	
Tumor size (measured endoscopically)	< 2 cm	55	6 (11)	1			
	≥ 2 cm	134	10 (8)	0.76	0.27-2.09	0.59	
Macroscopic type	Erosive	71	5 (7)	1			
	Papillary	26	2 (8)	1.11	0.21-5.75	0.9	
	Plaque-like	72	5 (7)	0.95	0.27-3.31	0.94	
	Ulcerative	8	2 (25)	5.58	1.06-29.32	0.04	
	Intraluminal mass	12	2 (17)	5.41	1.02-28.68	0.047	
Standard histopathological variable							
Tumor invasion depth level	m2	21	0	1.42	0.91-2.21		0.13
	m3	26	2 (8)				
	sm1	16	1 (6)				
	sm2	43	4 (9)				
	sm3	83	9 (11)				
Degree of differentiation	Well	36	1 (3)	1			
	Moderate	73	5 (7)	2.19	0.25-18.98	0.48	
	Poor	54	6 (11)	3.93	0.47-32.89	0.21	
	Basaloid	17	3 (18)	12.4	1.27-121.08	0.03	
	Spindle cell/ sarcomatoid	9	1 (11)	5.73	0.35 -92.90	0.22	
Angiolymphatic invasion	No	166	11 (7)	1			
	Yes	23	5 (22)	3.38	1.15-9.93	0.03	
Multicentric invasive lesions	No	173	15 (9)	1			
	Yes	16	1 (6)	0.92	0.12-7.00	0.93	
Number of lymph nodes dissected	< 14	85	7 (8)	1			
	≥ 14	104	9 (9)	0.95	0.36-2.57	0.93	
Measured histopathological variable							
Tumor thickness	< 3000 μm	82	6 (7)	1			
	≥ 3000 μm	107	10 (9)	1.53	0.56-4.21	0.42	
Submucosal invasion thickness	0	47	2 (4)	1.88	0.91-3.90		0.09
	< 2000 μm	80	7 (9)				
	≥ 2000 μm	62	7 (11)				
Diameter of the largest invasive lesion	< 2 cm	126	9 (7)	1			
	≥ 2 cm	63	7 (11)	2.56	0.92-7.15	0.07	
Immunohistochemical staining[2]							
P53	Complete loss	47	6 (13)	1.78	0.44-7.16	0.42	
	Weak, patchy	40	3 (8)	1			
	Diffuse, strong	34	6 (18)	2.31	0.58-9.25	0.24	
Cyclin D1	-	35	5 (14)	0.94	0.51-1.74		0.84
	+	37	5 (14)				
	++	47	5 (11)				
EGFR	-	52	9 (17)	0.63	0.31-1.28		0.2
	+	40	4 (10)				
	++	29	2 (7)				
VEGF	-	50	6 (12)	0.95	0.50-1.81		0.88
	+	33	3 (9)				
	++	33	4 (12)				
Multivariate Cox proportional hazards analysis							
Parameter							
Tumor location	Upper thoracic			3.83	1.23-11.96	0.02	
	Middle thoracic			1			
	Lower thoracic			1.95	0.50-7.54	0.34	
Angiolymphatic invasion				3.55	1.17-10.77	0.03	

[1]Excluding 10 patients with an unknown site of recurrence; [2]Available in tissue microarray cases. HR: Hazard ratio; CI: Confidence interval; 5-yr RFS: 5-year recurrence free survival; 10-yr RFS: 10-year recurrence free survival; NA: Not associated.

Table 6 Relationship between clinicopathological parameters and the likelihood of having early recurrence (≤ 24 mo) in the 199 pT1N0 esophageal squamous cell carcinoma patients *n* (%)

Univariate logistic regression							
Parameter		**Total**	**Early recurrence**	**Odds ratio**	**95%CI**	**Global *P***	***P*-for-trend**
Clinical variable							
Sex	Male	142	12 (9)	1			
	Female	57	6 (11)	1.28	0.45-3.58	0.65	
Age (yr)	< 60	121	15 (12)	1			
	≥ 60	78	3 (4)	0.28	0.08-1.01	0.052	
Endoscopic variable							
Tumor location	Upper thoracic	31	9 (29)	7.95	2.68-23.54	< 0.001	
	Middle thoracic	143	7 (5)	1			
	Lower thoracic	25	2 (8)	1.69	0.33-8.64	0.53	
Tumor size (endoscopically)	< 2 cm	59	4 (7)	1			
	≥ 2 cm	140	14 (10)	1.53	0.48-4.85	0.47	
Macroscopic	Erosive	73	4 (6)	1			
tumor types	Papillary	26	1 (4)	0.69	0.07-6.47	0.75	
	Plaque-like	79	7 (9)	1.68	0.47-5.98	0.43	
	Ulcerative	9	3 (33)	8.63	1.55-47.86	0.01	
	Intraluminal mass	12	3 (25)	5.75	1.10-29.95	0.04	
Standard histopathological variable							
Tumor invasion depth level	m2	21	0	1.78	1.05-3.01		0.03
	m3	26	1 (4)				
	sm1	18	2 (11)				
	sm2	45	2 (4)				
	sm3	89	13 (15)				
Degree of differentiation	Well	39	3 (8)	1			
	Moderate	76	6 (8)	1.03	0.24-4.35	0.97	
	Poor	56	4 (7)	0.92	0.20-4.38	0.92	
	Basaloid	19	4 (21)	3.2	0.64-16.07	0.16	
	Spindle cell/sarcomatoid	9	1 (11)	1.5	0.14-16.36	0.74	
Angiolymphatic invasion	No	172	10 (6)	1			
	Yes	27	8 (30)	6.82	2.40-19.38	< 0.001	
Multicentric invasive lesions	No	183	17 (9)	1			
	Yes	16	2 (13)	0.65	0.08-5.24	0.69	
Number of lymph nodes	< 14	90	11 (12)	1			
dissected	≥ 14	109		0.49	0.18-1.33	0.16	
Measured histopathological variable							
Tumor thickness	< 3000 μm	85	2(2)	1			
	≥ 3000 μm	114	16(14)	6.78	1.51-30.33	0.01	
Submucosal invasion thickness	0	47	1(2)	4.02	1.66 -9.73		0.001
	0-2000 μm	85	4(5)				
	≥ 2000 μm	67	13(19)				
Diameter of the largest single	< 2 cm	134	5(4)	1			
tongue of invasion	≥ 2 cm	65	13(20)	6.45	2.19-19.00	0.001	
Immunohistochemical staining[1]							
P53	Complete loss	50	7 (14)	1.34	0.36-4.98		0.66
	Weak, patchy	41	5 (12)	1			
	Diffuse, strong	37	4 (11)	1.15	0.28-4.63		0.85
Cyclin D1	-	38	4 (11)	1.32	0.69-2.54		0.4
	1+	39	4 (10)				
	2+	49	8 (16)				
EGFR	-	52	4 (8)	1.32	0.69-2.54		0.4
	1+	44	8 (18)				
	2+	32	4 (13)				
VEGF	-	54	4 (7)	1.59	0.83-3.04		0.16
	1+	34	5 (15)				
	2+	35	6 (17)				
Multivariate logistic regression							
Tumor location	Upper thoracic			7.73	2.15-27.78	0.002	
	Middle thoracic			1			
	Lower thoracic			1.18	0.20-6.86	0.85	
Angiolymphatic invasion				5.75	1.63-20.24	0.006	
Submucosal invasion thickness				2.64	0.92-7.60	0.07	
Diameter of the largest single tongue of invasion				4.13	1.17-14.56	0.03	

[1]Available in tissue microarray cases. OR: Odds ratio; CI: Confidence interval; NA: Not associated.

ESCC patient with a solitary lung metastasis achieve a long-term survival[24].

It should be noticed that one m2 case had a cervical lymph node recurrence at nearly 5 years after esophagectomy. This case had a tumor thickness of 325 μm and no adverse parameters. Therefore, long-term follow-up is needed for all patients with T1 ESCC after endoscopic resection or esophagectomy, even when the patients have no known adverse parameters.

We have identified certain clinicopathological features that are associated with an increased risk of tumor recurrence in pT1N0 thoracic ESCC patients after esophagectomy and thoracoabdominal two-field lymphadenectomy: (1) Patients with an upper thoracic location, ulcerative or intraluminal mass tumor type, deeper tumor invasion level, basaloid histology, angiolymphatic invasion, greater tumor thickness, greater submucosal invasion thickness, greater diameter of the largest single tongue of invasion, and/or completely negative aberrant p53 expression are at greater risk of tumor recurrence. A nomogram including tumor location, angiolymphatic invasion, and submucosal invasion thickness can be used to predict the likelihood of recurrence-free survival at different times after surgery; (2) Patients with an upper thoracic tumor location and/or angiolymphatic invasion have a higher risk of distant recurrence; and (3) Patients with an upper thoracic tumor location, angiolymphatic invasion, submucosal invasion thickness, and diameter of the largest single tongue of invasion have a higher risk of early recurrence.

All patients with T1 ESCC need long-term follow-up after endoscopic resection or esophagectomy, even patients without any adverse parameters. But this analysis should help clinicians select a subset of these patients who need especially close postoperative surveillance and/or chemoradiotherapy. Additional long-term follow-up studies are needed to confirm these findings.

ARTICLE HIGHLIGHTS

Research background

The prognosis of superficial (T1) esophageal squamous cell carcinoma (ESCC) is poor, compared with T1 gastric or colorectal cancer. The unfavorable prognosis of patients with T1 ESCC is due to high rates of both synchronous and metachronous metastases. Recurrences of T1 ESCC after esophagectomy are usually metachronous metastases. When recurrence occurs, the prognosis is similar in patients who were node-negative or node-positive at the time of the original surgery. However, only a few studies have evaluated the clinicopathological characteristics associated with an increased risk of a postoperative recurrence in pT1N0 ESCC patients. No previous studies have separately evaluated the clinicopathological characteristics that are associated with distant recurrence or early recurrence in pT1N0 ESCC patients.

Research motivation

The identification of pT1N0 ESCC cases at high risk for recurrence is a very important and challenging aspect of the clinical management of these patients, to ensure appropriate use and maximum benefit of additional therapies.

Research objectives

To investigate the clinicopathological characteristics that are associated with recurrence, distant recurrence, and early recurrence, in order to provide clues to optimal individual therapy.

Research methods

Clinicopathological characteristics associated with any recurrence or distant recurrence were evaluated using univariate and multivariate Cox proportional hazards models. Early recurrence (≤ 24 mo) and correlated parameters were assessed using univariate and multivariate logistic regression models.

Research results

We have identified certain clinicopathological features that are associated with an increased risk of tumor recurrence in pT1N0 thoracic ESCC patients. A nomogram including tumor location, angiolymphatic invasion, and submucosal invasion thickness can be used to predict the likelihood of recurrence-free survival at different times after surgery. Patients with an upper thoracic tumor location and/or angiolymphatic invasion have a higher risk of distant recurrence. Patients with an upper thoracic tumor location, angiolymphatic invasion, submucosal invasion thickness, and an greater diameter of the largest single tongue of invasion have a higher risk of early recurrence. Additional long-term follow-up studies are needed to confirm these findings.

Research conclusions

We evaluated the clinicopathological characteristics associated with an increased risk of a postoperative recurrence and separately evaluated the clinicopathological characteristics that are associated with distant recurrence or early recurrence in pT1N0 ESCC patients. This study should help clinicians select a subset of these patients who need especially close postoperative surveillance and/or chemoradiotherapy.

Research perspectives

Risk of tumor recurrence in pT1N0 ESCC patients can be predicted using certain clinicopathological features. This should be confirmed in more prospective studies and multi-center studies.

REFERENCES

1 **Liebermann-Meffert D**. Anatomical basis for the approach and extent of surgical treatment of esophageal cancer. *Dis Esophagus* 2001; **14**: 81-84 [PMID: 11553213]

2 **Mizutani M**, Murakami G, Nawata S, Hitrai I, Kimura W. Anatomy of right recurrent nerve node: why does early metastasis of esophageal cancer occur in it? *Surg Radiol Anat* 2006; **28**: 333-338 [PMID: 16718401 DOI: 10.1007/s00276-006-0115-y]

3 **Kuge K**, Murakami G, Mizobuchi S, Hata Y, Aikou T, Sasaguri S. Submucosal territory of the direct lymphatic drainage system to the thoracic duct in the human esophagus. *J Thorac Cardiovasc Surg* 2003; **125**: 1343-1349 [PMID: 12830054]

4 **Ozawa Y**, Kamei T, Nakano T, Taniyama Y, Miyagi S, Ohuchi N. Characteristics of Postoperative Recurrence in Lymph Node-Negative Superficial Esophageal Carcinoma. *World J Surg* 2016; **40**: 1663-1671 [PMID: 26908240 DOI: 10.1007/s00268-016-3454-9]

5 **Wang S**, Chen X, Fan J, Lu L. Prognostic Significance of Lymphovascular Invasion for Thoracic Esophageal Squamous Cell Carcinoma. *Ann Surg Oncol* 2016; **23**: 4101-4109 [PMID: 27436201 DOI: 10.1245/s10434-016-5416-8]

6 **Araki K**, Ohno S, Egashira A, Saeki H, Kawaguchi H, Sugimachi K. Pathologic features of superficial esophageal squamous cell carcinoma with lymph node and distal metastasis. *Cancer* 2002; **94**: 570-575 [PMID: 11900242 DOI: 10.1002/cncr.10190]

7 **Song Z**, Wang J, Lin B, Zhang Y. Analysis of the tumor length and other prognosis factors in pT1-2 node-negative esophageal squamous cell carcinoma in a Chinese population. *World J Surg Oncol* 2012; **10**: 273 [PMID: 23249675 DOI: 10.1186/1477-7819-10-273]

8 **Huang Q**, Luo K, Chen C, Wang G, Jin J, Kong M, Li B, Liu Q, Li J, Rong T, Chen H, Zhang L, Chen Y, Zhu C, Zheng B, Wen J, Zheng Y, Tan Z, Xie X, Yang H, Fu J. Identification and Validation of Lymphovascular Invasion as a Prognostic and Staging Factor in Node-Negative Esophageal Squamous Cell Carcinoma. *J*

Thorac Oncol 2016; **11**: 583-592 [PMID: 26792626 DOI: 10.1016/j.jtho.2015.12.109]
9 **Xue L**, Ren L, Zou S, Shan L, Liu X, Xie Y, Zhang Y, Lu J, Lin D, Dawsey SM, Wang G, Lu N. Parameters predicting lymph node metastasis in patients with superficial esophageal squamous cell carcinoma. *Mod Pathol* 2012; **25**: 1364-1377 [PMID: 22627741 DOI: 10.1038/modpathol.2012.89]
10 **Japan Esophageal Society.**. Japanese Classification of Esophageal Cancer, 11th Edition: part II and III. *Esophagus* 2017; **14**: 37-65 [PMID: 28111536 DOI: 10.1007/s10388-016-0556-2]
11 **Endoscopic Classification Review Group.**. Update on the paris classification of superficial neoplastic lesions in the digestive tract. *Endoscopy* 2005; **37**: 570-578 [PMID: 15933932 DOI: 10.1055/s-2005-861352]
12 **Bosman FT**, Carneiro F, Hruban RH, Theise ND. WHO classification of tumors of the digestive system 4ed. Lyon: IARC, 2010
13 **Setia N**, Agoston AT, Han HS, Mullen JT, Duda DG, Clark JW, Deshpande V, Mino-Kenudson M, Srivastava A, Lennerz JK, Hong TS, Kwak EL, Lauwers GY. A protein and mRNA expression-based classification of gastric cancer. *Mod Pathol* 2016; **29**: 772-784 [PMID: 27032689 DOI: 10.1038/modpathol.2016.55]
14 **Wang GQ**, Wei WQ, Hao CQ, Zhang JH, Lü N. [Natural progression of early esophageal squamous cell carcinoma]. *Zhonghua Zhong Liu Za Zhi* 2010; **32**: 600-602 [PMID: 21122412]
15 **Wang GQ**, Jiao GG, Chang FB, Fang WH, Song JX, Lu N, Lin DM, Xie YQ, Yang L. Long-term results of operation for 420 patients with early squamous cell esophageal carcinoma discovered by screening. *Ann Thorac Surg* 2004; **77**: 1740-1744 [PMID: 15111177]
16 **Natsugoe S**, Baba M, Shimada M, Kijima F, Kusano C, Yoshinaka H, Mueller J, Aikou T. Positive impact on surgical treatment for asymptomatic patients with esophageal carcinoma. *Hepatogastroenterology* 1999; **46**: 2854-2858 [PMID: 10576360]
17 **Law S**, Kwong DL, Kwok KF, Wong KH, Chu KM, Sham JS, Wong J. Improvement in treatment results and long-term survival of patients with esophageal cancer: impact of chemoradiation and change in treatment strategy. *Ann Surg* 2003; **238**: 339-347; discussion 347-348 [PMID: 14501500 DOI: 10.1097/01.sla.0000086545.45918.ee]
18 **Li H**, Zhang Q, Xu L, Chen Y, Wei Y, Zhou G. Factors predictive of prognosis after esophagectomy for squamous cell cancer. *J Thorac Cardiovasc Surg* 2009; **137**: 55-59 [PMID: 19154903 DOI: 10.1016/j.jtcvs.2008.05.024]
19 **Edge SB BD**, Compton CC, FritzAG, Greene FL, Trotti A III. AJCC cancer staging manual. 7th ed. In: Rice TW BE, Rusch VW, editor Esophagus and esopha-gogastric junction. 7th ed. New York: Springer, 2009: 103-115
20 **Rice TW**, Ishwaran H, Ferguson MK, Blackstone EH, Goldstraw P. Cancer of the Esophagus and Esophagogastric Junction: An Eighth Edition Staging Primer. *J Thorac Oncol* 2017; **12**: 36-42 [PMID: 27810391 DOI: 10.1016/j.jtho.2016.10.016]
21 **Kosugi S**, Kawaguchi Y, Kanda T, Ishikawa T, Sakamoto K, Akaike H, Fujii H, Wakai T. Cervical lymph node dissection for clinically submucosal carcinoma of the thoracic esophagus. *Ann Surg Oncol* 2013; **20**: 4016-4021 [PMID: 23892526 DOI: 10.1245/s10434-013-3141-0]
22 **Zhang BH**, Cheng GY, Xue Q, Gao SG, Sun KL, Wang YG, Mu JW, He J. Clinical outcomes of basaloid squamous cell carcinoma of the esophagus: a retrospective analysis of 142 cases. *Asian Pac J Cancer Prev* 2013; **14**: 1889-1894 [PMID: 23679289]
23 **Saito S**, Hosoya Y, Zuiki T, Hyodo M, Lefor A, Sata N, Nagase M, Nakazawa M, Matsubara D, Niki T, Yasuda Y. A clinicopathological study of basaloid squamous carcinoma of the esophagus. *Esophagus* 2009; **6**: 177-181
24 **Takemura M**, Yoshida K, Fujiwara Y, Sakurai K, Takii M. A case of long-term survival after pulmonary resection for metachronous pulmonary metastasis of basaloid squamous cell carcinoma of the esophagus. *Int J Surg Case Rep* 2012; **3**: 451-454 [PMID: 22721697 DOI: 10.1016/j.ijscr.2012.05.013]

P- Reviewer: Luyer MD, Otowa Y, Thota PN **S- Editor**: Wang XJ
L- Editor: Wang TQ **E- Editor**: Huang Y

World Journal of Gastroenterology

Submit a Manuscript: http://www.f6publishing.com

World J Gastroenterol 2018 December 7; 24(45): 5167-5178

DOI: 10.3748/wjg.v24.i45.5167

ISSN 1007-9327 (print) ISSN 2219-2840 (online)

ORIGINAL ARTICLE

Retrospective Study

Nomogram to predict overall survival after gallbladder cancer resection in China

Yi Bai, Zhi-Song Liu, Jian-Ping Xiong, Wei-Yu Xu, Jian-Zhen Lin, Jun-Yu Long, Fei Miao, Han-Chun Huang, Xue-Shuai Wan, Hai-Tao Zhao

Yi Bai, Jian-Ping Xiong, Wei-Yu Xu, Jian-Zhen Lin, Jun-Yu Long, Han-Chun Huang, Xue-Shuai Wan, Hai-Tao Zhao, Department of Liver Surgery, Peking Union Medical College Hospital, Chinese Academy of Medical Sciences and Peking Union Medical College, Beijing 100730, China

Zhi-Song Liu, Fei Miao, Department of Statistics, Tianjin University of Finance and Economics Pearl River College, Tianjin 301811, China

ORCID number: Yi Bai (0000-0002-1179-3734); Zhi-Song Liu (0000-0003-3213-4743); Jian-Ping Xiong (0000-0002-6163-2621); Wei-Yu Xu (0000-0002-2101-4829); Jian-Zhen Lin (0000-0002-4767-8834); Jun-Yu Long (0000-0001-5745-7165); Fei Miao (0000-0002-9617-961X); Han-Chun Huang (0000-0003-2626-3389); Xue-Shuai Wan (0000-0003-2140-5384); Hai-Tao Zhao (0000-0002-3444-8044).

Author contributions: Bai Y, Liu ZS, and Xiong JP contributed equally to this work; Bai Y conceived the research, collected and analyzed the clinical data, and wrote the manuscript that led to the submission; Xu WY, Xiong JP, and Huang HC helped to collect the clinical data and followed the patients; Liu ZS, Lin JZ, Long JY, and Miao F helped to analyze the data; Zhao HT and Wan XS revised the manuscript; Zhao HT provided financial support for this work; Zhao HT is the corresponding author; All authors read and approved the final manuscript.

Supported by Chinese Academy of Medical Sciences Innovation Fund for Medical Science, No. 2017-I2M-4-003; International Science and Technology Cooperation Projects, No. 2015DFA30650 and No. 2016YFE0107100; Capital Special Research Project for Health Development, No. 2014-2-4012; Beijing Natural Science Foundation, No. L172055; and National Ten-thousand Talent Program and Beijing Science and Technology Cooperation Special Award Subsidy Project.

Institutional review board statement: The publication of this manuscript has been reviewed and approved by the Peking Union Medical College Hospital institutional review board.

Informed consent statement: All patients and their families signed informed consent statements before surgery, and the type of surgical procedure was performed according to the approved guidelines.

Conflict-of-interest statement: We declare that the authors have no conflict of interest.

Data sharing statement: No additional data are available.

Manuscript source: Unsolicited manuscript

Correspondence author to: Hai-Tao Zhao, MD, Professor, Department of Liver Surgery, Peking Union Medical College Hospital, Chinese Academy of Medical Sciences and Peking Union Medical College, 1 Shuaifuyuan, Wangfujing, Beijing 100730, China. zhaoht@pumch.cn
Telephone: +86-10-69156042
Fax: +86-10-69156043

Received: September 19, 2018
Peer-review started: September 19, 2018
First decision: October 16, 2018
Revised: October 23, 2018
Accepted: November 9, 2018
Article in press: November 9, 2018
Published online: December 7, 2018

Abstract

AIM

To integrate clinically significant variables related

to prognosis after curative resection for gallbladder carcinoma (GBC) into a predictive nomogram.

METHODS

One hundred and forty-two GBC patients who underwent curative intent surgical resection at Peking Union Medical College Hospital (PUMCH) were included. This retrospective case study was conducted at PUMCH of the Chinese Academy of Medical Sciences and Peking Union Medical College (CAMS & PUMC) in China from January 1, 2003 to January 1, 2018. The continuous variable carbohydrate antigen 19-9 (CA19-9) was converted into a categorical variable (cCA19-9) based on the normal reference range. Stages 0 to IIIA were merged into one category, while the remaining stages were grouped into another category. Pathological grade X (GX) was treated as a missing value. A multivariate Cox proportional hazards model was used to select variables to construct a nomogram. Discrimination and calibration of the nomogram were performed *via* the concordance index (C-index) and calibration plots. The performance of the nomogram was estimated using the calibration curve. Receiver operating characteristic (ROC) curve analysis and decision curve analysis (DCA) were performed to evaluate the predictive accuracy and net benefit of the nomogram, respectively.

RESULTS

Of these 142 GBC patients, 55 (38.7%) were male, and the median and mean age were 64 and 63.9 years, respectively. Forty-eight (33.8%) patients in this cohort were censored in the survival analysis. The median survival time was 20 months. A series of methods, including the likelihood ratio test and Akaike information criterion (AIC) as well as stepwise, forward, and backward analyses, were used to select the model, and all yielded identical results. Jaundice [hazard ratio (HR) = 2.9; 95% confidence interval (CI): 1.60-5.27], cCA19-9 (HR = 3.2; 95%CI: 1.91-5.39), stage (HR = 1.89; 95%CI: 1.16-3.09), and resection (R) (HR = 2.82; 95%CI: 1.54-5.16) were selected as significant predictors and combined into a survival time predictive nomogram (C-index = 0.803; 95%CI: 0.766-0.839). High prediction accuracy (adjusted C-index = 0.797) was further verified *via* bootstrap validation. The calibration plot demonstrated good performance of the nomogram. ROC curve analysis revealed a high sensitivity and specificity. A high net benefit was proven by DCA.

CONCLUSION

A nomogram has been constructed to predict the overall survival of GBC patients who underwent radical surgery from a clinical database of GBC at PUMCH.

Key words: Nomogram; Survival; Prognosis; Gallbladder cancer; Resection

Core tip: A nomogram including jaundice, carbohydrate antigen 19-9 (CA19-9), American Joint Committee on Cancer tumor node metastasis stage, and incisional margin status was built to predict the survival of gallbladder cancer patients who underwent curative resection at Peking Union Medical College Hospital. After calibration and verification, this model was shown to have high predictive accuracy and good performance.

Bai Y, Liu ZS, Xiong JP, Xu WY, Lin JZ, Long JY, Miao F, Huang HC, Wan XS, Zhao HT. Nomogram to predict overall survival after gallbladder cancer resection in China. *World J Gastroenterol* 2018; 24(45): 5167-5178 Available from: URL: http://www.wjgnet.com/1007-9327/full/v24/i45/5167.htm DOI: http://dx.doi.org/10.3748/wjg.v24.i45.5167

INTRODUCTION

Gallbladder cancer (GBC) is a common biliary tract malignancy that ranks as the sixth most common digestive tract cancer[1,2]. Because of the lack of specific early screening methods and typical symptoms, most patients with GBC present with advanced-stage disease. Surgical resection remains the primary treatment for GBC because of the low sensitivity of GBC to radiotherapy (RT) and chemotherapy and because of a lack of effective drugs. Although the prevalence of GBC is low, the 5-year overall survival rate decreased from 20.1% from 2003-2005 to 16.4% from 2012-2015[3].

Although the American Joint Committee on Cancer (AJCC) staging system has published an updated eighth edition, this system does not offer precise prognostic information for individual patients[4]. Both physicians and patients are paying more attention to prognostic outcomes for GBC after surgical therapeutic interventions. Hence, a nomogram that accurately and specifically predicts overall survival is urgently needed. As a statistical predictive model, nomograms have been rapidly developed for most carcinoma types and are popular among doctors and patients because of their friendly and feasible interface[5,6]. More common tumors of the hepatobiliary system, such as hepatocellular carcinoma (HCC) and intrahepatic cholangiocarcinoma (ICC), have more explicit pathogenic factors and affect a relatively larger number of patients compared with GBC. Many nomograms suitable for these tumor types have been established to help clinicians accurately make rational decisions regarding diagnosis, treatment, and prognosis[7-9].

The Surveillance, Epidemiology, and End Results (SEER) Medicare database represents the American population and is an ideal research source for estimating cancer incidence and constructing survival models. In 2008, Wang *et al*[10] designed an individual predictive model considering the contribution of adjuvant RT to evaluate survival improvement in GBC patients after

resection. However, not everyone was sensitive to RT and chemotherapy due to differences in lymph node status and distant metastasis. Therefore, in 2011, they proposed another nomogram to further clarify specific GBC populations with the potential to obtain longer survival times after adjuvant chemoradiotherapy (CRT)[11]. For chronic cholecystitis, Zhou *et al*[12] developed an individualized diagnostic nomogram for stage I-II GBC in chronic cholecystitis patients with gallbladder wall thickening in 2016. Recently, a more accurate and effective survival model for predicting the prognosis of patients with nonmetastatic GBC after surgical resection derived from the SEER database was built by Zhang *et al*[13]. However, due to the limited number of GBC patients and disparate risk factors in China, to the best of our knowledge, no predictive model has thus far been established to evaluate the prognosis of patients with GBC in China.

The current study aimed to incorporate individual correlation determinants into a nomogram to predict overall survival for GBC patients after radical resection in China.

MATERIALS AND METHODS

Patients and treatments

From January 1, 2003 to January 1, 2018, 142 patients diagnosed with GBC *via* pathological examination after curative intent surgical resection at Peking Union Medical College Hospital (PUMCH) of the Chinese Academy of Medical Sciences and Peking Union Medical College (CAMS & PUMC) in Beijing, China were included in the current study. The inclusion criteria were as follows: (1) radical surgery; (2) GBC confirmed by pathological examination; (3) no antitumor treatment before or during surgery; (4) no other malignant tumors; and (5) pathological examination revealing a clear number of positive lymph nodes and the total number of lymph nodes obtained from the dissection. The exclusion criteria were as follows: (1) lack of a clear pathological diagnosis; (2) distant metastasis; (3) incomplete lymph node data; (4) nonprimary tumor; or (5) incomplete follow-up data.

Preoperative staging and surgical evaluation were performed based on imaging and laboratory examinations. Staging was further evaluated during surgery based on the findings and on the cryosection biopsy report. The following surgeries were performed according to the stage: for stage Tis-T1a patients, cholecystectomy was considered radical resection; for patients with stage T1b-T3/N0-1, cholecystectomy, hepatic wedge resection, and regional lymph node dissection were performed; for partial stage T3N2 patients, cholecystectomy, hepatic wedge resection, and enlarged lymph node dissection were performed; and for some patients with stage T4/N1-2, extended radical resection including combined semihepatic resection, peripheral organ resection, and hepatic pancreaticoduodenectomy were performed according to standard radical surgical procedures.

Ethics statement

The study was approved by the Medical Ethics Committee of PUMCH of the CAMS & PUMC. All patients provided written informed consent. The study was carried out according to the ethical standards of the World Medical Association Declaration of Helsinki[14].

Data collection

Demographic and clinical information and related variables were manually reviewed from the medical records. We retrospectively reviewed the medical records of patients to collect demographic data, body mass index (BMI), physical examination findings, serum laboratory test results, surgical records, pathological reports and imaging findings of cholecystolithiasis determined *via* ultrasonography, computerized tomography, and magnetic resonance imaging. Subjects involved in this study were those who underwent radical surgery without R2 excision and were diagnosed with GBC by histopathology. GBC stage and postoperative pathologic tumor node metastasis (pTNM) information were determined using the AJCC 8th edition (AJCC-8) classification system[4]. Incisional margins and tumor size were ascertained based on surgeon observations and final pathological assessments. All patients were followed routinely after discharge. The last follow-up time and vital status were recorded. After screening, 142 patients with confirmed GBC met the inclusion criteria.

Statistical analysis

Descriptive statistics for time-to-event variables and predictors were performed for quick screening of the data. Categorical variables are presented as numbers and percentages, and continuous variables are presented as the minimum, median, mean, maximum, and standard deviation. Some continuous variables were converted to categorical variables because their significance and linear relationships to outcomes were not satisfied after graphical and statistical assessments. For some categorical predictors, small categories were merged with others. The Kaplan-Meier (K-M) method was applied to compare survival curves for categories of individual predictors, and the log-rank test was used to determine the significance of these differences. Model selection methods, including the likelihood ratio test, Akaike information criterion (AIC), and stepwise, forward, and backward analyses, were used to construct a Cox proportional hazards model. Hazard ratios (HRs) and 95% confidence intervals (CIs) were estimated. Possible confounders and interactions in the model were detected. Schoenfeld residuals *vs* ranked survival time for selected predictors were analyzed to evaluate the proportional hazard assumption of the model. The predictive accuracy of the model was estimated by the concordance index (C-index). The overfit and predictive performance of the model were assessed *via* bootstrap validation. The clinically significant

Table 1 Descriptive statistics for time to event variable

Total	Event *n* (%)	Censored *n* (%)	Time (mo)	Survival probability	95%CI	Quartile	Point estimate	95%CI
142	94 (66.2)	48 (33.8)	12	0.638	0.562-0.724	50%	20	14-31
			36	0.360	0.284-0.458			

CI: Confidential interval.

variables calculated from the Cox proportional hazards model were integrated into a nomogram to predict the overall survival of patients undergoing GBC resection. The performance of the nomogram was estimated using a calibration curve. The predictive accuracy and net benefit of the nomogram were assessed *via* receiver operating characteristic (ROC) curve analysis and decision curve analysis (DCA), respectively. The significance level for all statistical tests was set at 0.05, and all tests were two-sided. Statistical analyses were performed using R version 3.5.0 software (http://www.r-project.org/). Extension packages, including "survival", "rms", "nomogramEx", and "survminer" were also used.

RESULTS

Survival outcomes and predictors

The study cohort consisted of 142 eligible patients who underwent GBC resection. Forty-eight (33.8%) patients were censored. The median survival time was 20 mo. The one- and 3-year survival probabilities were 63.8% and 36%, respectively (Table 1).

A detailed description of all the clinicopathologic and treatment characteristics can be found in Table 2. Notably, carbohydrate antigen 19-9 (CA19-9) as a candidate predictor spanned a wide range from a minimum value of 0.01 kU/L to a maximum value of 10524 kU/L. In addition, a large difference between the median and mean values resulted in obvious skewness. Both indicated that using CA19-9 as a continuous variable was not suitable for model construction due to its limited predictive role, as demonstrated by the relatively small coefficient. Hence, we converted CA19-9 into a categorical variable based on normal reference ranges to investigate its correlation with outcome. According to the latest AJCC staging system, we divided the patients into eight groups including stage 0, I, IIA, IIB, IIIA, IIIB, IVA, and IVB for predictor selection. We then combined stages 0 to IIIA into one category, while the remaining categories were combined due to few cases in some specific groups. In addition, pathological grade X (GX), which refers to a degree of pathological differentiation that cannot be assessed, accounted for 8.5% (12/142) of all participants and was treated as a missing value.

Model selection

To choose the significant predictive variables that correlated well with outcome, age at diagnosis, gender, jaundice, BMI, gallstones, diabetes, tumor size, CA19-9 levels, AJCC-8 stage, tumor differentiation, and surgical margins were incorporated statistics. For continuous variables, null model residuals (martingale residuals) *vs* age, BMI, and tumor size plotted with LOESS lines were performed to obtain preliminary assessments of their predictive potential for survival time. As shown in Figure 1, BMI and tumor size appeared to have a considerable nonlinear relationship with martingale residuals, indicating that the linear assumption of the model for BMI and tumor size with survival time may be rejected. Log transformation was subsequently attempted for BMI and tumor size; however, the linear correlation was little improved. Continuous predictors were thus converted into categorical variables. Notably, Figure 1 illustrates that the significance cutoff for BMI was approximately 24, which was consistent with the standard value for distinguishing normal and overweight in China; therefore, we converted BMI into two categories based on this cutoff. In addition, martingale residuals for BMI were closer to the fitted line than the other two variables, suggesting that BMI may be a potential predictor. We observed a scatter located in the top right of the tumor size graph (Figure 1), which can be considered a potential outlier because it robustly influenced the tendency of the fitted line. Cutoffs of approximately 2 and 5 were a better choice, consistent with the common classification criterion. For the predictor age, we initially used a univariate Cox model to assess the correlation between age and outcome, and the results showed that it was not a significant predictor. Because the fitted line appeared to be linear, and because there was no obvious cutoff, we evenly separated age into three categories (less than 55, 55 to 65, and older than 65 years) for further study (Figure 1). After conversion to categorical variables, we defined cCA19-9, cBMI, cTumor size, and cAge as the categorical forms of these variables to distinguish them from the continuous forms. Regarding the degree of tumor differentiation, 12 samples that could not be evaluated were treated as missing values, thus resulting in only 130 observations.

K-M survival curves for all predictors before adjustment for the other predictors were established. As shown in Figure 2, patients with jaundice had shorter survival times than patients without; patients with higher BMI exhibited longer survival times than patients with lower BMI; patients with lower CA19-9 levels showed

Table 2 Patient characteristics *n* (%)

Feature (Min, Median, Mean, Max, SD)	No. of patients
Age (35, 64, 63.9, 83, 10.2), years	
< 55	24 (16.9)
55-65	49 (34.5)
≥ 65	69 (48.6)
Gender	
Male	55 (38.7)
Female	87 (61.3)
Jaundice	
Absent	122 (85.9)
Present	20 (14.1)
Cholecystolithiasis	
Absent	67 (47.2)
Present	75 (52.8)
Diabetes	
Absent	32 (22.5)
Present	110 (77.5)
BMI (15.4, 23.5, 24.2, 32.3, 3.4)	
< 24	75 (52.8)
≥ 24	67 (47.2)
CA19-9 (0.01, 13.2, 66.4, 10524, 507.7), kU/L	
< 40	65 (45.8)
≥ 40	77 (54.2)
Tumor size (0.2, 3.0, 3.4, 13, 2.1), cm	
< 2	38 (26.8)
2-5	68 (47.9)
≥ 5	36 (25.3)
Primary tumor	
Tis	9 (6.3)
T1	9 (6.3)
T2	20 (14.1)
T3	93 (65.5)
T4	11 (7.8)
Regional lymph node	
N0	86 (60.6)
N1	43 (30.3)
N2	13 (9.1)
Stage	
0	9 (6.3)
I	9 (6.3)
ⅡA	10 (7.0)
ⅡB	3 (2.1)
ⅢA	49 (34.6)
ⅢB	40 (28.2)
ⅣA	9 (6.3)
ⅣB	13 (9.2)
Histologic grade	
G1	27 (19.0)
G2	53 (37.3)
G3	50 (35.2)
GX	12 (8.5)
Surgical margins	
R0	112 (78.9)
R1	30 (21.1)

Min: Minimum; Max: Maximum; SD: Standard deviation; No. of patients: Number of patients; BMI: Body mass index; CA19-9: Carbohydrate antigen 19-9; R: Resection.

longer survival times than patients with higher CA19-9; and patients in the lower stage group had longer survival times than patients in the higher stage group. Considering the surgical margin status, patients in the R0 category had longer survival times than patients in the R1 category. Risk tables for each indicator are shown below the corresponding K-M curves. Note that all categories of the following predictors had significant differences after the log-rank test: jaundice, cBMI, cCA19-9, stage, and R. However, cAge, gender, cholecystolithiasis, diabetes, cTumor size, and grade failed to reach significance in constructing the model.

Construction and diagnosis of a Cox proportional hazards model

Because the aforementioned predictors contained no missing values after excluding the degree of tumor differentiation, various model-selection criteria, including the likelihood ratio test, AIC, and stepwise, forward, and backward analyses, were utilized to construct the model for all 142 observation points. Notably, all methods yielded identical results.

To check for possible confounders, both univariate and multivariate models were established. Compared with the univariable model, the multivariable model showed that the CIs for jaundice (95%CI: 1.60-5.27), cCA19-9 (95%CI: 1.91-5.39), stage (95%CI: 1.16-3.09), and R (95%CI: 1.54-5.16) did not change significantly after combination with other predictors (Figure 3). Furthermore, we found that cCA19-9 was a confounder for BMI levels; thus, cBMI was excluded in the multivariate model. Moreover, interactions between each pair of predictors were examined, and no interactions were detected.

To further evaluate whether the proportional hazards assumption was valid, Schoenfeld residuals were analyzed with respect to ranked survival time for selected predictors. All fitted lines derived from individual scatter plots seemed to be horizontal (Figure 4). Furthermore, statistical tests were performed on Schoenfeld residuals *vs* ranked survival time for each predictor. The *P*-values for jaundice, cCA19-9, stage, and R were 0.8075, 0.8798, 0.6082, and 0.7919, respectively. The *P*-value for the global test was 0.9837. In conclusion, all the results indicated that the proportional hazards assumption was satisfied.

Construction and validation of the nomogram

The predictive ability of the model was assessed by calculating the C-index, which was 0.803 (95%CI: 0.766-0.839). Bootstrap validation was applied to estimate the overfit of the model. The adjusted C-index representing the bias-corrected estimate of model performance in the future was 0.797 after 1000 iterations, demonstrating good predictive accuracy for the nomogram.

The nomogram that predicts the survival time of patients with GBC after surgical resection is displayed in Figure 5A. The nomogram was developed based on the results of the Cox proportional hazards model in Figure 3. In this nomogram, each factor was ascribed a weighted point total that indicated a survival prognosis. One- and three-year survival probabilities can be measured using this nomogram. For instance, the presence of jaundice was assigned 92 points, while a CA19-9 level ≥ 40 kU/L was assigned 100 points. The higher a

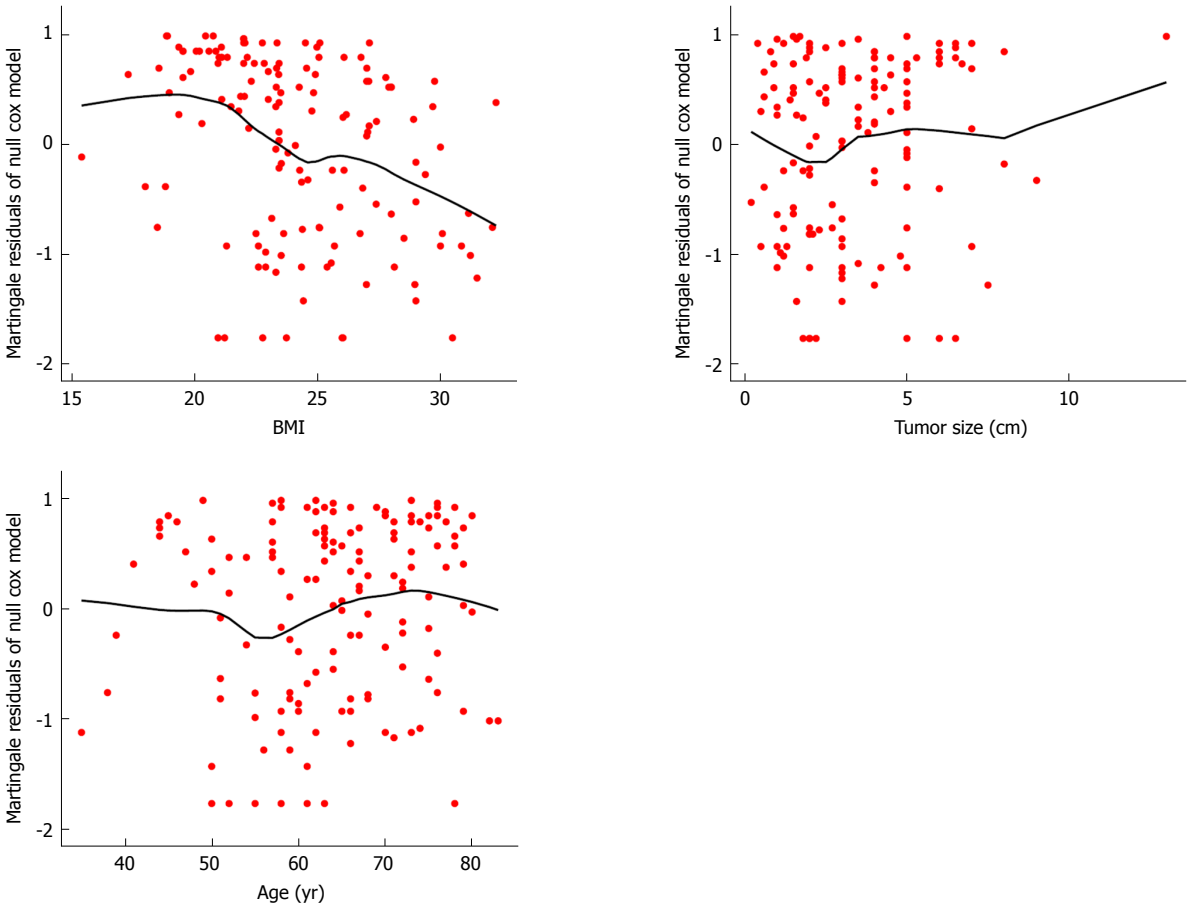

Figure 1 Graphical assessment for continuous predictors. Null model residuals (martingale residuals) *vs* body mass index, tumor size, and age were plotted with LOESS line to obtain a preliminary assessment of which of these predictors should be incorporated into the model. BMI: Body mass index.

patient scores, the poorer the prognosis. In addition, the performance of the nomogram was graphically evaluated using a calibration curve (Figure 5B). The predicted line overlapped well with the reference line, demonstrating the good performance of the nomogram. Similarly, we compared the predictive accuracy between the combined model and individual predictors, including jaundice, CA19-9, stage, and R, *via* ROC curve analysis. The area under the curve (AUC) of the nomogram was significantly larger than those of other single variables (Figure 6A). Finally, to determine whether the predictive nomogram was clinically useful, DCA was performed to evaluate the net benefit of the models. Compared with jaundice, CA19-9, stage, and R, the combined model offered the best clinical utility, as calculated within the favorable probability. Hence, this nomogram is the best model for predicting GBC patient survival, which might help clinicians with patient counseling, decision-making, and follow-up scheduling.

DISCUSSION

GBC is a common biliary tract tumor around the world. Due to its occult onset and lack of specific symptoms and early screening methods, most GBC patients already present with advanced-stage disease at diagnosis, which results in difficulty implementing curative intent surgical resection. GBC always behaves as a highly malignant tumor with a dismal prognosis[15,16]. Less than 5% of GBC patients survive for longer than 5 years[1]. The five-year survival rate of GBC patients has been declining in China according to the latest statistical report[3]. Obtaining accurate prognostic information is necessary to help physicians make better clinical decisions and perform consultations with patients regarding life expectancy after resection of tumor masses. Nomograms are alternative prognostic assessment tools for most cancers because they include more clinically related factors and offer more reliable prognostic information tailored to individual patients than the traditional AJCC TNM staging system. Nomograms are predictive tools that generate user-friendly graphical interfaces to calculate probabilities of clinical outcomes, such as diagnosis, recurrence, and prognosis, based on related, statistically significant variables[5,6,17]. The present study was the first to propose a nomogram for predicting the survival times of patients undergoing GBC resection in China. The nomogram suggested that the absence of jaundice, lower preoperative CA19-9 levels, lower AJCC TNM stage, and incisional margins without tumor cells correlated well with a long survival time. Notably, given the very broad data distribution and considerable discrepancies

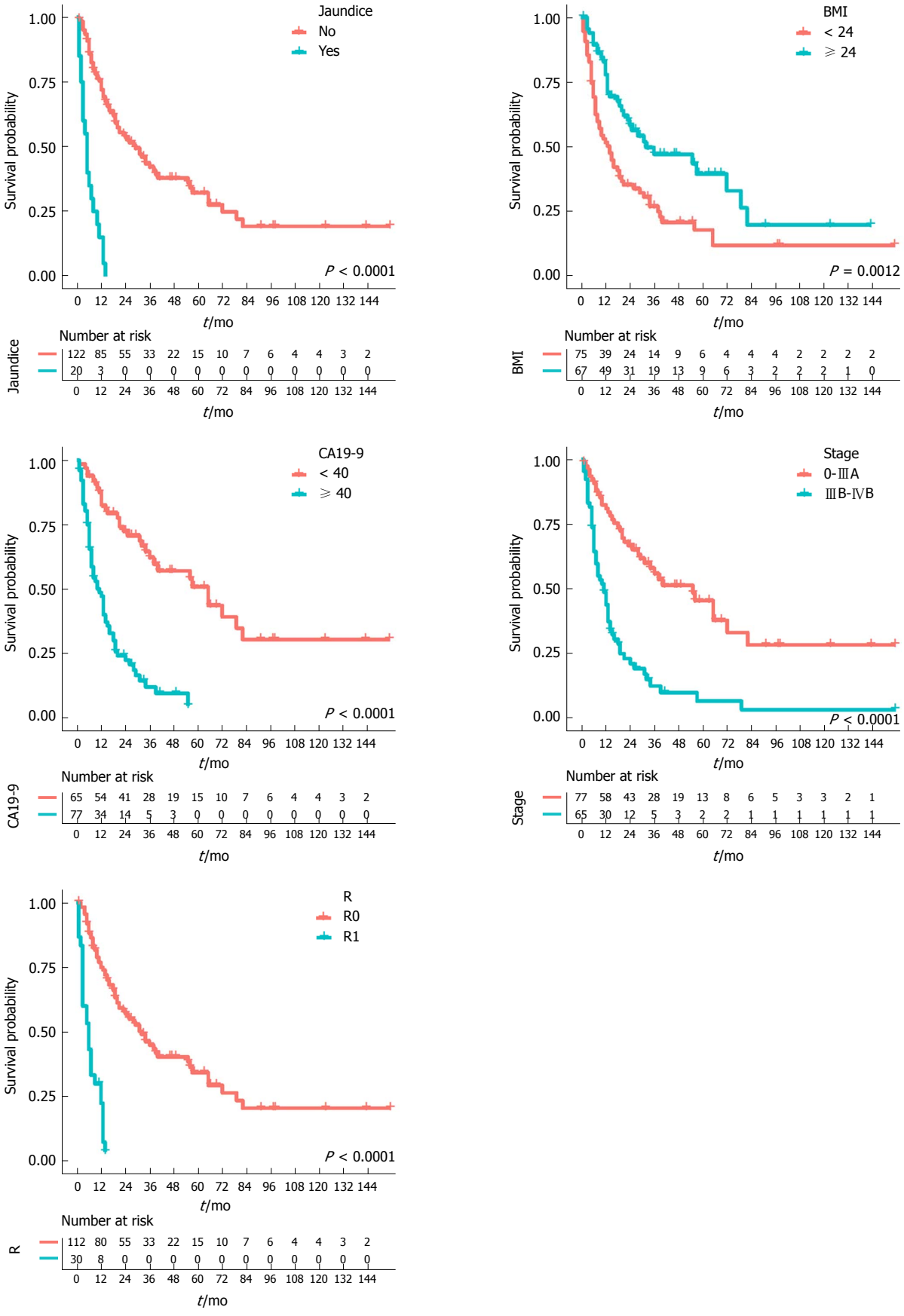

Figure 2 Kaplan-Meier survival curves for each predictor. Kaplan-Meier survival curves showing the overall survival rates in gallbladder cancer patients according to different category types. All predictors are statistically significant (*P*-values are shown in the bottom right corner). Time-dependent numbers at risk are listed at the bottom. BMI: Body mass index; CA19-9: Carbohydrate antigen 19-9; R: Resection.

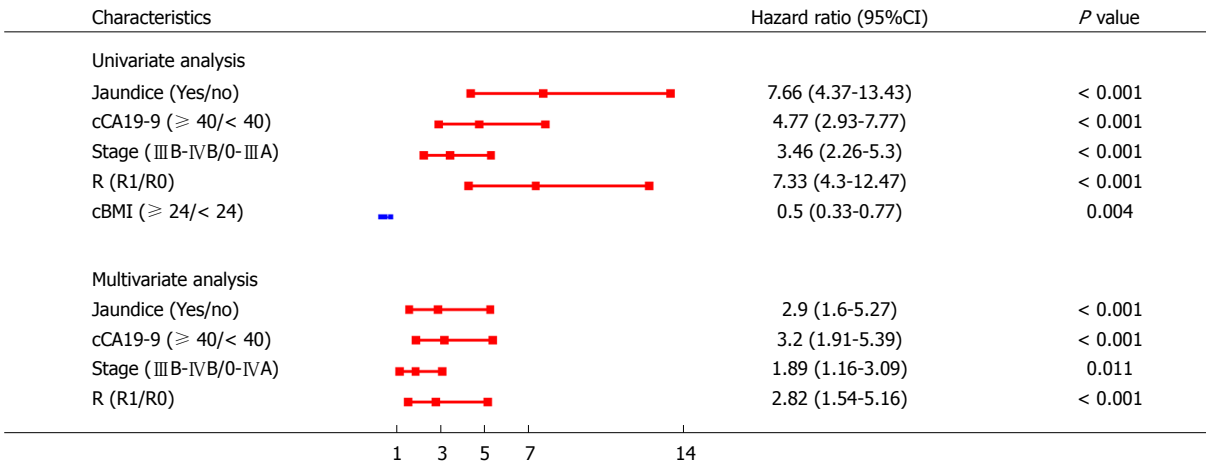

Figure 3 Cox proportional hazards model. Absence of jaundice and lower groups of categorical carbohydrate antigen 19-9, stage, resection, and categorical body mass index were used as the baseline. Red represents statistically significant factors incorporated to the model after both univariate and multivariate analysis, while blue represents factors that were excluded after multivariate analysis. cCA19-9: Categorical carbohydrate antigen 19-9; R: Resection; cBMI: Categorical body mass index.

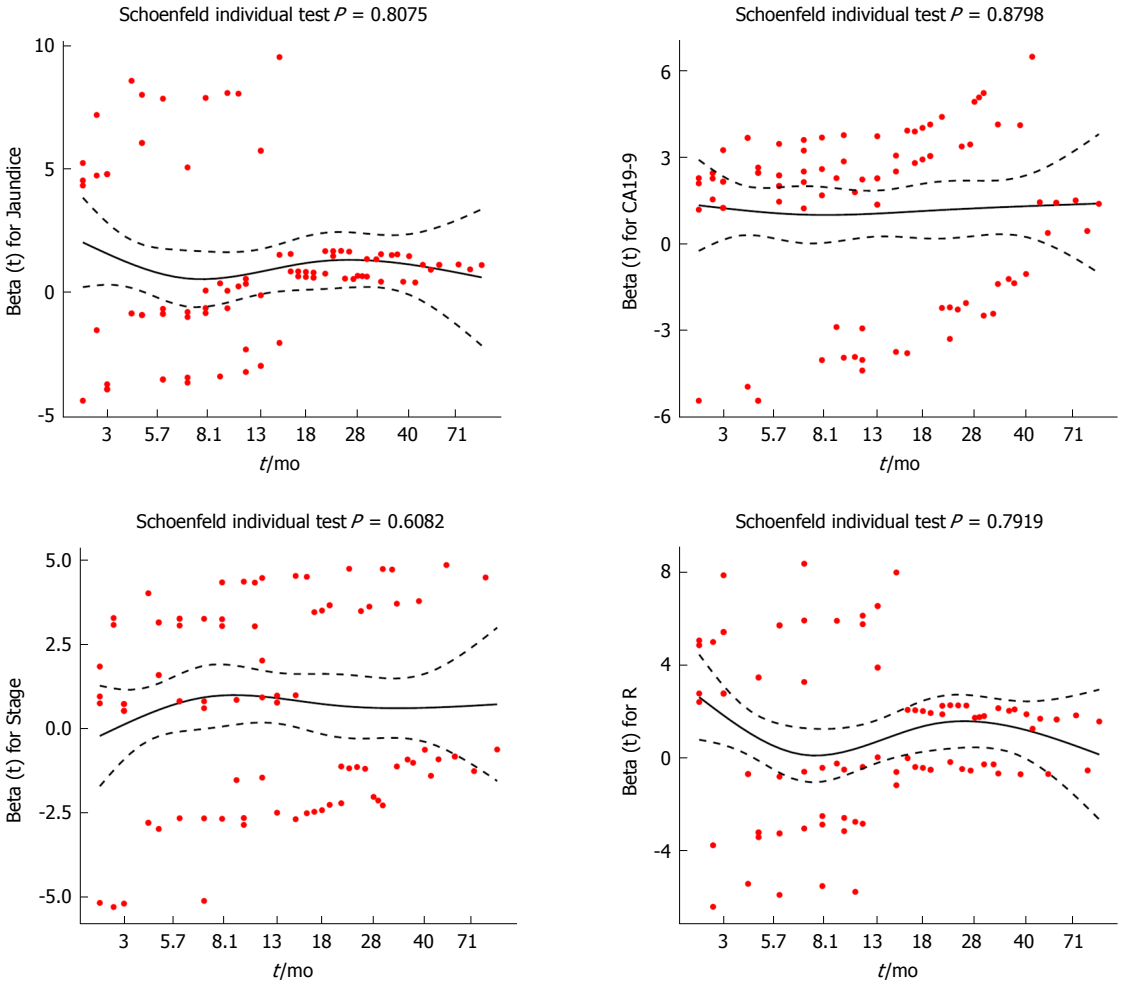

Figure 4 Schoenfeld residuals *vs* ranked survival time for selected predictors. The X-axis represents the survival time, while the Beta values referring to jaundice, carbohydrate antigen 19-9, stage, and resection are shown on the Y-axis. CA19-9: Carbohydrate antigen 19-9; R: Resection.

between the median and mean, we converted CA19-9 into a categorical variable to evaluate its relationship with outcome. In addition, we demonstrated that categorical forms of continuous variables, including BMI, tumor size, and age, were better choices for model selection. Moreover, for 12 patients with GX disease who were treated as having missing values, we did not use conventional modeling methods to first

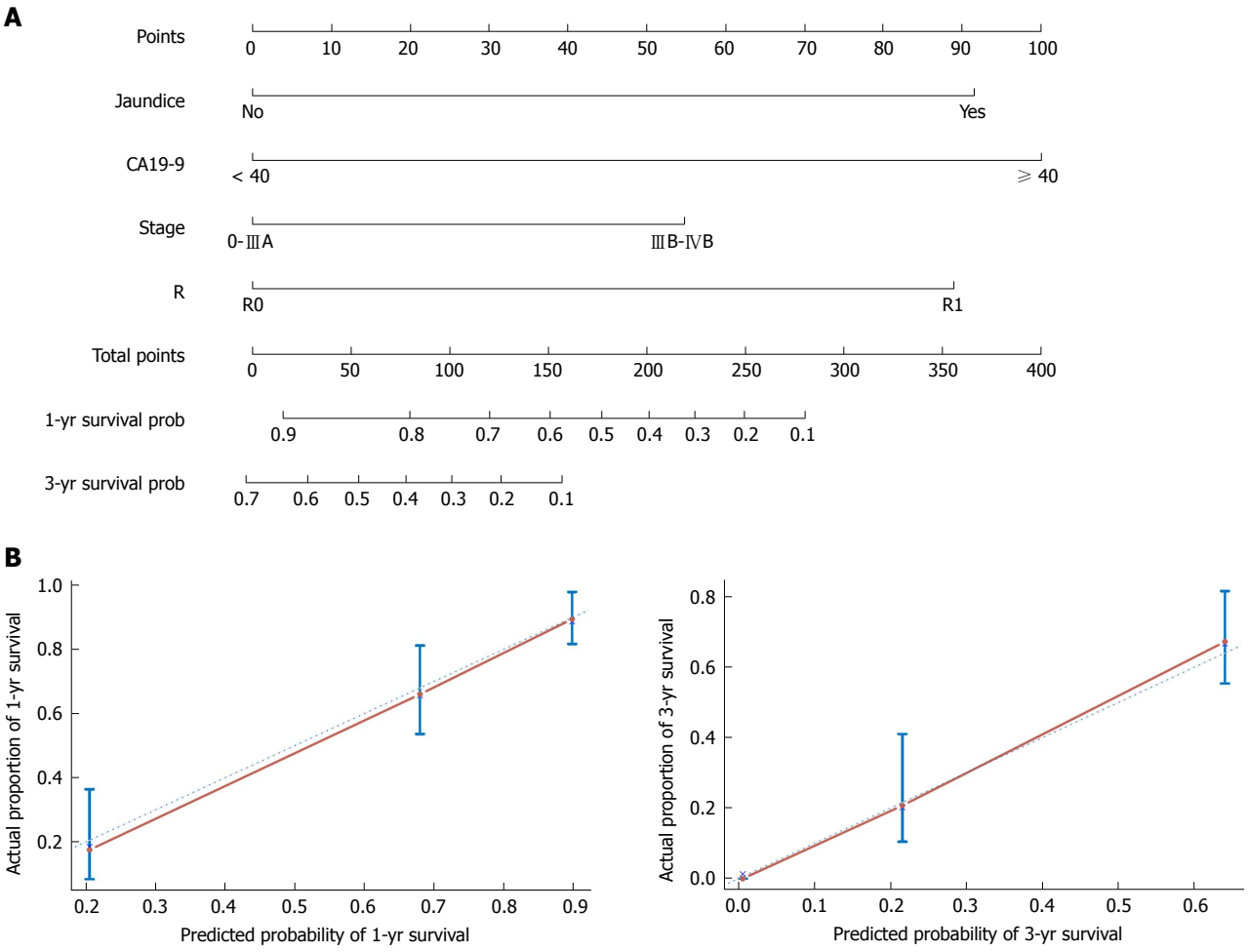

Figure 5 Nomogram and calibration plot. A: A nomogram to predict the survival time of postsurgery gallbladder cancer (GBC) patients. Patient's jaundice condition is located in the row labeled "Jaundice", and a straight line is drawn up to the row labeled "Points" to determine the corresponding points. This process is then repeated for each of the remaining factors. After the total points are summed, a straight line is drawn from the appropriate total point number location to the rows labeled "1-yr survival prob" and "3-yr survival prob" to predict patient survival probability; B: Calibration curves for predicting 1- and 5-yr overall survival for GBC patients after radical resection. Actual survival measured *via* Kaplan-Meier analysis is shown on the Y-axis, and the nomogram-predicted survival is shown on the X-axis. CA19-9: Carbohydrate antigen 19-9.

construct and then validate a nomogram. Instead, we first checked the predictive potential of each candidate variable. Importantly, after statistical analysis, we found that cCA19-9 was a confounder for BMI levels and thus excluded cBMI from nomogram construction.

The SEER database of the National Cancer Institute, which represents approximately 26% of the US population, can be used to obtain enough clinical information on rare tumor types, such as GBC. Wang *et al*[10,11] successively built two nomograms derived from the SEER database to evaluate the survival benefit of adjuvant RT, adjuvant chemotherapy, or CRT for patients with GBC. The first model demonstrated that patients with node-positive and/or T2 stage or higher disease had the greatest benefit from adjuvant RT[10]. The second nomogram found that patients with at least T2 or N1 disease had a survival benefit from adjuvant CRT[11]. Both studies indicated the potential for age at diagnosis, gender, race, extent of the primary tumor, and nodal status to influence the survival time of GBC patients. Interestingly, there are some differences between our results. The main reason may be that the study patients were from two different countries, leading to heterogeneity in ethnicity. In addition, environmental factors, such as living conditions, eating habits, and other risk factors, may also have contributed to the different results[16,18,19]. Furthermore, GBC is a rare tumor in China; thus, large, multi-institutional study cohorts are lacking. In addition, we lacked a population-based cancer registry database similar to the SEER database. Our cohort was thus relatively small, and it was difficult to perform the same study strategy, which caused discrepancies in the results.

Recently, Zhang *et al*[13] constructed a model to predict the survival of patients with nonmetastatic GBC after surgical resection derived from the SEER database. Compared with the studies by Wang *et al*[10,11], they identified additional predictors, including tumor size, histological grade, lymph node excision, and chemotherapy. Their nomogram performed better than the seventh edition of the AJCC Cancer Staging system, further demonstrating the superiority of nomograms.

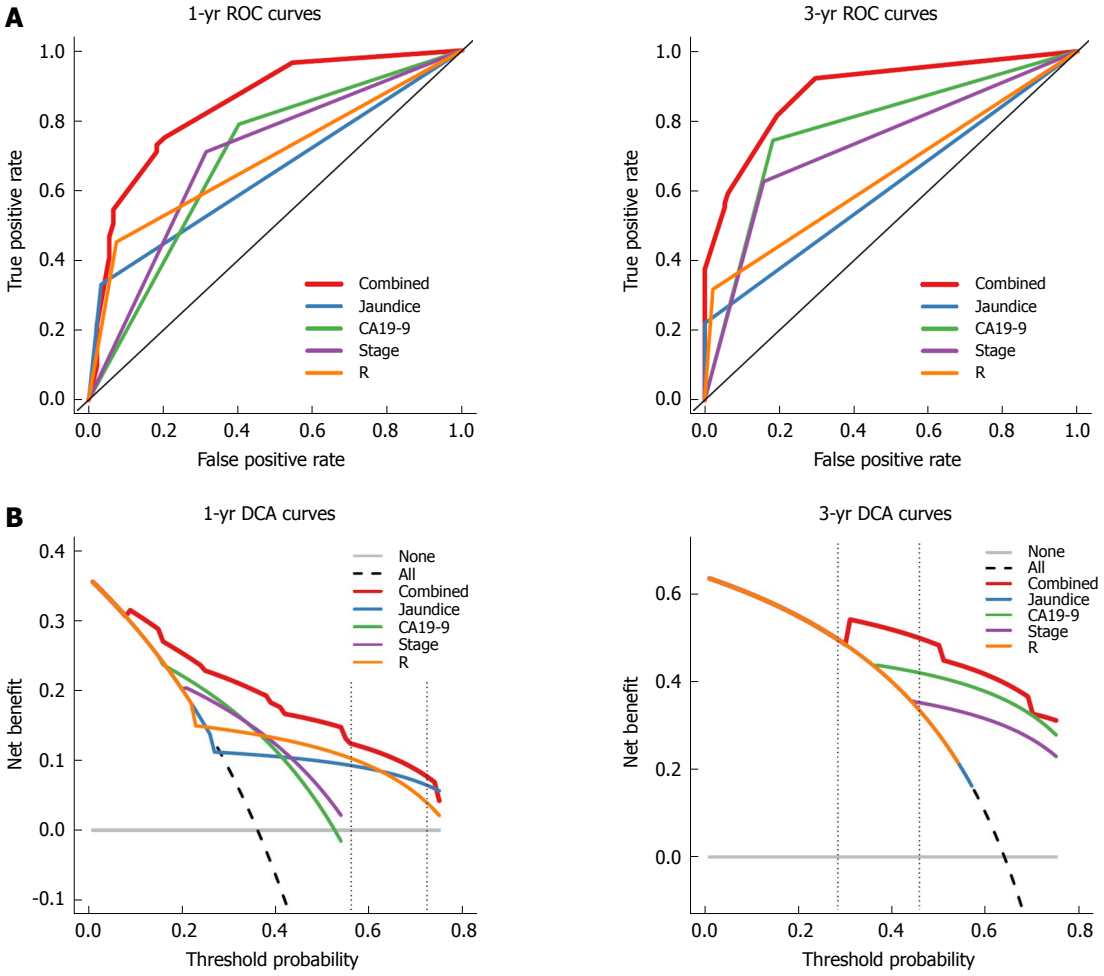

Figure 6 Receiver operating characteristic and decision curve analysis of the nomogram for 1- and 3-yr survival. A: Time-dependent receiver operating characteristic curve analysis for the sensitivity and specificity of the nomograms. The combined nomogram (red solid line) had higher accuracy compared with the individual indicators; B: Time-dependent decision curve analysis for the clinical benefit of the nomograms and the corresponding scope of application. The black dotted line represents the assumption that all patients survive in the first and third year. The gray solid line represents the assumption that no patients survive in the first or third year. The red solid line represents the combined nomogram. The threshold probability between two vertical dashed lines represents the 95%CI of 1- and 3-yr survival probability in the null model. ROC: Receiver operating characteristic; DCA: Decision curve analysis.

Among these variables, tumor size, which had no correlation with prognosis in our model, was treated as two classified variables in their model. The AJCC standard does not use tumor size to assess T stage, which is in line with our results, indicating that tumor size plays a minor role in survival in GBC. Notably, continuous variables do not typically have a purely linear relationship with prognosis. After analyzing martingale residuals *vs* BMI, tumor size, and age, we found that converting these continuous variables into categorical variables was a better strategy for model selection. Furthermore, in contrast to conventional modeling methods, due to missing data regarding the grade variable, we first evaluated potential factors one by one to select five variables, including jaundice, cBMI, cCA19-9 levels, stage, and R that significantly affected outcome. For cCA19-9, which was a confounder of BMI levels and showed no interactions with each pair of predictors, four predictors other than cBMI were considered to establish the final nomogram. Overall, our research strategy was particularly suitable for a small study sample and single-center rare tumor cohorts, especially those with partial missing data. More importantly, our nomogram, which was based on a previously reported strategy, exhibited high predictive accuracy (C-index: 0.803; 95%CI: 0.766-0.839) and model performance (adjusted C-index: 0.797).

There are several potential limitations in this study. Our research cohort was from a single institution (PUMCH, which is one of the most famous hospitals where GBC patients from Beijing and the surrounding can seek diagnosis and treatment) with a small clinical database. The study results may not be widely used in patients from other institutions or countries because of selection bias and the lack of external validation. However, compared with patient cohorts from some other institutions in China, the clinical characteristics were similar, indicating the individualized epidemiology of GBC in China[20]. In addition, these shortcomings may to some extent be transformed into advantages because compared with large-scale multicenter studies,

a predictive nomogram built from a single institution study may have a high sensitivity and specificity due to decreased heterogeneity caused by demographic, clinical, and tumor-related characteristics. Clinicians are devoted to constructing models with general applicability and high accuracy at all times. However, this aim is always hard to fulfill due to the contradictions between heterogeneity and homogeneity. The establishment of a nomogram based on a single institution for survival prediction of rare tumors may be an alternative choice. Here, we introduced the details of a modeling method to facilitate the wide application of this research strategy.

In summary, jaundice, preoperative CA19-9 levels, AJCC-8 stage, and surgical margin status played vital roles in influencing survival time and were incorporated into a nomogram to predict outcomes for postoperative GBC patients. This model had high predictive accuracy and performed well after bootstrap validation and calibration. This type of research strategy should be widely used to construct specific nomograms according to different institutional databases, especially for rare tumors with small patient sample sizes with some missing data.

ARTICLE HIGHLIGHTS

Research background

Gallbladder cancer (GBC) is a rare tumor type with dismal outcomes. With advances in medical science, GBC patients have more treatment choices in addition to surgical resection, including chemotherapy, radiotherapy, targeted therapy, and immunotherapy. However, 5-year survival rates are surprisingly decreasing in China. Hence, screening GBC prognostic risk factors and constructing a prognostic model with high predictive accuracy and clinical utility for assessing the survival time of patients undergoing curative intent resection for GBC are of great importance.

Research motivation

Nomograms can integrate several independent prognostic factors for tumor patients into one model according by weighting each indicator to predict their overall survival. Compared with a single prediction indicator, this method can therefore provide more accurate and personalized prognostic information. Unfortunately, because of rare samples and ambiguous risk factors, nomograms to estimate survival time in GBC patients, especially in China, remain limited.

Research objectives

To establish a nomogram with easy use and high performance for predicting the survival of GBC patients undergoing radical resection in China, which will help doctors make rational decisions with respect to treatment, prognosis, and follow-up.

Research methods

To select survival-related predictors, clinical parameters consisting of age, gender, jaundice, cholecystolithiasis, diabetes, body mass index (BMI), carbohydrate antigen 19-9 (CA19-9), tumor size, pathological stage, histologic grade, and surgical margins derived from 142 GBC patients after curative intent surgical resection at Peking Union Medical College Hospital (PUMCH) were incorporated into a univariate Cox regression analysis. Model selection criteria, including the likelihood ratio test, Akaike information criterion (AIC), and stepwise, forward, and backward analyses, were applied. Jaundice, CA19-9, pathological stage, and resection (R) were combined into a survival-time predictive nomogram. The predictive accuracy of the model was estimated using the concordance index (C-index). The performance of the nomogram was estimated using a calibration curve. The predictive accuracy and net benefit of the nomogram were assessed *via* receiver operating characteristic (ROC) curve analysis and decision curve analysis (DCA), respectively.

Research results

A nomogram consisting of jaundice, CA19-9 levels, pathological stage, and resection margin status was constructed to predict the survival time of GBC patients after curative resection. More importantly, our nomogram exhibited high predictive accuracy (C-index: 0.803; 95%CI: 0.766-0.839) and model performance (adjusted C-index: 0.797). Due to limited samples, more samples are needed to optimize model performance.

Research conclusions

A nomogram was constructed to predict the overall survival of GBC patients who underwent radical surgery from a clinical database of GBC at PUMCH. In addition to a conventional nomogram construction strategy, continuous predictors were first converted into categorical variables after graphical assessment. Then, optimal cutoffs were selected regarding both normal references and martingale residuals. Schoenfeld residuals were analyzed with respect to ranked survival time for selected predictors, including jaundice, CA19-9 levels, pathological stage, and R, to further evaluate whether the proportional hazards assumption was valid. Finally, the predictive accuracy and clinical utility of nomogram were checked *via* ROC curve analysis and DCA, respectively. In summary, this study not only introduced a novel nomogram construction method to optimize model performance but also provided more detail information for clinicians to perform patient counseling, decision-making, and follow-up scheduling.

Research perspectives

This study describes a modeling method based on a single institution for survival prediction of rare tumors. This model had high predictive accuracy and performed well after bootstrap validation and calibration. This research strategy should be widely used to construct specific nomograms according to different institutional databases, especially for rare tumors with small sample sizes of patients with some missing data.

REFERENCES

1 **Hundal R**, Shaffer EA. Gallbladder cancer: epidemiology and outcome. *Clin Epidemiol* 2014; **6**: 99-109 [PMID: 24634588 DOI: 10.2147/CLEP.S37357]

2 **Wernberg JA**, Lucarelli DD. Gallbladder cancer. *Surg Clin North Am* 2014; **94**: 343-360 [PMID: 24679425 DOI: 10.1016/j.suc.2014.01.009]

3 **Zeng H**, Chen W, Zheng R, Zhang S, Ji JS, Zou X, Xia C, Sun K, Yang Z, Li H, Wang N, Han R, Liu S, Li H, Mu H, He Y, Xu Y, Fu Z, Zhou Y, Jiang J, Yang Y, Chen J, Wei K, Fan D, Wang J, Fu F, Zhao D, Song G, Chen J, Jiang C, Zhou X, Gu X, Jin F, Li Q, Li Y, Wu T, Yan C, Dong J, Hua Z, Baade P, Bray F, Jemal A, Yu XQ, He J. Changing cancer survival in China during 2003-15: a pooled analysis of 17 population-based cancer registries. *Lancet Glob Health* 2018; **6**: e555-e567 [PMID: 29653628 DOI: 10.1016/S2214-109X(18)30127-X]

4 **Amin MB**, Greene FL, Edge SB, Compton CC, Gershenwald JE, Brookland RK, Meyer L, Gress DM, Byrd DR, Winchester DP. The Eighth Edition AJCC Cancer Staging Manual: Continuing to build a bridge from a population-based to a more "personalized" approach to cancer staging. *CA Cancer J Clin* 2017; **67**: 93-99 [PMID: 28094848 DOI: 10.3322/caac.21388]

5 **Balachandran VP**, Gonen M, Smith JJ, DeMatteo RP. Nomograms in oncology: more than meets the eye. *Lancet Oncol* 2015; **16**: e173-e180 [PMID: 25846097 DOI: 10.1016/S1470-2045(14)71116-7]

6 **Iasonos A**, Schrag D, Raj GV, Panageas KS. How to build and interpret a nomogram for cancer prognosis. *J Clin Oncol* 2008; **26**: 1364-1370 [PMID: 18323559 DOI: 10.1200/JCO.2007.12.9791]

7 **Groot Koerkamp B**, Wiggers JK, Gonen M, Doussot A, Allen PJ, Besselink MG, Blumgart LH, Busch OR, D'Angelica MI, DeMatteo RP, Gouma DJ, Kingham TP, van Gulik TM, Jarnagin WR. Survival after resection of perihilar cholangiocarcinoma-development and

external validation of a prognostic nomogram. *Ann Oncol* 2015; **26**: 1930-1935 [PMID: 26133967 DOI: 10.1093/annonc/mdv279]
8 **Hyder O**, Marques H, Pulitano C, Marsh JW, Alexandrescu S, Bauer TW, Gamblin TC, Sotiropoulos GC, Paul A, Barroso E, Clary BM, Aldrighetti L, Ferrone CR, Zhu AX, Popescu I, Gigot JF, Mentha G, Feng S, Pawlik TM. A nomogram to predict long-term survival after resection for intrahepatic cholangiocarcinoma: an Eastern and Western experience. *JAMA Surg* 2014; **149**: 432-438 [PMID: 24599477 DOI: 10.1001/jamasurg.2013.5168]
9 **Wan G**, Gao F, Chen J, Li Y, Geng M, Sun L, Liu Y, Liu H, Yang X, Wang R, Feng Y, Wang X. Nomogram prediction of individual prognosis of patients with hepatocellular carcinoma. *BMC Cancer* 2017; **17**: 91 [PMID: 28143427 DOI: 10.1186/s12885-017-3062-6]
10 **Wang SJ**, Fuller CD, Kim JS, Sittig DF, Thomas CR Jr, Ravdin PM. Prediction model for estimating the survival benefit of adjuvant radiotherapy for gallbladder cancer. *J Clin Oncol* 2008; **26**: 2112-2117 [PMID: 18378567 DOI: 10.1200/JCO.2007.14.7934]
11 **Wang SJ**, Lemieux A, Kalpathy-Cramer J, Ord CB, Walker GV, Fuller CD, Kim JS, Thomas CR Jr. Nomogram for predicting the benefit of adjuvant chemoradiotherapy for resected gallbladder cancer. *J Clin Oncol* 2011; **29**: 4627-4632 [PMID: 22067404 DOI: 10.1200/JCO.2010.33.8020]
12 **Zhou D**, Wang JD, Yang Y, Yu WL, Zhang YJ, Quan ZW. Individualized nomogram improves diagnostic accuracy of stage I-II gallbladder cancer in chronic cholecystitis patients with gallbladder wall thickening. *Hepatobiliary Pancreat Dis Int* 2016; **15**: 180-188 [PMID: 27020635 DOI: 10.1016/s1499-3872(16)60073-5]
13 **Zhang W**, Hong HJ, Chen YL. Establishment of a Gallbladder Cancer-Specific Survival Model to Predict Prognosis in Non-metastatic Gallbladder Cancer Patients After Surgical Resection. *Dig Dis Sci* 2018 [PMID: 29736837 DOI: 10.1007/s10620-018-5103-7]
14 **General Assembly of the World Medical Association**. World Medical Association Declaration of Helsinki: ethical principles for medical research involving human subjects. *J Am Coll Dent* 2014; **81**: 14-18 [PMID: 25951678]
15 **Aloia TA**, Járufe N, Javle M, Maithel SK, Roa JC, Adsay V, Coimbra FJ, Jarnagin WR. Gallbladder cancer: expert consensus statement. *HPB* (Oxford) 2015; **17**: 681-690 [PMID: 26172135 DOI: 10.1111/hpb.12444]
16 **Randi G**, Franceschi S, La Vecchia C. Gallbladder cancer worldwide: geographical distribution and risk factors. *Int J Cancer* 2006; **118**: 1591-1602 [PMID: 16397865 DOI: 10.1002/ijc.21683]
17 **Wang Y**, Li J, Xia Y, Gong R, Wang K, Yan Z, Wan X, Liu G, Wu D, Shi L, Lau W, Wu M, Shen F. Prognostic nomogram for intrahepatic cholangiocarcinoma after partial hepatectomy. *J Clin Oncol* 2013; **31**: 1188-1195 [PMID: 23358969 DOI: 10.1200/JCO.2012.41.5984]
18 **Figueiredo JC**, Haiman C, Porcel J, Buxbaum J, Stram D, Tambe N, Cozen W, Wilkens L, Le Marchand L, Setiawan VW. Sex and ethnic/racial-specific risk factors for gallbladder disease. *BMC Gastroenterol* 2017; **17**: 153 [PMID: 29221432 DOI: 10.1186/s12876-017-0678-6]
19 **Goldin RD**, Roa JC. Gallbladder cancer: a morphological and molecular update. *Histopathology* 2009; **55**: 218-229 [PMID: 19490172 DOI: 10.1111/j.1365-2559.2008.03192.x]
20 **Shen HX**, Song HW, Xu XJ, Jiao ZY, Ti ZY, Li ZY, Ren B, Chen C, Ma L, Zhao YL, Zhang GJ, Ma JC, Geng XL, Zhang XD, Shi JS, Wang L, Geng ZM. Clinical epidemiological survey of gallbladder carcinoma in northwestern China, 2009-2013: 2379 cases in 17 centers. *Chronic Dis Transl Med* 2017; **3**: 60-66 [PMID: 29063057 DOI: 10.1016/j.cdtm.2017.01.003]

P- Reviewer: Higuchi K, Jung DH, Seo DW **S- Editor**: Ma RY
L- Editor: Wang TQ **E- Editor**: Huang Y

World Journal of Gastroenterology

Submit a Manuscript: http://www.f6publishing.com

World J Gastroenterol 2018 December 7; 24(45): 5179-5188

DOI: 10.3748/wjg.v24.i45.5179

ISSN 1007-9327 (print) ISSN 2219-2840 (online)

ORIGINAL ARTICLE

Observational Study

Narrow band imaging and white light endoscopy in the characterization of a polypectomy scar: A single-blind observational study

Fausto Riu Pons, Montserrat Andreu, Javier Gimeno Beltran, Marco Antonio Álvarez-Gonzalez, Agustín Seoane Urgorri, Josep Maria Dedeu, Luis Barranco Priego, Xavier Bessa

Fausto Riu Pons, Montserrat Andreu, Marco Antonio Álvarez-Gonzalez, Agustín Seoane Urgorri, Josep Maria Dedeu, Luis Barranco Priego, Xavier Bessa, Gastroenterology Department, Hospital del Mar, Barcelona 08003, Spain

Fausto Riu Pons, Montserrat Andreu, Javier Gimeno Beltran, Marco Antonio Álvarez-Gonzalez, Agustín Seoane Urgorri, Josep Maria Dedeu, Luis Barranco Priego, Xavier Bessa, IMIM (Hospital del Mar Medical Research Institute), Barcelona 08003, Spain

Fausto Riu Pons, Montserrat Andreu, Marco Antonio Álvarez-Gonzalez, Josep Maria Dedeu, Xavier Bessa, Department of Medicine, Autonomous University of Barcelona, Barcelona 08003, Spain

Montserrat Andreu, Pompeu Fabra University, Barcelona 08003, Spain

Javier Gimeno Beltran, Pathology Department, Hospital del Mar, Barcelona 08003, Spain.

ORCID number: Fausto Riu Pons (0000-0002-6576-4226); Montserrat Andreu (0000-0003-4286-1098); Javier Gimeno Beltran (0000-0001-6085-5228); Marco Antonio Álvarez-Gonzalez (0000-0002-9312-0268); Agustín Seoane Urgorri (0000-0001-8023-4445); Josep Maria Dedeu (0000-0003-0522-1032); Luis Barranco Priego (0000-0002-7352-7415); Xavier Bessa (0000-0003-4680-1228).

Author contributions: Riu Pons F, Andreu M and Bessa X designed research and wrote the paper; Gimeno Beltran J supervised the pathological assessment; Riu Pons F, Álvarez-Gonzalez MA, Seoane Urgorri A, Dedeu JM and Barranco Priego L performed the follow-up colonoscopy; Riu Pons F, Andreu M and Bessa X analyzed data.

Institutional review board statement: The study was reviewed and approved by the institutional review board of Parc de Salut Mar, 21 April 2015 (protocol number: 2015/6152/I).

Informed consent statement: All patients gave their written informed consent prior to study inclusion.

Conflict-of-interest statement: There are no conflicts of interest to report for any of the authors.

Data sharing statement: The dataset and statistical code is available from the corresponding author at FRiu@parcdesalutmar.cat

STROBE statement: Registration: ClinicalTrials.gov, NCT02448693. The manuscript followed the guidelines of the STROBE statement.

Manuscript source: Unsolicited manuscript

Correspondence author to: Fausto Riu Pons, MD, Senior Researcher, Gastroenterology Department, Hospital del Mar, Passeig Marítim 25-29, Barcelona 08003, Spain. friu@parcdesalutmar.cat
Telephone: +34-93-2483217

Received: August 20, 2018
Peer-review started: August 20, 2018
First decision: October 14, 2018
Revised: October 18, 2018
Accepted: November 16, 2018
Article in press: November 16, 2018
Published online: December 7, 2018

Abstract

AIM

To assess the incremental benefit of narrow band imaging (NBI) and white light endoscopy (WLE), randomizing the initial technique for the detection of residual neoplasia at the polypectomy scar after an endoscopic piecemeal mucosal resection (EPMR).

METHODS

We conducted an observational study in an academic center to assess the incremental benefit of NBI and WLE randomly applied 1:1 (NBI-WLE or WLE-NBI) in the follow-up of a post-EPMR scar by the same endoscopist.

RESULTS

A total of 112 EPMR scars were included. The median baseline polyp size was 20 mm (interquartile range: 14-30). At first review, NBI and WLE showed good sensitivity (85.0% *vs* 78.9%), specificity (77.1% *vs* 84.2%) and overall accuracy (80.0% *vs* 82.5%). NBI after WLE (WLE-NBI group) improved accuracy, but this difference was not statistically significant [area under the curve (AUC): 86.8% *vs* 81.6%, P = 0.15]. WLE after NBI (NBI-WLE group) did not improve accuracy (AUC: 81.4% *vs* 81.1%, P = 0.9). Overall, recurrence was found in 39/112 (34.8%) lesions.

CONCLUSION

Although no statistically significant differences were found between the two techniques at the first post-EPMR assessment, the use of NBI after WLE may improve residual neoplasia detection. Nevertheless, biopsy is still required in the first scar review.

Key words: Colonoscopy; Narrow band imaging; Endoscopic mucosal resection

Core tip: Endoscopic mucosal resection of colon polyps in a piecemeal fashion requires a first close follow-up to detect residual neoplasia. There are limited data on the optimal approach to reviewing polypectomy scars with narrow band imaging (NBI). In this prospective observational study, which randomized the initial technique for the detection of residual neoplasia, NBI was slightly more accurate than white light endoscopy. To improve the assessment of polypectomy scars, high-definition endoscopes with NBI should be the rule. However, biopsies are still required at the first follow-up, even if there are no macroscopically evident lesions.

Riu Pons F, Andreu M, Gimeno Beltran J, Álvarez-Gonzalez MA, Seoane Urgorri A, Dedeu JM, Barranco Priego L, Bessa X. Narrow band imaging and white light endoscopy in the characterization of a polypectomy scar: A single-blind observational study. *World J Gastroenterol* 2018; 24(45): 5179-5188 Available from: URL: http://www.wjgnet.com/1007-9327/full/v24/i45/5179.htm DOI: http://dx.doi.org/10.3748/wjg.v24.i45.5179

INTRODUCTION

Resection of non-pedunculated polyps, usually large sessile colonic polyps, increases technical difficulty and often requires fragmented resection or endoscopic piecemeal mucosal resection (EPMR)[1]. EPMR has been associated with lesion recurrence in 16%-27% of cases[2-4]. Consequently, clinical guidelines recommend endoscopic follow-up between 3 mo and 6 mo after piecemeal resection of colorectal polyps to check for residual neoplasia[5,6].

Narrow band imaging (NBI) improves visibility and identification of the surface and vascular structures of colon polyps. This technique uses optical interference filters to spectrally narrow the bandwidths used in conventional white light, providing more visual detail to superficial mucosal structures, and enhancing visualization of the superficial mucosal capillaries in neoplastic tissue[7]. In contrast to conventional chromoendoscopy, NBI is easy to activate by pressing a button on the handle of the endoscope.

Virtual or conventional chromoendoscopy is applied during polyp resection, defining the edge of the lesion. There have been few studies using conventional chromoscopy[8] or NBI in the examination of the EPMR scar. In 2011, Rogart *et al*[9] compared the accuracy of NBI with that of standard white light for the detection of residual neoplasia at the resection site in 60 discrete lesions (from the upper gastrointestinal tract to colon). In 27 out of 43 (63%) lesions detected, the extension of the residual scar was greater with NBI than with white light. However, this finding does not reveal whether the use of this technique could improve the detection of residual tumor after piecemeal polypectomy, avoiding complications, time and the costs of biopsy and histological analysis.

In this context, the European Society of Gastrointestinal Endoscopy (ESGE) published the first guideline on advanced endoscopic imaging for the detection and differentiation of colorectal neoplasia and recommends conventional or virtual chromoendoscopy such as NBI in the evaluation of patients with a piecemeal polypectomy scar (a strong recommendation, but with low quality evidence)[10]. A recent paper by Desomer *et al*[11] was the first to describe a standardized imaging protocol with high-definition WLE and sequential NBI for post-endoscopic mucosal resection (EMR) scar assessment, showing that this protocol is highly accurate in the endoscopic detection of residual or recurrence adenoma in the EMR scar, however, both techniques were always applied sequentially in the same order (WLE plus NBI) precluding to conclude the global accuracy depending on

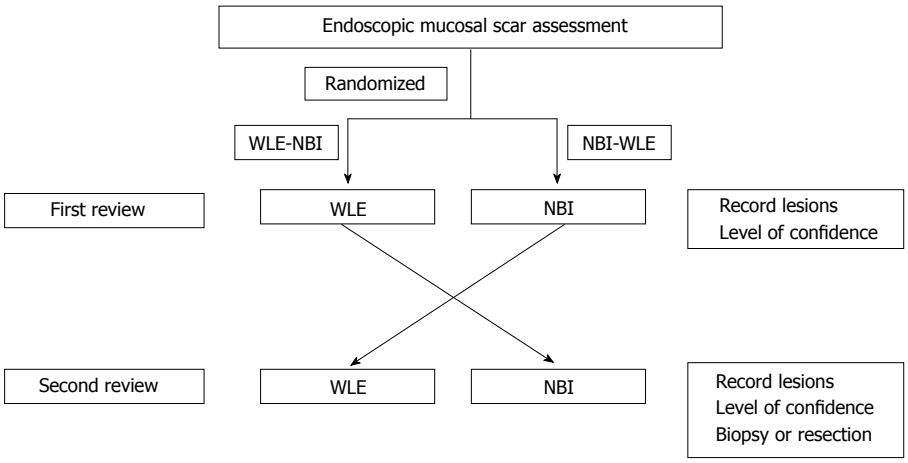

Figure 1 Study protocol. Prediction of residual adenoma/hyperplastic tissue by the endoscopist with a level of confidence: Positive or: Negative. WLE: White light endoscopy; NBI: Narrow band imaging.

the order of scar exploration of which technique at first is relevant.

Therefore, the present study was designed to assess the incremental benefit of NBI and WLE, randomizing the initial technique for the detection of residual neoplasia at the polypectomy scar after EPMR.

MATERIALS AND METHODS

Study design and population

An observational study was conducted from May 2015 to May 2016 at the Endoscopy Unit of Hospital del Mar in Barcelona (Spain) to compare the accuracy of both NBI and high-definition WLE in detecting residual neoplastic tissue after EPMR of a colonic polyp.

The study protocol, in compliance with the ethical guidelines of the 1975 Declaration of Helsinki, was approved by the institutional review board of Parc de Salut Mar, 21 April 2015 (protocol number: 2015/6152/I) and registered at ClinicalTrials.gov (NCT02448693). Written informed consent was obtained from all patients included in the study.

We included from the electronic database of the Endoscopy Unit consecutive patients with a minimum age of 18 years who had undergone a baseline colonoscopy in the last 12 mo with one or more sessile or flat polyp removed in a piecemeal fashion regardless of size. All baseline colonoscopies were performed by general gastroenterologists or expert endoscopists. Patients were excluded from follow-up colonoscopy if an advanced colorectal cancer (CRC) was found at the baseline colonoscopy, or if they did not attend follow-up or did not provide informed consent, or if they had a high risk of complications due to sedation -including patients with high comorbidity (American Society of Anesthesiologists, ASA grade IV and higher)- or had inadequate bowel preparation defined by the Boston bowel preparation score[12].

Procedure

Follow-up colonoscopies were performed by five experienced senior endoscopists (experience of > 4000 colonoscopies) using high-definition colonoscopes with NBI (EVIS EXERA III CV-190; Olympus Inc., Tokyo, Japan)[13]. All colonoscopies fulfilled the best standards of quality (cecal intubation, bowel preparation cleanliness and endoscope time withdrawal). All patients underwent bowel preparation using split-dose 4 L of oral polyethylene glycol-based solution. Level of consciousness was monitored by propofol alone or combined with midazolam and fentanyl at the discretion of the endoscopist. An anesthesia specialist was consulted in individual cases.

Each procedure was performed by the same endoscopist. Randomization was done before the initiation of the procedure. Allocation concealment of the first technique was computer-generated by the biomedical research consulting service of Hospital del Mar Medical Research Institute (IMIM), Barcelona. In addition, three specialized pathologists were blinded to the study protocol and samples were received as scar polypectomy for assessment. Colon inspection was done with WLE during withdrawal. At the proximity of the scar or scars, if there was multiplicity, WLE and NBI were used randomly one after the other (WLE-NBI or NBI-WLE group). If NBI was the first technique used, it was switched prior to scar detection, avoiding, as far as possible, a glance with WLE (Figure 1).

At first scar review, any macroscopically suspicious lesion or nodularity (evaluation site) was assigned a level of confidence, recorded on a data sheet by the endoscopist. The level of confidence represented a prediction of visual residual neoplasia graded as positive: High confidence of diagnostic certainty or negative: Low confidence or normal appearing scar. The morphology of each evaluation site was described as flat or nodular elevated. Residual neoplasia was defined for any adenoma or serrated tissue that was confirmed on histopathological analysis. After the first examination, the endoscopist switched to the second endoscopic technique and reviewed the polypectomy scar again.

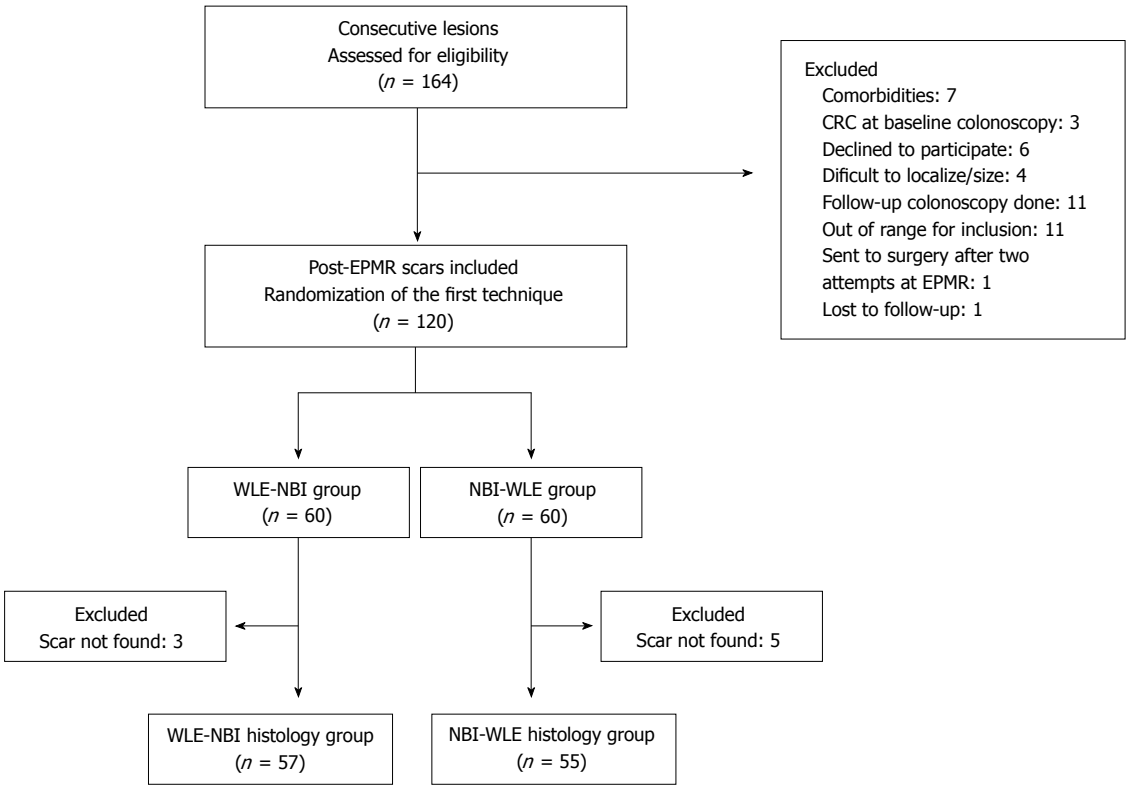

Figure 2 Flow diagram of study selection. WLE: White light endoscopy; NBI: Narrow band imaging; EPMR: Endoscopic piecemeal mucosal resection; CRC: Colorectal cancer.

Any newly detected or suspicious lesions were classified by making another prediction with a level of confidence and recorded separately from the first review on a data sheet. For newly suspected irregularities considered as positive, the first review was being graded as negative. After both evaluations, all of the sites were biopsied (up to three), including an apparently normal scar. If detected lesions were larger than 5 mm, the endoscopist could use any additional therapeutic arsenal to destroy the residual tissue by means of cold snare, diathermy, EMR or argon plasma coagulation. The rest of the colon was inspected following conventional standards with WLE.

Data from the baseline colonoscopy included: lesion size and location, Paris classification[14], NBI International Colorectal Endoscopic (NICE) classification[15], histology, ASA classification, use of clips, use of endoscopic tattooing to mark the lesion, number of resected specimens from EPMR (categorized as 2-5 or > 5 specimens)[16], endoscopists who performed EPMR, and median time from baseline colonoscopy to evaluation.

The primary outcome was the accuracy of NBI and WLE in detecting residual neoplasia in a polypectomy scar, with pathological analysis as the gold standard.

Statistical analysis

Continuous variables were compared using the *t*-test, if normally distributed, and the Mann-Whitney test if not. Categorical variables were compared using the chi-square test or Fisher's exact test. The accuracy of each technique in detecting residual neoplasia was assessed globally for each scar. Receiver operating characteristic (ROC) curve analyses were performed to reveal the relationship between the sensitivity and specificity of NBI and WLE. Kappa statistics were used to assess interobserver agreement between endoscopists for each technique and with histology. The threshold values of kappa defined by Landis and Koch[17] are: 0.0 agreement no greater than chance alone, 0.01-0.2 slight, 0.21-0.4 fair, 0.41-0.6 moderate, 0.61-0.8 substantial and 0.81-1.0 near perfect agreement. *P* values < 0.05 were considered to be statistically significant. Statistical analyses were performed using STATA/IC 13.1 (StataCorp, College Station, TX, United States).

On the basis of previous studies[9], we aimed to improve sensitivity in the detection of residual tissue after an EPMR (WLE *vs* NBI) from 70% to 85%. A sample size of 120 lesions (60 in each of the two groups) achieved 80% power to detect a difference, with alpha = 0.05.

RESULTS

Baseline characteristics

A total of 164 EPMR in 156 patients were assessed for eligibility. One hundred twenty lesions from 111 patients were included in this study and 44 were excluded as shown in Figure 2. The enrolled patients were randomly

Table 1 Baseline patient's characteristics *n* (%)

Total number of lesions	112
Mean age, years (SD)	67.7 (10.1)
Sex ratio, % male	57.1
Weight (Kg, SD)	74.7 (15.4)
BMI (Kg/m^2, SD)	27.6 (5.1)
Family History of CRC	27 (24.1)
Personal History of CRC	7 (6.3)
Current smoking	20 (17.9)
Diabetes	19 (17.0)
Lesion size, mm (median, interquartile range)	20 (14-30)
Categorical size	
10-19 mm	47 (42.0)
20-39 mm	52 (46.4)
≥ 40 mm	13 (11.6)
Location of the lesion	
Cecum	15 (13.4)
Ascending	53 (47.3)
Transverse	20 (17.9)
Descending	4 (3.6)
Sigmoid	10 (8.9)
Rectum	10 (8.9)
ASA classification	
ASA I	18 (16.1)
ASA II	56 (50.0)
ASA III	38 (33.9)
Paris classification	
0-Is	48 (42.9)
0-IIa	50 (44.6)
Other combinations (IIa + Is/IIc)	14 (12.5)
NICE classification	
NICE I	17 (15.2)
NICE II	94 (83.9)
NICE III	1 (0.9)
Number of resected pieces	
2-5 pieces	46 (41.1)
> 5 pieces	66 (58.9)
Baseline histology	
Hyperplastic	4 (3.6)
Adenoma with LGD	53 (47.3)
Adenoma with HGD	39 (34.8)
Sessile serrated adenoma (SSA)	11 (9.8)
Traditional serrated adenoma (TSA)	2 (1.8)
Adenocarcinoma (pT1 stage)	3 (2.7)
Use of clips	59 (52.7)
Clips per lesion (median, interquartile range)	3 (1-3)
Use of clips	
Prophylactic	56 (94.9)
Intraprocedural bleeding	2 (3.4)
Suspicion of deep mural injury	1 (1.7)
Tattooed lesion after EPMR	38 (33.9)
Endoscopist who performed piecemeal EMR	
Expert endoscopists	98 (87.5)
General gastroenterologists	14 (12.5)
Median time to review (months, interquartile range)	3.9 (3.0-5.3)

BMI: Body mass index; ASA: American society of anesthesia; CRC: Colorectal cancer; EMR: Endoscopic mucosal resection; LGD: Low-grade dysplasia; HGD: High-grade dysplasia; EPMR: Endoscopic piecemeal mucosal resection.

divided into two groups (WLE-NBI or NBI-WLE). After randomization, 8 lesions were excluded because the scar was not found, and therefore 112 scars were finally included to the analysis.

The patients' baseline characteristics of one hundred twelve scars are depicted in Table 1. Male gender was more prevalent (57.1% males) and the mean age was 67.7 years (SD: 10.1) at the time of the EPMR procedure. The median size of the lesion was 20 mm (interquartile range: 14-30). Lesions were most frequently located proximal from the cecum to the transverse colon (78.6%). Polyp morphology was sessile 0-Is (42.9%), superficial elevated 0-IIa (44.6%), or other non-polypoid combinations (12.5%), with predominantly adenoma with low-grade dysplasia (47.3%). The resection technique was using saline injection with indigo carmine and optionally diluted adrenaline.

Endoscopic clips were used in 59 of 112 lesions (52.7%), with a median of three clips (interquartile range: 1-3) per session. The reasons for clipping were mostly for prophylactic measures in 56 patients (94.9%), intraprocedural bleeding in two patients (3.4%) and suspicion of deep mural injury in one patient (1.7%). All the complications were successfully managed endoscopically with no clinically significant post-procedural bleeding or late complications.

Comparison of NBI and WLE

The median time from initial resection to scar review was 3.9 mo (interquartile range: 3.0-5.3). The characteristics of WLE-NBI and NBI-WLE are shown in Table 2. Both groups were similar, including the presence of clips that remained at the polypectomy scar, except for the median size of baseline polyps, which were larger in the WLE-NBI group.

Assessment of WLE and NBI with histology

Among the 112 lesions, a minimum of one biopsy per scar was assessed, two different biopsies in 25 scars, and up to three in three scars. When comparing the two techniques with histology as the gold standard, we analyzed those lesions as a whole scar.

In the WLE-NBI group, a first inspection with WLE obtained 78.9% sensitivity, 84.2% specificity, 71.4% positive predictive value (PPV) and 88.9% negative predictive value (NPV). The addition of a second review with NBI slightly increased sensitivity to 89.5% and NPV to 94.1%, without modifying specificity (84.2%) or PPV (73.9%).

Similar findings were demonstrated by the area under the ROC curve for a global assessment. As shown in Table 3, the addition of NBI was followed by a slight but not significant increase in accuracy: WLE 81.6% (95%CI: 70.5%-92.7%) *vs* NBI 86.8% (95%CI: 77.6%-96.0%, $P = 0.15$, Figure 3).

In the NBI-WLE group, in which the first review was thorough NBI examination, we obtained 85.0% sensitivity, 77.1% specificity, 68.0% PPV and 90.0% NPV. Adding a second review with WLE did not increase sensitivity (80.0%) but improved specificity (82.9%) and PPV (72.7%) with similar NPV (87.9%).

As shown in Table 3, the AUC was similar for each technique: NBI 81.1% (95%CI: 70.4%-91.8%) *vs* WLE 81.4% (95%CI: 70.4%-92.4%, $P = 0.9$, Figure 3).

Table 2 Characteristics between groups at protocol study

	WLE-NBI (n = 57)	NBI-WLE (n = 55)	P value
Sex (male, %)	54.4	60.0	0.36
Age (yr)	67.3	68.2	0.65
BMI (mean)	28.2	27.0	0.23
Baseline polyp size			0.002
10-19 mm	16 (28.1)	31 (56.4)	
20-39 mm	30 (52.6)	22 (40.0)	
≥ 40 mm	11 (19.3)	2 (3.6)	
Location, right sided (%)	79.0	78.2	0.92
Paris Classification			0.34
0-Is	26 (45.6)	22 (40.0)	
0-IIa	22 (38.6)	28 (50.9)	
Other Combinations	9 (15.8)	5 (9.1)	
NICE Classification			0.90
NICE I	8 (14.0)	9 (16.4)	
NICE II	48 (84.2)	46 (83.6)	
NICE III	1 (1.8)	0 (0)	
Baseline histology			0.78
Hyperplastic	2 (3.5)	2 (3.6)	
Adenoma with LGD	26 (45.6)	27 (49.1)	
Adenoma with HGD	22 (38.6)	17 (30.9)	
Sessile Serrated Adenoma (SSA)	5 (8.8)	6 (10.9)	
Traditional serrated adenoma	0 (0)	2 (3.6)	
Adenocarcinoma (pT1 stage)	2 (3.5)	1 (1.8)	
Morphology of scar on site 1			0.12
Flat	29 (50.9)	20 (36.4)	
Nodular elevated	28 (49.1)	35 (63.6)	
Presence of clips on scar	3 (5.3)	8 (14.6)	0.12
Residual neoplasia on histology assessment			0.74
Negative	38 (66.7)	35 (63.6)	
Positive	19 (33.3)	20 (36.4)	
Polyps resected (mean, SD)	2.4 (2.7)	2.4 (2.7)	0.92
Mean time baseline EPMR colonoscopy (min)	55.9	51.9	0.38

WLE: White light endoscopy; NBI: Narrow band imaging; BMI: Body mass index; LGD: Low-grade dysplasia; HGD: High-grade dysplasia; EPMR: Endoscopic piecemeal mucosal resection.

Table 3 Diagnostic performance of white light endoscopy and narrow band imaging for each group

	WLE-NBI group			NBI-WLE group		
	WLE (95%CI)	NBI (95%CI)		NBI (95%CI)	WLE (95%CI)	
Sensitivity	78.9% (56.7-91.5)	89.5% (68.6-97.1)		85.0% (64.0-94.8)	80.0% (58.4-91.9)	
Specificity	84.2% (69.6-92.6)	84.2% (69.6-92.6)		77.1% (61.0-87.9)	82.9% (67.3-91.9)	
False positive	15.8% (7.4-30.4)	15.80% (7.4-30.4)		22.9% (12.1-39.0)	17.1% (8.1-32.7)	
False negative	21.1% (8.5-43.3)	10.50% (2.9-31.4)		15.00% (5.2-36.0)	20.0% (8.1-41.6)	
PPV	71.4% (50.0-86.2)	73.9% (53.5-87.5)		68.0% (48.4-82.8)	72.7% (51.8-86.8)	
NPV	88.9% (74.7-95.6)	94.1% (80.9-98.4)		90.0% (74.4-96.5)	87.9% (72.7-95.2)	
LR +	5 (2.3-10.8)	5.7 (2.7-12.0)		3.7 (2.0-7.0)	4.7 (2.2-10.0)	
LR -	0.3 (0.1-0.6)	0.1 (0.03-0.5)		0.2 (0.1-0.6)	0.2 (0.1-0.6)	
Global accuracy	82.5% (70.6-90.2)	86.0% (74.7-92.7)		80.0% (67.6-88.4)	81.8% (69.7-89.8)	
AUC	81.6% (70.5-92.7)	86.8% (77.6-96.0)	P = 0.15	81.1% (70.4-91.8)	81.4% (70.4-92.4)	P = 0.9

CI: Confidence interval; WLE: White light endoscopy; NBI: Narrow band imaging; PPV: Positive predictive value; NPV: Negative predictive value; LR: Likelihood ratio; AUC: Area under the curve.

There was also a high degree of interobserver agreement between WLE and NBI (Kappa value, 0.91) and good concordance with histology (WLE: Kappa, 0.62 and NBI: Kappa, 0.65).

None of the patients had major complications due to the colonoscopy assessment.

Residual neoplasia in scar tissue

Of the 112 scars detected at the endoscopic follow-up, 39 (34.8%) had residual neoplastic lesions on histologic assessment (Figure 4): 1 (2.6%) hyperplastic polyp, 29 (74.4%) adenomas with low-grade dysplasia, 5 (12.8%) adenomas with high-grade dysplasia, 3 (7.7%) sessile serrated polyps and 1 (2.6%) carcinoma. The latter case, considered a high-grade dysplastic adenoma at the baseline piecemeal polypectomy, was a flat depressed (0-IIc) unresectable lesion on colonoscopy follow-up.

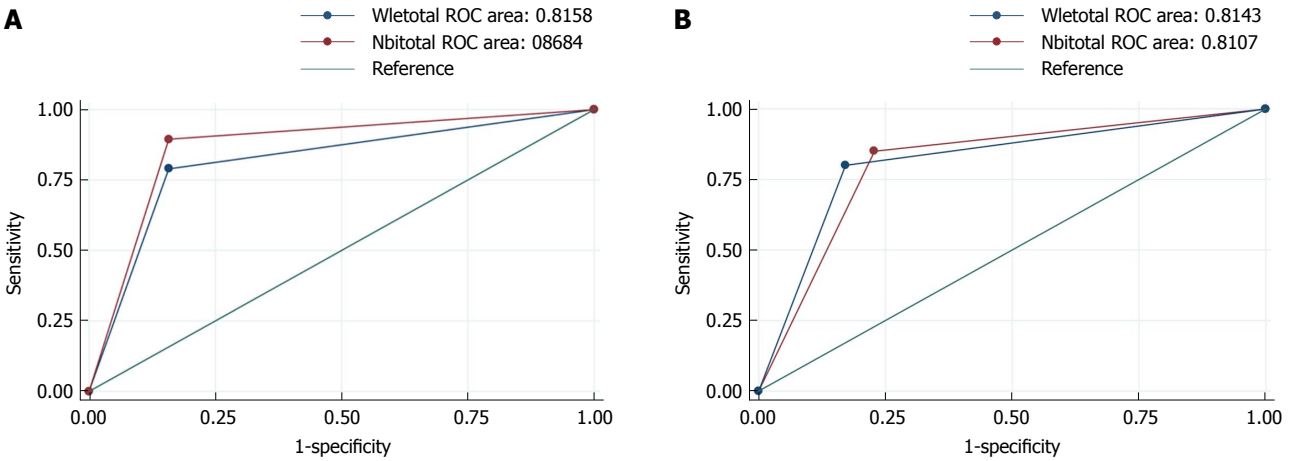

Figure 3 Receiver operating characteristic curve. Global assessment of white light endoscopy (WLE) and narrow band imaging (NBI) is drawn for each group. A: WLE-NBI; B: NBI-WLE. The cut-off of the best area under the operating characteristic curve (ROC) curve is the true positive rate (sensitivity) plotted to the false positive rate (1.0-specificity). The closer the ROC curve to the upper left corner, the higher the accuracy of the test.

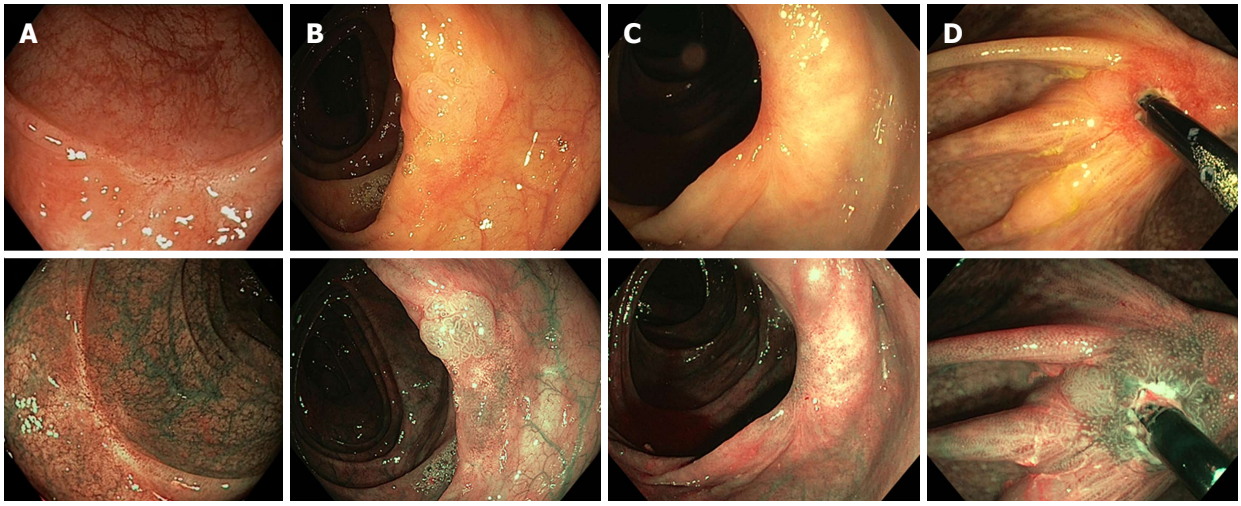

Figure 4 Examples of endoscopic mucosal scar with white light endoscopy and narrow band imaging (above and below and from left to right). A: Normal scar; B: Clear residual tissue of a surprisingly sessile serrated polyp/adenoma with no dysplasia on either the scar or endoscopic piecemeal mucosal resection; C: Apparent normal tissue with low-grade dysplasia at histology; D: Small residual tissue with low-grade dysplasia surrounding a clip (a clip artifact).

DISCUSSION

We found that NBI and WLE showed high sensitivity, specificity and very good accuracy in detecting residual neoplasia. Of importance, in the first review with both techniques, the global assessment was almost equivalent (AUC: 82%). Sensitivity and NPV were improved only by NBI after WLE but this difference was not statistically significant.

Current ESGE guidelines of advanced colonoscopic imaging suggest the use of conventional or virtual chromoendoscopy at the piecemeal polypectomy scar, but there is scarce evidence[10]. In 183 lesions, Desomer *et al*[11] demonstrated that NBI achieves higher sensitivity and specificity than WLE alone (sensitivity: 93.3% *vs* 66.7%; specificity: 94.1% *vs* 96.1%). However, a ROC curve for global assessment would have been desirable to discriminate statistically significant differences. Despite the higher accuracy of WLE+NBI, the false negative result, meaning to give a negative diagnosis but was actually positive on histology, was 6.7%, indicating that a surveillance and histology protocol need to be implemented before biopsies can be omitted.

Globally, we identified 34.8% of patients with residual neoplasia, which is higher than values reported in the literature[2-4]. In most of the patients, the residual neoplastic tissue was treated endoscopically. However, due to the primary outcome of the study, we did not undertake a second follow-up to determine the persistence of residual neoplasia subsequently. Knabe *et al*[18] reported a similarly high recurrence of 31.7% at the first follow-up, and pointed out that 7% of macroscopically inconspicuous polypectomy scars were found to have occult residual adenoma. This highlights that a substantial proportion of large EPMR confers incomplete resection and some scars can harbor late

recurrence. In our study, the use of NBI after WLE yielded a false negative rate of 11%. These lesions could have been missed had we not taken biopsies from the scar.

Of note, almost half of the lesions were clipped, mostly as a prophylactic measure. Their use or presence at the scar did not influence characterization or recurrence. This type of closure makes a nodularity of elevated normal mucosa or a granulation tissue, also called the clip artifact[19]. However, even though we did not evaluate the morphology of the clip artifact, the presence of a nodule or irregularity should be meticulously inspected and, if there is inconclusive focal change, biopsies or excision should be performed[20].

There are some explanations that plausibly strengthen our findings. First, for this study, we used high-definition colonoscopes (series 190 from Olympus). The vascularity or the pit pattern of the polypectomy scar seems to be well defined even with WLE. Second, the strength of randomization involves the assignment of a grade of suspicion each time the endoscopist detects irregularities from the normal or fibrotic mucosa. Our results suggest that switching the filter to NBI or WLE does not alter the first impression (near perfect agreement with a kappa of 0.91).

Our study has some limitations. First, this is a single-center study and the observed results should be compared with those of other centers with different level of expertise. In addition, we excluded patients with high comorbidity who had undergone EPMR to avoid losses or other complications related to sedation at follow-up colonoscopy.

Second, randomization of the two techniques in which the introduction of the colonoscope was on WLE could have biased the results for the NBI-WLE group. However, the results of NBI as the first evaluation were similar to those of WLE as the first (AUC: 81.1% *vs* 81.6%, respectively) and were slightly better than those for the WLE-NBI group (AUC: 86.8%). Other possible scenarios would have been insertion by a first endoscopist and assessment by a second endoscopist, or two different endoscopists at the same time for each technique. This would have introduced other bias by having two endoscopists in the same room, and the results would be less homogeneous between endoscopists.

Third, the median baseline polyp size was statistically significant between the two groups at the follow-up colonoscopy to evaluate the scar. We assume this non-intentional distribution was due to randomization of a small sample. However, there was no difference in the scar morphology or the number of residual tissue in the histology sample between the two groups.

Finally, the median time to review was short, which did not allow recurrence to be distinguished from residual tissue. Moreover, we did not carry out surveillance after 6 mo, which could have increased the proportion of late recurrences detected. Due to the primary outcome in our study, we could not extrapolate the risk factors for recurrence. There is robust evidence from a meta-analysis of potential predictors of local recurrence, and the recurrence risk can be stratified by using the Sydney EMR recurrence tool[21,22].

In conclusion, this prospective observational study of recurrence at endoscopic resection scars assessed by expert observers did not show a difference in the detection of recurrence at the EPMR scar depending on whether the initial technique was NBI or WLE but there was a slight accuracy improvement in the WLE-NBI group although non-significant. Biopsies are still required in the first review of the scar in all cases, either when there is any suspicious nodularity or clip artifact, even if no macroscopically evident lesion is observed. Although non-targeted forceps biopsy is an imperfect gold standard, larger lesions resected in a piecemeal fashion should be monitored at 3-6 mo to detect and resect residual tissue.

ARTICLE HIGHLIGHTS

Research background

Endoscopic mucosal resection of colon polyps in a piecemeal fashion (EPMR) requires a first close follow-up at 3-6 mo. In addition, the European Society of Gastrointestinal Endoscopy recommends the use of advanced endoscopic imaging for the detection and differentiation of residual neoplasia at the polypectomy scar, but with low quality of evidence.

Research motivation

There are limited data on the best approach with the use of narrow band imaging (NBI) compared with white light endoscopy (WLE) to review a polypectomy scar.

Research objectives

This study was designed to assess the incremental benefit of NBI and WLE, randomizing the initial technique for the detection of residual neoplasia at the polypectomy scar after an EPMR.

Research methods

We conducted an observational study of 120 polypectomy scars in 111 patients who had undergone a baseline colonoscopy with piecemeal polyp resection regardless of size and prospectively assigned to follow-up colonoscopy with random application of NBI and WLE 1:1 at the proximity of the scar. Patients were distributed in two groups (NBI-WLE or WLE-NBI). Five experienced endoscopists used Olympus 190 series for the assessment. Any macroscopically suspicious lesion was recorded as positive, with high confidence of a definitive diagnosis, or as negative. After the first examination, the endoscopist switched to the second technique and reviewed the polypectomy scar again, making a second prediction. After both evaluations, all of the sites were biopsied, including apparently normal scars. All resected specimens were blinded to the three specialized pathologists. The primary outcome was the accuracy of NBI and WLE in detecting residual neoplasia in the polypectomy scar, with pathological analysis as the gold standard. Receiver operating characteristic (ROC) curve analyses were performed to reveal the relationship between the sensitivity and specificity of NBI and WLE, and Kappa statistics were used to assess interobserver agreement between endoscopists for each technique and with histology.

Research results

After randomization, 8 lesions were excluded from the final assessment

because the scar was not found, and therefore 112 scars were finally included to the analysis. In the WLE-NBI group, a first inspection with WLE showed 78.9% sensitivity, 84.2% specificity, 71.4% positive predictive value (PPV) and 88.9% negative predictive value (NPV). The addition of a second review with NBI slightly increased sensitivity to 89.5% and NPV to 94.1%, without modifying specificity (84.2%) or PPV (73.9%). The addition of NBI was followed by a slight but non- significant increase in accuracy, shown by the area under the ROC curve (AUC): WLE 81.6% *vs* NBI 86.8% (P = 0.15). In the NBI-WLE group, which underwent the first review with NBI, the results in terms of sensitivity and specificity were almost equivalent. There were no differences in the AUC with NBI (81.1%) *vs* WLE (81.4%) (P = 0.9). There was a high degree of interobserver agreement between WLE and NBI (Kappa value, 0.91) and good concordance with histology (WLE: Kappa 0.62 and NBI: Kappa, 0.65). Of the 112 scars detected at the endoscopic follow-up, 39 (34.8%) had residual neoplastic lesions on histologic assessment.

Research conclusions

We found that NBI and WLE showed high sensitivity, specificity and very good accuracy in detecting residual neoplasia. Sensitivity and NPV were improved only when NBI was performed after WLE but this difference was not statistically significant. In our study we identified a higher rate of patients with residual neoplasia. Due to the primary outcome of the study, we did not undertake a second follow-up. Despite the use of NBI after WLE, we found a false negative rate of 11%. These lesions could have been missed if we had not taken biopsies from the scar. For this reason, we believe that biopsies are still required in the first review of the scars in all cases, even if there are no macroscopically evident lesions, although we recognize that this is an imperfect gold standard. Monitoring EPMR at 3 to 6 mo is mandatory to detect and resect residual tissue.

Research perspectives

The future direction in this field will probably focus on the use of optical magnification or other digital improvements in image enhancing techniques.

ACKNOWLEDGMENTS

This study was awarded as the best poster in the XXVI Catalan Society of Digestology Congress. Lleida (Spain) January 2017.

REFERENCES

1 **Burgess NG**, Bahin FF, Bourke MJ. Colonic polypectomy (with videos). *Gastrointest Endosc* 2015; **81**: 813-835 [PMID: 25805461 DOI: 10.1016/j.gie.2014.12.027]
2 **Moss A**, Williams SJ, Hourigan LF, Brown G, Tam W, Singh R, Zanati S, Burgess NG, Sonson R, Byth K, Bourke MJ. Long-term adenoma recurrence following wide-field endoscopic mucosal resection (WF-EMR) for advanced colonic mucosal neoplasia is infrequent: results and risk factors in 1000 cases from the Australian Colonic EMR (ACE) study. *Gut* 2015; **64**: 57-65 [PMID: 24986245 DOI: 10.1136/gutjnl-2013-305516]
3 **Khashab M**, Eid E, Rusche M, Rex DK. Incidence and predictors of "late" recurrences after endoscopic piecemeal resection of large sessile adenomas. *Gastrointest Endosc* 2009; **70**: 344-349 [PMID: 19249767 DOI: 10.1016/j.gie.2008.10.037]
4 **Buchner AM**, Guarner-Argente C, Ginsberg GG. Outcomes of EMR of defiant colorectal lesions directed to an endoscopy referral center. *Gastrointest Endosc* 2012; **76**: 255-263 [PMID: 22657404 DOI: 10.1016/j.gie.2012.02.060]
5 **Atkin WS**, Valori R, Kuipers EJ, Hoff G, Senore C, Segnan N, Jover R, Schmiegel W, Lambert R, Pox C; International Agency for Research on Cancer. European guidelines for quality assurance in colorectal cancer screening and diagnosis. First Edition--Colonoscopic surveillance following adenoma removal. *Endoscopy* 2012; **44** Suppl 3: SE151-SE163 [PMID: 23012119 DOI: 10.1055/s-0032-1309821]
6 **Lieberman DA**, Rex DK, Winawer SJ, Giardiello FM, Johnson DA, Levin TR. Guidelines for colonoscopy surveillance after screening and polypectomy: a consensus update by the US Multi-Society Task Force on Colorectal Cancer. *Gastroenterology* 2012; **143**: 844-857 [PMID: 22763141 DOI: 10.1053/j.gastro.2012.06.001]
7 **Machida H**, Sano Y, Hamamoto Y, Muto M, Kozu T, Tajiri H, Yoshida S. Narrow-band imaging in the diagnosis of colorectal mucosal lesions: a pilot study. *Endoscopy* 2004; **36**: 1094-1098 [PMID: 15578301 DOI: 10.1055/s-2004-826040]
8 **Hurlstone DP**, Sanders DS, Cross SS, Adam I, Shorthouse AJ, Brown S, Drew K, Lobo AJ. Colonoscopic resection of lateral spreading tumours: a prospective analysis of endoscopic mucosal resection. *Gut* 2004; **53**: 1334-1339 [PMID: 15306595 DOI: 10.1136/gut.2003.036913]
9 **Rogart JN**, Aslanian HR, Siddiqui UD. Narrow band imaging to detect residual or recurrent neoplastic tissue during surveillance endoscopy. *Dig Dis Sci* 2011; **56**: 472-478 [PMID: 20532981 DOI: 10.1007/s10620-010-1289-z]
10 **Kamiński MF**, Hassan C, Bisschops R, Pohl J, Pellisé M, Dekker E, Ignjatovic-Wilson A, Hoffman A, Longcroft-Wheaton G, Heresbach D, Dumonceau JM, East JE. Advanced imaging for detection and differentiation of colorectal neoplasia: European Society of Gastrointestinal Endoscopy (ESGE) Guideline. *Endoscopy* 2014; **46**: 435-449 [PMID: 24639382 DOI: 10.1055/s-0034-1365348]
11 **Desomer L**, Tutticci N, Tate DJ, Williams SJ, McLeod D, Bourke MJ. A standardized imaging protocol is accurate in detecting recurrence after EMR. *Gastrointest Endosc* 2017; **85**: 518-526 [PMID: 27343411 DOI: 10.1016/j.gie.2016.06.031]
12 **Lai EJ**, Calderwood AH, Doros G, Fix OK, Jacobson BC. The Boston bowel preparation scale: a valid and reliable instrument for colonoscopy-oriented research. *Gastrointest Endosc* 2009; **69**: 620-625 [PMID: 19136102 DOI: 10.1016/j.gie.2008.05.057]
13 **ASGE Technology Committee**. High-definition and high-magnification endoscopes. *Gastrointest Endosc* 2014; **80**: 919-927 [PMID: 25442091 DOI: 10.1016/j.gie.2014.06.019]
14 The Paris endoscopic classification of superficial neoplastic lesions: esophagus, stomach, and colon: November 30 to December 1, 2002. *Gastrointest Endosc* 2003; **58**: S3-S43 [PMID: 14652541 DOI: 10.1016/S0016-5107(03)02159-X]
15 **Hewett DG**, Kaltenbach T, Sano Y, Tanaka S, Saunders BP, Ponchon T, Soetikno R, Rex DK. Validation of a simple classification system for endoscopic diagnosis of small colorectal polyps using narrow-band imaging. *Gastroenterology* 2012; **143**: 599-607.e1 [PMID: 22609383 DOI: 10.1053/j.gastro.2012.05.006]
16 **Sakamoto T**, Matsuda T, Otake Y, Nakajima T, Saito Y. Predictive factors of local recurrence after endoscopic piecemeal mucosal resection. *J Gastroenterol* 2012; **47**: 635-640 [PMID: 22223177 DOI: 10.1007/s00535-011-0524-5]
17 **Landis JR**, Koch GG. The measurement of observer agreement for categorical data. *Biometrics* 1977; **33**: 159-174 [PMID: 843571 DOI: 10.2307/2529310]
18 **Knabe M**, Pohl J, Gerges C, Ell C, Neuhaus H, Schumacher B. Standardized long-term follow-up after endoscopic resection of large, nonpedunculated colorectal lesions: a prospective two-center study. *Am J Gastroenterol* 2014; **109**: 183-189 [PMID: 24343549 DOI: 10.1038/ajg.2013.419]
19 **Sreepati G**, Vemulapalli KC, Rex DK. Clip artifact after closure of large colorectal EMR sites: incidence and recognition. *Gastrointest Endosc* 2015; **82**: 344-349 [PMID: 25843616 DOI: 10.1016/j.gie.2014.12.059]
20 **Pellisé M**, Desomer L, Burgess NG, Williams SJ, Sonson R, McLeod D, Bourke MJ. The influence of clips on scars after EMR: clip artifact. *Gastrointest Endosc* 2016; **83**: 608-616 [PMID: 26364966 DOI: 10.1016/j.gie.2015.08.071]
21 **Belderbos TD**, Leenders M, Moons LM, Siersema PD. Local recurrence after endoscopic mucosal resection of nonpedunculated colorectal lesions: systematic review and meta-analysis. *Endoscopy* 2014; **46**: 388-402 [PMID: 24671869 DOI: 10.1055/s-0034-1364970]

22 **Tate DJ**, Desomer L, Klein A, Brown G, Hourigan LF, Lee EY, Moss A, Ormonde D, Raftopoulos S, Singh R, Williams SJ, Zanati S, Byth K, Bourke MJ. Adenoma recurrence after piecemeal colonic EMR is predictable: the Sydney EMR recurrence tool. *Gastrointest Endosc* 2017; **85**: 647-656.e6 [PMID: 27908600 DOI: 10.1016/j.gie.2016.11.027]

P- Reviewer: Aoki T, Fei BY, Tsuji Y **S- Editor**: Wang XJ
L- Editor: A **E- Editor**: Huang Y

Published by **Baishideng Publishing Group Inc**
7901 Stoneridge Drive, Suite 501, Pleasanton, CA 94588, USA
Telephone: +1-925-223-8242
Fax: +1-925-223-8243
E-mail: bpgoffice@wjgnet.com
Help Desk: http://www.f6publishing.com/helpdesk
http://www.wjgnet.com

ISSN 1007-9327